

Climate Change 2007

The Physical Science Basis

The Intergovernmental Panel on Climate Change (IPCC) was set up jointly by the World Meteorological Organization and the United Nations Environment Programme to provide an authoritative international statement of scientific understanding of climate change. The IPCC's periodic assessments of the causes, impacts and possible response strategies to climate change are the most comprehensive and up-to-date reports available on the subject, and form the standard reference for all concerned with climate change in academia, government and industry worldwide. Through three working groups, many hundreds of international experts assess climate change in this Fourth Assessment Report. The Report consists of three main volumes under the umbrella title *Climate Change 2007*, all available from Cambridge University Press:

Climate Change 2007 - The Physical Science Basis

Contribution of Working Group I to the Fourth Assessment Report of the IPCC
(ISBN 978 0521 88009-1 Hardback; 978 0521 70596-7 Paperback)

Climate Change 2007 - Impacts, Adaptation and Vulnerability

Contribution of Working Group II to the Fourth Assessment Report of the IPCC
(978 0521 88010-7 Hardback; 978 0521 70597-4 Paperback)

Climate Change 2007 - Mitigation of Climate Change

Contribution of Working Group III to the Fourth Assessment Report of the IPCC
(978 0521 88011-4 Hardback; 978 0521 70598-1 Paperback)

Climate Change 2007 - The Physical Science Basis is the most comprehensive and up-to-date scientific assessment of past, present and future climate change. The report provides:

- the most complete and quantitative assessment of how human activities are affecting the radiative energy balance in the atmosphere
- a more extensive assessment of changes observed throughout the climate system than ever before using the latest measurements covering the atmosphere, land surface, oceans, and snow, ice and frozen ground
- a detailed assessment of past climate change and its causes
- the first probabilistic assessment of climate model simulations and projections using detailed atmosphere-ocean coupled models from 18 modelling centres around the world
- a detailed assessment of climate change observations, modelling, and attribution for every continent

Simply put, this latest assessment of the IPCC will again form the standard scientific reference for all those concerned with climate change and its consequences, including students and researchers in environmental science, meteorology, climatology, biology, ecology and atmospheric chemistry, and policy makers in governments and industry worldwide.

From reviews of the Third Assessment Report – Climate Change 2001:

‘The detail is truly amazing ... invaluable works of reference ... no reference or science library should be without a set [of the IPCC volumes] ... unreservedly recommended to all readers.’

Journal of Meteorology

‘This well-edited set of three volumes will surely be the standard reference for nearly all arguments related with global warming and climate change in the next years. It should not be missing in the libraries of atmospheric and climate research institutes and those administrative and political institutions which have to deal with global change and sustainable development.’

Meteorologische Zeitschrift

‘... likely to remain a vital reference work until further research renders the details outdated by the time of the next survey ... another significant step forward in the understanding of the likely impacts of climate change on a global scale.’

International Journal of Climatology

‘The IPCC has conducted what is arguably the largest, most comprehensive and transparent study ever undertaken by mankind ... The result is a work of substance and authority, which only the foolish would deride.’

Wind Engineering

‘... the weight of evidence presented, the authority that IPCC commands and the breadth of view can hardly fail to impress and earn respect. Each of the volumes is essentially a remarkable work of reference, containing a plethora of information and copious bibliographies. There can be few natural scientists who will not want to have at least one of these volumes to hand on their bookshelves, at least until further research renders the details outdated by the time of the next survey.’

The Holocene

‘The subject is explored in great depth and should prove valuable to policy makers, researchers, analysts, and students.’

American Meteorological Society

From reviews of the Second Assessment Report – Climate Change 1995:

‘... essential reading for anyone interested in global environmental change, either past, present or future. ... These volumes have a deservedly high reputation’

Geological Magazine

‘... a tremendous achievement of coordinating the contributions of well over a thousand individuals to produce an authoritative, state-of-the-art review which will be of great value to decision-makers and the scientific community at large ... an indispensable reference.’

International Journal of Climatology

‘... a wealth of clear, well-organized information that is all in one place ... there is much to applaud.’

Environment International

Climate Change 2007

The Physical Science Basis

Edited by

Susan Solomon

Co-Chair,
IPCC Working Group I

Dahe Qin

Co-Chair,
IPCC Working Group I

Martin Manning

Head, Technical Support Unit
IPCC Working Group I

Melinda Marquis

Kristen Averyt

Melinda M.B. Tignor

Henry LeRoy Miller, Jr.

Technical Support Unit, IPCC Working Group I

Zhenlin Chen

China Meteorological Administration

Contribution of Working Group I
to the Fourth Assessment Report of the
Intergovernmental Panel on Climate Change

Published for the Intergovernmental Panel on Climate Change

 **CAMBRIDGE**
UNIVERSITY PRESS

CAMBRIDGE UNIVERSITY PRESS

Cambridge, New York, Melbourne, Madrid, Cape Town, Singapore, São Paulo, Delhi

Cambridge University Press

32 Avenue of the Americas, New York, NY 10013-2473, USA

www.cambridge.org

Information on this title: www.cambridge.org/9780521880091

© Intergovernmental Panel on Climate Change 2007

This publication is in copyright. Subject to statutory exception and to the provisions of relevant collective licensing agreements, no reproduction of any part may take place without the written permission of Cambridge University Press.

First published 2007

Printed in Canada by Friesens

A catalog record for this publication is available from the British Library.

ISBN 978-0-521-88009-1 hardback

ISBN 978-0-521-70596-7 paperback

Cambridge University Press has no responsibility for the persistence or accuracy of URLs for external or third-party Internet Web sites referred to in this publication and does not guarantee that any content on such Web sites is, or will remain, accurate or appropriate.

Please use the following reference to the whole report:

IPCC, 2007: *Climate Change 2007: The Physical Science Basis. Contribution of Working Group I to the Fourth Assessment Report of the Intergovernmental Panel on Climate Change* [Solomon, S., D. Qin, M. Manning, Z. Chen, M. Marquis, K.B. Averyt, M. Tignor and H.L. Miller (eds.)]. Cambridge University Press, Cambridge, United Kingdom and New York, NY, USA, 996 pp.

Cover photo:

The Blue Marble western and eastern hemispheres. These images integrate land, ocean, sea ice and clouds into a visual representation of the earth's climate system. They are based on space-borne earth observation data from NASA's MODIS (MODerate resolution Imaging Spectroradiometer) sensor aboard the TERRA and AQUA satellites. These images are part of the Blue Marble dataset which is freely available at <http://bluemarble.nasa.gov>. They are further documented in Stöckli, R., Vermote, E., Saleous, N., Simmon, R., and Herring, D. (2006). True color earth data set includes seasonal dynamics. EOS, 87(5):49, 55.

Foreword

Representing the first major global assessment of climate change science in six years, “Climate Change 2007 – The Physical Science Basis” has quickly captured the attention of both policymakers and the general public. The report confirms that our scientific understanding of the climate system and its sensitivity to greenhouse gas emissions is now richer and deeper than ever before. It also portrays a dynamic research sector that will provide ever greater insights into climate change over the coming years.

The rigor and credibility of this report owes much to the unique nature of the Intergovernmental Panel on Climate Change (IPCC). Established by the World Meteorological Organization and the United Nations Environment Programme in 1988, the IPCC is both an intergovernmental body and a network of the world’s leading climate change scientists and experts.

The chapters forming the bulk of this report describe scientists’ assessment of the state-of-knowledge in their respective fields. They were written by 152 coordinating lead authors and lead authors from over 30 countries and reviewed by over 600 experts. A large number of government reviewers also contributed review comments.

The Summary for Policymakers was approved by officials from 113 governments and represents their understanding – and their ownership – of the entire underlying report. It is this combination of expert and government review that constitutes the strength of the IPCC.

The IPCC does not conduct new research. Instead, its mandate is to make policy-relevant – as opposed to policy-prescriptive – assessments of the existing worldwide literature on the scientific, technical and socio-economic aspects of climate change. Its earlier assessment reports helped to inspire governments to adopt and implement the United Nations Framework Convention on Climate Change and the Kyoto Protocol. The current report will also be highly relevant as Governments consider their options for moving forward together to address the challenge of climate change.

Climate Change 2007 – the Physical Science Basis is the first volume of the IPCC’s Fourth Assessment Report. The second volume considers climate change impacts, vulnerabilities and adaptation options, while the third volume assesses the opportunities for and the costs of mitigation. A fourth volume provides a synthesis of the IPCC’s overall findings.

The Physical Science Basis was made possible by the commitment and voluntary labor of the world’s leading climate scientists. We would like to express our gratitude to all the Coordinating Lead Authors, Lead Authors, Contributing Authors, Review Editors and Reviewers. We would also like to thank the staff of the Working Group I Technical Support Unit and the IPCC Secretariat for their dedication in coordinating the production of another successful IPCC report.

Many Governments have supported the participation of their resident scientists in the IPCC process and contributed to the IPCC Trust Fund, thus also assuring the participation of experts from developing countries and countries with economies in transition. The governments of Italy, China, New Zealand and Norway hosted drafting sessions, while the Government of France hosted the final plenary that approved and accepted the report. The Government of the United States of America funded the Working Group I Technical Support Unit.

Finally, we would like to thank Dr R.K. Pachauri, Chairman of the IPCC, for his sound direction and tireless and able guidance of the IPCC, and Dr. Susan Solomon and Prof. Dahe Qin, the Co-Chairs of Working Group I, for their skillful leadership of Working Group I through the production of this report.



M. Jarraud
Secretary General
World Meteorological Organization



A. Steiner
Executive Director
United Nations Environment Programme

Preface

This Working Group I contribution to the IPCC's Fourth Assessment Report (AR4) provides a comprehensive assessment of the physical science of climate change and continues to broaden the view of that science, following on from previous Working Group I assessments. The results presented here are based on the extensive scientific literature that has become available since completion of the IPCC's Third Assessment Report, together with expanded data sets, new analyses, and more sophisticated climate modelling capabilities.

This report has been prepared in accordance with rules and procedures established by the IPCC and used for previous assessment reports. The report outline was agreed at the 21st Session of the Panel in November 2003 and the lead authors were accepted at the 31st Session of the IPCC Bureau in April 2004. Drafts prepared by the authors were subject to two rounds of review and revision during which over 30,000 written comments were submitted by over 650 individual experts as well as by governments and international organizations. Review Editors for each chapter have ensured that all substantive government and expert review comments received appropriate consideration. The Summary for Policymakers was approved line-by-line and the underlying chapters were then accepted at the 10th Session of IPCC Working Group I from 29 January to 1 February 2007.

Scope of the Report

The Working Group I report focuses on those aspects of the current understanding of the physical science of climate change that are judged to be most relevant to policymakers. It does not attempt to review the evolution of scientific understanding or to cover all of climate science. Furthermore, this assessment is based on the relevant scientific literature available to the authors in mid-2006 and the reader should recognize that some topics covered here may be subject to further rapid development.

A feature of recent climate change research is the breadth of observations now available for different components of the climate system, including the atmosphere, oceans, and cryosphere. Additional observations and new analyses have broadened our understanding and enabled many uncertainties to be reduced. New information has also led to some new questions in areas such as unanticipated changes in ice sheets, their potential effect on sea level rise, and the implications of complex interactions between climate change and biogeochemistry.

In considering future projections of climate change, this report follows decisions made by the Panel during the AR4 scoping and approval process to use emission scenarios that have been previously assessed by the IPCC for consistency across the three Working Groups. However, the value of information from new climate models related to climate stabilization has also been recognized. In order to address both topics, climate modelling groups have conducted climate simulations that included idealized experiments in which atmospheric composition is held constant. Together with climate model ensemble simulations, including many model runs for the 20th and 21st centuries, this assessment has been able to consider far more simulations than any previous assessment of climate change.

The IPCC assessment of the effects of climate change and of options for responding to or avoiding such effects, are assessed by Working Groups II and III and so are not covered here. In particular, while this Working Group I report presents results for a range of emission scenarios consistent with previous reports, an updated assessment of the plausible range of future emissions can only be conducted by Working Group III.

The Structure of this Report

This Working Group I assessment includes, for the first time, an introductory chapter, Chapter 1, which covers the ways in which climate change science has progressed, including an overview of the methods used in climate change science, the role of climate models and evolution in the treatment of uncertainties.

Chapters 2 and 7 cover the changes in atmospheric constituents (both gases and aerosols) that affect the radiative energy balance in the atmosphere and determine the Earth's climate. Chapter 2 presents a perspective based on observed change in the atmosphere and covers the central concept of radiative forcing. Chapter 7 complements this by considering the interactions between the biogeochemical cycles that affect atmospheric constituents and climate change, including aerosol/cloud interactions.

Chapters 3, 4 and 5 cover the extensive range of observations now available for the atmosphere and surface, for snow, ice and frozen ground, and for the oceans respectively. While observed changes in these components of the climate system are closely inter-related through physical processes, the separate chapters allow a more focused assessment of available data and their uncertainties, including remote sensing data from satellites. Chapter 5 includes observed changes in sea level, recognizing the strong interconnections between these and ocean heat content.

Chapter 6 presents a palaeoclimatic perspective and assesses the evidence for past climate change and the extent to which that is explained by our present scientific understanding. It includes a new assessment of reconstructed temperatures for the past 1300 years.

Chapter 8 covers the ways in which physical processes are simulated in climate models and the evaluation of models against observed climate, including its average state and variability. Chapter 9 covers the closely related issue of the extent to which observed climate change can be attributed to different causes, both natural and anthropogenic.

Chapter 10 covers the use of climate models for projections of global climate including their uncertainties. It shows results for different levels of future greenhouse gases, providing a probabilistic assessment of a range of physical climate system responses and the time scales and inertia associated with such responses. Chapter 11 covers regional climate change projections consistent with the global projections. It includes an assessment of model reliability at regional levels and the factors that can significantly influence regional scale climate change.

The Summary for Policymakers (SPM) and Technical Summary (TS) of this report follow a parallel structure and each includes cross references to the chapter and section where the material being summarized can be found in the underlying report. In this way these summary components of the report provide a road-map to the content of the entire report and the reader is encouraged to use the SPM and TS in that way.

An innovation in this report is the inclusion of 19 Frequently Asked Questions, in which the authors provide scientific answers to a range of general questions in a form that will be useful for a broad range of teaching purposes. Finally the report is accompanied by about 250 pages of supplementary material that was reviewed along with the chapter drafts and is made available on CDROM and in web-based versions of the report to provide an additional level of detail, such as results for individual climate models.

Some key policy-relevant questions and issues addressed in this report and the relevant chapters

Question	Chapters
How has the science of climate change advanced since the IPCC began?	1
What is known about the natural and anthropogenic agents that contribute to climate change, and the underlying processes that are involved?	2, 6, 7
How has climate been observed to change during the period of instrumental measurements?	3, 4, 5
What is known of palaeoclimatic changes, before the instrumental era, over time scales of hundreds to millions of years, and the processes that caused them?	6, 9
How well do we understand human and natural contributions to recent climate change, and how well can we simulate changes in climate using models?	8, 9
How is climate projected to change in the future, globally and regionally?	10, 11
What is known about past and projected changes in sea level, including the role of changes in glaciers and ice sheets?	4, 5, 6, 10
Are extremes such as heavy precipitation, droughts, and heat waves changing and why, and how are they expected to change in the future?	3, 5, 9, 10, 11

Acknowledgments

This assessment has benefited greatly from the very high degree of co-operation that exists within the international climate science community and its coordination by the World Meteorological Organization World Climate Research Program (WCRP) and the International Geosphere Biosphere Program (IGBP). In particular we wish to acknowledge the enormous commitment by the individuals and agencies of 14 climate modelling groups from around the world, as well as the archiving and distribution of an unprecedented amount (over 30 Terabytes) of climate model output by the Program for Climate Model Diagnosis and Intercomparison (PCMDI). This has enabled a more detailed comparison among current climate models and a more comprehensive assessment of the potential nature of long term climate change than ever before.

We must emphasise that this report has been entirely dependent on the expertise, hard work, and commitment to excellence shown throughout by our Coordinating Lead Authors and Lead Authors with important help by many Contributing Authors. In addition we would like to express our sincere appreciation of the work carried out by the expert reviewers and acknowledge the value of the very large number of constructive comments received. Our Review Editors have similarly played a critical role in assisting the authors to deal with these comments.

The Working Group I Bureau, Kansri Boonpragob, Filippo Giorgi, Bubu Jallow, Jean Jouzel, Maria Martelo and David Wratt have played the role of an editorial board in assisting with the selection of authors and with guiding the initial outline of the report. They have provided

constructive support to the Working Group Co-Chairs throughout for which we are very grateful.

Our sincere thanks go to the hosts and organizers of the four lead author meetings that were necessary for the preparation of the report and we gratefully acknowledge the support received from governments and agencies in Italy, China, New Zealand and Norway. The final Working Group I approval session was made possible by Mr Marc Gillet through the generosity of the government of France and the session was greatly facilitated by Francis Hayes, the WMO Conference Officer.

It is a pleasure to acknowledge the tireless work of the staff of the Working Group I Technical Support Unit, Melinda Marquis, Kristen Averyt, Melinda Tignor, Roy Miller, Tahl Kestin and Scott Longmore, who were ably assisted by Zhenlin Chen, Barbara Keppler, MaryAnn Pykkonen, Kyle Terran, Lelani Arris, and Marilyn Anderson. Graphics support and layout by Michael Shibao and Paula Megenhardt is gratefully appreciated. We thank Reto Stockli for kindly providing images of the Earth from space for the cover of this report. Assistance in helping the Co-Chairs to organize and edit the Frequently Asked Questions by David Wratt, David Fahey, and Susan Joy Hassol, is also appreciated. We should also like to thank Renate Christ, Secretary of the IPCC, and Secretariat staff Jian Liu, Rudie Bourgeois, Annie Courtin and Joelle Fernandez who provided logistical support for government liaison and travel of experts from developing countries and transitional economy countries.

Rajendra K. Pachauri
IPCC Chairman

Susan Solomon
IPCC WGI Co-Chair

Dahe Qin
IPCC WGI Co-Chair

Martin Manning
IPCC WGI TSU Head

Contents

Foreword	v
Preface	vii
Summary for Policymakers	1
Technical Summary	19
1 Historical Overview of Climate Change Science	93
2 Changes in Atmospheric Constituents and Radiative Forcing	129
3 Observations: Atmospheric Surface and Climate Change	235
4 Observations: Changes in Snow, Ice and Frozen Ground	337
5 Observations: Ocean Climate Change and Sea Level	385
6 Palaeoclimate	433
7 Coupling Between Changes in the Climate System and Biogeochemistry	499
8 Climate Models and their Evaluation	589
9 Understanding and Attributing Climate Change	663
10 Global Climate Projections	747
11 Regional Climate Projections	847
Annex I: Glossary	941
Annex II: Contributors to the IPCC WGI Fourth Assessment Report	955
Annex III: Reviewers of the IPCC WGI Fourth Assessment Report	969
Annex IV: Acronyms	981
Index	989

A report of Working Group I of the Intergovernmental Panel on Climate Change

Summary for Policymakers

Drafting Authors:

Richard B. Alley, Terje Berntsen, Nathaniel L. Bindoff, Zhenlin Chen, Amnat Chidthaisong, Pierre Friedlingstein, Jonathan M. Gregory, Gabriele C. Hegerl, Martin Heimann, Bruce Hewitson, Brian J. Hoskins, Fortunat Joos, Jean Jouzel, Vladimir Kattsov, Ulrike Lohmann, Martin Manning, Taroh Matsuno, Mario Molina, Neville Nicholls, Jonathan Overpeck, Dahe Qin, Graciela Raga, Venkatachalam Ramaswamy, Jiawen Ren, Matilde Rusticucci, Susan Solomon, Richard Somerville, Thomas F. Stocker, Peter A. Stott, Ronald J. Stouffer, Penny Whetton, Richard A. Wood, David Wratt

Draft Contributing Authors:

J. Arblaster, G. Brasseur, J.H. Christensen, K.L. Denman, D.W. Fahey, P. Forster, E. Jansen, P.D. Jones, R. Knutti, H. Le Treut, P. Lemke, G. Meehl, P. Mote, D.A. Randall, D.A. Stone, K.E. Trenberth, J. Willebrand, F. Zwiers

This Summary for Policymakers should be cited as:

IPCC, 2007: Summary for Policymakers. In: *Climate Change 2007: The Physical Science Basis. Contribution of Working Group I to the Fourth Assessment Report of the Intergovernmental Panel on Climate Change* [Solomon, S., D. Qin, M. Manning, Z. Chen, M. Marquis, K.B. Averyt, M. Tignor and H.L. Miller (eds.)]. Cambridge University Press, Cambridge, United Kingdom and New York, NY, USA.

Introduction

The Working Group I contribution to the IPCC Fourth Assessment Report describes progress in understanding of the human and natural drivers of climate change,¹ observed climate change, climate processes and attribution, and estimates of projected future climate change. It builds upon past IPCC assessments and incorporates new findings from the past six years of research. Scientific progress since the Third Assessment Report (TAR) is based upon large amounts of new and more comprehensive data, more sophisticated analyses of data, improvements in understanding of processes and their simulation in models and more extensive exploration of uncertainty ranges.

The basis for substantive paragraphs in this Summary for Policymakers can be found in the chapter sections specified in curly brackets.

Human and Natural Drivers of Climate Change

Changes in the atmospheric abundance of greenhouse gases and aerosols, in solar radiation and in land surface properties alter the energy balance of the climate system. These changes are expressed in terms of radiative forcing,² which is used to compare how a range of human and natural factors drive warming or cooling influences on global climate. Since the TAR, new observations and related modelling of greenhouse gases, solar activity, land surface properties and some aspects of aerosols have led to improvements in the quantitative estimates of radiative forcing.

Global atmospheric concentrations of carbon dioxide, methane and nitrous oxide have increased markedly as a result of human activities since 1750 and now far exceed pre-industrial values determined from ice cores spanning many thousands of years (see Figure SPM.1). The global increases in carbon dioxide concentration are due primarily to fossil fuel use and land use change, while those of methane and nitrous oxide are primarily due to agriculture. {2.3, 6.4, 7.3}

- Carbon dioxide is the most important anthropogenic greenhouse gas (see Figure SPM.2). The global atmospheric concentration of carbon dioxide has increased from a pre-industrial value of about 280 ppm to 379 ppm³ in 2005. The atmospheric concentration of carbon dioxide in 2005 exceeds by far the natural range over the last 650,000 years (180 to 300 ppm) as determined from ice cores. The annual carbon dioxide concentration growth rate was larger during the last 10 years (1995–2005 average: 1.9 ppm per year), than it has been since the beginning of continuous direct atmospheric measurements (1960–2005 average: 1.4 ppm per year) although there is year-to-year variability in growth rates. {2.3, 7.3}
- The primary source of the increased atmospheric concentration of carbon dioxide since the pre-industrial period results from fossil fuel use, with land-use change providing another significant but smaller contribution. Annual fossil carbon dioxide emissions⁴ increased from an average of 6.4 [6.0 to 6.8]⁵ GtC (23.5 [22.0 to 25.0] GtCO₂) per year in the 1990s to 7.2 [6.9 to 7.5] GtC (26.4 [25.3 to 27.5] GtCO₂) per year in 2000–2005 (2004 and 2005 data are interim estimates). Carbon dioxide emissions associated with land-use change

¹ *Climate change* in IPCC usage refers to any change in climate over time, whether due to natural variability or as a result of human activity. This usage differs from that in the United Nations Framework Convention on Climate Change, where climate change refers to a change of climate that is attributed directly or indirectly to human activity that alters the composition of the global atmosphere and that is in addition to natural climate variability observed over comparable time periods.

² *Radiative forcing* is a measure of the influence that a factor has in altering the balance of incoming and outgoing energy in the Earth-atmosphere system and is an index of the importance of the factor as a potential climate change mechanism. Positive forcing tends to warm the surface while negative forcing tends to cool it. In this report, radiative forcing values are for 2005 relative to pre-industrial conditions defined at 1750 and are expressed in watts per square metre (W m⁻²). See Glossary and Section 2.2 for further details.

³ ppm (parts per million) or ppb (parts per billion, 1 billion = 1,000 million) is the ratio of the number of greenhouse gas molecules to the total number of molecules of dry air. For example, 300 ppm means 300 molecules of a greenhouse gas per million molecules of dry air.

⁴ Fossil carbon dioxide emissions include those from the production, distribution and consumption of fossil fuels and as a by-product from cement production. An emission of 1 GtC corresponds to 3.67 GtCO₂.

⁵ In general, uncertainty ranges for results given in this Summary for Policymakers are 90% uncertainty intervals unless stated otherwise, that is, there is an estimated 5% likelihood that the value could be above the range given in square brackets and 5% likelihood that the value could be below that range. Best estimates are given where available. Assessed uncertainty intervals are not always symmetric about the corresponding best estimate. Note that a number of uncertainty ranges in the Working Group I TAR corresponded to 2 standard deviations (95%), often using expert judgement.

CHANGES IN GREENHOUSE GASES FROM ICE CORE AND MODERN DATA

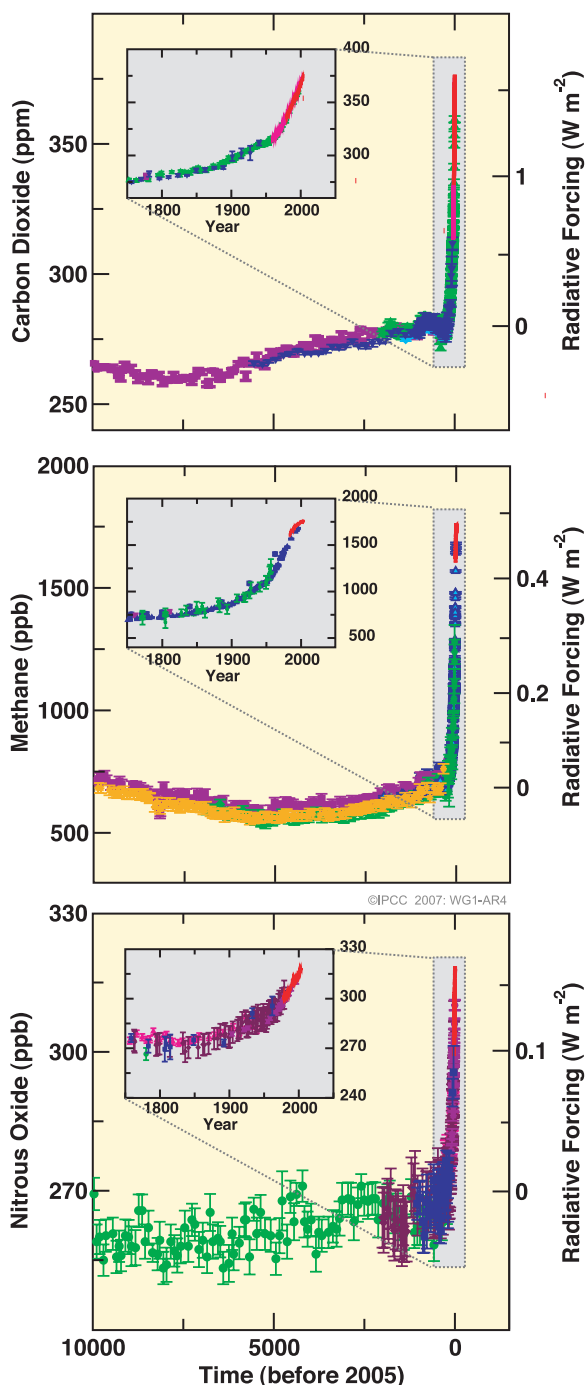


Figure SPM.1. Atmospheric concentrations of carbon dioxide, methane and nitrous oxide over the last 10,000 years (large panels) and since 1750 (inset panels). Measurements are shown from ice cores (symbols with different colours for different studies) and atmospheric samples (red lines). The corresponding radiative forcings are shown on the right hand axes of the large panels. {Figure 6.4}

are estimated to be 1.6 [0.5 to 2.7] GtC (5.9 [1.8 to 9.9] GtCO₂) per year over the 1990s, although these estimates have a large uncertainty. {7.3}

- The global atmospheric concentration of methane has increased from a pre-industrial value of about 715 ppb to 1732 ppb in the early 1990s, and was 1774 ppb in 2005. The atmospheric concentration of methane in 2005 exceeds by far the natural range of the last 650,000 years (320 to 790 ppb) as determined from ice cores. Growth rates have declined since the early 1990s, consistent with total emissions (sum of anthropogenic and natural sources) being nearly constant during this period. It is *very likely*⁶ that the observed increase in methane concentration is due to anthropogenic activities, predominantly agriculture and fossil fuel use, but relative contributions from different source types are not well determined. {2.3, 7.4}
- The global atmospheric nitrous oxide concentration increased from a pre-industrial value of about 270 ppb to 319 ppb in 2005. The growth rate has been approximately constant since 1980. More than a third of all nitrous oxide emissions are anthropogenic and are primarily due to agriculture. {2.3, 7.4}

The understanding of anthropogenic warming and cooling influences on climate has improved since the TAR, leading to *very high confidence*⁷ that the global average net effect of human activities since 1750 has been one of warming, with a radiative forcing of +1.6 [+0.6 to +2.4] W m⁻² (see Figure SPM.2). {2.3., 6.5, 2.9}

- The combined radiative forcing due to increases in carbon dioxide, methane, and nitrous oxide is +2.30 [+2.07 to +2.53] W m⁻², and its rate of increase during the industrial era is *very likely* to have been unprecedented in more than 10,000 years (see Figures

⁶ In this Summary for Policymakers, the following terms have been used to indicate the assessed likelihood, using expert judgement, of an outcome or a result: *Virtually certain* > 99% probability of occurrence, *Extremely likely* > 95%, *Very likely* > 90%, *Likely* > 66%, *More likely than not* > 50%, *Unlikely* < 33%, *Very unlikely* < 10%, *Extremely unlikely* < 5% (see Box TS.1 for more details).

⁷ In this Summary for Policymakers the following levels of confidence have been used to express expert judgements on the correctness of the underlying science: *very high confidence* represents at least a 9 out of 10 chance of being correct; *high confidence* represents about an 8 out of 10 chance of being correct (see Box TS.1)

SPM.1 and SPM.2). The carbon dioxide radiative forcing increased by 20% from 1995 to 2005, the largest change for any decade in at least the last 200 years. {2.3, 6.4}

- Anthropogenic contributions to aerosols (primarily sulphate, organic carbon, black carbon, nitrate and dust) together produce a cooling effect, with a total direct radiative forcing of -0.5 [-0.9 to -0.1] $W m^{-2}$ and an indirect cloud albedo forcing of -0.7 [-1.8 to -0.3] $W m^{-2}$. These forcings are now better understood than at the time of the TAR due to improved *in situ*, satellite and ground-based measurements and more

comprehensive modelling, but remain the dominant uncertainty in radiative forcing. Aerosols also influence cloud lifetime and precipitation. {2.4, 2.9, 7.5}

- Significant anthropogenic contributions to radiative forcing come from several other sources. Tropospheric ozone changes due to emissions of ozone-forming chemicals (nitrogen oxides, carbon monoxide, and hydrocarbons) contribute $+0.35$ [$+0.25$ to $+0.65$] $W m^{-2}$. The direct radiative forcing due to changes in halocarbons⁸ is $+0.34$ [$+0.31$ to $+0.37$] $W m^{-2}$. Changes in surface albedo, due to land cover changes and deposition of black carbon aerosols on snow, exert

RADIATIVE FORCING COMPONENTS

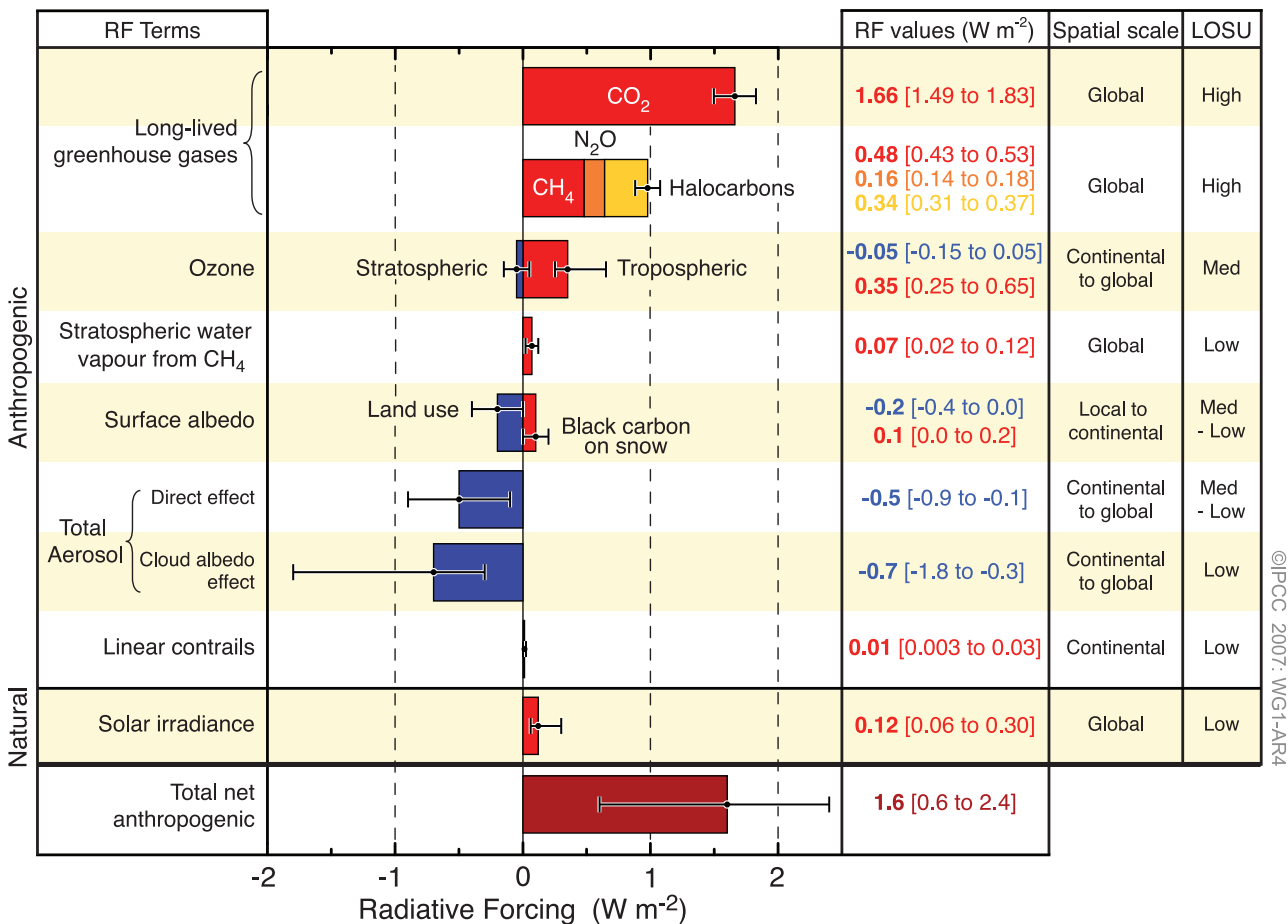


Figure SPM.2. Global average radiative forcing (RF) estimates and ranges in 2005 for anthropogenic carbon dioxide (CO_2), methane (CH_4), nitrous oxide (N_2O) and other important agents and mechanisms, together with the typical geographical extent (spatial scale) of the forcing and the assessed level of scientific understanding (LOSU). The net anthropogenic radiative forcing and its range are also shown. These require summing asymmetric uncertainty estimates from the component terms, and cannot be obtained by simple addition. Additional forcing factors not included here are considered to have a very low LOSU. Volcanic aerosols contribute an additional natural forcing but are not included in this figure due to their episodic nature. The range for linear contrails does not include other possible effects of aviation on cloudiness. {2.9, Figure 2.20}

⁸ Halocarbon radiative forcing has been recently assessed in detail in IPCC's Special Report on Safeguarding the Ozone Layer and the Global Climate System (2005).

respective forcings of -0.2 [-0.4 to 0.0] and $+0.1$ [0.0 to $+0.2$] W m^{-2} . Additional terms smaller than ± 0.1 W m^{-2} are shown in Figure SPM.2. {2.3, 2.5, 7.2}

- Changes in solar irradiance since 1750 are estimated to cause a radiative forcing of $+0.12$ [$+0.06$ to $+0.30$] W m^{-2} , which is less than half the estimate given in the TAR. {2.7}

Direct Observations of Recent Climate Change

Since the TAR, progress in understanding how climate is changing in space and in time has been gained through improvements and extensions of numerous datasets and data analyses, broader geographical coverage, better understanding of uncertainties, and a wider variety of measurements. Increasingly comprehensive observations are available for glaciers and snow cover since the 1960s, and for sea level and ice sheets since about the past decade. However, data coverage remains limited in some regions.

Warming of the climate system is unequivocal, as is now evident from observations of increases in global average air and ocean temperatures, widespread melting of snow and ice, and rising global average sea level (see Figure SPM.3). {3.2, 4.2, 5.5}

- Eleven of the last twelve years (1995–2006) rank among the 12 warmest years in the instrumental record of global surface temperature⁹ (since 1850). The updated 100-year linear trend (1906 to 2005) of 0.74°C [0.56°C to 0.92°C] is therefore larger than the corresponding trend for 1901 to 2000 given in the TAR of 0.6°C [0.4°C to 0.8°C]. The linear warming trend over the last 50 years (0.13°C [0.10°C to 0.16°C] per decade) is nearly twice that for the last 100 years. The total temperature increase from 1850–1899 to 2001–2005 is 0.76°C [0.57°C to 0.95°C]. Urban heat island effects are real but local, and have a negligible influence (less than 0.006°C per decade over land and zero over the oceans) on these values. {3.2}
- New analyses of balloon-borne and satellite measurements of lower- and mid-tropospheric temperature show warming rates that are similar to those of the surface temperature record and are consistent within their respective uncertainties, largely reconciling a discrepancy noted in the TAR. {3.2, 3.4}
- The average atmospheric water vapour content has increased since at least the 1980s over land and ocean as well as in the upper troposphere. The increase is broadly consistent with the extra water vapour that warmer air can hold. {3.4}
- Observations since 1961 show that the average temperature of the global ocean has increased to depths of at least 3000 m and that the ocean has been absorbing more than 80% of the heat added to the climate system. Such warming causes seawater to expand, contributing to sea level rise (see Table SPM.1). {5.2, 5.5}
- Mountain glaciers and snow cover have declined on average in both hemispheres. Widespread decreases in glaciers and ice caps have contributed to sea level rise (ice caps do not include contributions from the Greenland and Antarctic Ice Sheets). (See Table SPM.1.) {4.6, 4.7, 4.8, 5.5}
- New data since the TAR now show that losses from the ice sheets of Greenland and Antarctica have *very likely* contributed to sea level rise over 1993 to 2003 (see Table SPM.1). Flow speed has increased for some Greenland and Antarctic outlet glaciers, which drain ice from the interior of the ice sheets. The corresponding increased ice sheet mass loss has often followed thinning, reduction or loss of ice shelves or loss of floating glacier tongues. Such dynamical ice loss is sufficient to explain most of the Antarctic net mass loss and approximately half of the Greenland net mass loss. The remainder of the ice loss from Greenland has occurred because losses due to melting have exceeded accumulation due to snowfall. {4.6, 4.8, 5.5}
- Global average sea level rose at an average rate of 1.8 [1.3 to 2.3] mm per year over 1961 to 2003. The rate was faster over 1993 to 2003: about 3.1 [2.4 to 3.8] mm per year. Whether the faster rate for 1993 to 2003 reflects decadal variability or an increase in the longer-term trend is unclear. There is *high confidence* that

⁹ The average of near-surface air temperature over land and sea surface temperature.

CHANGES IN TEMPERATURE, SEA LEVEL AND NORTHERN HEMISPHERE SNOW COVER

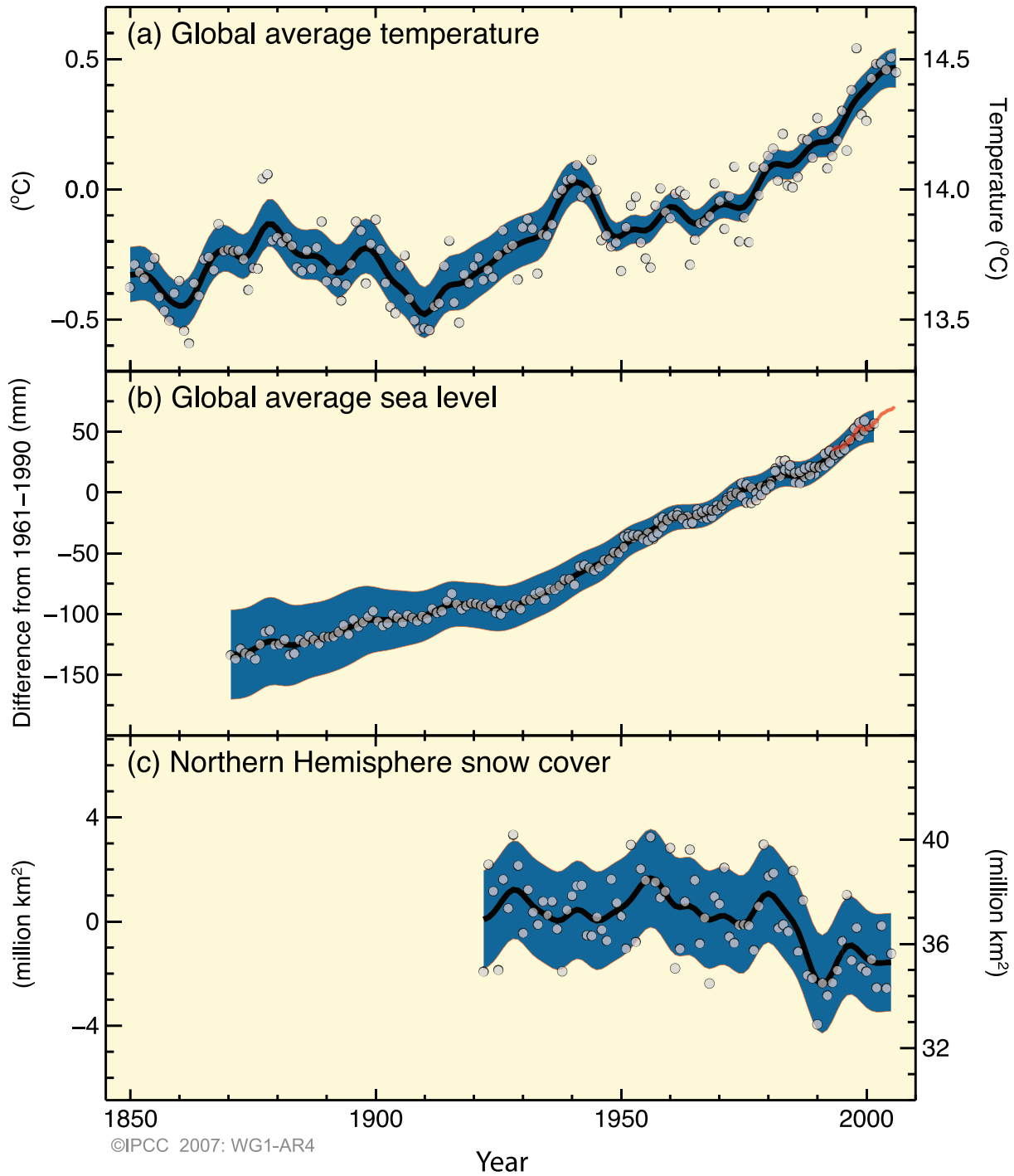


Figure SPM.3. Observed changes in (a) global average surface temperature, (b) global average sea level from tide gauge (blue) and satellite (red) data and (c) Northern Hemisphere snow cover for March–April. All changes are relative to corresponding averages for the period 1961–1990. Smoothed curves represent decadal average values while circles show yearly values. The shaded areas are the uncertainty intervals estimated from a comprehensive analysis of known uncertainties (a and b) and from the time series (c). {FAQ 3.1, Figure 1, Figure 4.2, Figure 5.13}

the rate of observed sea level rise increased from the 19th to the 20th century. The total 20th-century rise is estimated to be 0.17 [0.12 to 0.22] m. {5.5}

- For 1993 to 2003, the sum of the climate contributions is consistent within uncertainties with the total sea level rise that is directly observed (see Table SPM.1). These estimates are based on improved satellite and *in situ* data now available. For the period 1961 to 2003, the sum of climate contributions is estimated to be smaller than the observed sea level rise. The TAR reported a similar discrepancy for 1910 to 1990. {5.5}

At continental, regional and ocean basin scales, numerous long-term changes in climate have been observed. These include changes in arctic temperatures and ice, widespread changes in precipitation amounts, ocean salinity, wind patterns and aspects of extreme weather including droughts, heavy precipitation, heat waves and the intensity of tropical cyclones.¹⁰ {3.2, 3.3, 3.4, 3.5, 3.6, 5.2}

- Average arctic temperatures increased at almost twice the global average rate in the past 100 years. Arctic temperatures have high decadal variability, and a warm period was also observed from 1925 to 1945. {3.2}

- Satellite data since 1978 show that annual average arctic sea ice extent has shrunk by 2.7 [2.1 to 3.3]% per decade, with larger decreases in summer of 7.4 [5.0 to 9.8]% per decade. These values are consistent with those reported in the TAR. {4.4}

- Temperatures at the top of the permafrost layer have generally increased since the 1980s in the Arctic (by up to 3°C). The maximum area covered by seasonally frozen ground has decreased by about 7% in the Northern Hemisphere since 1900, with a decrease in spring of up to 15%. {4.7}

- Long-term trends from 1900 to 2005 have been observed in precipitation amount over many large regions.¹¹ Significantly increased precipitation has been observed in eastern parts of North and South America, northern Europe and northern and central Asia. Drying has been observed in the Sahel, the Mediterranean, southern Africa and parts of southern Asia. Precipitation is highly variable spatially and temporally, and data are limited in some regions. Long-term trends have not been observed for the other large regions assessed.¹¹ {3.3, 3.9}

- Changes in precipitation and evaporation over the oceans are suggested by freshening of mid- and high-latitude waters together with increased salinity in low-latitude waters. {5.2}

Table SPM.1. Observed rate of sea level rise and estimated contributions from different sources. {5.5, Table 5.3}

Source of sea level rise	Rate of sea level rise (mm per year)	
	1961–2003	1993–2003
Thermal expansion	0.42 ± 0.12	1.6 ± 0.5
Glaciers and ice caps	0.50 ± 0.18	0.77 ± 0.22
Greenland Ice Sheet	0.05 ± 0.12	0.21 ± 0.07
Antarctic Ice Sheet	0.14 ± 0.41	0.21 ± 0.35
Sum of individual climate contributions to sea level rise	1.1 ± 0.5	2.8 ± 0.7
Observed total sea level rise	1.8 ± 0.5 ^a	3.1 ± 0.7 ^a
Difference (Observed minus sum of estimated climate contributions)	0.7 ± 0.7	0.3 ± 1.0

Table note:

^a Data prior to 1993 are from tide gauges and after 1993 are from satellite altimetry.

¹⁰ Tropical cyclones include hurricanes and typhoons.

¹¹ The assessed regions are those considered in the regional projections chapter of the TAR and in Chapter 11 of this report.

- Mid-latitude westerly winds have strengthened in both hemispheres since the 1960s. {3.5}
- More intense and longer droughts have been observed over wider areas since the 1970s, particularly in the tropics and subtropics. Increased drying linked with higher temperatures and decreased precipitation has contributed to changes in drought. Changes in sea surface temperatures, wind patterns and decreased snowpack and snow cover have also been linked to droughts. {3.3}
- The frequency of heavy precipitation events has increased over most land areas, consistent with warming and observed increases of atmospheric water vapour. {3.8, 3.9}
- Widespread changes in extreme temperatures have been observed over the last 50 years. Cold days, cold nights and frost have become less frequent, while hot days, hot nights and heat waves have become more frequent (see Table SPM.2). {3.8}

Table SPM.2. Recent trends, assessment of human influence on the trend and projections for extreme weather events for which there is an observed late-20th century trend. {Tables 3.7, 3.8, 9.4; Sections 3.8, 5.5, 9.7, 11.2–11.9}

Phenomenon ^a and direction of trend	Likelihood that trend occurred in late 20th century (typically post 1960)	Likelihood of a human contribution to observed trend ^b	Likelihood of future trends based on projections for 21st century using SRES scenarios
Warmer and fewer cold days and nights over most land areas	<i>Very likely^c</i>	<i>Likely^d</i>	<i>Virtually certain^d</i>
Warmer and more frequent hot days and nights over most land areas	<i>Very likely^e</i>	<i>Likely (nights)^d</i>	<i>Virtually certain^d</i>
Warm spells/heat waves. Frequency increases over most land areas	<i>Likely</i>	<i>More likely than not^f</i>	<i>Very likely</i>
Heavy precipitation events. Frequency (or proportion of total rainfall from heavy falls) increases over most areas	<i>Likely</i>	<i>More likely than not^f</i>	<i>Very likely</i>
Area affected by droughts increases	<i>Likely in many regions since 1970s</i>	<i>More likely than not</i>	<i>Likely</i>
Intense tropical cyclone activity increases	<i>Likely in some regions since 1970</i>	<i>More likely than not^f</i>	<i>Likely</i>
Increased incidence of extreme high sea level (excludes tsunamis) ^g	<i>Likely</i>	<i>More likely than not^{f,h}</i>	<i>Likelyⁱ</i>

Table notes:

^a See Table 3.7 for further details regarding definitions.

^b See Table TS.4, Box TS.5 and Table 9.4.

^c Decreased frequency of cold days and nights (coldest 10%).

^d Warming of the most extreme days and nights each year.

^e Increased frequency of hot days and nights (hottest 10%).

^f Magnitude of anthropogenic contributions not assessed. Attribution for these phenomena based on expert judgement rather than formal attribution studies.

^g Extreme high sea level depends on average sea level and on regional weather systems. It is defined here as the highest 1% of hourly values of observed sea level at a station for a given reference period.

^h Changes in observed extreme high sea level closely follow the changes in average sea level. {5.5} It is *very likely* that anthropogenic activity contributed to a rise in average sea level. {9.5}

ⁱ In all scenarios, the projected global average sea level at 2100 is higher than in the reference period. {10.6} The effect of changes in regional weather systems on sea level extremes has not been assessed.

- There is observational evidence for an increase in intense tropical cyclone activity in the North Atlantic since about 1970, correlated with increases of tropical sea surface temperatures. There are also suggestions of increased intense tropical cyclone activity in some other regions where concerns over data quality are greater. Multi-decadal variability and the quality of the tropical cyclone records prior to routine satellite observations in about 1970 complicate the detection of long-term trends in tropical cyclone activity. There is no clear trend in the annual numbers of tropical cyclones. {3.8}

Some aspects of climate have not been observed to change. {3.2, 3.8, 4.4, 5.3}

- A decrease in diurnal temperature range (DTR) was reported in the TAR, but the data available then extended only from 1950 to 1993. Updated observations reveal that DTR has not changed from 1979 to 2004 as both day- and night-time temperature have risen at about the same rate. The trends are highly variable from one region to another. {3.2}
- Antarctic sea ice extent continues to show interannual variability and localised changes but no statistically significant average trends, consistent with the lack of warming reflected in atmospheric temperatures averaged across the region. {3.2, 4.4}
- There is insufficient evidence to determine whether trends exist in the meridional overturning circulation (MOC) of the global ocean or in small-scale phenomena such as tornadoes, hail, lightning and dust-storms. {3.8, 5.3}

A Palaeoclimatic Perspective

Palaeoclimatic studies use changes in climatically sensitive indicators to infer past changes in global climate on time scales ranging from decades to millions of years. Such proxy data (e.g., tree ring width) may be influenced by both local temperature and other factors such as precipitation, and are often representative of particular seasons rather than full years. Studies since the TAR draw increased confidence from additional data showing coherent behaviour across multiple indicators in different parts of the world. However, uncertainties generally increase with time into the past due to increasingly limited spatial coverage.

Palaeoclimatic information supports the interpretation that the warmth of the last half century is unusual in at least the previous 1,300 years. The last time the polar regions were significantly warmer than present for an extended period (about 125,000 years ago), reductions in polar ice volume led to 4 to 6 m of sea level rise. {6.4, 6.6}

- Average Northern Hemisphere temperatures during the second half of the 20th century were *very likely* higher than during any other 50-year period in the last 500 years and *likely* the highest in at least the past 1,300 years. Some recent studies indicate greater variability in Northern Hemisphere temperatures than suggested in the TAR, particularly finding that cooler periods existed in the 12th to 14th, 17th and 19th centuries. Warmer periods prior to the 20th century are within the uncertainty range given in the TAR. {6.6}
- Global average sea level in the last interglacial period (about 125,000 years ago) was *likely* 4 to 6 m higher than during the 20th century, mainly due to the retreat of polar ice. Ice core data indicate that average polar temperatures at that time were 3°C to 5°C higher than present, because of differences in the Earth's orbit. The Greenland Ice Sheet and other arctic ice fields *likely* contributed no more than 4 m of the observed sea level rise. There may also have been a contribution from Antarctica. {6.4}

Understanding and Attributing Climate Change

This assessment considers longer and improved records, an expanded range of observations and improvements in the simulation of many aspects of climate and its variability based on studies since the TAR. It also considers the results of new attribution studies that have evaluated whether observed changes are quantitatively consistent with the expected response to external forcings and inconsistent with alternative physically plausible explanations.

Most of the observed increase in global average temperatures since the mid-20th century is *very likely* due to the observed increase in anthropogenic greenhouse gas concentrations.¹² This is an advance since the TAR's conclusion that "most of the observed warming over the last 50 years is *likely* to have been due to the increase in greenhouse gas concentrations". Discernible human influences now extend to other aspects of climate, including ocean warming, continental-average temperatures, temperature extremes and wind patterns (see Figure SPM.4 and Table SPM.2). {9.4, 9.5}

- It is *likely* that increases in greenhouse gas concentrations alone would have caused more warming than observed because volcanic and anthropogenic aerosols have offset some warming that would otherwise have taken place. {2.9, 7.5, 9.4}
- The observed widespread warming of the atmosphere and ocean, together with ice mass loss, support the conclusion that it is *extremely unlikely* that global climate change of the past 50 years can be explained without external forcing, and *very likely* that it is not due to known natural causes alone. {4.8, 5.2, 9.4, 9.5, 9.7}
- Warming of the climate system has been detected in changes of surface and atmospheric temperatures in the upper several hundred metres of the ocean, and in contributions to sea level rise. Attribution studies have established anthropogenic contributions to all of these changes. The observed pattern of tropospheric warming and stratospheric cooling is *very likely* due to the combined influences of greenhouse gas increases and stratospheric ozone depletion. {3.2, 3.4, 9.4, 9.5}
- It is *likely* that there has been significant anthropogenic warming over the past 50 years averaged over each continent except Antarctica (see Figure SPM.4). The observed patterns of warming, including greater warming over land than over the ocean, and their changes over time, are only simulated by models that include anthropogenic forcing. The ability of coupled climate models to simulate the observed temperature evolution on each of six continents provides stronger evidence of human influence on climate than was available in the TAR. {3.2, 9.4}
- Difficulties remain in reliably simulating and attributing observed temperature changes at smaller scales. On these scales, natural climate variability is relatively larger, making it harder to distinguish changes expected due to external forcings. Uncertainties in local forcings and feedbacks also make it difficult to estimate the contribution of greenhouse gas increases to observed small-scale temperature changes. {8.3, 9.4}
- Anthropogenic forcing is *likely* to have contributed to changes in wind patterns,¹³ affecting extra-tropical storm tracks and temperature patterns in both hemispheres. However, the observed changes in the Northern Hemisphere circulation are larger than simulated in response to 20th-century forcing change. {3.5, 3.6, 9.5, 10.3}
- Temperatures of the most extreme hot nights, cold nights and cold days are *likely* to have increased due to anthropogenic forcing. It is *more likely than not* that anthropogenic forcing has increased the risk of heat waves (see Table SPM.2). {9.4}

¹² Consideration of remaining uncertainty is based on current methodologies.

¹³ In particular, the Southern and Northern Annular Modes and related changes in the North Atlantic Oscillation. {3.6, 9.5, Box TS.2}

GLOBAL AND CONTINENTAL TEMPERATURE CHANGE

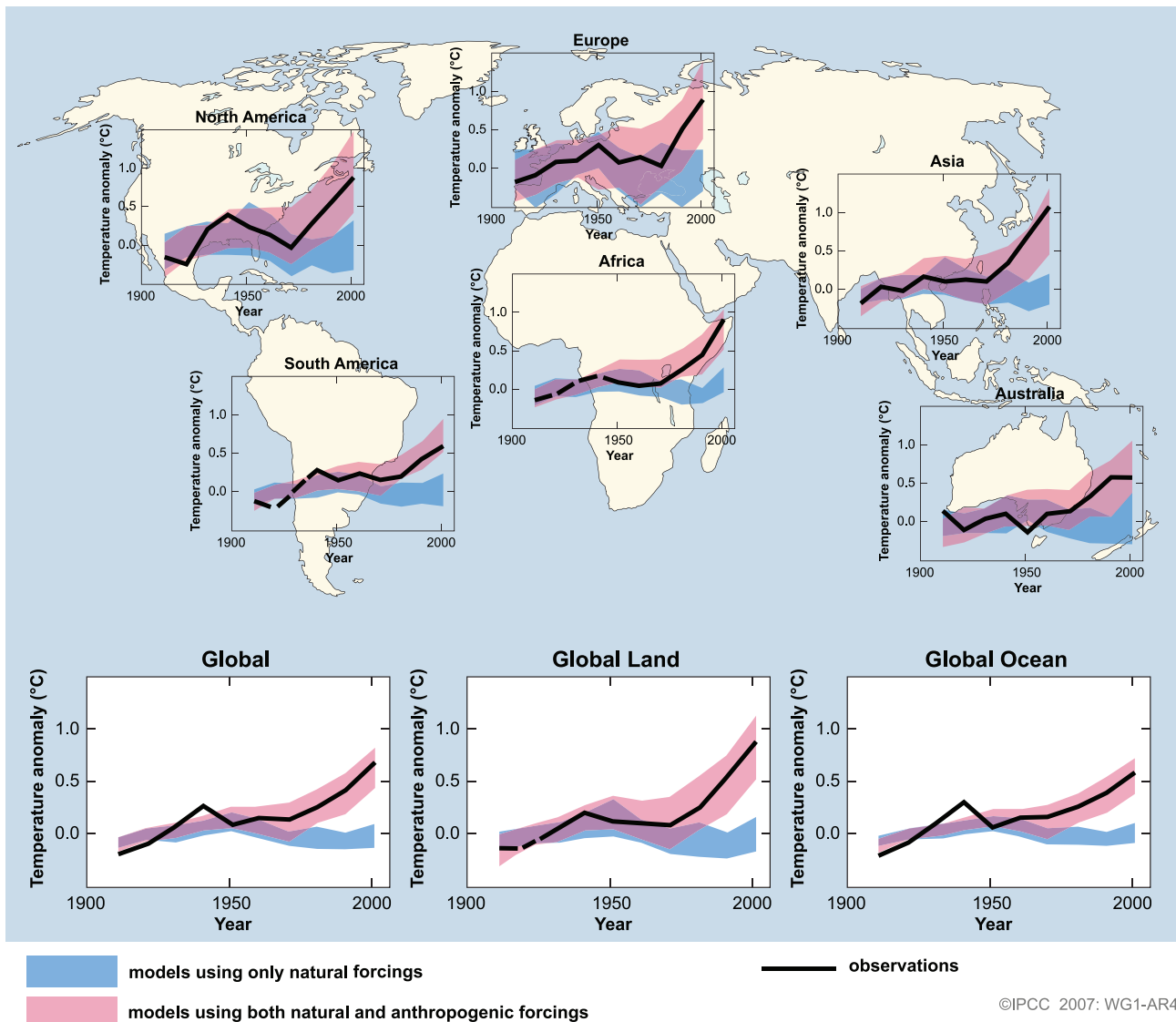


Figure SPM.4. Comparison of observed continental- and global-scale changes in surface temperature with results simulated by climate models using natural and anthropogenic forcings. Decadal averages of observations are shown for the period 1906 to 2005 (black line) plotted against the centre of the decade and relative to the corresponding average for 1901–1950. Lines are dashed where spatial coverage is less than 50%. Blue shaded bands show the 5–95% range for 19 simulations from five climate models using only the natural forcings due to solar activity and volcanoes. Red shaded bands show the 5–95% range for 58 simulations from 14 climate models using both natural and anthropogenic forcings. {FAQ 9.2, Figure 1}

Analysis of climate models together with constraints from observations enables an assessed *likely* range to be given for climate sensitivity for the first time and provides increased confidence in the understanding of the climate system response to radiative forcing. {6.6, 8.6, 9.6, Box 10.2}

- The equilibrium climate sensitivity is a measure of the climate system response to sustained radiative forcing. It is not a projection but is defined as the global average surface warming following a doubling of carbon dioxide concentrations. It is *likely* to be in the range 2°C to 4.5°C with a best estimate of about 3°C, and is *very unlikely* to be less than 1.5°C. Values substantially higher than 4.5°C cannot be excluded, but agreement of models with observations is not as good for those values. Water vapour changes represent the largest feedback affecting climate sensitivity and are now better understood than in the TAR. Cloud feedbacks remain the largest source of uncertainty. {8.6, 9.6, Box 10.2}
- It is *very unlikely* that climate changes of at least the seven centuries prior to 1950 were due to variability generated within the climate system alone. A significant fraction of the reconstructed Northern Hemisphere inter-decadal temperature variability over those centuries is *very likely* attributable to volcanic eruptions and changes in solar irradiance, and it is *likely* that anthropogenic forcing contributed to the early 20th-century warming evident in these records. {2.7, 2.8, 6.6, 9.3}

Projections of Future Changes in Climate

A major advance of this assessment of climate change projections compared with the TAR is the large number of simulations available from a broader range of models. Taken together with additional information from observations, these provide a quantitative basis for estimating likelihoods for many aspects of future climate change. Model simulations cover a range of possible futures including idealised emission or concentration assumptions. These include SRES¹⁴ illustrative marker scenarios for the 2000 to 2100 period and model experiments with greenhouse gases and aerosol concentrations held constant after year 2000 or 2100.

For the next two decades, a warming of about 0.2°C per decade is projected for a range of SRES emission scenarios. Even if the concentrations of all greenhouse gases and aerosols had been kept constant at year 2000 levels, a further warming of about 0.1°C per decade would be expected. {10.3, 10.7}

- Since IPCC's first report in 1990, assessed projections have suggested global average temperature increases between about 0.15°C and 0.3°C per decade for 1990 to 2005. This can now be compared with observed values of about 0.2°C per decade, strengthening confidence in near-term projections. {1.2, 3.2}
- Model experiments show that even if all radiative forcing agents were held constant at year 2000 levels, a further warming trend would occur in the next two decades at a rate of about 0.1°C per decade, due mainly to the slow response of the oceans. About twice as much warming (0.2°C per decade) would be expected if emissions are within the range of the SRES scenarios. Best-estimate projections from models indicate that decadal average warming over each inhabited continent by 2030 is insensitive to the choice among SRES scenarios and is *very likely* to be at least twice as large as the corresponding model-estimated natural variability during the 20th century. {9.4, 10.3, 10.5, 11.2–11.7, Figure TS-29}

¹⁴ SRES refers to the *IPCC Special Report on Emission Scenarios* (2000). The SRES scenario families and illustrative cases, which did not include additional climate initiatives, are summarised in a box at the end of this Summary for Policymakers. Approximate carbon dioxide equivalent concentrations corresponding to the computed radiative forcing due to anthropogenic greenhouse gases and aerosols in 2100 (see p. 823 of the TAR) for the SRES B1, A1T, B2, A1B, A2 and A1FI illustrative marker scenarios are about 600, 700, 800, 850, 1250 and 1,550 ppm respectively. Scenarios B1, A1B and A2 have been the focus of model intercomparison studies and many of those results are assessed in this report.

Continued greenhouse gas emissions at or above current rates would cause further warming and induce many changes in the global climate system during the 21st century that would *very likely* be larger than those observed during the 20th century. {10.3}

- Advances in climate change modelling now enable best estimates and *likely* assessed uncertainty ranges to be given for projected warming for different emission scenarios. Results for different emission scenarios are provided explicitly in this report to avoid loss of this policy-relevant information. Projected global average surface warmings for the end of the 21st century (2090–2099) relative to 1980–1999 are shown in Table SPM.3. These illustrate the differences between lower and higher SRES emission scenarios, and the projected warming uncertainty associated with these scenarios. {10.5}
- Best estimates and *likely* ranges for global average surface air warming for six SRES emissions marker scenarios are given in this assessment and are shown in Table SPM.3. For example, the best estimate for the low scenario (B1) is 1.8°C (*likely* range is 1.1°C to 2.9°C), and the best estimate for the high scenario (A1FI) is 4.0°C (*likely* range is 2.4°C to 6.4°C). Although these projections are broadly consistent with the span quoted in the TAR (1.4°C to 5.8°C), they are not directly comparable (see Figure SPM.5). The Fourth Assessment Report is more advanced as it provides best estimates and an assessed likelihood range for each of the marker scenarios. The new assessment of the *likely* ranges now relies on a larger number of climate models of increasing complexity and realism, as well as new information regarding the nature of feedbacks from the carbon cycle and constraints on climate response from observations. {10.5}
- Warming tends to reduce land and ocean uptake of atmospheric carbon dioxide, increasing the fraction of anthropogenic emissions that remains in the atmosphere. For the A2 scenario, for example, the climate-carbon cycle feedback increases the corresponding global average warming at 2100 by more than 1°C. Assessed upper ranges for temperature projections are larger than in the TAR (see Table SPM.3) mainly because the broader range of models now available suggests stronger climate-carbon cycle feedbacks. {7.3, 10.5}
- Model-based projections of global average sea level rise at the end of the 21st century (2090–2099) are shown in Table SPM.3. For each scenario, the midpoint of the range in Table SPM.3 is within 10% of the

Table SPM.3. Projected global average surface warming and sea level rise at the end of the 21st century. {10.5, 10.6, Table 10.7}

Case	Temperature Change (°C at 2090-2099 relative to 1980-1999) ^a		Sea Level Rise (m at 2090-2099 relative to 1980-1999)
	Best estimate	<i>Likely</i> range	Model-based range excluding future rapid dynamical changes in ice flow
Constant Year 2000 concentrations ^b	0.6	0.3 – 0.9	NA
B1 scenario	1.8	1.1 – 2.9	0.18 – 0.38
A1T scenario	2.4	1.4 – 3.8	0.20 – 0.45
B2 scenario	2.4	1.4 – 3.8	0.20 – 0.43
A1B scenario	2.8	1.7 – 4.4	0.21 – 0.48
A2 scenario	3.4	2.0 – 5.4	0.23 – 0.51
A1FI scenario	4.0	2.4 – 6.4	0.26 – 0.59

Table notes:

^a These estimates are assessed from a hierarchy of models that encompass a simple climate model, several Earth System Models of Intermediate Complexity and a large number of Atmosphere-Ocean General Circulation Models (AOGCMs).

^b Year 2000 constant composition is derived from AOGCMs only.

MULTI-MODEL AVERAGES AND ASSESSED RANGES FOR SURFACE WARMING

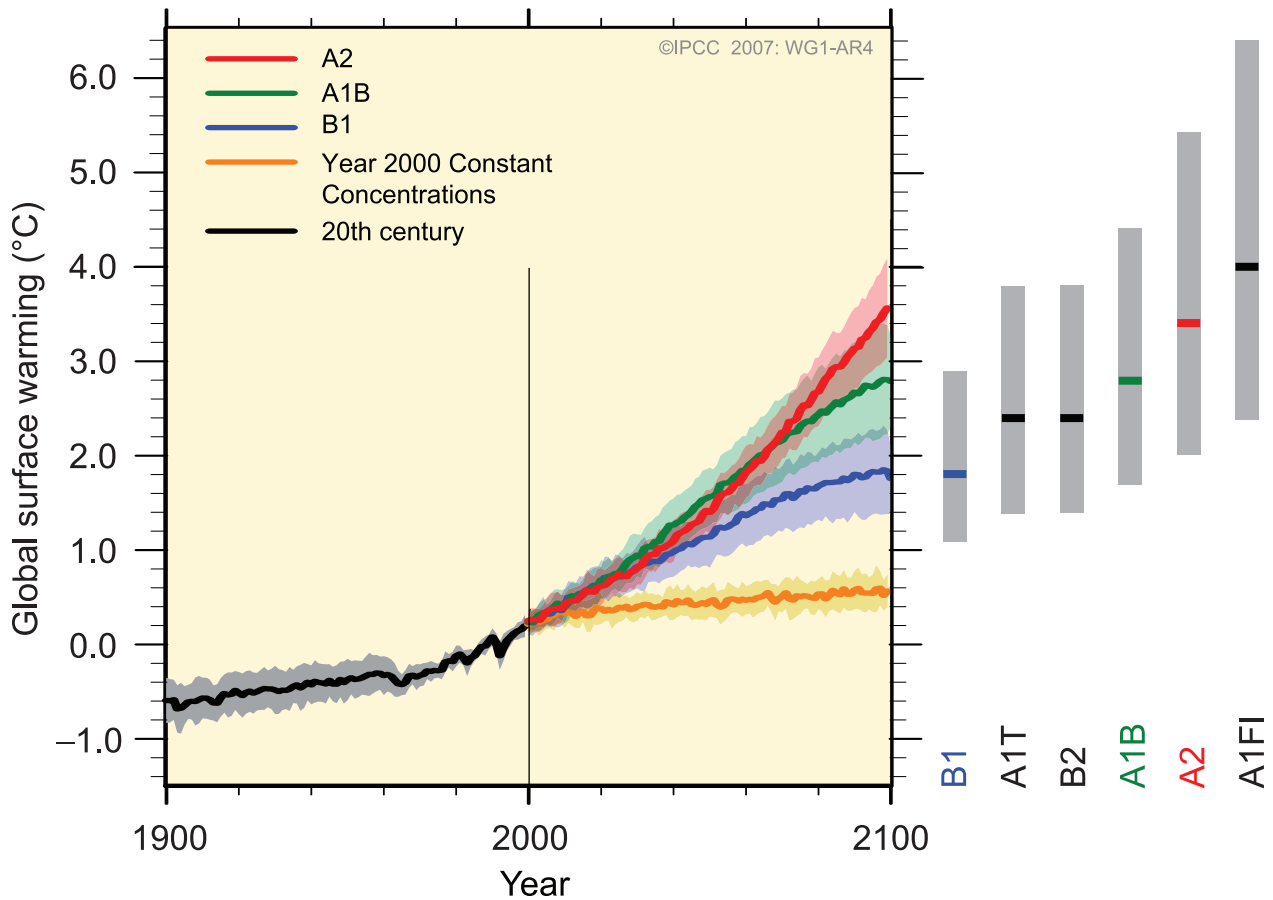


Figure SPM.5. Solid lines are multi-model global averages of surface warming (relative to 1980–1999) for the scenarios A2, A1B and B1, shown as continuations of the 20th century simulations. Shading denotes the ± 1 standard deviation range of individual model annual averages. The orange line is for the experiment where concentrations were held constant at year 2000 values. The grey bars at right indicate the best estimate (solid line within each bar) and the **likely** range assessed for the six SRES marker scenarios. The assessment of the best estimate and **likely** ranges in the grey bars includes the AOGCMs in the left part of the figure, as well as results from a hierarchy of independent models and observational constraints. {Figures 10.4 and 10.29}

TAR model average for 2090–2099. The ranges are narrower than in the TAR mainly because of improved information about some uncertainties in the projected contributions.¹⁵ {10.6}

- Models used to date do not include uncertainties in climate-carbon cycle feedback nor do they include the full effects of changes in ice sheet flow, because a basis in published literature is lacking. The projections include a contribution due to increased ice flow from Greenland and Antarctica at the rates observed for 1993 to 2003, but these flow rates could increase or decrease in the future. For example, if this contribution were to grow linearly with global average temperature change,

the upper ranges of sea level rise for SRES scenarios shown in Table SPM.3 would increase by 0.1 to 0.2 m. Larger values cannot be excluded, but understanding of these effects is too limited to assess their likelihood or provide a best estimate or an upper bound for sea level rise. {10.6}

- Increasing atmospheric carbon dioxide concentrations lead to increasing acidification of the ocean. Projections based on SRES scenarios give reductions in average global surface ocean pH¹⁶ of between 0.14 and 0.35 units over the 21st century, adding to the present decrease of 0.1 units since pre-industrial times. {5.4, Box 7.3, 10.4}

¹⁵ TAR projections were made for 2100, whereas projections in this report are for 2090–2099. The TAR would have had similar ranges to those in Table SPM.3 if it had treated the uncertainties in the same way.

¹⁶ Decreases in pH correspond to increases in acidity of a solution. See Glossary for further details.

There is now higher confidence in projected patterns of warming and other regional-scale features, including changes in wind patterns, precipitation and some aspects of extremes and of ice. {8.2, 8.3, 8.4, 8.5, 9.4, 9.5, 10.3, 11.1}

- Projected warming in the 21st century shows scenario-independent geographical patterns similar to those observed over the past several decades. Warming is expected to be greatest over land and at most high northern latitudes, and least over the Southern Ocean and parts of the North Atlantic Ocean (see Figure SPM.6). {10.3}
- Snow cover is projected to contract. Widespread increases in thaw depth are projected over most permafrost regions. {10.3, 10.6}
- Sea ice is projected to shrink in both the Arctic and Antarctic under all SRES scenarios. In some projections, arctic late-summer sea ice disappears almost entirely by the latter part of the 21st century. {10.3}
- It is *very likely* that hot extremes, heat waves and heavy precipitation events will continue to become more frequent. {10.3}
- Based on a range of models, it is *likely* that future tropical cyclones (typhoons and hurricanes) will become more intense, with larger peak wind speeds and more heavy precipitation associated with ongoing increases of tropical sea surface temperatures. There is less confidence in projections of a global decrease in numbers of tropical cyclones. The apparent increase in the proportion of very intense storms since 1970 in some regions is much larger than simulated by current models for that period. {9.5, 10.3, 3.8}

PROJECTIONS OF SURFACE TEMPERATURES

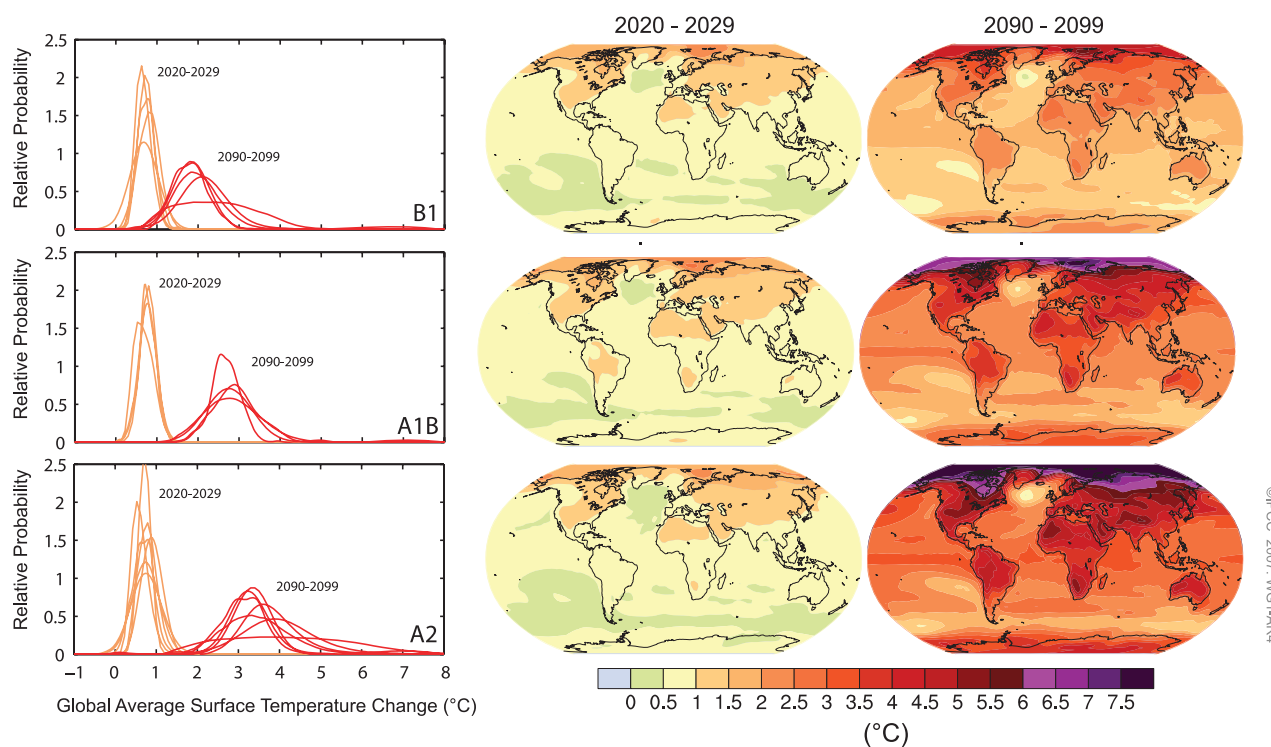


Figure SPM.6. Projected surface temperature changes for the early and late 21st century relative to the period 1980–1999. The central and right panels show the AOGCM multi-model average projections for the B1 (top), A1B (middle) and A2 (bottom) SRES scenarios averaged over the decades 2020–2029 (centre) and 2090–2099 (right). The left panels show corresponding uncertainties as the relative probabilities of estimated global average warming from several different AOGCM and Earth System Model of Intermediate Complexity studies for the same periods. Some studies present results only for a subset of the SRES scenarios, or for various model versions. Therefore the difference in the number of curves shown in the left-hand panels is due only to differences in the availability of results. {Figures 10.8 and 10.28}

PROJECTED PATTERNS OF PRECIPITATION CHANGES

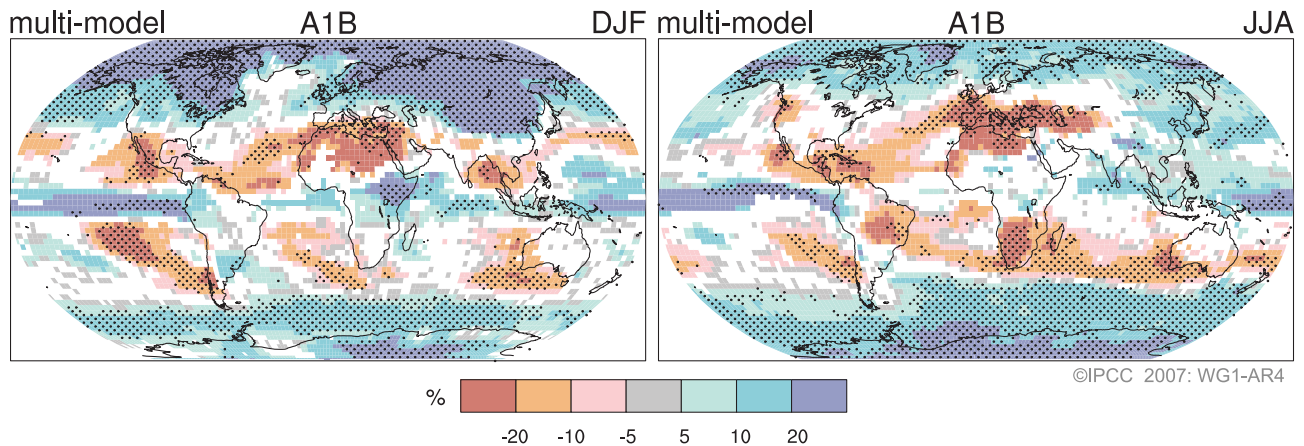


Figure SPM.7. Relative changes in precipitation (in percent) for the period 2090–2099, relative to 1980–1999. Values are multi-model averages based on the SRES A1B scenario for December to February (left) and June to August (right). White areas are where less than 66% of the models agree in the sign of the change and stippled areas are where more than 90% of the models agree in the sign of the change. {Figure 10.9}

- Extratropical storm tracks are projected to move poleward, with consequent changes in wind, precipitation and temperature patterns, continuing the broad pattern of observed trends over the last half-century. {3.6, 10.3}
 - Since the TAR, there is an improving understanding of projected patterns of precipitation. Increases in the amount of precipitation are *very likely* in high latitudes, while decreases are *likely* in most subtropical land regions (by as much as about 20% in the A1B scenario in 2100, see Figure SPM.7), continuing observed patterns in recent trends. {3.3, 8.3, 9.5, 10.3, 11.2 to 11.9}
 - Based on current model simulations, it is *very likely* that the meridional overturning circulation (MOC) of the Atlantic Ocean will slow down during the 21st century. The multi-model average reduction by 2100 is 25% (range from zero to about 50%) for SRES emission scenario A1B. Temperatures in the Atlantic region are projected to increase despite such changes due to the much larger warming associated with projected increases in greenhouse gases. It is *very unlikely* that the MOC will undergo a large abrupt transition during the 21st century. Longer-term changes in the MOC cannot be assessed with confidence. {10.3, 10.7}
- Anthropogenic warming and sea level rise would continue for centuries due to the time scales associated with climate processes and feedbacks, even if greenhouse gas concentrations were to be stabilised. {10.4, 10.5, 10.7}**
- Climate-carbon cycle coupling is expected to add carbon dioxide to the atmosphere as the climate system warms, but the magnitude of this feedback is uncertain. This increases the uncertainty in the trajectory of carbon dioxide emissions required to achieve a particular stabilisation level of atmospheric carbon dioxide concentration. Based on current understanding of climate-carbon cycle feedback, model studies suggest that to stabilise at 450 ppm carbon dioxide could require that cumulative emissions over the 21st century be reduced from an average of approximately 670 [630 to 710] GtC (2460 [2310 to 2600] GtCO₂) to approximately 490 [375 to 600] GtC (1800 [1370 to 2200] GtCO₂). Similarly, to stabilise at 1000 ppm, this feedback could require that cumulative emissions be reduced from a model average of approximately 1415 [1340 to 1490] GtC (5190 [4910 to 5460] GtCO₂) to approximately 1100 [980 to 1250] GtC (4030 [3590 to 4580] GtCO₂). {7.3, 10.4}

- If radiative forcing were to be stabilised in 2100 at B1 or A1B levels¹⁴ a further increase in global average temperature of about 0.5°C would still be expected, mostly by 2200. {10.7}
- If radiative forcing were to be stabilised in 2100 at A1B levels¹⁴, thermal expansion alone would lead to 0.3 to 0.8 m of sea level rise by 2300 (relative to 1980–1999). Thermal expansion would continue for many centuries, due to the time required to transport heat into the deep ocean. {10.7}
- Contraction of the Greenland Ice Sheet is projected to continue to contribute to sea level rise after 2100. Current models suggest that ice mass losses increase with temperature more rapidly than gains due to precipitation and that the surface mass balance becomes negative at a global average warming (relative to pre-industrial values) in excess of 1.9°C to 4.6°C. If a negative surface mass balance were sustained for millennia, that would lead to virtually complete elimination of the Greenland Ice Sheet and a resulting contribution to sea level rise of about 7 m. The corresponding future temperatures in Greenland are comparable to those inferred for the last interglacial period 125,000 years ago, when palaeoclimatic information suggests reductions of polar land ice extent and 4 to 6 m of sea level rise. {6.4, 10.7}
- Dynamical processes related to ice flow not included in current models but suggested by recent observations could increase the vulnerability of the ice sheets to warming, increasing future sea level rise. Understanding of these processes is limited and there is no consensus on their magnitude. {4.6, 10.7}
- Current global model studies project that the Antarctic Ice Sheet will remain too cold for widespread surface melting and is expected to gain in mass due to increased snowfall. However, net loss of ice mass could occur if dynamical ice discharge dominates the ice sheet mass balance. {10.7}
- Both past and future anthropogenic carbon dioxide emissions will continue to contribute to warming and sea level rise for more than a millennium, due to the time scales required for removal of this gas from the atmosphere. {7.3, 10.3}

THE EMISSION SCENARIOS OF THE IPCC SPECIAL REPORT ON EMISSION SCENARIOS (SRES)¹⁷

A1. The A1 storyline and scenario family describes a future world of very rapid economic growth, global population that peaks in mid-century and declines thereafter, and the rapid introduction of new and more efficient technologies. Major underlying themes are convergence among regions, capacity building and increased cultural and social interactions, with a substantial reduction in regional differences in per capita income. The A1 scenario family develops into three groups that describe alternative directions of technological change in the energy system. The three A1 groups are distinguished by their technological emphasis: fossil-intensive (A1FI), non-fossil energy sources (A1T) or a balance across all sources (A1B) (where balanced is defined as not relying too heavily on one particular energy source, on the assumption that similar improvement rates apply to all energy supply and end use technologies).

A2. The A2 storyline and scenario family describes a very heterogeneous world. The underlying theme is self-reliance and preservation of local identities. Fertility patterns across regions converge very slowly, which results in continuously increasing population. Economic development is primarily regionally oriented and per capita economic growth and technological change more fragmented and slower than other storylines.

B1. The B1 storyline and scenario family describes a convergent world with the same global population, that peaks in mid-century and declines thereafter, as in the A1 storyline, but with rapid change in economic structures toward a service and information economy, with reductions in material intensity and the introduction of clean and resource-efficient technologies. The emphasis is on global solutions to economic, social and environmental sustainability, including improved equity, but without additional climate initiatives.

B2. The B2 storyline and scenario family describes a world in which the emphasis is on local solutions to economic, social and environmental sustainability. It is a world with continuously increasing global population, at a rate lower than A2, intermediate levels of economic development, and less rapid and more diverse technological change than in the B1 and A1 storylines. While the scenario is also oriented towards environmental protection and social equity, it focuses on local and regional levels.

An illustrative scenario was chosen for each of the six scenario groups A1B, A1FI, A1T, A2, B1 and B2. All should be considered equally sound.

The SRES scenarios do not include additional climate initiatives, which means that no scenarios are included that explicitly assume implementation of the United Nations Framework Convention on Climate Change or the emissions targets of the Kyoto Protocol.

¹⁷ Emission scenarios are not assessed in this Working Group I Report of the IPCC. This box summarising the SRES scenarios is taken from the TAR and has been subject to prior line-by-line approval by the Panel.

A report accepted by Working Group I of the Intergovernmental Panel on Climate Change but not approved in detail

“Acceptance” of IPCC Reports at a Session of the Working Group or Panel signifies that the material has not been subject to line-by-line discussion and agreement, but nevertheless presents a comprehensive, objective and balanced view of the subject matter.

Technical Summary

Coordinating Lead Authors:

Susan Solomon (USA), Dahe Qin (China), Martin Manning (USA, New Zealand)

Lead Authors:

Richard B. Alley (USA), Terje Berntsen (Norway), Nathaniel L. Bindoff (Australia), Zhenlin Chen (China), Amnat Chidthaisong (Thailand), Jonathan M. Gregory (UK), Gabriele C. Hegerl (USA, Germany), Martin Heimann (Germany, Switzerland), Bruce Hewitson (South Africa), Brian J. Hoskins (UK), Fortunat Joos (Switzerland), Jean Jouzel (France), Vladimir Kattsov (Russia), Ulrike Lohmann (Switzerland), Taroh Matsuno (Japan), Mario Molina (USA, Mexico), Neville Nicholls (Australia), Jonathan Overpeck (USA), Graciela Raga (Mexico, Argentina), Venkatachalam Ramaswamy (USA), Jiawen Ren (China), Matilde Rusticucci (Argentina), Richard Somerville (USA), Thomas F. Stocker (Switzerland), Ronald J. Stouffer (USA), Penny Whetton (Australia), Richard A. Wood (UK), David Wratt (New Zealand)

Contributing Authors:

J. Arblaster (USA, Australia), G. Brasseur (USA, Germany), J.H. Christensen (Denmark), K.L. Denman (Canada), D.W. Fahey (USA), P. Forster (UK), J. Haywood (UK), E. Jansen (Norway), P.D. Jones (UK), R. Knutti (Switzerland), H. Le Treut (France), P. Lemke (Germany), G. Meehl (USA), D. Randall (USA), D.A. Stone (UK, Canada), K.E. Trenberth (USA), J. Willebrand (Germany), F. Zwiers (Canada)

Review Editors:

Kansri Boonpragob (Thailand), Filippo Giorgi (Italy), Bubu Pateh Jallow (The Gambia)

This Technical Summary should be cited as:

Solomon, S., D. Qin, M. Manning, R.B. Alley, T. Berntsen, N.L. Bindoff, Z. Chen, A. Chidthaisong, J.M. Gregory, G.C. Hegerl, M. Heimann, B. Hewitson, B.J. Hoskins, F. Joos, J. Jouzel, V. Kattsov, U. Lohmann, T. Matsuno, M. Molina, N. Nicholls, J. Overpeck, G. Raga, V. Ramaswamy, J. Ren, M. Rusticucci, R. Somerville, T.F. Stocker, P. Whetton, R.A. Wood and D. Wratt, 2007: Technical Summary. In: *Climate Change 2007: The Physical Science Basis. Contribution of Working Group I to the Fourth Assessment Report of the Intergovernmental Panel on Climate Change* [Solomon, S., D. Qin, M. Manning, Z. Chen, M. Marquis, K.B. Averyt, M. Tignor and H.L. Miller (eds.)]. Cambridge University Press, Cambridge, United Kingdom and New York, NY, USA.

Table of Contents

TS.1 Introduction	21	TS.4 Understanding and Attributing Climate Change	58
TS.2 Changes in Human and Natural Drivers of Climate	21	TS.4.1 Advances in Attribution of Changes in Global-Scale Temperature in the Instrumental Period: Atmosphere, Ocean and Ice	58
Box TS.1: Treatment of Uncertainties in the Working Group I Assessment	22	Box TS.7: Evaluation of Atmosphere–Ocean General Circulation Models	59
TS.2.1 Greenhouse Gases	23	TS.4.2 Attribution of Spatial and Temporal Changes in Temperature.....	62
TS.2.2 Aerosols.....	29	TS.4.3 Attribution of Changes in Circulation, Precipitation and Other Climate Variables	64
TS.2.3 Aviation Contrails and Cirrus, Land Use and Other Effects	30	TS.4.4 Palaeoclimate Studies of Attribution	64
TS.2.4 Radiative Forcing Due to Solar Activity and Volcanic Eruptions	30	TS.4.5 Climate Response to Radiative Forcing.....	64
TS.2.5 Net Global Radiative Forcing, Global Warming Potentials and Patterns of Forcing	31	TS.5 Projections of Future Changes in Climate	66
TS.2.6 Surface Forcing and the Hydrologic Cycle	35	Box TS.8: Hierarchy of Global Climate Models	67
TS.3 Observations of Changes in Climate	35	TS.5.1 Understanding Near-Term Climate Change	68
TS.3.1 Atmospheric Changes: Instrumental Record	35	Box TS.9: Committed Climate Change.....	68
Box TS.2: Patterns (Modes) of Climate Variability	39	TS.5.2 Large-Scale Projections for the 21st Century	69
TS.3.2 Changes in the Cryosphere: Instrumental Record	43	TS.5.3 Regional-Scale Projections	74
Box TS.3: Ice Sheet Dynamics and Stability.....	44	Box TS.10: Regional Downscaling	74
TS.3.3 Changes in the Ocean: Instrumental Record	47	TS.5.4 Coupling Between Climate Change and Changes in Biogeochemical Cycles.....	77
Box TS.4: Sea Level.....	51	TS.5.5 Implications of Climate Processes and their Time Scales for Long-Term Projections.....	79
TS.3.4 Consistency Among Observations	51	TS.6 Robust Findings and Key Uncertainties	81
Box TS.5: Extreme Weather Events.....	53	TS.6.1 Changes in Human and Natural Drivers of Climate	81
TS.3.5 A Palaeoclimatic Perspective	54	TS.6.2 Observations of Changes in Climate.....	82
Box TS.6: Orbital Forcing.....	56	TS.6.3 Understanding and Attributing Climate Change	86
		TS.6.4 Projections of Future Changes in Climate	87

TS.1 Introduction

In the six years since the IPCC's Third Assessment Report (TAR), significant progress has been made in understanding past and recent climate change and in projecting future changes. These advances have arisen from large amounts of new data, more sophisticated analyses of data, improvements in the understanding and simulation of physical processes in climate models and more extensive exploration of uncertainty ranges in model results. The increased confidence in climate science provided by these developments is evident in this Working Group I contribution to the IPCC's Fourth Assessment Report.

While this report provides new and important policy-relevant information on the scientific understanding of climate change, the complexity of the climate system and the multiple interactions that determine its behaviour impose limitations on our ability to understand fully the future course of Earth's global climate. There is still an incomplete physical understanding of many components of the climate system and their role in climate change. Key uncertainties include aspects of the roles played by clouds, the cryosphere, the oceans, land use and couplings between climate and biogeochemical cycles. The areas of science covered in this report continue to undergo rapid progress and it should be recognised that the present assessment reflects scientific understanding based on the peer-reviewed literature available in mid-2006.

The key findings of the IPCC Working Group I assessment are presented in the Summary for Policymakers. This Technical Summary provides a more detailed overview of the scientific basis for those findings and provides a road map to the chapters of the underlying report. It focuses on key findings, highlighting what is new since the TAR. The structure of the Technical Summary is as follows:

- Section 2: an overview of current scientific understanding of the natural and anthropogenic drivers of changes in climate;
- Section 3: an overview of observed changes in the climate system (including the atmosphere, oceans and cryosphere) and their relationships to physical processes;
- Section 4: an overview of explanations of observed climate changes based on climate models and physical

understanding, the extent to which climate change can be attributed to specific causes and a new evaluation of climate sensitivity to greenhouse gas increases;

- Section 5: an overview of projections for both near- and far-term climate changes including the time scales of responses to changes in forcing, and probabilistic information about future climate change; and
- Section 6: a summary of the most robust findings and the key uncertainties in current understanding of physical climate change science.

Each paragraph in the Technical Summary reporting substantive results is followed by a reference in curly brackets to the corresponding chapter section(s) of the underlying report where the detailed assessment of the scientific literature and additional information can be found.

TS.2 Changes in Human and Natural Drivers of Climate

The Earth's global mean climate is determined by incoming energy from the Sun and by the properties of the Earth and its atmosphere, namely the reflection, absorption and emission of energy within the atmosphere and at the surface. Although changes in received solar energy (e.g., caused by variations in the Earth's orbit around the Sun) inevitably affect the Earth's energy budget, the properties of the atmosphere and surface are also important and these may be affected by climate feedbacks. The importance of climate feedbacks is evident in the nature of past climate changes as recorded in ice cores up to 650,000 years old.

Changes have occurred in several aspects of the atmosphere and surface that alter the global energy budget of the Earth and can therefore cause the climate to change. Among these are increases in greenhouse gas concentrations that act primarily to increase the atmospheric absorption of outgoing radiation, and increases in aerosols (microscopic airborne particles or droplets) that act to reflect and absorb incoming solar radiation and change cloud radiative properties. Such changes cause a radiative forcing of the climate system.¹ Forcing agents can differ considerably from one another in terms of the magnitudes of forcing, as well as spatial and temporal features. Positive and negative radiative forcings contribute to increases and decreases, respectively, in

¹ 'Radiative forcing' is a measure of the influence a factor has in altering the balance of incoming and outgoing energy in the Earth-atmosphere system and is an index of the importance of the factor as a potential climate change mechanism. Positive forcing tends to warm the surface while negative forcing tends to cool it. In this report, radiative forcing values are for changes relative to a pre-industrial background at 1750, are expressed in Watts per square metre ($W m^{-2}$) and, unless otherwise noted, refer to a global and annual average value. See Glossary for further details.

Box TS.1: Treatment of Uncertainties in the Working Group I Assessment

The importance of consistent and transparent treatment of uncertainties is clearly recognised by the IPCC in preparing its assessments of climate change. The increasing attention given to formal treatments of uncertainty in previous assessments is addressed in Section 1.6. To promote consistency in the general treatment of uncertainty across all three Working Groups, authors of the Fourth Assessment Report have been asked to follow a brief set of guidance notes on determining and describing uncertainties in the context of an assessment.² This box summarises the way that Working Group I has applied those guidelines and covers some aspects of the treatment of uncertainty specific to material assessed here.

Uncertainties can be classified in several different ways according to their origin. Two primary types are ‘value uncertainties’ and ‘structural uncertainties’. Value uncertainties arise from the incomplete determination of particular values or results, for example, when data are inaccurate or not fully representative of the phenomenon of interest. Structural uncertainties arise from an incomplete understanding of the processes that control particular values or results, for example, when the conceptual framework or model used for analysis does not include all the relevant processes or relationships. Value uncertainties are generally estimated using statistical techniques and expressed probabilistically. Structural uncertainties are generally described by giving the authors’ collective judgment of their confidence in the correctness of a result. In both cases, estimating uncertainties is intrinsically about describing the limits to knowledge and for this reason involves expert judgment about the state of that knowledge. A different type of uncertainty arises in systems that are either chaotic or not fully deterministic in nature and this also limits our ability to project all aspects of climate change.

The scientific literature assessed here uses a variety of other generic ways of categorising uncertainties. Uncertainties associated with ‘random errors’ have the characteristic of decreasing as additional measurements are accumulated, whereas those associated with ‘systematic errors’ do not. In dealing with climate records, considerable attention has been given to the identification of systematic errors or unintended biases arising from data sampling issues and methods of analysing and combining data. Specialised statistical methods based on quantitative analysis have been developed for the detection and attribution of climate change and for producing probabilistic projections of future climate parameters. These are summarised in the relevant chapters.

The uncertainty guidance provided for the Fourth Assessment Report draws, for the first time, a careful distinction between levels of confidence in scientific understanding and the likelihoods of specific results. This allows authors to express high confidence that an event is extremely unlikely (e.g., rolling a dice twice and getting a six both times), as well as high confidence that an event is about as likely as not (e.g., a tossed coin coming up heads). Confidence and likelihood as used here are distinct concepts but are often linked in practice.

The standard terms used to define levels of confidence in this report are as given in the IPCC Uncertainty Guidance Note, namely:

Confidence Terminology	Degree of confidence in being correct
<i>Very high confidence</i>	At least 9 out of 10 chance
<i>High confidence</i>	About 8 out of 10 chance
<i>Medium confidence</i>	About 5 out of 10 chance
<i>Low confidence</i>	About 2 out of 10 chance
<i>Very low confidence</i>	Less than 1 out of 10 chance

Note that ‘low confidence’ and ‘very low confidence’ are only used for areas of major concern and where a risk-based perspective is justified.

Chapter 2 of this report uses a related term ‘level of scientific understanding’ when describing uncertainties in different contributions to radiative forcing. This terminology is used for consistency with the Third Assessment Report, and the basis on which the authors have determined particular levels of scientific understanding uses a combination of approaches consistent with the uncertainty guidance note as explained in detail in Section 2.9.2 and Table 2.11.

(continued)

² The IPCC Uncertainty Guidance Note is included in Supplementary Material for this report.

The standard terms used in this report to define the likelihood of an outcome or result where this can be estimated probabilistically are:

Likelihood Terminology	Likelihood of the occurrence/ outcome
<i>Virtually certain</i>	> 99% probability
<i>Extremely likely</i>	> 95% probability
<i>Very likely</i>	> 90% probability
<i>Likely</i>	> 66% probability
<i>More likely than not</i>	> 50% probability
<i>About as likely as not</i>	33 to 66% probability
<i>Unlikely</i>	< 33% probability
<i>Very unlikely</i>	< 10% probability
<i>Extremely unlikely</i>	< 5% probability
<i>Exceptionally unlikely</i>	< 1% probability

The terms ‘extremely likely’, ‘extremely unlikely’ and ‘more likely than not’ as defined above have been added to those given in the IPCC Uncertainty Guidance Note in order to provide a more specific assessment of aspects including attribution and radiative forcing.

Unless noted otherwise, values given in this report are assessed best estimates and their uncertainty ranges are 90% confidence intervals (i.e., there is an estimated 5% likelihood of the value being below the lower end of the range or above the upper end of the range). Note that in some cases the nature of the constraints on a value, or other information available, may indicate an asymmetric distribution of the uncertainty range around a best estimate. In such cases, the uncertainty range is given in square brackets following the best estimate.

global average surface temperature. This section updates the understanding of estimated anthropogenic and natural radiative forcings.

The overall response of global climate to radiative forcing is complex due to a number of positive and negative feedbacks that can have a strong influence on the climate system (see e.g., Sections 4.5 and 5.4). Although water vapour is a strong greenhouse gas, its concentration in the atmosphere changes in response to changes in surface climate and this must be treated as a feedback effect and not as a radiative forcing. This section also summarises changes in the surface energy budget and its links to the hydrological cycle. Insights into the effects of agents such as aerosols on precipitation are also noted.

TS.2.1 Greenhouse Gases

The dominant factor in the radiative forcing of climate in the industrial era is the increasing concentration of various greenhouse gases in the atmosphere. Several of the major greenhouse gases occur naturally but increases in their atmospheric concentrations over the last 250 years are due largely to human activities. Other greenhouse gases are entirely the result of human activities. The contribution of each greenhouse gas to radiative forcing

over a particular period of time is determined by the change in its concentration in the atmosphere over that period and the effectiveness of the gas in perturbing the radiative balance. Current atmospheric concentrations of the different greenhouse gases considered in this report vary by more than eight orders of magnitude (factor of 10^8), and their radiative efficiencies vary by more than four orders of magnitude (factor of 10^4), reflecting the enormous diversity in their properties and origins.

The current concentration of a greenhouse gas in the atmosphere is the net result of the history of its past emissions and removals from the atmosphere. The gases and aerosols considered here are emitted to the atmosphere by human activities or are formed from precursor species emitted to the atmosphere. These emissions are offset by chemical and physical removal processes. With the important exception of carbon dioxide (CO_2), it is generally the case that these processes remove a specific fraction of the amount of a gas in the atmosphere each year and the inverse of this removal rate gives the mean lifetime for that gas. In some cases, the removal rate may vary with gas concentration or other atmospheric properties (e.g., temperature or background chemical conditions).

Long-lived greenhouse gases (LLGHGs), for example, CO_2 , methane (CH_4) and nitrous oxide (N_2O), are

chemically stable and persist in the atmosphere over time scales of a decade to centuries or longer, so that their emission has a long-term influence on climate. Because these gases are long lived, they become well mixed throughout the atmosphere much faster than they are removed and their global concentrations can be accurately estimated from data at a few locations. Carbon dioxide does not have a specific lifetime because it is continuously cycled between the atmosphere, oceans and land biosphere and its net removal from the atmosphere involves a range of processes with different time scales.

Short-lived gases (e.g., sulphur dioxide and carbon monoxide) are chemically reactive and generally removed by natural oxidation processes in the atmosphere, by removal at the surface or by washout in precipitation; their concentrations are hence highly variable. Ozone is a significant greenhouse gas that is formed and destroyed by chemical reactions involving other species in the atmosphere. In the troposphere, the human influence on ozone occurs primarily through changes in precursor gases that lead to its formation, whereas in the stratosphere, the human influence has been primarily through changes in ozone removal rates caused by chlorofluorocarbons (CFCs) and other ozone-depleting substances.

TS.2.1.1 Changes in Atmospheric Carbon Dioxide, Methane and Nitrous Oxide

Current concentrations of atmospheric CO₂ and CH₄ far exceed pre-industrial values found in polar ice core records of atmospheric composition dating back 650,000 years. Multiple lines of evidence confirm that the post-industrial rise in these gases does not stem from natural mechanisms (see Figure TS.1 and Figure TS.2). {2.3, 6.3–6.5, FAQ 7.1}

The total radiative forcing of the Earth’s climate due to increases in the concentrations of the LLGHGs CO₂, CH₄ and N₂O, and very likely the rate of increase in the total forcing due to these gases over the period since 1750, are unprecedented in more than 10,000 years (Figure TS.2). It is very likely that the sustained rate of increase in the combined radiative forcing from these greenhouse gases of about +1 W m⁻² over the past four decades is at least six times faster than at any time during the two millennia before the Industrial Era, the period for which ice core data have the required temporal resolution. The radiative forcing due to these LLGHGs has the highest level of confidence of any forcing agent. {2.3, 6.4}

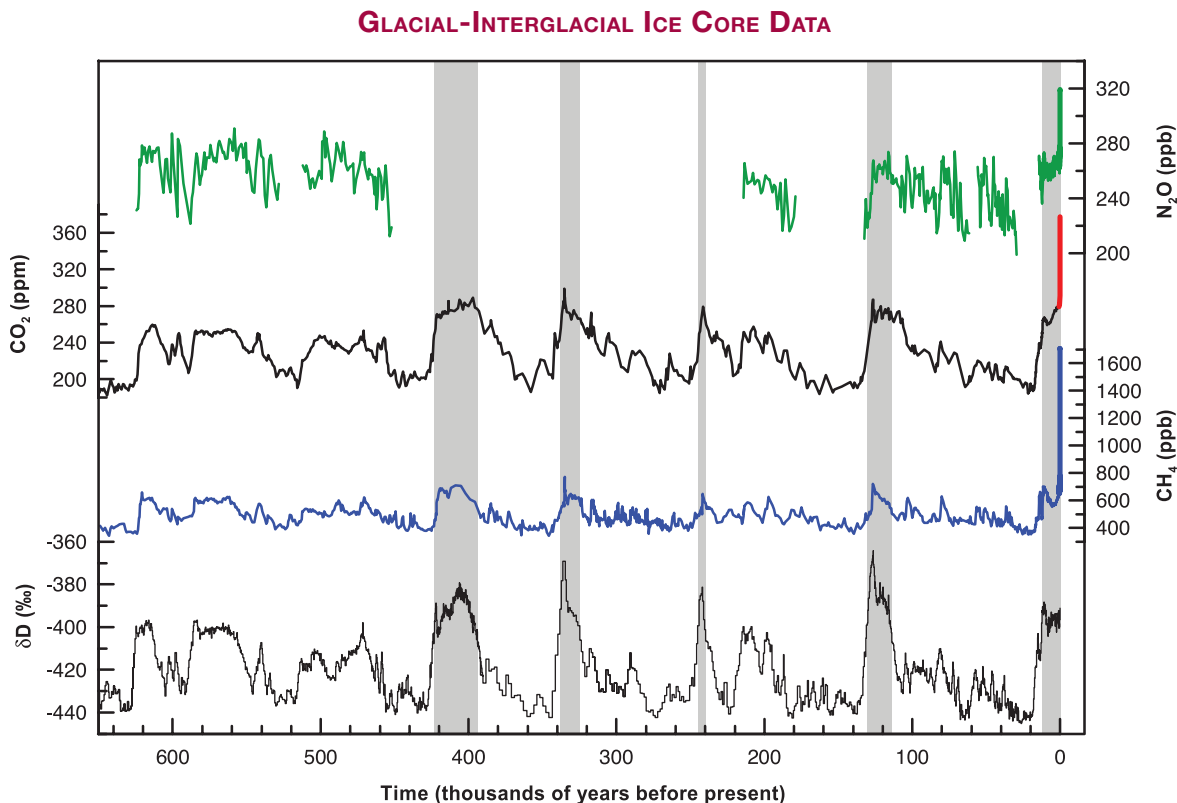


Figure TS.1. Variations of deuterium (δD) in antarctic ice, which is a proxy for local temperature, and the atmospheric concentrations of the greenhouse gases carbon dioxide (CO_2), methane (CH_4), and nitrous oxide (N_2O) in air trapped within the ice cores and from recent atmospheric measurements. Data cover 650,000 years and the shaded bands indicate current and previous interglacial warm periods. {Adapted from Figure 6.3}

CHANGES IN GREENHOUSE GASES FROM ICE CORE AND MODERN DATA

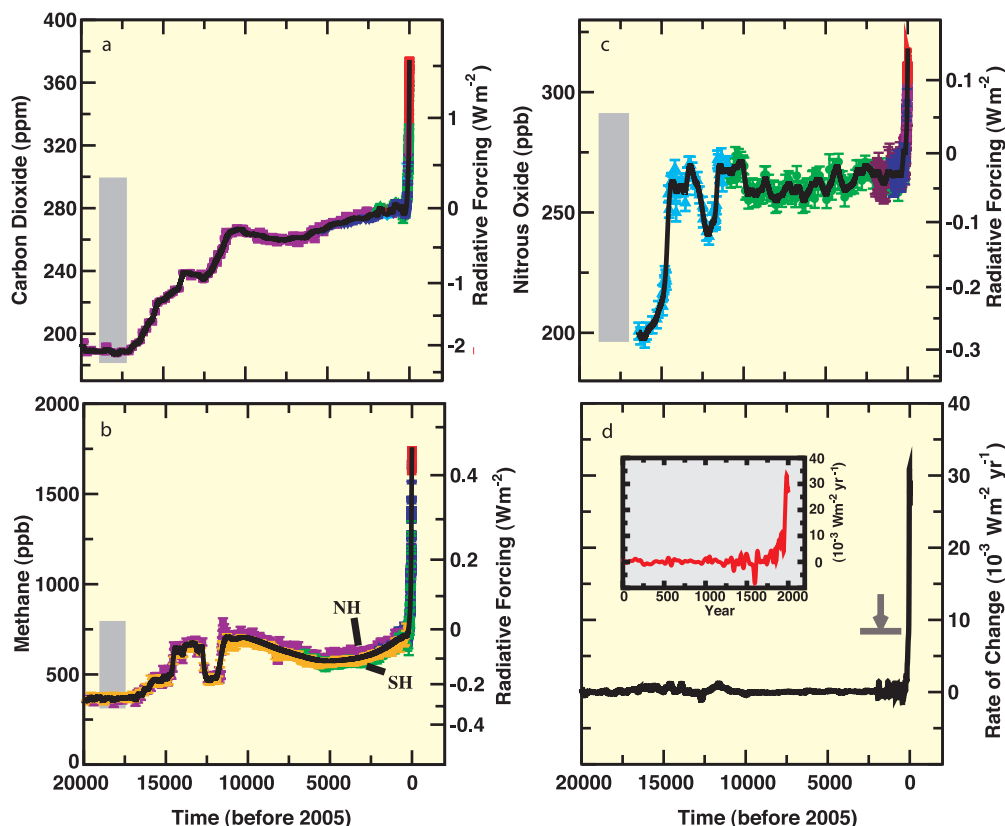


Figure TS.2. The concentrations and radiative forcing by (a) carbon dioxide (CO_2), (b) methane (CH_4), (c) nitrous oxide (N_2O) and (d) the rate of change in their combined radiative forcing over the last 20,000 years reconstructed from antarctic and Greenland ice and firn data (symbols) and direct atmospheric measurements (panels a,b,c, red lines). The grey bars show the reconstructed ranges of natural variability for the past 650,000 years. The rate of change in radiative forcing (panel d, black line) has been computed from spline fits to the concentration data. The width of the age spread in the ice data varies from about 20 years for sites with a high accumulation of snow such as Law Dome, Antarctica, to about 200 years for low-accumulation sites such as Dome C, Antarctica. The arrow shows the peak in the rate of change in radiative forcing that would result if the anthropogenic signals of CO_2 , CH_4 , and N_2O had been smoothed corresponding to conditions at the low-accumulation Dome C site. The negative rate of change around 1600 shown in the higher-resolution inset in panel d results from a CO_2 decrease of about 10 ppm in the Law Dome record. {Figure 6.4}

The concentration of atmospheric CO_2 has increased from a pre-industrial value of about 280 ppm to 379 ppm in 2005. Atmospheric CO_2 concentration increased by only 20 ppm over the 8000 years prior to industrialisation; multi-decadal to centennial-scale variations were less than 10 ppm and likely due mostly to natural processes. However, since 1750, the CO_2 concentration has risen by nearly 100 ppm. The annual CO_2 growth rate was larger during the last 10 years (1995–2005 average: 1.9 ppm yr^{-1}) than it has been since continuous direct atmospheric measurements began (1960–2005 average: 1.4 ppm yr^{-1}). {2.3, 6.4, 6.5}

Increases in atmospheric CO_2 since pre-industrial times are responsible for a radiative forcing of $+1.66 \pm 0.17 \text{ W m}^{-2}$; a contribution which dominates all other radiative forcing agents considered in this report. For the decade from 1995 to 2005, the growth rate of CO_2

in the atmosphere led to a 20% increase in its radiative forcing. {2.3, 6.4, 6.5}

Emissions of CO_2 from fossil fuel use and from the effects of land use change on plant and soil carbon are the primary sources of increased atmospheric CO_2 . Since 1750, it is estimated that about 2/3rds of anthropogenic CO_2 emissions have come from fossil fuel burning and about 1/3rd from land use change. About 45% of this CO_2 has remained in the atmosphere, while about 30% has been taken up by the oceans and the remainder has been taken up by the terrestrial biosphere. About half of a CO_2 pulse to the atmosphere is removed over a time scale of 30 years; a further 30% is removed within a few centuries; and the remaining 20% will typically stay in the atmosphere for many thousands of years. {7.3}

In recent decades, emissions of CO_2 have continued to increase (see Figure TS.3). Global annual fossil

CO₂ emissions³ increased from an average of 6.4 ± 0.4 GtC yr⁻¹ in the 1990s to 7.2 ± 0.3 GtC yr⁻¹ in the period 2000 to 2005. Estimated CO₂ emissions associated with land use change, averaged over the 1990s, were⁴ 0.5 to 2.7 GtC yr⁻¹, with a central estimate of 1.6 Gt yr⁻¹. Table TS.1 shows the estimated budgets of CO₂ in recent decades. {2.3, 6.4, 7.3, FAQ 7.1}

Since the 1980s, natural processes of CO₂ uptake by the terrestrial biosphere (i.e., the residual land sink in Table TS.1) and by the oceans have removed about 50% of anthropogenic emissions (i.e., fossil CO₂ emissions and land use change flux in Table TS.1). These removal processes are influenced by the atmospheric CO₂ concentration and by changes in climate. Uptake by the oceans and the terrestrial biosphere have been similar in magnitude but the terrestrial biosphere uptake is more variable and was higher in the 1990s than in the 1980s by about 1 GtC yr⁻¹. Observations demonstrate that dissolved CO₂ concentrations in the surface ocean (pCO₂) have been increasing nearly everywhere, roughly following the atmospheric CO₂ increase but with large regional and temporal variability. {5.4, 7.3}

Carbon uptake and storage in the terrestrial biosphere arise from the net difference between uptake due to vegetation growth, changes in reforestation and sequestration, and emissions due to heterotrophic respiration, harvest, deforestation, fire, damage by pollution and other disturbance factors affecting biomass and soils. Increases and decreases in fire frequency in different regions have affected net carbon

uptake, and in boreal regions, emissions due to fires appear to have increased over recent decades. Estimates of net CO₂ surface fluxes from inverse studies using networks of atmospheric data demonstrate significant land uptake in the mid-latitudes of the Northern Hemisphere (NH) and near-zero land-atmosphere fluxes in the tropics, implying that tropical deforestation is approximately balanced by regrowth. {7.3}

Short-term (interannual) variations observed in the atmospheric CO₂ growth rate are primarily controlled by changes in the flux of CO₂ between the atmosphere and the terrestrial biosphere, with a smaller but significant fraction due to variability in ocean fluxes (see Figure TS.3). Variability in the terrestrial biosphere flux is driven by climatic fluctuations, which affect the uptake of CO₂ by plant growth and the return of CO₂ to the atmosphere by the decay of organic material through heterotrophic respiration and fires. El Niño-Southern Oscillation (ENSO) events are a major source of interannual variability in atmospheric CO₂ growth rate, due to their effects on fluxes through land and sea surface temperatures, precipitation and the incidence of fires. {7.3}

The direct effects of increasing atmospheric CO₂ on large-scale terrestrial carbon uptake cannot be quantified reliably at present. Plant growth can be stimulated by increased atmospheric CO₂ concentrations and by nutrient deposition (fertilization effects). However, most experiments and studies show that such responses appear to be relatively short lived and strongly coupled

Table TS.1. Global carbon budget. By convention, positive values are CO₂ fluxes (GtC yr⁻¹) into the atmosphere and negative values represent uptake from the atmosphere (i.e., 'CO₂ sinks'). Fossil CO₂ emissions for 2004 and 2005 are based on interim estimates. Due to the limited number of available studies, for the net land-to-atmosphere flux and its components, uncertainty ranges are given as 65% confidence intervals and do not include interannual variability (see Section 7.3). NA indicates that data are not available.

	1980s	1990s	2000–2005
Atmospheric increase	3.3 ± 0.1	3.2 ± 0.1	4.1 ± 0.1
Fossil carbon dioxide emissions	5.4 ± 0.3	6.4 ± 0.4	7.2 ± 0.3
Net ocean-to-atmosphere flux	-1.8 ± 0.8	-2.2 ± 0.4	-2.2 ± 0.5
Net land-to-atmosphere flux	-0.3 ± 0.9	-1.0 ± 0.6	-0.9 ± 0.6
<i>Partitioned as follows</i>			
Land use change flux	1.4 (0.4 to 2.3)	1.6 (0.5 to 2.7)	NA
Residual land sink	-1.7 (-3.4 to 0.2)	-2.6 (-4.3 to -0.9)	NA

³ Fossil CO₂ emissions include those from the production, distribution and consumption of fossil fuels and from cement production. Emission of 1 GtC corresponds to 3.67 GtCO₂.

⁴ As explained in Section 7.3, uncertainty ranges for land use change emissions, and hence for the full carbon cycle budget, can only be given as 65% confidence intervals.

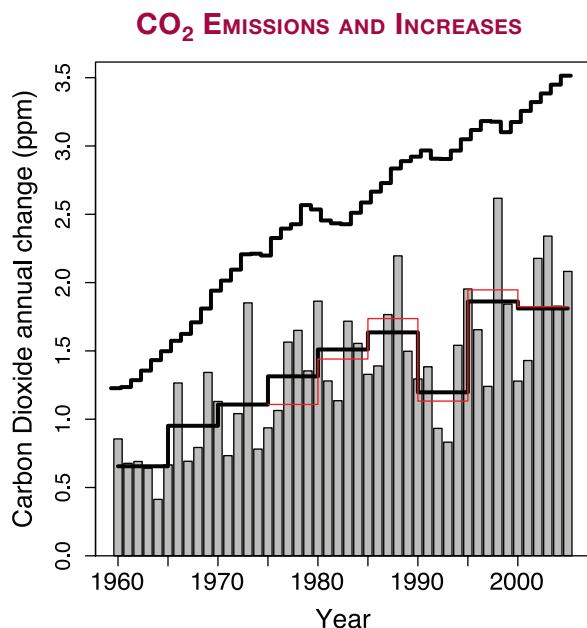


Figure TS.3. Annual changes in global mean CO₂ concentration (grey bars) and their five-year means from two different measurement networks (red and lower black stepped lines). The five-year means smooth out short-term perturbations associated with strong ENSO events in 1972, 1982, 1987 and 1997. Uncertainties in the five-year means are indicated by the difference between the red and lower black lines and are of order 0.15 ppm. The upper stepped line shows the annual increases that would occur if all fossil fuel emissions stayed in the atmosphere and there were no other emissions. {Figure 7.4}

to other effects such as availability of water and nutrients. Likewise, experiments and studies of the effects of climate (temperature and moisture) on heterotrophic respiration of litter and soils are equivocal. Note that the effect of climate change on carbon uptake is addressed separately in section TS.5.4. {7.3}

The CH₄ abundance in 2005 of about 1774 ppb is more than double its pre-industrial value. Atmospheric CH₄ concentrations varied slowly between 580 and 730 ppb over the last 10,000 years, but increased by about 1000 ppb in the last two centuries, representing the fastest changes in this gas over at least the last 80,000 years. In the late 1970s and early 1980s, CH₄ growth rates displayed maxima above 1% yr⁻¹, but since the early 1990s have decreased significantly and were close to zero for the six-year period from 1999 to 2005. Increases in CH₄ abundance occur when emissions exceed removals. The recent decline in growth rates implies that emissions now approximately match removals, which are due primarily to oxidation by the hydroxyl radical (OH). Since the TAR, new studies using two independent tracers (methyl chloroform and ¹⁴CO) suggest no significant long-term change in the global abundance of OH. Thus,

the slowdown in the atmospheric CH₄ growth rate since about 1993 is *likely* due to the atmosphere approaching an equilibrium during a period of near-constant total emissions. {2.3, 7.4, FAQ 7.1}

Increases in atmospheric CH₄ concentrations since pre-industrial times have contributed a radiative forcing of +0.48 ± 0.05 W m⁻². Among greenhouse gases, this forcing remains second only to that of CO₂ in magnitude. {2.3}

Current atmospheric CH₄ levels are due to continuing anthropogenic emissions of CH₄, which are greater than natural emissions. Total CH₄ emissions can be well determined from observed concentrations and independent estimates of removal rates. Emissions from individual sources of CH₄ are not as well quantified as the total emissions but are mostly biogenic and include emissions from wetlands, ruminant animals, rice agriculture and biomass burning, with smaller contributions from industrial sources including fossil fuel-related emissions. This knowledge of CH₄ sources, combined with the small natural range of CH₄ concentrations over the past 650,000 years (Figure TS.1) and their dramatic increase since 1750 (Figure TS.2), make it *very likely* that the observed long-term changes in CH₄ are due to anthropogenic activity. {2.3, 6.4, 7.4}

In addition to its slowdown over the last 15 years, the growth rate of atmospheric CH₄ has shown high interannual variability, which is not yet fully explained. The largest contributions to interannual variability during the 1996 to 2001 period appear to be variations in emissions from wetlands and biomass burning. Several studies indicate that wetland CH₄ emissions are highly sensitive to temperature and are also affected by hydrological changes. Available model estimates all indicate increases in wetland emissions due to future climate change but vary widely in the magnitude of such a positive feedback effect. {7.4}

The N₂O concentration in 2005 was 319 ppb, about 18% higher than its pre-industrial value. Nitrous oxide increased approximately linearly by about 0.8 ppb yr⁻¹ over the past few decades. Ice core data show that the atmospheric concentration of N₂O varied by less than about 10 ppb for 11,500 years before the onset of the industrial period. {2.3, 6.4, 6.5}

The increase in N₂O since the pre-industrial era now contributes a radiative forcing of +0.16 ± 0.02 W m⁻² and is due primarily to human activities, particularly agriculture and associated land use change. Current estimates are that about 40% of total N₂O emissions are anthropogenic but individual source estimates remain subject to significant uncertainties. {2.3, 7.4}

TS.2.1.3 Changes in Atmospheric Halocarbons, Stratospheric Ozone, Tropospheric Ozone and Other Gases

CFCs and hydrochlorofluorocarbons (HCFCs) are greenhouse gases that are purely anthropogenic in origin and used in a wide variety of applications. Emissions of these gases have decreased due to their phase-out under the Montreal Protocol, and the atmospheric concentrations of CFC-11 and CFC-113 are now decreasing due to natural removal processes. Observations in polar firn cores since the TAR have now extended the available time series information for some of these greenhouse gases. Ice core and *in situ* data confirm that industrial sources are the cause of observed atmospheric increases in CFCs and HCFCs. {2.3}

The Montreal Protocol gases contributed $+0.32 \pm 0.03 \text{ W m}^{-2}$ to direct radiative forcing in 2005, with CFC-12 continuing to be the third most important long-lived radiative forcing agent. These gases as a group contribute about 12% of the total forcing due to LLGHGs. {2.3}

The concentrations of industrial fluorinated gases covered by the Kyoto Protocol (hydrofluorocarbons (HFCs), perfluorocarbons (PFCs), sulphur hexafluoride (SF_6)) are relatively small but are increasing rapidly. Their total radiative forcing in 2005 was $+0.017 \text{ W m}^{-2}$. {2.3}

Tropospheric ozone is a short-lived greenhouse gas produced by chemical reactions of precursor species in the atmosphere and with large spatial and temporal variability. Improved measurements and modelling have advanced the understanding of chemical precursors that lead to the formation of tropospheric ozone, mainly carbon monoxide, nitrogen oxides (including sources and possible long-term trends in lightning) and formaldehyde. Overall, current models are successful in describing the principal features of the present global tropospheric ozone distribution on the basis of underlying processes. New satellite and *in situ* measurements provide important global constraints for these models; however, there is less confidence in their ability to reproduce the changes in ozone associated with large changes in emissions or climate, and in the simulation of observed long-term trends in ozone concentrations over the 20th century. {7.4}

Tropospheric ozone radiative forcing is estimated to be $+0.35$ [$+0.25$ to $+0.65$] W m^{-2} with a *medium* level of scientific understanding. The best estimate of this radiative forcing has not changed since the TAR. Observations show that trends in tropospheric ozone during the last few decades vary in sign and magnitude at many locations, but there are

indications of significant upward trends at low latitudes. Model studies of the radiative forcing due to the increase in tropospheric ozone since pre-industrial times have increased in complexity and comprehensiveness compared with models used in the TAR. {2.3, 7.4}

Changes in tropospheric ozone are linked to air quality and climate change. A number of studies have shown that summer daytime ozone concentrations correlate strongly with temperature. This correlation appears to reflect contributions from temperature-dependent biogenic volatile organic carbon emissions, thermal decomposition of peroxyacetyl nitrate, which acts as a reservoir for nitrogen oxides (NO_x), and association of high temperatures with regional stagnation. Anomalously hot and stagnant conditions during the summer of 1988 were responsible for the highest surface-level ozone year on record in the north-eastern USA. The summer heat wave in Europe in 2003 was also associated with exceptionally high local ozone at the surface. {Box 7.4}

The radiative forcing due to the destruction of stratospheric ozone is caused by the Montreal Protocol gases and is re-evaluated to be $-0.05 \pm 0.10 \text{ W m}^{-2}$, weaker than in the TAR, with a medium level of scientific understanding. The trend of greater and greater depletion of global stratospheric ozone observed during the 1980s and 1990s is no longer occurring; however, global stratospheric ozone is still about 4% below pre-1980 values and it is not yet clear whether ozone recovery has begun. In addition to the chemical destruction of ozone, dynamical changes may have contributed to NH mid-latitude ozone reduction. {2.3}

Direct emission of water vapour by human activities makes a negligible contribution to radiative forcing. However, as global mean temperatures increase, tropospheric water vapour concentrations increase and this represents a key feedback but not a forcing of climate change. Direct emission of water to the atmosphere by anthropogenic activities, mainly irrigation, is a possible forcing factor but corresponds to less than 1% of the natural sources of atmospheric water vapour. The direct injection of water vapour into the atmosphere from fossil fuel combustion is significantly lower than that from agricultural activity. {2.5}

Based on chemical transport model studies, the radiative forcing from increases in stratospheric water vapour due to oxidation of CH_4 is estimated to be $+0.07 \pm 0.05 \text{ W m}^{-2}$. The level of scientific understanding is low because the contribution of CH_4 to the corresponding vertical structure of the water vapour change near the tropopause is uncertain. Other potential human causes of stratospheric water vapour increases that could contribute to radiative forcing are poorly understood. {2.3}

TS.2.2 Aerosols

Direct aerosol radiative forcing is now considerably better quantified than previously and represents a major advance in understanding since the time of the TAR, when several components had a very low level of scientific understanding. A total direct aerosol radiative forcing combined across all aerosol types can now be given for the first time as $-0.5 \pm 0.4 \text{ W m}^{-2}$, with a medium-low level of scientific understanding.

Atmospheric models have improved and many now represent all aerosol components of significance. Aerosols vary considerably in their properties that affect the extent to which they absorb and scatter radiation, and thus different types may have a net cooling or warming effect. Industrial aerosol consisting mainly of a mixture of sulphates, organic and black carbon, nitrates and industrial dust is clearly discernible over many continental regions of the NH. Improved *in situ*, satellite and surface-based measurements (see Figure TS.4) have enabled verification of global aerosol model simulations. These improvements allow quantification of the total direct aerosol radiative forcing for the first time, representing an important advance since the TAR. The direct radiative forcing for individual species remains less certain and is estimated from models to be $-0.4 \pm 0.2 \text{ W m}^{-2}$ for sulphate, $-0.05 \pm 0.05 \text{ W m}^{-2}$ for fossil fuel organic carbon, $+0.2 \pm 0.15 \text{ W m}^{-2}$ for fossil fuel black carbon, $+0.03 \pm 0.12 \text{ W m}^{-2}$ for biomass burning, $-0.1 \pm 0.1 \text{ W m}^{-2}$ for nitrate and $-0.1 \pm 0.2 \text{ W m}^{-2}$ for mineral dust. Two recent emission inventory studies support data from ice cores and suggest that global anthropogenic sulphate emissions decreased over the 1980 to 2000 period and that the geographic distribution of sulphate forcing has also changed. {2.4, 6.6}

Significant changes in the estimates of the direct radiative forcing due to biomass-burning, nitrate and mineral dust aerosols have occurred since the TAR. For biomass-burning aerosol, the estimated direct radiative forcing is now revised from being negative to near zero due to the estimate being strongly influenced by the occurrence of these aerosols over clouds. For the first time, the radiative forcing due to nitrate aerosol is given. For mineral dust, the range in the direct radiative forcing is reduced due to a reduction in the estimate of its anthropogenic fraction. {2.4}

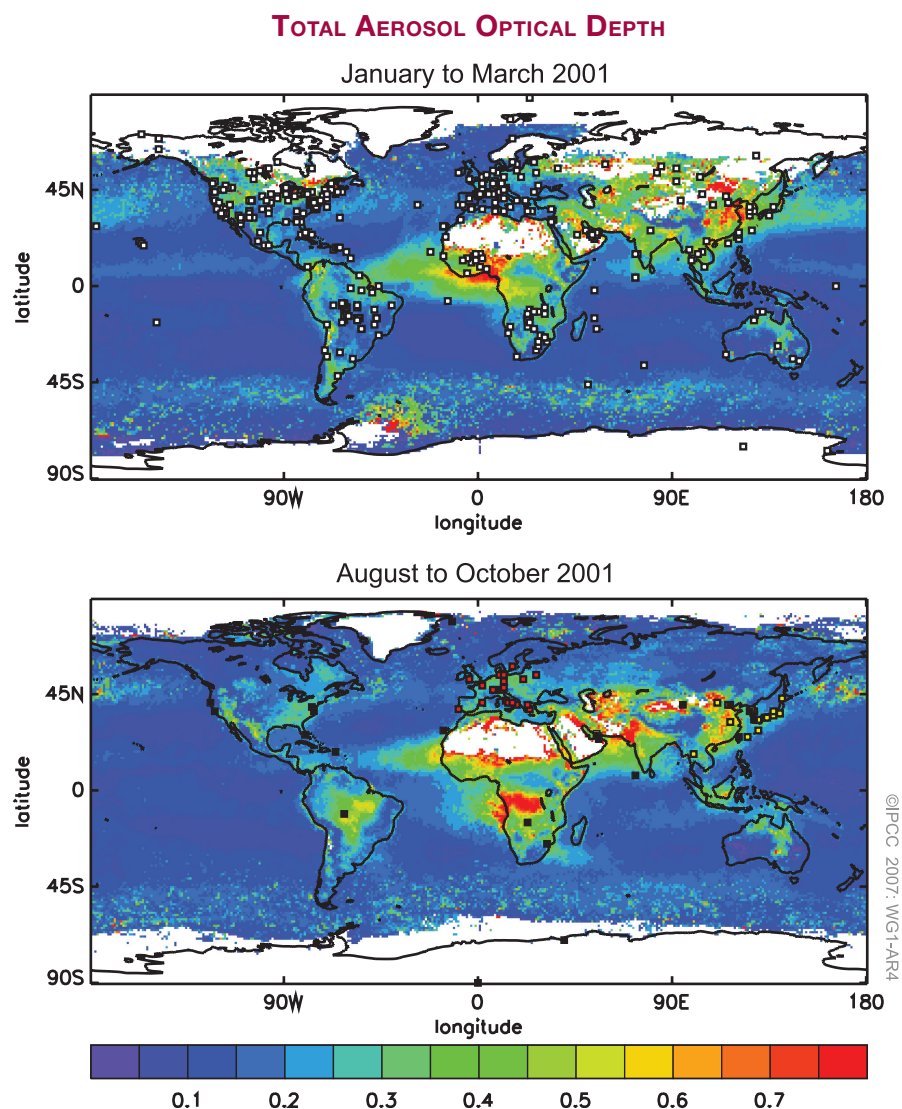


Figure TS.4. (Top) The total aerosol optical depth (due to natural plus anthropogenic aerosols) at a mid-visible wavelength determined by satellite measurements for January to March 2001 and (bottom) August to October 2001, illustrating seasonal changes in industrial and biomass-burning aerosols. Data are from satellite measurements, complemented by two different kinds of ground-based measurements at locations shown in the two panels (see Section 2.4.2 for details). {Figure 2.11}

Anthropogenic aerosols effects on water clouds cause an indirect cloud albedo effect (referred to as the first indirect effect in the TAR), which has a best estimate for the first time of -0.7 [-0.3 to -1.8] W m^{-2} . The number of global model estimates of the albedo effect for liquid water clouds has increased substantially since the TAR, and the estimates have been evaluated in a more rigorous way. The estimate for this radiative forcing comes from multiple model studies incorporating more aerosol species and describing aerosol-cloud interaction processes in greater detail. Model studies including more aerosol species or constrained by satellite observations tend to yield a relatively weaker cloud albedo effect. Despite the advances and progress since the TAR and the reduction in the spread of the estimate of the forcing, there remain large uncertainties in both measurements and modelling of processes, leading to a low level of scientific understanding, which is an elevation from the very low rank in the TAR. {2.4, 7.5, 9.2}

Other effects of aerosol include a cloud lifetime effect, a semi-direct effect and aerosol-ice cloud interactions. These are considered to be part of the climate response rather than radiative forcings. {2.4, 7.5}

TS.2.3 Aviation Contrails and Cirrus, Land Use and Other Effects

Persistent linear contrails from global aviation contribute a small radiative forcing of $+0.01$ [$+0.003$ to $+0.03$] W m^{-2} , with a low level of scientific understanding. This best estimate is smaller than the estimate in the TAR. This difference results from new observations of contrail cover and reduced estimates of contrail optical depth. No best estimates are available for the net forcing from spreading contrails. Their effects on cirrus cloudiness and the global effect of aviation aerosol on background cloudiness remain unknown. {2.6}

Human-induced changes in land cover have increased the global surface albedo, leading to a radiative forcing of -0.2 ± 0.2 W m^{-2} , the same as in the TAR, with a medium-low level of scientific understanding. Black carbon aerosols deposited on snow reduce the surface albedo and are estimated to yield an associated radiative forcing of $+0.1 \pm 0.1$ W m^{-2} , with a low level of scientific understanding. Since the TAR, a number of estimates of the forcing from land use changes have been made, using better techniques, exclusion of feedbacks in the evaluation and improved incorporation of large-scale observations. Uncertainties in the estimate include mapping and characterisation of present-day vegetation and historical state, parametrization of surface radiation processes and biases in models'

climate variables. The presence of soot particles in snow leads to a decrease in the albedo of snow and a positive forcing, and could affect snowmelt. Uncertainties are large regarding the manner in which soot is incorporated in snow and the resulting optical properties. {2.5}

The impacts of land use change on climate are expected to be locally significant in some regions, but are small at the global scale in comparison with greenhouse gas warming. Changes in the land surface (vegetation, soils, water) resulting from human activities can significantly affect local climate through shifts in radiation, cloudiness, surface roughness and surface temperatures. Changes in vegetation cover can also have a substantial effect on surface energy and water balance at the regional scale. These effects involve non-radiative processes (implying that they cannot be quantified by a radiative forcing) and have a very low level of scientific understanding. {2.5, 7.2, 9.3, Box 11.4}

The release of heat from anthropogenic energy production can be significant over urban areas but is not significant globally. {2.5}

TS.2.4 Radiative Forcing Due to Solar Activity and Volcanic Eruptions

Continuous monitoring of total solar irradiance now covers the last 28 years. The data show a well-established 11-year cycle in irradiance that varies by 0.08% from solar cycle minima to maxima, with no significant long-term trend. New data have more accurately quantified changes in solar spectral fluxes over a broad range of wavelengths in association with changing solar activity. Improved calibrations using high-quality overlapping measurements have also contributed to a better understanding. Current understanding of solar physics and the known sources of irradiance variability suggest comparable irradiance levels during the past two solar cycles, including at solar minima. The primary known cause of contemporary irradiance variability is the presence on the Sun's disk of sunspots (compact, dark features where radiation is locally depleted) and faculae (extended bright features where radiation is locally enhanced). {2.7}

The estimated direct radiative forcing due to changes in the solar output since 1750 is $+0.12$ [$+0.06$ to $+0.3$] W m^{-2} , which is less than half of the estimate given in the TAR, with a low level of scientific understanding. The reduced radiative forcing estimate comes from a re-evaluation of the long-term change in solar irradiance since 1610 (the Maunder Minimum) based upon: a new reconstruction using a model of solar magnetic flux variations that does not invoke geomagnetic,

cosmogenic or stellar proxies; improved understanding of recent solar variations and their relationship to physical processes; and re-evaluation of the variations of Sun-like stars. While this leads to an elevation in the level of scientific understanding from very low in the TAR to low in this assessment, uncertainties remain large because of the lack of direct observations and incomplete understanding of solar variability mechanisms over long time scales. {2.7, 6.6}

Empirical associations have been reported between solar-modulated cosmic ray ionization of the atmosphere and global average low-level cloud cover but evidence for a systematic indirect solar effect remains ambiguous. It has been suggested that galactic cosmic rays with sufficient energy to reach the troposphere could alter the population of cloud condensation nuclei and hence microphysical cloud properties (droplet number and concentration), inducing changes in cloud processes analogous to the indirect cloud albedo effect of tropospheric aerosols and thus causing an indirect solar forcing of climate. Studies have probed various correlations with clouds in particular regions or using limited cloud types or limited time periods; however, the cosmic ray time series does not appear to correspond to global total cloud cover after 1991 or to global low-level cloud cover after 1994. Together with the lack of a proven physical mechanism and the plausibility of other causal factors affecting changes in cloud cover, this makes the association between galactic cosmic ray-induced changes in aerosol and cloud formation controversial. {2.7}

Explosive volcanic eruptions greatly increase the concentration of stratospheric sulphate aerosols. A single eruption can thereby cool global mean climate for a few years. Volcanic aerosols perturb both the stratosphere and surface/troposphere radiative energy budgets and climate in an episodic manner, and many past events are evident in ice core observations of sulphate as well as temperature records. There have been no explosive volcanic events since the 1991 Mt. Pinatubo eruption capable of injecting significant material to the stratosphere. However, the potential exists for volcanic eruptions much larger than the 1991 Mt. Pinatubo eruption, which could produce larger radiative forcing and longer-term cooling of the climate system. {2.7, 6.4, 6.6, 9.2}

TS.2.5 Net Global Radiative Forcing, Global Warming Potentials and Patterns of Forcing

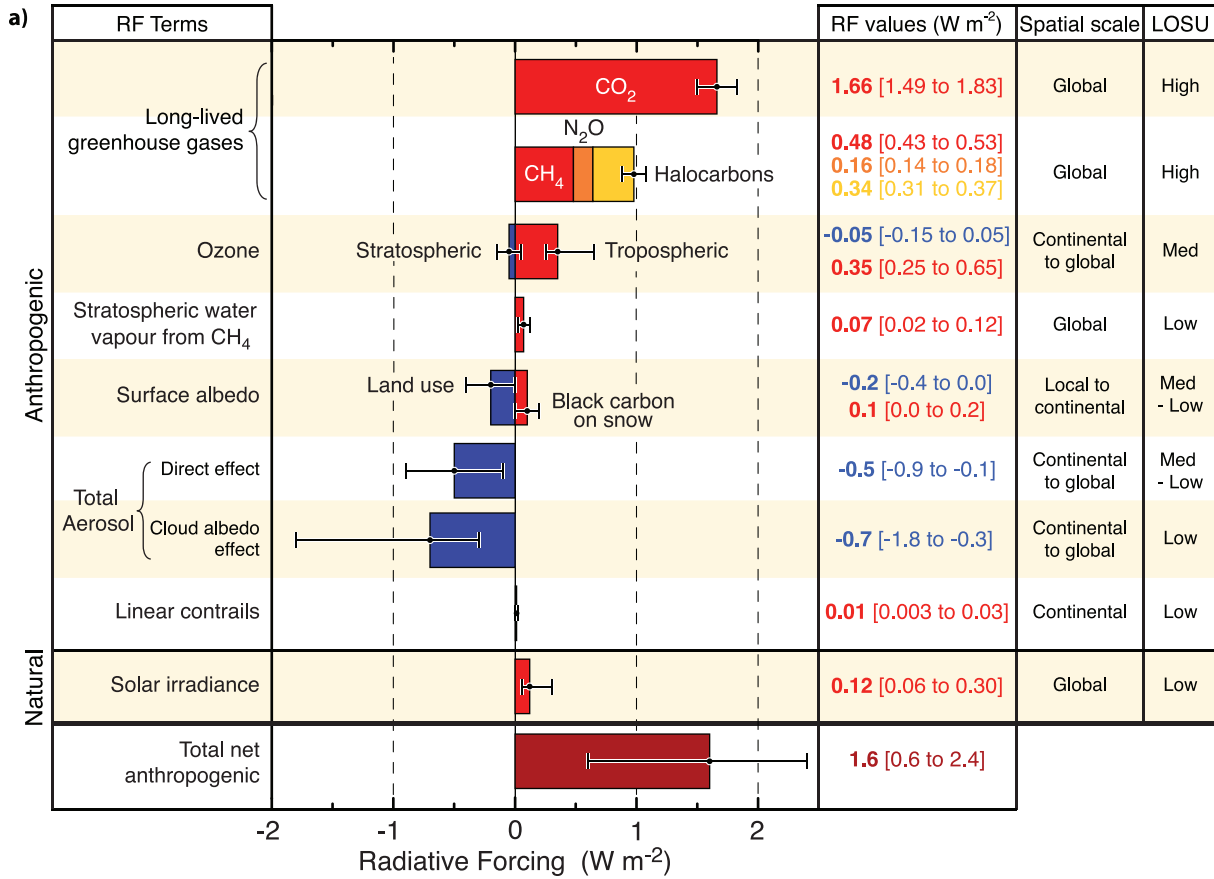
The understanding of anthropogenic warming and cooling influences on climate has improved

since the TAR, leading to very high confidence that the effect of human activities since 1750 has been a net positive forcing of +1.6 [+0.6 to +2.4] W m⁻². Improved understanding and better quantification of the forcing mechanisms since the TAR make it possible to derive a combined net anthropogenic radiative forcing for the first time. Combining the component values for each forcing agent and their uncertainties yields the probability distribution of the combined anthropogenic radiative forcing estimate shown in Figure TS.5; the most likely value is about an order of magnitude larger than the estimated radiative forcing from changes in solar irradiance. Since the range in the estimate is +0.6 to +2.4 W m⁻², there is very high confidence in the net positive radiative forcing of the climate system due to human activity. The LLGHGs together contribute +2.63 ± 0.26 W m⁻², which is the dominant radiative forcing term and has the highest level of scientific understanding. In contrast, the total direct aerosol, cloud albedo and surface albedo effects that contribute negative forcings are less well understood and have larger uncertainties. The range in the net estimate is increased by the negative forcing terms, which have larger uncertainties than the positive terms. The nature of the uncertainty in the estimated cloud albedo effect introduces a noticeable asymmetry in the distribution. Uncertainties in the distribution include structural aspects (e.g., representation of extremes in the component values, absence of any weighting of the radiative forcing mechanisms, possibility of unaccounted for but as yet unquantified radiative forcings) and statistical aspects (e.g., assumptions about the types of distributions describing component uncertainties). {2.7, 2.9}

The Global Warming Potential (GWP) is a useful metric for comparing the potential climate impact of the emissions of different LLGHGs (see Table TS.2). Global Warming Potentials compare the integrated radiative forcing over a specified period (e.g., 100 years) from a unit mass pulse emission and are a way of comparing the potential climate change associated with emissions of different greenhouse gases. There are well-documented shortcomings of the GWP concept, particularly in using it to assess the impact of short-lived species. {2.10}

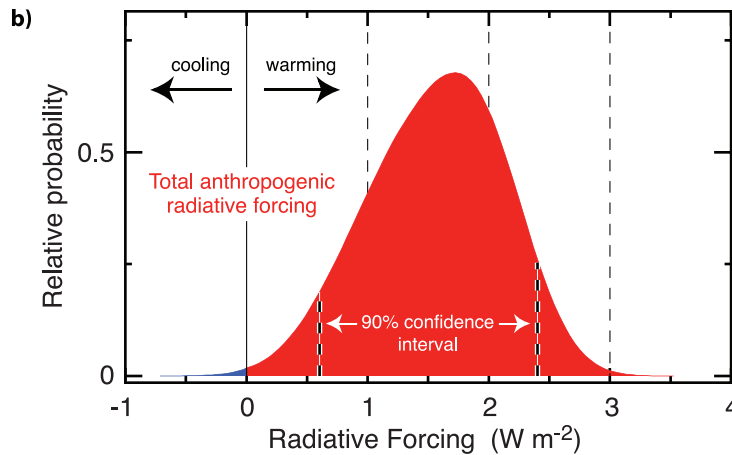
For the magnitude and range of realistic forcings considered, evidence suggests an approximately linear relationship between global mean radiative forcing and global mean surface temperature response. The spatial patterns of radiative forcing vary between different forcing agents. However, the spatial signature of the climate response is not generally expected to match that of the forcing. Spatial patterns of climate response

GLOBAL MEAN RADIATIVE FORCINGS



©IPCC 2007: WG1-AR4

PROBABILITY DISTRIBUTION



©IPCC 2007: WG1-AR4

Figure TS.5. (a) Global mean radiative forcings (RF) and their 90% confidence intervals in 2005 for various agents and mechanisms. Columns on the right-hand side specify best estimates and confidence intervals (RF values); typical geographical extent of the forcing (Spatial scale); and level of scientific understanding (LOSU) indicating the scientific confidence level as explained in Section 2.9. Errors for CH_4 , N_2O and halocarbons have been combined. The net anthropogenic radiative forcing and its range are also shown. Best estimates and uncertainty ranges can not be obtained by direct addition of individual terms due to the asymmetric uncertainty ranges for some factors; the values given here were obtained from a Monte Carlo technique as discussed in Section 2.9. Additional forcing factors not included here are considered to have a very low LOSU. Volcanic aerosols contribute an additional form of natural forcing but are not included due to their episodic nature. The range for linear contrails does not include other possible effects of aviation on cloudiness. (b) Probability distribution of the global mean combined radiative forcing from all anthropogenic agents shown in (a). The distribution is calculated by combining the best estimates and uncertainties of each component. The spread in the distribution is increased significantly by the negative forcing terms, which have larger uncertainties than the positive terms. {2.9.1, 2.9.2; Figure 2.20}

Table TS.2. Lifetimes, radiative efficiencies and direct (except for CH₄) global warming potentials (GWP) relative to CO₂. (Table 2.14)

Industrial Designation or Common Name (years)	Chemical Formula	Lifetime (years)	Radiative Efficiency (W m ⁻² ppb ⁻¹)	Global Warming Potential for Given Time Horizon			
				SAR [†] (100-yr)	20-yr	100-yr	500-yr
Carbon dioxide	CO ₂	See below ^a	^b 1.4x10 ⁻⁵	1	1	1	1
Methane ^c	CH ₄	12 ^c	3.7x10 ⁻⁴	21	72	25	7.6
Nitrous oxide	N ₂ O	114	3.03x10 ⁻³	310	289	298	153
Substances controlled by the Montreal Protocol							
CFC-11	CCl ₃ F	45	0.25	3,800	6,730	4,750	1,620
CFC-12	CCl ₂ F ₂	100	0.32	8,100	11,000	10,900	5,200
CFC-13	CClF ₃	640	0.25		10,800	14,400	16,400
CFC-113	CCl ₂ FCClF ₂	85	0.3	4,800	6,540	6,130	2,700
CFC-114	CClF ₂ CClF ₂	300	0.31		8,040	10,000	8,730
CFC-115	CClF ₂ CF ₃	1,700	0.18		5,310	7,370	9,990
Halon-1301	CBrF ₃	65	0.32	5,400	8,480	7,140	2,760
Halon-1211	CBrClF ₂	16	0.3		4,750	1,890	575
Halon-2402	CBrF ₂ CBrF ₂	20	0.33		3,680	1,640	503
Carbon tetrachloride	CCl ₄	26	0.13	1,400	2,700	1,400	435
Methyl bromide	CH ₃ Br	0.7	0.01		17	5	1
Methyl chloroform	CH ₃ CCl ₃	5	0.06		506	146	45
HCFC-22	CHClF ₂	12	0.2	1,500	5,160	1,810	549
HCFC-123	CHCl ₂ CF ₃	1.3	0.14	90	273	77	24
HCFC-124	CHClFCF ₃	5.8	0.22	470	2,070	609	185
HCFC-141b	CH ₃ CCl ₂ F	9.3	0.14		2,250	725	220
HCFC-142b	CH ₃ CClF ₂	17.9	0.2	1,800	5,490	2,310	705
HCFC-225ca	CHCl ₂ CF ₂ CF ₃	1.9	0.2		429	122	37
HCFC-225cb	CHClFCF ₂ CClF ₂	5.8	0.32		2,030	595	181
Hydrofluorocarbons							
HFC-23	CHF ₃	270	0.19	11,700	12,000	14,800	12,200
HFC-32	CH ₂ F ₂	4.9	0.11	650	2,330	675	205
HFC-125	CHF ₂ CF ₃	29	0.23	2,800	6,350	3,500	1,100
HFC-134a	CH ₂ FCF ₃	14	0.16	1,300	3,830	1,430	435
HFC-143a	CH ₃ CF ₃	52	0.13	3,800	5,890	4,470	1,590
HFC-152a	CH ₃ CHF ₂	1.4	0.09	140	437	124	38
HFC-227ea	CF ₃ CHF ₂ CF ₃	34.2	0.26	2,900	5,310	3,220	1,040
HFC-236fa	CF ₃ CH ₂ CF ₃	240	0.28	6,300	8,100	9,810	7,660
HFC-245fa	CHF ₂ CH ₂ CF ₃	7.6	0.28		3,380	1030	314
HFC-365mfc	CH ₃ CF ₂ CH ₂ CF ₃	8.6	0.21		2,520	794	241
HFC-43-10mee	CF ₃ CHFCH ₂ CF ₂ CF ₃	15.9	0.4	1,300	4,140	1,640	500
Perfluorinated compounds							
Sulphur hexafluoride	SF ₆	3,200	0.52	23,900	16,300	22,800	32,600
Nitrogen trifluoride	NF ₃	740	0.21		12,300	17,200	20,700
PFC-14	CF ₄	50,000	0.10	6,500	5,210	7,390	11,200
PFC-116	C ₂ F ₆	10,000	0.26	9,200	8,630	12,200	18,200

Table TS.2 (continued)

Industrial Designation or Common Name (years)	Chemical Formula	Lifetime (years)	Radiative Efficiency (W m ⁻² ppb ⁻¹)	Global Warming Potential for Given Time Horizon			
				SAR [‡] (100-yr)	20-yr	100-yr	500-yr
Perfluorinated compounds (continued)							
PFC-218	C ₃ F ₈	2,600	0.26	7,000	6,310	8,830	12,500
PFC-318	c-C ₄ F ₈	3,200	0.32	8,700	7,310	10,300	14,700
PFC-3-1-10	C ₄ F ₁₀	2,600	0.33	7,000	6,330	8,860	12,500
PFC-4-1-12	C ₅ F ₁₂	4,100	0.41		6,510	9,160	13,300
PFC-5-1-14	C ₆ F ₁₄	3,200	0.49	7,400	6,600	9,300	13,300
PFC-9-1-18	C ₁₀ F ₁₈	>1,000 ^d	0.56		>5,500	>7,500	>9,500
trifluoromethyl sulphur pentafluoride	SF ₅ CF ₃	800	0.57		13,200	17,700	21,200
Fluorinated ethers							
HFE-125	CHF ₂ OCF ₃	136	0.44		13,800	14,900	8,490
HFE-134	CHF ₂ OCHF ₂	26	0.45		12,200	6,320	1,960
HFE-143a	CH ₃ OCF ₃	4.3	0.27		2,630	756	230
HCFE-235da2	CHF ₂ OCHClCF ₃	2.6	0.38		1,230	350	106
HFE-245cb2	CH ₃ OCF ₂ CHF ₂	5.1	0.32		2,440	708	215
HFE-245fa2	CHF ₂ OCH ₂ CF ₃	4.9	0.31		2,280	659	200
HFE-254cb2	CH ₃ OCF ₂ CHF ₂	2.6	0.28		1,260	359	109
HFE-347mcc3	CH ₃ OCF ₂ CF ₂ CF ₃	5.2	0.34		1,980	575	175
HFE-347pcf2	CHF ₂ CF ₂ OCH ₂ CF ₃	7.1	0.25		1,900	580	175
HFE-356pcc3	CH ₃ OCF ₂ CF ₂ CHF ₂	0.33	0.93		386	110	33
HFE-449sl (HFE-7100)	C ₄ F ₉ OCH ₃	3.8	0.31		1,040	297	90
HFE-569sf2 (HFE-7200)	C ₄ F ₉ OC ₂ H ₅	0.77	0.3		207	59	18
HFE-43-10pccc124 (H-Galden 1040x)	CHF ₂ OCF ₂ OC ₂ F ₄ OCHF ₂	6.3	1.37		6,320	1,870	569
HFE-236ca12 (HG-10)	CHF ₂ OCF ₂ OCHF ₂	12.1	0.66		8,000	2,800	860
HFE-338pcc13 (HG-01)	CHF ₂ OCF ₂ CF ₂ OCHF ₂	6.2	0.87		5,100	1,500	460
Perfluoropolyethers							
PFPME	CF ₃ OCF(CF ₃)CF ₂ OCF ₂ OCF ₃	800	0.65		7,620	10,300	12,400
Hydrocarbons and other compounds – Direct Effects							
Dimethylether	CH ₃ OCH ₃	0.015	0.02		1	1	<<1
Methylene chloride	CH ₂ Cl ₂	0.38	0.03		31	8.7	2.7
Methyl chloride	CH ₃ Cl	1.0	0.01		45	13	4

Notes:

[‡] SAR refers to the IPCC Second Assessment Report (1995) used for reporting under the UNFCCC.

^a The CO₂ response function used in this report is based on the revised version of the Bern Carbon cycle model used in Chapter 10 of this report (Bern2.5CC; Joos et al. 2001) using a background CO₂ concentration value of 378 ppm. The decay of a pulse of CO₂ with time t is given by

$$a_0 + \sum_{i=1}^3 a_i \cdot e^{-t/\tau_i} \quad \text{where } a_0 = 0.217, a_1 = 0.259, a_2 = 0.338, a_3 = 0.186, \tau_1 = 172.9 \text{ years}, \tau_2 = 18.51 \text{ years}, \text{ and } \tau_3 = 1.186 \text{ years, for } t < 1,000 \text{ years.}$$

^b The radiative efficiency of CO₂ is calculated using the IPCC (1990) simplified expression as revised in the TAR, with an updated background concentration value of 378 ppm and a perturbation of +1 ppm (see Section 2.10.2).

^c The perturbation lifetime for CH₄ is 12 years as in the TAR (see also Section 7.4). The GWP for CH₄ includes indirect effects from enhancements of ozone and stratospheric water vapour (see Section 2.10).

^d The assumed lifetime of 1000 years is a lower limit.

are largely controlled by climate processes and feedbacks. For example, sea ice-albedo feedbacks tend to enhance the high-latitude response. Spatial patterns of response are also affected by differences in thermal inertia between land and sea areas. {2.8, 9.2}

The pattern of response to a radiative forcing can be altered substantially if its structure is favourable for affecting a particular aspect of the atmospheric structure or circulation. Modelling studies and data comparisons suggest that mid- to high-latitude circulation patterns are *likely* to be affected by some forcings such as volcanic eruptions, which have been linked to changes in the Northern Annular Mode (NAM) and North Atlantic Oscillation (NAO) (see Section 3.1 and Box TS.2). Simulations also suggest that absorbing aerosols, particularly black carbon, can reduce the solar radiation reaching the surface and can warm the atmosphere at regional scales, affecting the vertical temperature profile and the large-scale atmospheric circulation. {2.8, 7.5, 9.2}

The spatial patterns of radiative forcings for ozone, aerosol direct effects, aerosol-cloud interactions and land use have considerable uncertainties. This is in contrast to the relatively high confidence in the spatial pattern of radiative forcing for the LLGHGs. The net positive radiative forcing in the Southern Hemisphere (SH) *very likely* exceeds that in the NH because of smaller aerosol concentrations in the SH. {2.9}

TS 2.6 Surface Forcing and the Hydrologic Cycle

Observations and models indicate that changes in the radiative flux at the Earth's surface affect the surface heat and moisture budgets, thereby involving the hydrologic cycle. Recent studies indicate that some forcing agents can influence the hydrologic cycle differently than others through their interactions with clouds. In particular, changes in aerosols may have affected precipitation and other aspects of the hydrologic cycle more strongly than other anthropogenic forcing agents. Energy deposited at the surface directly affects evaporation and sensible heat transfer. The instantaneous radiative flux change at the surface (hereafter called 'surface forcing') is a useful diagnostic tool for understanding changes in the heat and moisture surface budgets and the accompanying climate change. However, unlike radiative forcing, it cannot be used to quantitatively compare the effects of different agents on the equilibrium global mean surface temperature change. Net radiative forcing and surface forcing have different equator-to-pole gradients in the NH, and are different between the NH and SH. {2.9, 7.2, 7.5, 9.5}

TS.3 Observations of Changes in Climate

This assessment evaluates changes in the Earth's climate system, considering not only the atmosphere, but also the ocean and the cryosphere, as well as phenomena such as atmospheric circulation changes, in order to increase understanding of trends, variability and processes of climate change at global and regional scales. Observational records employing direct methods are of variable length as described below, with global temperature estimates now beginning as early as 1850. Observations of extremes of weather and climate are discussed, and observed changes in extremes are described. The consistency of observed changes among different climate variables that allows an increasingly comprehensive picture to be drawn is also described. Finally, palaeoclimatic information that generally employs indirect proxies to infer information about climate change over longer time scales (up to millions of years) is also assessed.

TS.3.1 Atmospheric Changes: Instrumental Record

This assessment includes analysis of global and hemispheric means, changes over land and ocean and distributions of trends in latitude, longitude and altitude. Since the TAR, improvements in observations and their calibration, more detailed analysis of methods and extended time series allow more in-depth analyses of changes including atmospheric temperature, precipitation, humidity, wind and circulation. Extremes of climate are a key expression of climate variability, and this assessment includes new data that permit improved insights into the changes in many types of extreme events including heat waves, droughts, heavy precipitation and tropical cyclones (including hurricanes and typhoons). {3.2–3.4, 3.8}

Furthermore, advances have occurred since the TAR in understanding how a number of seasonal and long-term anomalies can be described by patterns of climate variability. These patterns arise from internal interactions and from the differential effects on the atmosphere of land and ocean, mountains and large changes in heating. Their response is often felt in regions far removed from their physical source through atmospheric teleconnections associated with large-scale waves in the atmosphere. Understanding temperature and precipitation anomalies associated with the dominant patterns of climate variability is essential to understanding many regional climate anomalies and why these may differ from those at the global scale. Changes in storm tracks, the jet streams,

regions of preferred blocking anticyclones and changes in monsoons can also occur in conjunction with these preferred patterns of variability. {3.5–3.7}

TS.3.1.1 Global Average Temperatures

2005 and 1998 were the warmest two years in the instrumental global surface air temperature record since 1850. Surface temperatures in 1998 were enhanced by the major 1997–1998 El Niño but no such strong anomaly was present in 2005. Eleven of the last 12 years (1995 to 2006) – the exception being 1996 – rank among the 12 warmest years on record since 1850. {3.2}

The global average surface temperature has increased, especially since about 1950. The updated 100-year trend (1906–2005) of $0.74^{\circ}\text{C} \pm 0.18^{\circ}\text{C}$ is larger than the 100-year warming trend at the time of the TAR (1901–2000) of $0.6^{\circ}\text{C} \pm 0.2^{\circ}\text{C}$ due to additional warm years. The total temperature increase from 1850–1899 to 2001–2005 is $0.76^{\circ}\text{C} \pm 0.19^{\circ}\text{C}$. The rate of warming averaged over the last 50 years ($0.13^{\circ}\text{C} \pm 0.03^{\circ}\text{C}$ per decade) is nearly twice that for the last 100 years. Three different global estimates all show consistent warming trends. There is also consistency between the data sets in their separate land and ocean domains, and between sea surface temperature (SST) and nighttime marine air temperature (see Figure TS.6). {3.2}

Recent studies confirm that effects of urbanisation and land use change on the global temperature record are negligible (less than 0.006°C per decade over land and zero over the ocean) as far as hemispheric- and continental-scale averages are concerned. All observations are subject to data quality and consistency checks to correct for potential biases. The real but local effects of urban areas are accounted for in the land temperature data sets used. Urbanisation and land use effects are not relevant to the widespread oceanic warming that has been observed. Increasing evidence suggests that urban heat island effects also affect precipitation, cloud and diurnal temperature range (DTR). {3.2}

The global average DTR has stopped decreasing. A decrease in DTR of approximately 0.1°C per decade was reported in the TAR for the period 1950 to 1993. Updated observations reveal that DTR has not changed from 1979 to 2004 as both day- and night time temperature have risen at about the same rate. The trends are highly variable from one region to another. {3.2}

New analyses of radiosonde and satellite measurements of lower- and mid-tropospheric temperature show warming rates that are generally consistent with each other and with those in the surface temperature record within their respective uncertainties for the periods 1958 to 2005 and 1979 to 2005. This largely resolves a discrepancy noted in the TAR (see Figure TS.7). The radiosonde record is markedly less spatially complete than the surface record and increasing evidence suggests that a number of radiosonde data sets are unreliable, especially in the tropics. Disparities remain among different tropospheric temperature trends estimated from satellite Microwave Sounding Unit (MSU) and advanced MSU measurements since 1979, and all likely still contain residual errors. However, trend estimates have been substantially improved and data set differences reduced since the TAR, through adjustments for changing satellites, orbit decay and drift in local crossing time (diurnal cycle effects). It appears that the satellite tropospheric temperature record is broadly consistent with surface temperature trends provided that the stratospheric influence on MSU channel 2 is accounted for. The range across different data sets of global surface warming since 1979 is 0.16°C to 0.18°C per decade, compared to 0.12°C to 0.19°C per decade for MSU-derived estimates of tropospheric temperatures. It is likely that there is increased warming with altitude from the surface through much of the troposphere in the tropics, pronounced cooling in the stratosphere, and a trend towards a higher tropopause. {3.4}

Stratospheric temperature estimates from adjusted radiosondes, satellites and reanalyses are all in qualitative agreement, with a cooling of between 0.3°C and 0.6°C per decade since 1979 (see Figure TS.7). Longer radiosonde records (back to 1958) also indicate stratospheric cooling but are subject to substantial instrumental uncertainties. The rate of cooling increased after 1979 but has slowed in the last decade. It is *likely* that radiosonde records overestimate stratospheric cooling, owing to changes in sondes not yet taken into account. The trends are not monotonic, because of stratospheric warming episodes that follow major volcanic eruptions. {3.4}

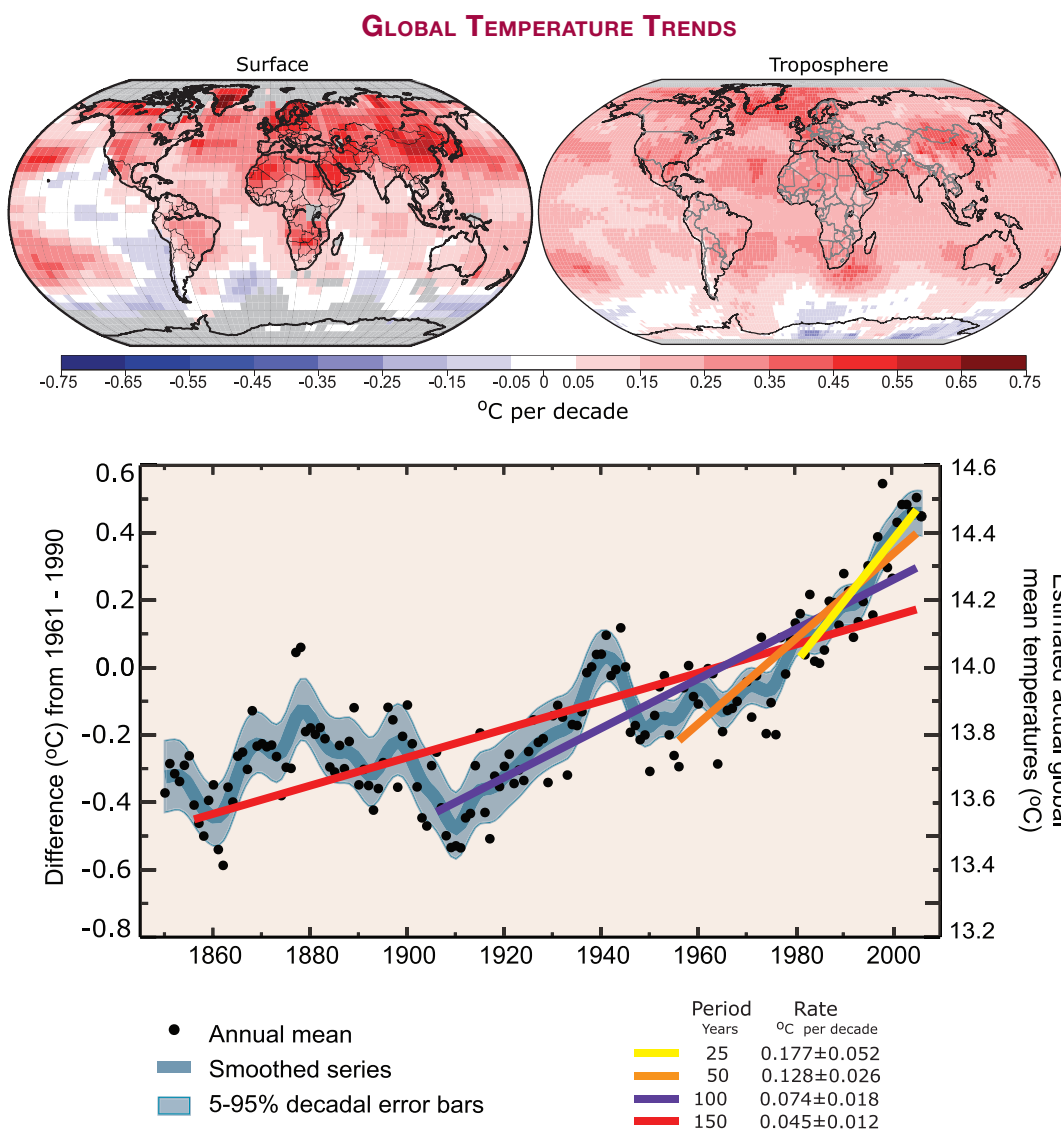


Figure TS.6. (Top) Patterns of linear global temperature trends over the period 1979 to 2005 estimated at the surface (left), and for the troposphere from satellite records (right). Grey indicates areas with incomplete data. (Bottom) Annual global mean temperatures (black dots) with linear fits to the data. The left hand axis shows temperature anomalies relative to the 1961 to 1990 average and the right hand axis shows estimated actual temperatures, both in °C. Linear trends are shown for the last 25 (yellow), 50 (orange), 100 (purple) and 150 years (red). The smooth blue curve shows decadal variations (see Appendix 3.A), with the decadal 90% error range shown as a pale blue band about that line. The total temperature increase from the period 1850 to 1899 to the period 2001 to 2005 is $0.76\text{ °C} \pm 0.19\text{ °C}$. {FAQ 3.1, Figure 1.}

TS.3.1.2 Spatial Distribution of Changes in Temperature, Circulation and Related Variables

Surface temperatures over land regions have warmed at a faster rate than over the oceans in both hemispheres. Longer records now available show significantly faster rates of warming over land than ocean in the past two decades (about 0.27 °C vs. 0.13 °C per decade). {3.2}

The warming in the last 30 years is widespread over the globe, and is greatest at higher northern latitudes. The greatest warming has occurred in the NH winter (DJF) and spring (MAM). Average arctic temperatures have been increasing at almost twice the rate of the rest of the world in the past 100 years. However, arctic temperatures are highly variable. A slightly longer arctic warm period, almost as warm as the present, was observed from 1925 to 1945, but its geographical distribution appears to have been different from the recent warming since its extent was not global. {3.2}

There is evidence for long-term changes in the large-scale atmospheric circulation, such as a poleward shift and strengthening of the westerly winds. Regional climate trends can be very different from the global average, reflecting changes in the circulations and interactions of the atmosphere and ocean and the other components of the climate system. Stronger mid-latitude westerly wind maxima have occurred in both hemispheres in most seasons from at least 1979 to the late 1990s, and poleward displacements of corresponding Atlantic and southern polar front jet streams have been documented. The westerlies in the NH increased from the 1960s to the 1990s but have since returned to values close to the long-term average. The increased strength of the westerlies in the NH changes the flow from oceans to continents, and is a major factor in the observed winter changes in storm tracks and related patterns of precipitation and temperature trends at mid- and high-latitudes. Analyses of wind and significant wave height support reanalysis-based evidence for changes in NH extratropical storms from the start of the reanalysis record in the late 1970s until the late 1990s. These changes are accompanied by a tendency towards stronger winter polar vortices throughout the troposphere and lower stratosphere. {3.2, 3.5}

Many regional climate changes can be described in terms of preferred patterns of climate variability and therefore as changes in the occurrence of indices that characterise the strength and phase of these patterns. The importance, over all time scales, of fluctuations in the westerlies and storm tracks in the North Atlantic has often been noted, and these fluctuations are described by the NAO (see Box TS.2 for an explanation of this and other preferred patterns). The characteristics of fluctuations in the zonally averaged westerlies in the two hemispheres have more recently been described by their respective ‘annular modes’, the Northern and Southern Annular Modes (NAM and SAM). The observed changes can be expressed as a shift of the circulation towards the structure associated with one sign of these preferred patterns. The increased mid-latitude westerlies in the North Atlantic can be largely viewed as reflecting either NAO or NAM changes; multi-decadal variability is also evident in the Atlantic, both in the atmosphere and the ocean. In the SH, changes in circulation related to an increase in the

OBSERVED AIR TEMPERATURES

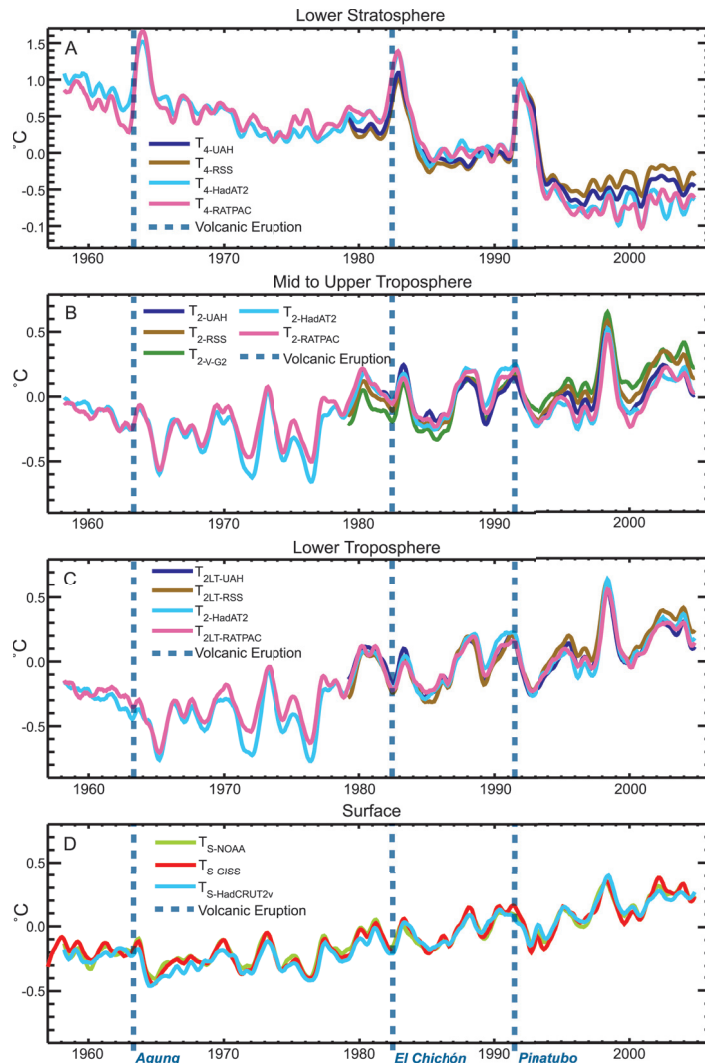


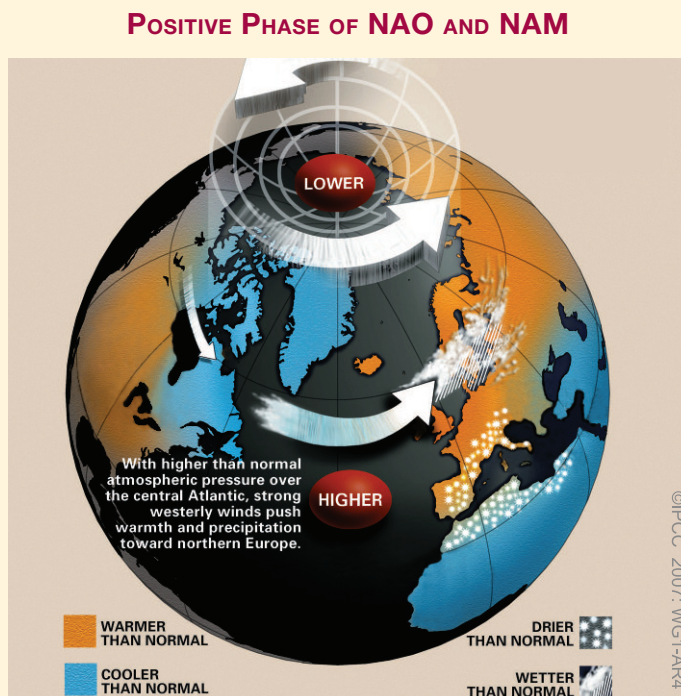
Figure TS.7. Observed surface (D) and upper air temperatures for the lower troposphere (C), mid- to upper troposphere (B) and lower stratosphere (A), shown as monthly mean anomalies relative to the period 1979 to 1997 smoothed with a seven-month running mean filter. Dashed lines indicate the times of major volcanic eruptions. {Figure 3.17}

SAM from the 1960s to the present are associated with strong warming over the Antarctic Peninsula and, to a lesser extent, cooling over parts of continental Antarctica. Changes have also been observed in ocean-atmosphere interactions in the Pacific. The ENSO is the dominant mode of global-scale variability on interannual time scales although there have been times when it is less apparent. The 1976–1977 climate shift, related to the phase change in the Pacific Decadal Oscillation (PDO) towards more El Niño events and changes in the evolution of ENSO, has affected many areas, including most tropical monsoons. For instance, over North America, ENSO and Pacific-

Box TS.2: Patterns (Modes) of Climate Variability

Analysis of atmospheric and climatic variability has shown that a significant component of it can be described in terms of fluctuations in the amplitude and sign of indices of a relatively small number of preferred patterns of variability. Some of the best known of these are:

- El Niño-Southern Oscillation (ENSO), a coupled fluctuation in the atmosphere and the equatorial Pacific Ocean, with preferred time scales of two to about seven years. ENSO is often measured by the difference in surface pressure anomalies between Tahiti and Darwin and the SSTs in the central and eastern equatorial Pacific. ENSO has global teleconnections.
- North Atlantic Oscillation (NAO), a measure of the strength of the Icelandic Low and the Azores High, and of the westerly winds between them, mainly in winter. The NAO has associated fluctuations in the storm track, temperature and precipitation from the North Atlantic into Eurasia (see Box TS.2, Figure 1).
- Northern Annular Mode (NAM), a winter fluctuation in the amplitude of a pattern characterised by low surface pressure in the Arctic and strong mid-latitude westerlies. The NAM has links with the northern polar vortex and hence the stratosphere.
- Southern Annular Mode (SAM), the fluctuation of a pattern with low antarctic surface pressure and strong mid-latitude westerlies, analogous to the NAM, but present year round.
- Pacific-North American (PNA) pattern, an atmospheric large-scale wave pattern featuring a sequence of tropospheric high- and low-pressure anomalies stretching from the subtropical west Pacific to the east coast of North America.
- Pacific Decadal Oscillation (PDO), a measure of the SSTs in the North Pacific that has a very strong correlation with the North Pacific Index (NPI) measure of the depth of the Aleutian Low. However, it has a signature throughout much of the Pacific.



Box TS.2, Figure 1. A schematic of the changes associated with the positive phase of the NAO and NAM. The changes in pressure and winds are shown, along with precipitation changes. Warm colours indicate areas that are warmer than normal and blue indicates areas that are cooler than normal.

The extent to which all these preferred patterns of variability can be considered to be true modes of the climate system is a topic of active research. However, there is evidence that their existence can lead to larger-amplitude regional responses to forcing than would otherwise be expected. In particular, a number of the observed 20th-century climate changes can be viewed in terms of changes in these patterns. It is therefore important to test the ability of climate models to simulate them (see Section TS.4, Box TS.7) and to consider the extent to which observed changes related to these patterns are linked to internal variability or to anthropogenic climate change. {3.6, 8.4}

North American (PNA) teleconnection-related changes appear to have led to contrasting changes across the continent, as the western part has warmed more than the eastern part, while the latter has become cloudier and wetter. There is substantial low-frequency atmospheric variability in the Pacific sector over the 20th century, with extended periods of weakened (1900–1924; 1947–1976) as well as strengthened (1925–1946; 1977–2003) circulation. {3.2, 3.5, 3.6}

Changes in extremes of temperature are consistent with warming. Observations show widespread reductions in the number of frost days in mid-latitude regions, increases in the number of warm extremes (warmest 10% of days or nights) and a reduction in the number of daily cold extremes (coldest 10% of days or nights) (see Box TS.5). The most marked changes are for cold nights, which have declined over the 1951 to 2003 period for all regions where data are available (76% of the land). {3.8}

Heat waves have increased in duration beginning in the latter half of the 20th century. The record-breaking heat wave over western and central Europe in the summer of 2003 is an example of an exceptional recent extreme. That summer (JJA) was the warmest since comparable instrumental records began around 1780 (1.4°C above the previous warmest in 1807). Spring drying of the land surface over Europe was an important factor in the occurrence of the extreme 2003 temperatures. Evidence suggests that heat waves have also increased in frequency and duration in other locations. The very strong correlation between observed dryness and high temperatures over land in the tropics during summer highlights the important role moisture plays in moderating climate. {3.8, 3.9}

There is insufficient evidence to determine whether trends exist in such events as tornadoes, hail, lightning and dust storms which occur at small spatial scales. {3.8}

TS.3.1.3 Changes in the Water Cycle: Water Vapour, Clouds, Precipitation and Tropical Storms

Tropospheric water vapour is increasing (Figure TS.8). Surface specific humidity has generally increased since 1976 in close association with higher temperatures over both land and ocean. Total column water vapour has increased over the global oceans by $1.2 \pm 0.3\%$ per decade (95% confidence limits) from 1988 to 2004. The observed regional changes are consistent in pattern and amount with the changes in SST and the assumption of a near-constant relative humidity increase in water vapour mixing ratio. The additional atmospheric water vapour implies increased moisture availability for precipitation. {3.4}

ATMOSPHERIC WATER VAPOUR

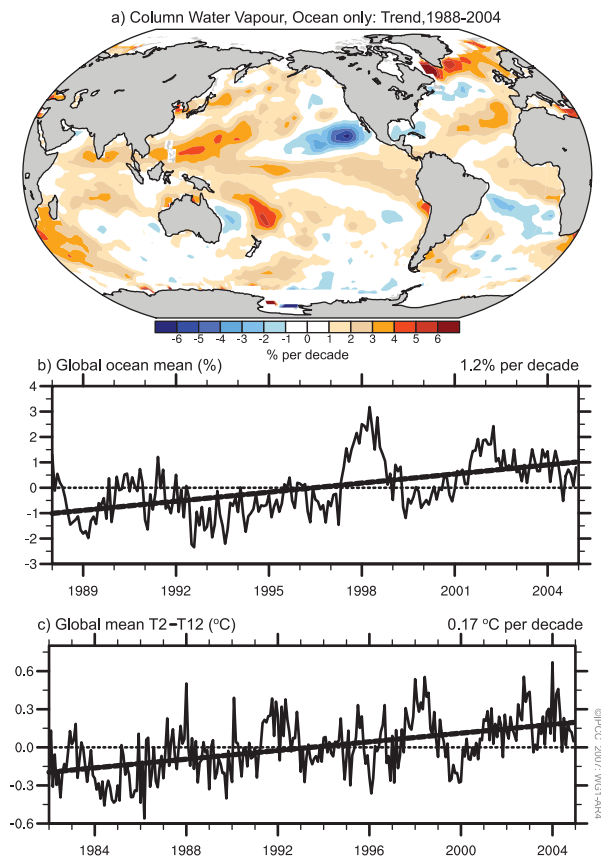


Figure TS.8. (a) Linear trends in precipitable water (total column water vapour) over the period 1988 to 2004 (% per decade) and (b) the monthly time series of anomalies, relative to the period shown, over the global ocean with linear trend. (c) The global mean (80°N to 80°S) radiative signature of upper-tropospheric moistening is given by monthly time series of combinations of satellite brightness temperature anomalies (°C), relative to the period 1982 to 2004, with the dashed line showing the linear trend of the key brightness temperature in °C per decade. {3.4, Figures 3.20 and 3.21}

Upper-tropospheric water vapour is also increasing. Due to instrumental limitations, it is difficult to assess long-term changes in water vapour in the upper troposphere, where it is of radiative importance. However, the available data now show evidence for global increases in upper-tropospheric specific humidity over the past two decades (Figure TS.8). These observations are consistent with the observed increase in temperatures and represent an important advance since the TAR. {3.4}

Cloud changes are dominated by ENSO. Widespread (but not ubiquitous) decreases in continental DTR have coincided with increases in cloud amounts. Surface and satellite observations disagree on changes in total and low-level cloud changes over the ocean. However, radiation

changes at the top of the atmosphere from the 1980s to 1990s (possibly related in part to the ENSO phenomenon) appear to be associated with reductions in tropical upper-level cloud cover, and are consistent with changes in the energy budget and in observed ocean heat content. {3.4}

‘Global dimming’ is not global in extent and it has not continued after 1990. Reported decreases in solar radiation at the Earth’s surface from 1970 to 1990 have an urban bias. Further, there have been increases since about 1990. An increasing aerosol load due to human activities decreases regional air quality and the amount of solar radiation reaching the Earth’s surface. In some areas, such as Eastern Europe, recent observations of a reversal in the sign of this effect link changes in solar radiation to concurrent air quality improvements. {3.4}

Long-term trends in precipitation amounts from 1900 to 2005 have been observed in many large regions (Figure TS.9). Significantly increased precipitation has been observed in the eastern parts of North and South America, northern Europe and northern and central Asia. Drying has been observed in the Sahel, the Mediterranean, southern Africa and parts of southern Asia. Precipitation is highly variable spatially and temporally, and robust long-term trends have not been established for other large regions.⁵ {3.3}

Substantial increases in heavy precipitation events have been observed. It is *likely* that there have been increases in the number of heavy precipitation events (e.g., above the 95th percentile) in many land regions since about 1950, even in those regions where there has been a reduction in total precipitation amount. Increases have also been reported for rarer precipitation events (1 in 50 year return period), but only a few regions have sufficient data to assess such trends reliably (see Figure TS.10). {3.8}

There is observational evidence for an increase of intense tropical cyclone activity in the North Atlantic since about 1970, correlated with increases in tropical SSTs. There are also suggestions of increased intense tropical cyclone activity in some other regions where concerns over data quality are greater. Multi-decadal variability and the quality of the tropical cyclone records prior to routine satellite observations in about 1970 complicate the detection of long-term trends in tropical cyclone activity and there is no clear trend in the annual numbers of tropical cyclones. Estimates of the potential destructiveness of tropical cyclones suggest a substantial upward trend since the mid-1970s, with a trend towards longer lifetimes and greater intensity. Trends are also apparent in SST, a critical variable known to influence

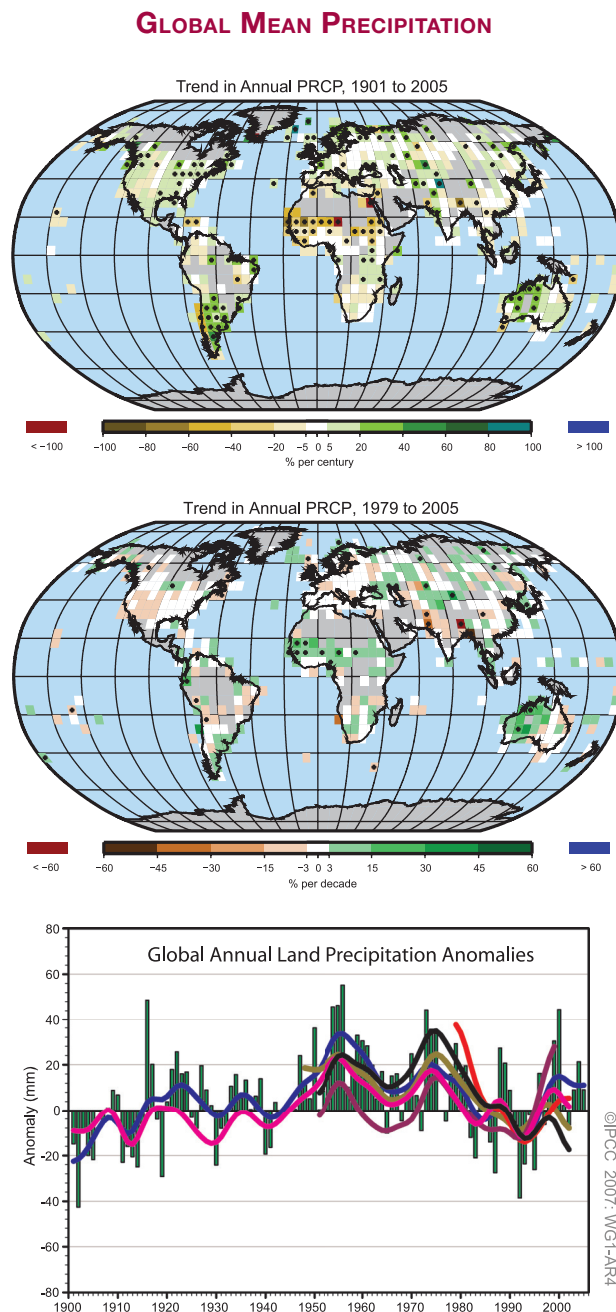


Figure TS.9. (Top) Distribution of linear trends of annual land precipitation amounts over the period 1901 to 2005 (% per century) and (middle) 1979 to 2005 (% per decade). Areas in grey have insufficient data to produce reliable trends. The percentage is based on the 1961 to 1990 period. (Bottom) Time series of annual global land precipitation anomalies with respect to the 1961 to 1990 base period for 1900 to 2005. The smooth curves show decadal variations (see Appendix 3.A) for different data sets. {3.3, Figures 3.12 and 3.13}

⁵ The assessed regions are those considered in the regional projections chapter of the TAR and in Chapter 11 of this report.

ANNUAL PRECIPITATION TRENDS

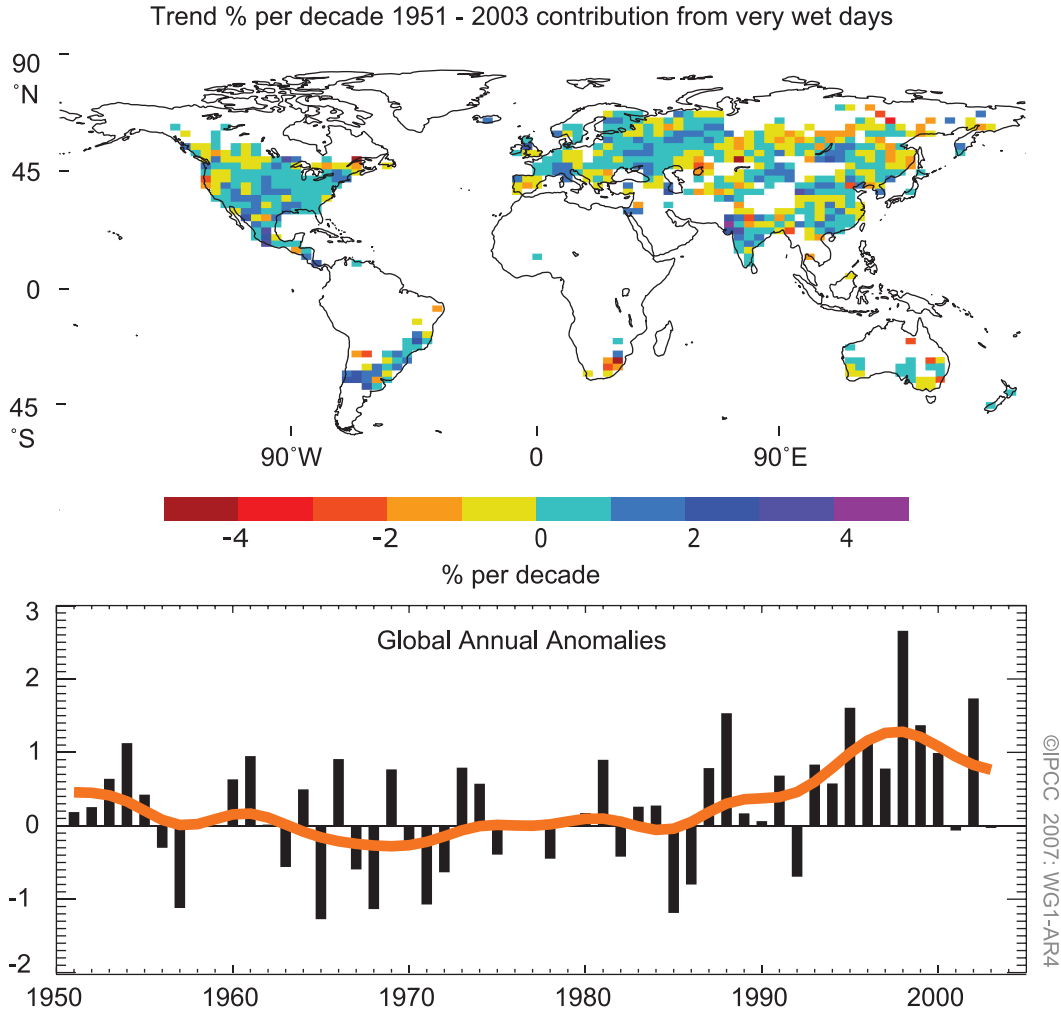


Figure TS.10. (Top) Observed trends (% per decade) over the period 1951 to 2003 in the contribution to total annual precipitation from very wet days (i.e., corresponding to the 95th percentile and above). White land areas have insufficient data for trend determination. (Bottom) Anomalies (%) of the global (regions with data shown in top panel) annual time series of very wet days (with respect to 1961–1990) defined as the percentage change from the base period average (22.5%). The smooth orange curve shows decadal variations (see Appendix 3.A). {Figure 3.39}

ANNUAL SEA-SURFACE TEMPERATURE ANOMALIES

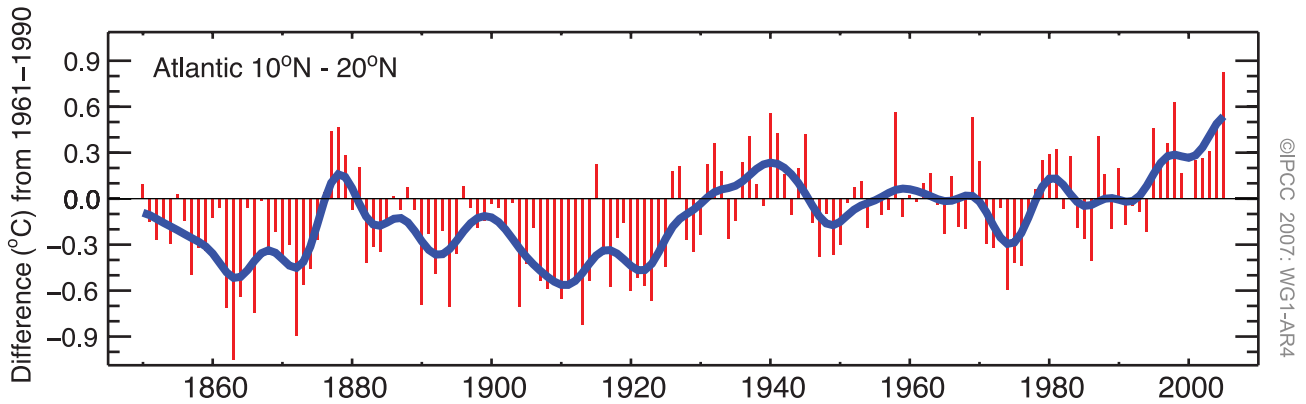


Figure TS.11. Tropical Atlantic (10°N–20°N) sea surface temperature annual anomalies (°C) in the region of Atlantic hurricane formation, relative to the 1961 to 1990 mean. {Figure 3.33}

tropical cyclone development (see Figure TS.11). Variations in the total numbers of tropical cyclones result from ENSO and decadal variability, which also lead to a redistribution of tropical storm numbers and tracks. The numbers of hurricanes in the North Atlantic have been above normal (based on 1981–2000) in nine of the years from 1995 to 2005. {3.8}

More intense and longer droughts have been observed over wider areas, particularly in the tropics and subtropics since the 1970s. While there are many different measures of drought, many studies use precipitation changes together with temperature.⁶ Increased drying due to higher temperatures and decreased land precipitation have contributed to these changes. {3.3}

TS.3.2 Changes in the Cryosphere: Instrumental Record

Currently, ice permanently covers 10% of the land surface, with only a tiny fraction occurring outside Antarctica and Greenland. Ice also covers approximately 7% of the oceans in the annual mean. In midwinter, snow covers approximately 49% of the land surface in the NH. An important property of snow and ice is its high surface albedo. Because up to 90% of the incident solar radiation is reflected by snow and ice surfaces, while only about 10% is reflected by the open ocean or forested lands, changes in snow and ice cover are important feedback mechanisms in climate change. In addition, snow and ice are effective insulators. Seasonally frozen ground is more extensive than snow cover, and its presence is important for energy and moisture fluxes. Therefore, frozen surfaces play important roles in energy and climate processes. {4.1}

The cryosphere stores about 75% of the world's freshwater. At a regional scale, variations in mountain snowpack, glaciers and small ice caps play a crucial role in freshwater availability. Since the change from ice to liquid water occurs at specific temperatures, ice is a component of the climate system that could be subject to abrupt change following sufficient warming. Observations and analyses of changes in ice have expanded and improved since the TAR, including shrinkage of mountain glacier volume, decreases in snow cover, changes in permafrost and frozen ground, reductions in arctic sea ice extent, coastal thinning of the Greenland Ice Sheet exceeding inland thickening from increased snowfall, and reductions in seasonally frozen ground and river and lake ice cover.

These allow an improved understanding of how the cryosphere is changing, including its contributions to recent changes in sea level. The periods from 1961 to the present and from 1993 to the present are a focus of this report, due to the availability of directly measured glacier mass balance data and altimetry observations of the ice sheets, respectively. {4.1}

Snow cover has decreased in most regions, especially in spring. Northern Hemisphere snow cover observed by satellite over the 1966 to 2005 period decreased in every month except November and December, with a stepwise drop of 5% in the annual mean in the late 1980s (see Figure TS.12). In the SH, the few long records or proxies mostly show either decreases or no changes in the past 40 years or more. Northern Hemisphere April snow cover extent is strongly correlated with 40°N to 60°N April temperature, reflecting the feedback between snow and temperature. {4.2}

Decreases in snowpack have been documented in several regions worldwide based upon annual time series of mountain snow water equivalent and snow depth. Mountain snow can be sensitive to small changes in temperature, particularly in temperate climatic zones where the transition from rain to snow is generally closely associated with the altitude of the freezing level. Declines in mountain snowpack in western North America and in the Swiss Alps are largest at lower, warmer elevations. Mountain snow water equivalent has declined since 1950 at 75% of the stations monitored in western North America. Mountain snow depth has also declined in the Alps and in southeastern Australia. Direct observations of snow depth are too limited to determine changes in the Andes, but temperature measurements suggest that the altitude where snow occurs (above the snow line) has probably risen in mountainous regions of South America. {4.2}

Permafrost and seasonally frozen ground in most regions display large changes in recent decades. Changes in permafrost conditions can affect river runoff, water supply, carbon exchange and landscape stability, and can cause damage to infrastructure. Temperature increases at the top of the permafrost layer of up to 3°C since the 1980s have been reported. Permafrost warming has also been observed with variable magnitude in the Canadian Arctic, Siberia, the Tibetan Plateau and Europe. The permafrost base is thawing at a rate ranging from 0.04 m yr⁻¹ in Alaska to 0.02 m yr⁻¹ on the Tibetan Plateau. {4.7}

The maximum area covered by seasonally frozen ground decreased by about 7% in the NH over the

⁶ Precipitation and temperature are combined in the Palmer Drought Severity Index (PDSI), considered in this report as one measure of drought. The PDSI does not include variables such as wind speed, solar radiation, cloudiness and water vapour but is a superior measure to precipitation alone.

Box TS.3: Ice Sheet Dynamics and Stability

Ice sheets are thick, broad masses of ice formed mainly from compaction of snow. They spread under their own weight, transferring mass towards their margins where it is lost primarily by runoff of surface melt water or by calving of icebergs into marginal seas or lakes. Ice sheets flow by deformation within the ice or melt water-lubricated sliding over materials beneath. Rapid basal motion requires that the basal temperature be raised to the melting point by heat from the Earth's interior, delivered by melt water transport, or from the 'friction' of ice motion. Sliding velocities under a given gravitational stress can differ by several orders of magnitude, depending on the presence or absence of deformable sediment, the roughness of the substrate and the supply and distribution of water. Basal conditions are generally poorly characterised, introducing important uncertainties to the understanding of ice sheet stability. {4.6}

Ice flow is often channelled into fast-moving ice streams (that flow between slower-moving ice walls) or outlet glaciers (with rock walls). Enhanced flow in ice streams arises either from higher gravitational stress linked to thicker ice in bedrock troughs, or from increased basal lubrication. {4.6}

Ice discharged across the coast often remains attached to the ice sheet to become a floating ice shelf. An ice shelf moves forward, spreading and thinning under its own weight, and fed by snowfall on its surface and ice input from the ice sheet. Friction at ice shelf sides and over local shoals slows the flow of the ice shelf and thus the discharge from the ice sheet. An ice shelf loses mass by calving icebergs from the front and by basal melting into the ocean cavity beneath. Studies suggest an ocean warming of 1°C could increase ice shelf basal melt by 10 m yr⁻¹, but inadequate knowledge of the largely inaccessible ice shelf cavities restricts the accuracy of such estimates. {4.6}

The palaeo-record of previous ice ages indicates that ice sheets shrink in response to warming and grow in response to cooling, and that shrinkage can be far faster than growth. The volumes of the Greenland and Antarctic Ice Sheets are equivalent to approximately 7 m and 57 m of sea level rise, respectively. Palaeoclimatic data indicate that substantial melting of one or both ice sheets has likely occurred in the past. However, ice core data show that neither ice sheet was completely removed during warm periods of at least the past million years. Ice sheets can respond to environmental forcing over very long time scales, implying that commitments to future changes may result from current warming. For example, a surface warming may take more than 10,000 years to penetrate to the bed and change temperatures there. Ice velocity over most of an ice sheet changes slowly in response to changes in the ice sheet shape or surface temperature, but large velocity changes may occur rapidly in ice streams and outlet glaciers in response to changing basal conditions, penetration of surface melt water to the bed or changes in the ice shelves into which they flow. {4.6, 6.4}

Models currently configured for long integrations remain most reliable in their treatment of surface accumulation and ablation, as for the TAR, but do not include full treatments of ice dynamics; thus, analyses of past changes or future projections using such models may underestimate ice flow contributions to sea level rise, but the magnitude of such an effect is unknown. {8.2}

latter half of the 20th century, with a decrease in spring of up to 15%. Its maximum depth has decreased by about 0.3 m in Eurasia since the mid-20th century. In addition, maximum seasonal thaw depth increased by about 0.2 m in the Russian Arctic from 1956 to 1990. {4.7}

On average, the general trend in NH river and lake ice over the past 150 years indicates that the freeze-up date has become later at an average rate of 5.8 ± 1.9 days per century, while the breakup date has occurred earlier, at a rate of 6.5 ± 1.4 days per century. However, considerable spatial variability has also been observed, with some regions showing trends of opposite sign. {4.3}

Annual average arctic sea ice extent has shrunk by about $2.7 \pm 0.6\%$ per decade since 1978 based upon satellite observations (see Figure TS.13). The decline in summer extent is larger than in winter extent, with the summer minimum declining at a rate of about $7.4 \pm 2.4\%$ per decade. Other data indicate that the summer decline began around 1970. Similar observations in the Antarctic

reveal larger interannual variability but no consistent trends during the period of satellite observations. In contrast to changes in continental ice such as ice sheets and glaciers, changes in sea ice do not directly contribute to sea level change (because this ice is already floating), but can contribute to salinity changes through input of freshwater. {4.4}

During the 20th century, glaciers and ice caps have experienced widespread mass losses and have contributed to sea level rise. Mass loss of glaciers and ice caps (excluding those around the ice sheets of Greenland and Antarctica) is estimated to be 0.50 ± 0.18 mm yr⁻¹ in sea level equivalent (SLE) between 1961 and 2003, and 0.77 ± 0.22 mm yr⁻¹ SLE between 1991 and 2003. The late 20th-century glacier wastage *likely* has been a response to post-1970 warming. {4.5}

Recent observations show evidence for rapid changes in ice flow in some regions, contributing to sea level rise and suggesting that the dynamics of ice

motion may be a key factor in future responses of ice shelves, coastal glaciers and ice sheets to climate change. Thinning or loss of ice shelves in some near-coastal regions of Greenland, the Antarctic Peninsula and West Antarctica has been associated with accelerated flow of nearby glaciers and ice streams, suggesting that ice shelves (including short ice shelves of kilometres or tens of kilometres in length) could play a larger role

in stabilising or restraining ice motion than previously thought. Both oceanic and atmospheric temperatures appear to contribute to the observed changes. Large summer warming in the Antarctic Peninsula region *very likely* played a role in the subsequent rapid breakup of the Larsen B Ice Shelf in 2002 by increasing summer melt water, which drained into crevasses and wedged them open. Models do not accurately capture all of the physical processes that appear to be involved in observed iceberg calving (as in the breakup of Larsen B). {4.6}

CHANGES IN SNOW COVER

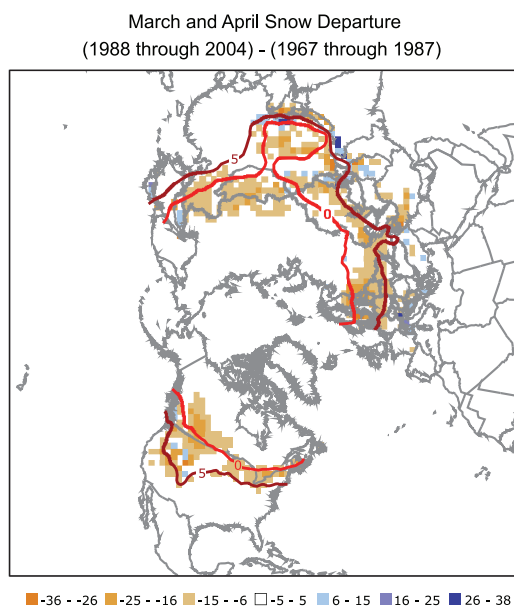
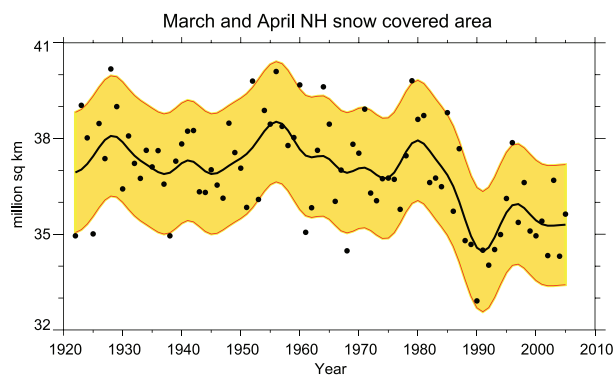


Figure TS.12. (Top) Northern Hemisphere March–April snow-covered area from a station-derived snow cover index (prior to 1972) and from satellite data (during and after 1972). The smooth curve shows decadal variations (see Appendix 3.A) with the 5 to 95% data range shaded in yellow. (Bottom) Differences in the distribution of March–April snow cover between earlier (1967–1987) and later (1988–2004) portions of the satellite era (expressed in percent coverage). Tan colours show areas where snow cover has declined. Red curves show the 0°C and 5°C isotherms averaged for March–April 1967 to 2004, from the Climatic Research Unit (CRU) gridded land surface temperature version 2 (CRUTEM2v) data. The greatest decline generally tracks the 0°C and 5°C isotherms, reflecting the strong feedback between snow and temperature. {Figures 4.2, 4.3}

CHANGES IN SEA ICE EXTENT

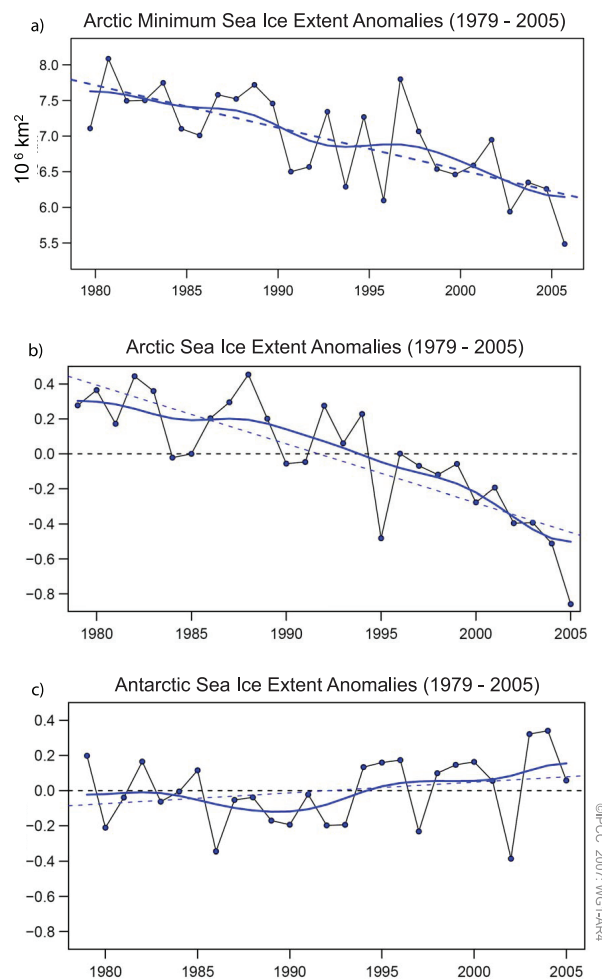


Figure TS.13. (a) Arctic minimum sea ice extent; (b) arctic sea ice extent anomalies; and (c) antarctic sea ice extent anomalies all for the period 1979 to 2005. Symbols indicate annual values while the smooth blue curves show decadal variations (see Appendix 3.A). The dashed lines indicate the linear trends. (a) Results show a linear trend of $-60 \pm 20 \times 10^3 \text{ km}^2 \text{ yr}^{-1}$, or approximately -7.4% per decade. (b) The linear trend is $-33 \pm 7.4 \times 10^3 \text{ km}^2 \text{ yr}^{-1}$ (equivalent to approximately -2.7% per decade) and is significant at the 95% confidence level. (c) Antarctic results show a small positive trend of $5.6 \pm 9.2 \times 10^3 \text{ km}^2 \text{ yr}^{-1}$, which is not statistically significant. {Figures 4.8 and 4.9}

The Greenland and Antarctic Ice Sheets taken together have *very likely* contributed to the sea level rise of the past decade. It is *very likely* that the Greenland Ice Sheet shrunk from 1993 to 2003, with thickening in central regions more than offset by increased melting in coastal regions. Whether the ice sheets have been growing or shrinking over time scales of longer than a decade is not well established from observations. Lack of agreement between techniques and the small number of estimates preclude assignment of best estimates or statistically rigorous error bounds for changes in ice sheet mass balances. However, acceleration of outlet glaciers drains ice from the interior and has been observed in both ice sheets (see Figure TS.14). Assessment of the data and techniques suggests a mass balance for the Greenland Ice Sheet of -50 to -100 Gt yr⁻¹ (shrinkage contributing to raising global sea level by 0.14 to

0.28 mm yr⁻¹) during 1993 to 2003, with even larger losses in 2005. There are greater uncertainties for earlier time periods and for Antarctica. The estimated range in mass balance for the Greenland Ice Sheet over the period 1961 to 2003 is between growth of 25 Gt yr⁻¹ and shrinkage by 60 Gt yr⁻¹ (-0.07 to $+0.17$ mm yr⁻¹ SLE). Assessment of all the data yields an estimate for the overall Antarctic Ice Sheet mass balance ranging from growth of 100 Gt yr⁻¹ to shrinkage of 200 Gt yr⁻¹ (-0.27 to $+0.56$ mm yr⁻¹ SLE) from 1961 to 2003, and from $+50$ to -200 Gt yr⁻¹ (-0.14 to $+0.55$ mm yr⁻¹ SLE) from 1993 to 2003. The recent changes in ice flow are *likely* to be sufficient to explain much or all of the estimated antarctic mass imbalance, with recent changes in ice flow, snowfall and melt water runoff sufficient to explain the mass imbalance of Greenland. {4.6, 4.8}

RATES OF OBSERVED SURFACE ELEVATION CHANGE

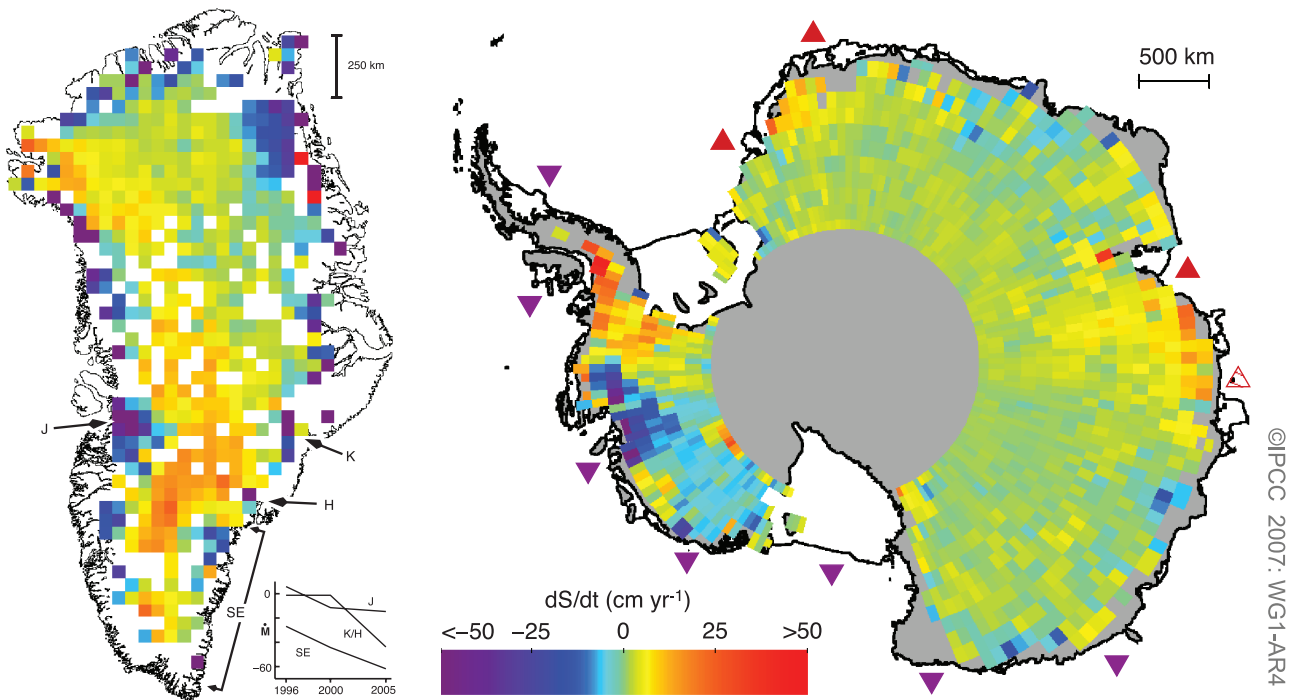


Figure TS.14. Rates of observed recent surface elevation change for Greenland (left; 1989–2005) and Antarctica (right; 1992–2005). Red hues indicate a rising surface and blue hues a falling surface, which typically indicate an increase or loss in ice mass at a site, although changes over time in bedrock elevation and in near-surface density can be important. For Greenland, the rapidly thinning outlet glaciers Jakobshavn (J), Kangerdlugssuaq (K), Helheim (H) and areas along the southeast coast (SE) are shown, together with their estimated mass balance vs. time (with K and H combined, in Gt yr⁻¹, with negative values indicating loss of mass from the ice sheet to the ocean). For Antarctica, ice shelves estimated to be thickening or thinning by more than 30 cm yr⁻¹ are shown by point-down purple triangles (thinning) and point-up red triangles (thickening) plotted just seaward of the relevant ice shelves. (Figures 4.17 and 4.19)

TS.3.3 Changes in the Ocean: Instrumental Record

The ocean plays an important role in climate and climate change. The ocean is influenced by mass, energy and momentum exchanges with the atmosphere. Its heat capacity is about 1000 times larger than that of the atmosphere and the ocean's net heat uptake is therefore many times greater than that of the atmosphere (see Figure TS.15). Global observations of the heat taken up by the ocean can now be shown to be a definitive test of changes in the global energy budget. Changes in the amount of energy taken up by the upper layers of the ocean also play a crucial role for climate variations on seasonal to interannual time scales, such as El Niño. Changes in the transport of heat and SSTs have important effects upon many regional climates worldwide. Life in the sea is dependent on the biogeochemical status of the ocean and is affected by changes in its physical state and circulation. Changes in ocean biogeochemistry can also feed back into the climate system, for example, through changes in uptake or release of radiatively active gases such as CO₂. {5.1, 7.3}

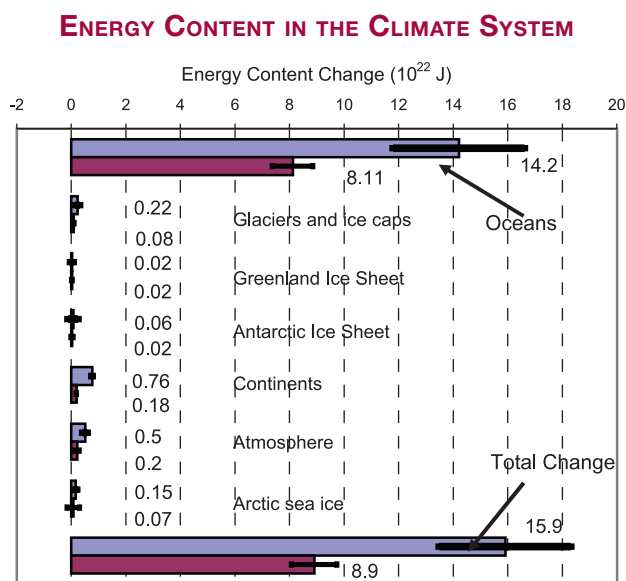


Figure TS.15. Energy content changes in different components of the Earth system for two periods (1961–2003 and 1993–2003). Blue bars are for 1961 to 2003; burgundy bars are for 1993 to 2003. Positive energy content change means an increase in stored energy (i.e., heat content in oceans, latent heat from reduced ice or sea ice volumes, heat content in the continents excluding latent heat from permafrost changes, and latent and sensible heat and potential and kinetic energy in the atmosphere). All error estimates are 90% confidence intervals. No estimate of confidence is available for the continental heat gain. Some of the results have been scaled from published results for the two respective periods. {Figure 5.4}

Global mean sea level variations are driven in part by changes in density, through thermal expansion or contraction of the ocean's volume. Local changes in sea level also have a density-related component due to temperature and salinity changes. In addition, exchange of water between oceans and other reservoirs (e.g., ice sheets, mountain glaciers, land water reservoirs and the atmosphere) can change the ocean's mass and hence contribute to changes in sea level. Sea level change is not geographically uniform because processes such as ocean circulation changes are not uniform across the globe (see Box TS.4). {5.5}

Oceanic variables can be useful for climate change detection, in particular temperature and salinity changes below the surface mixed layer where the variability is smaller and signal-to-noise ratio is higher. Observations analysed since the TAR have provided new evidence for changes in global ocean heat content and salinity, sea level, thermal expansion contributions to sea level rise, water mass evolution and biogeochemical cycles. {5.5}

TS.3.3.1 Changes in Ocean Heat Content and Circulation

The world ocean has warmed since 1955, accounting over this period for more than 80% of the changes in the energy content of the Earth's climate system. A total of 7.9 million vertical profiles of ocean temperature allows construction of improved global time series (see Figure TS.16). Analyses of the global oceanic heat budget have been replicated by several independent analysts and are robust to the method used. Data coverage limitations require averaging over decades for the deep ocean and observed decadal variability in the global heat content is not fully understood. However, inadequacies in the distribution of data (particularly coverage in the Southern Ocean and South Pacific) could contribute to the apparent decadal variations in heat content. During the period 1961 to 2003, the 0 to 3000 m ocean layer has taken up about 14.1×10^{22} J, equivalent to an average heating rate of 0.2 W m^{-2} (per unit area of the Earth's surface). During 1993 to 2003, the corresponding rate of warming in the shallower 0 to 700 m ocean layer was higher, about $0.5 \pm 0.18 \text{ W m}^{-2}$. Relative to 1961 to 2003, the period 1993 to 2003 had high rates of warming but in 2004 and 2005 there has been some cooling compared to 2003. {5.1–5.3}

Warming is widespread over the upper 700 m of the global ocean. The Atlantic has warmed south of 45°N. The warming is penetrating deeper in the Atlantic Ocean Basin than in the Pacific, Indian and Southern Oceans, due to the

GLOBAL OCEAN HEAT CONTENT (0 - 700 m)

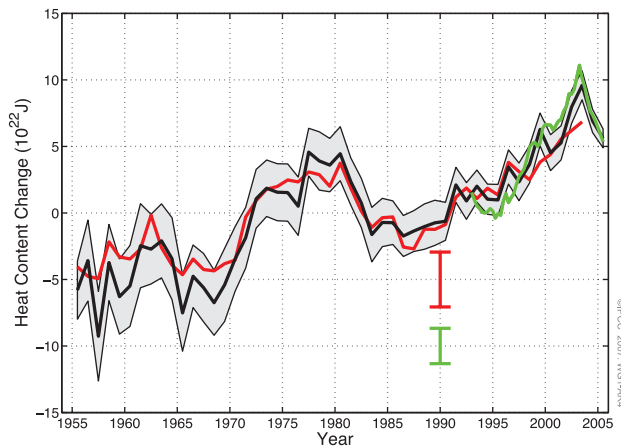


Figure TS.16. Time series of global ocean heat content (10^{22} J) for the 0 to 700 m layer. The three coloured lines are independent analyses of the oceanographic data. The black and red curves denote the deviation from their 1961 to 1990 average and the shorter green curve denotes the deviation from the average of the black curve for the period 1993 to 2003. The 90% uncertainty range for the black curve is indicated by the grey shading and for the other two curves by the error bars. (Figure 5.1)

deep overturning circulation cell that occurs in the North Atlantic. The SH deep overturning circulation shows little evidence of change based on available data. However, the upper layers of the Southern Ocean contribute strongly to the overall warming. At least two seas at subtropical latitudes (Mediterranean and Japan/East China Sea) are warming. While the global trend is one of warming, significant decadal variations have been observed in the global time series, and there are large regions where the oceans are cooling. Parts of the North Atlantic, North Pacific and equatorial Pacific have cooled over the last 50 years. The changes in the Pacific Ocean show ENSO-like spatial patterns linked in part to the PDO. {5.2, 5.3}

Parts of the Atlantic meridional overturning circulation exhibit considerable decadal variability, but data do not support a coherent trend in the overturning circulation. {5.3}

TS.3.3.2 Changes in Ocean Biogeochemistry and Salinity

The uptake of anthropogenic carbon since 1750 has led to the ocean becoming more acidic, with an average decrease in surface pH of 0.1 units.⁷ Uptake of CO_2 by the ocean changes its chemical equilibrium. Dissolved

CO_2 forms a weak acid, so as dissolved CO_2 increases, pH decreases (i.e., the ocean becomes more acidic). The overall pH change is computed from estimates of anthropogenic carbon uptake and simple ocean models. Direct observations of pH at available stations for the last 20 years also show trends of decreasing pH, at a rate of about 0.02 pH units per decade. Decreasing ocean pH decreases the depth below which calcium carbonate dissolves and increases the volume of the ocean that is undersaturated with respect to the minerals aragonite (a meta-stable form of calcium carbonate) and calcite, which are used by marine organisms to build their shells. Decreasing surface ocean pH and rising surface temperatures also act to reduce the ocean buffer capacity for CO_2 and the rate at which the ocean can take up excess atmospheric CO_2 . {5.4, 7.3}

The oxygen concentration of the ventilated thermocline (about 100 to 1000 m) decreased in most ocean basins between 1970 and 1995. These changes may reflect a reduced rate of ventilation linked to upper-level warming and/or changes in biological activity. {5.4}

There is now widespread evidence for changes in ocean salinity at gyre and basin scales in the past half century (see Figure TS.17) with the near-surface waters in the more evaporative regions increasing in salinity in almost all ocean basins. These changes in salinity imply changes in the hydrological cycle over the oceans. In the high-latitude regions in both hemispheres, the surface waters show an overall freshening consistent with these regions having greater precipitation, although higher runoff, ice melting, advection and changes in the meridional overturning circulation may also contribute. The subtropical latitudes in both hemispheres are characterised by an increase in salinity in the upper 500 m. The patterns are consistent with a change in the Earth's hydrological cycle, in particular with changes in precipitation and inferred larger water transport in the atmosphere from low latitudes to high latitudes and from the Atlantic to the Pacific. {5.2}

TS.3.3.3 Changes in Sea Level

Over the 1961 to 2003 period, the average rate of global mean sea level rise is estimated from tide gauge data to be 1.8 ± 0.5 mm yr^{-1} (see Figure TS.18). For the purpose of examining the sea level budget, best estimates and 5 to 95% confidence intervals are provided for all land ice contributions. The average

⁷ Acidity is a measure of the concentration of H^+ ions and is reported in pH units, where $\text{pH} = -\log(\text{H}^+)$. A pH decrease of 1 unit means a 10-fold increase in the concentration of H^+ , or acidity.

LINEAR TRENDS OF ZONALLY AVERAGED SALINITY (1955 - 1998)

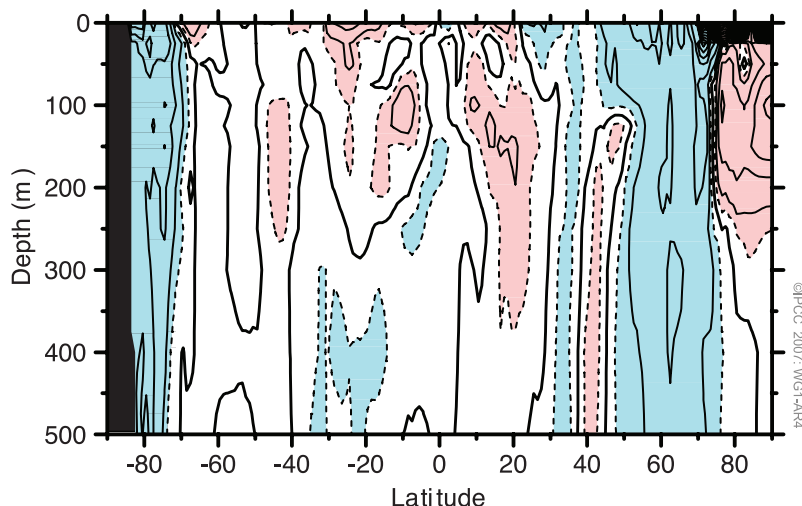


Figure TS.17. Linear trends (1955–1998) of zonally averaged salinity (Practical Salinity Scale) for the World Ocean. The contour interval is 0.01 per decade and dashed contours are ± 0.005 per decade. The dark, solid line is the zero contour. Red shading indicates values equal to or greater than 0.005 per decade and blue shading indicates values equal to or less than -0.005 per decade. {Figure 5.5}

thermal expansion contribution to sea level rise for this period was $0.42 \pm 0.12 \text{ mm yr}^{-1}$, with significant decadal variations, while the contribution from glaciers, ice caps and ice sheets is estimated to have been $0.7 \pm 0.5 \text{ mm yr}^{-1}$ (see Table TS.3). The sum of these estimated climate-related contributions for about the past four decades thus amounts to $1.1 \pm 0.5 \text{ mm yr}^{-1}$, which is less than the best estimate from the tide gauge observations (similar to the discrepancy noted in the TAR). Therefore, the sea level budget for 1961 to 2003 has not been closed satisfactorily. {4.8, 5.5}

The global average rate of sea level rise measured by TOPEX/Poseidon satellite altimetry during 1993 to 2003 is $3.1 \pm 0.7 \text{ mm yr}^{-1}$. This observed rate for the recent period is close to the estimated total of $2.8 \pm 0.7 \text{ mm yr}^{-1}$ for the climate-related contributions due to thermal expansion ($1.6 \pm 0.5 \text{ mm yr}^{-1}$) and changes in land ice ($1.2 \pm 0.4 \text{ mm yr}^{-1}$). Hence, the understanding of the budget has improved significantly for this recent period, with the climate contributions constituting the main factors in the sea level budget (which is closed to within known errors). Whether the faster rate for 1993 to 2003 compared to 1961 to 2003 reflects decadal variability or an increase in the longer-term trend is unclear. The

tide gauge record indicates that faster rates similar to that observed in 1993 to 2003 have occurred in other decades since 1950. {5.5, 9.5}

There is *high confidence* that the rate of sea level rise accelerated between the mid-19th and the mid-20th centuries based upon tide gauge and geological data. A recent reconstruction of sea level change back to 1870 using the best available tide records provides high confidence that the rate of sea level rise accelerated over the period 1870 to 2000. Geological observations indicate that during the previous 2000 years, sea level change was small, with average rates in the range 0.0 to 0.2 mm yr^{-1} . The use of proxy sea level data from archaeological sources is well established in the Mediterranean and indicates that oscillations in sea level from about AD 1 to AD 1900 did not exceed $\pm 0.25 \text{ m}$. The available evidence

indicates that the onset of modern sea level rise started between the mid-19th and mid-20th centuries. {5.5}

Precise satellite measurements since 1993 now provide unambiguous evidence of regional variability of sea level change. In some regions, rates of rise during this period are up to several times the global mean,

GLOBAL MEAN SEA LEVEL

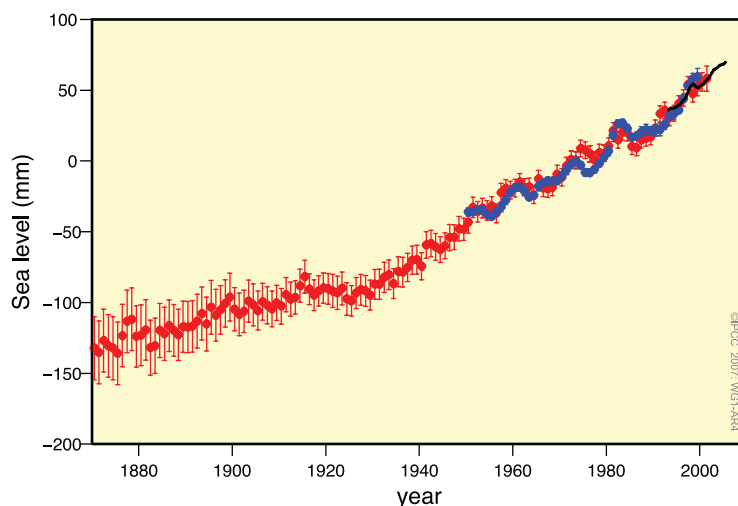


Figure TS.18. Annual averages of the global mean sea level based on reconstructed sea level fields since 1870 (red), tide gauge measurements since 1950 (blue) and satellite altimetry since 1992 (black). Units are in mm relative to the average for 1961 to 1990. Error bars are 90% confidence intervals. {Figure 5.13}

Table TS.3. Contributions to sea level rise based upon observations (left columns) compared to models used in this assessment (right columns; see Section 9.5 and Appendix 10.A for details). Values are presented for 1993 to 2003 and for the last four decades, including observed totals. {Adapted from Tables 5.3 and 9.2}

Sources of Sea Level Rise	Sea Level Rise (mm yr ⁻¹)			
	1961–2003		1993–2003	
	Observed	Modelled	Observed	Modelled
Thermal expansion	0.42 ± 0.12	0.5 ± 0.2	1.6 ± 0.5	1.5 ± 0.7
Glaciers and ice caps	0.50 ± 0.18	0.5 ± 0.2	0.77 ± 0.22	0.7 ± 0.3
Greenland Ice Sheet	0.05 ± 0.12 ^a		0.21 ± 0.07 ^a	
Antarctic Ice Sheet	0.14 ± 0.41 ^a		0.21 ± 0.35 ^a	
Sum of individual climate contributions to sea level rise	1.1 ± 0.5	1.2 ± 0.5	2.8 ± 0.7	2.6 ± 0.8
Observed total sea level rise	1.8 ± 0.5 (tide gauges)		3.1 ± 0.7 (satellite altimeter)	
Difference (Observed total minus the sum of observed climate contributions)	0.7 ± 0.7		0.3 ± 1.0	

Notes:

^a prescribed based upon observations (see Section 9.5)

while in other regions sea level is falling. The largest sea level rise since 1992 has taken place in the western Pacific and eastern Indian Oceans (see Figure TS.19). Nearly all of the Atlantic Ocean shows sea level rise during the past decade, while sea level in the eastern Pacific and western Indian Oceans has been falling. These temporal and spatial variations in regional sea level rise are influenced in part by patterns of coupled ocean-atmosphere variability, including ENSO and the NAO. The pattern of observed sea level change since 1992 is similar to the thermal expansion computed from ocean temperature changes, but different from the thermal expansion pattern of the last 50 years, indicating the importance of regional decadal variability. {5.5}

Observations suggest increases in extreme high water at a broad range of sites worldwide since 1975. Longer records are limited in space and under-sampled in time, so a global analysis over the entire 20th century is not feasible. In many locations, the secular changes in extremes were similar to those in mean sea level. At others, changes in atmospheric conditions such as storminess were more important in determining long-term trends. Interannual variability in high water extremes was positively correlated with regional mean sea level, as well as to indices of regional climate such as ENSO in the Pacific and NAO in the Atlantic. {5.5}

SEA LEVEL CHANGE PATTERNS

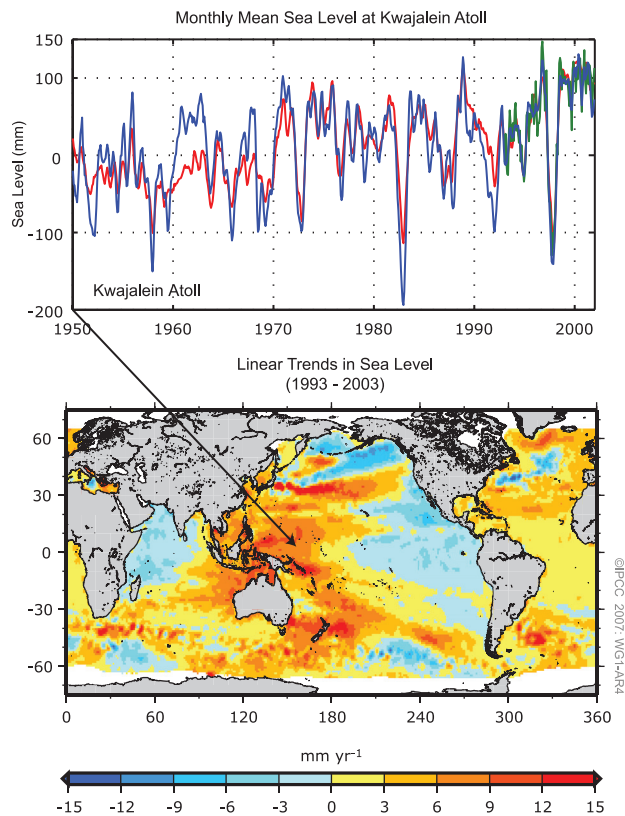


Figure TS.19. (Top) Monthly mean sea level (mm) curve for 1950 to 2000 at Kwajalein (8°44'N, 167°44'E). The observed sea level (from tide gauge measurements) is in blue, the reconstructed sea level in red and the satellite altimetry record in green. Annual and semiannual signals have been removed from each time series and the tide gauge data have been smoothed. (Bottom) Geographic distribution of short-term linear trends in mean sea level for 1993 to 2003 (mm yr⁻¹) based on TOPEX/Poseidon satellite altimetry. {Figures 5.15 and 5.18}

Box TS.4: Sea Level

The level of the sea at the shoreline is determined by many factors that operate over a great range of temporal scales: hours to days (tides and weather), years to millennia (climate), and longer. The land itself can rise and fall and such regional land movements need to be accounted for when using tide gauge measurements for evaluating the effect of oceanic climate change on coastal sea level. Coastal tide gauges indicate that global average sea level rose during the 20th century. Since the early 1990s, sea level has also been observed continuously by satellites with near-global coverage. Satellite and tide gauge data agree at a wide range of spatial scales and show that global average sea level has continued to rise during this period. Sea level changes show geographical variation because of several factors, including the distributions of changes in ocean temperature, salinity, winds and ocean circulation. Regional sea level is affected by climate variability on shorter time scales, for instance associated with El Niño and the NAO, leading to regional interannual variations which can be much greater or weaker than the global trend.

Based on ocean temperature observations, the thermal expansion of seawater as it warms has contributed substantially to sea level rise in recent decades. Climate models are consistent with the ocean observations and indicate that thermal expansion is expected to continue to contribute to sea level rise over the next 100 years. Since deep ocean temperatures change only slowly, thermal expansion would continue for many centuries even if atmospheric concentrations of greenhouse gases were stabilised.

Global average sea level also rises or falls when water is transferred from land to ocean or vice versa. Some human activities can contribute to sea level change, especially by the extraction of groundwater and construction of reservoirs. However, the major land store of freshwater is the water frozen in glaciers, ice caps and ice sheets. Sea level was more than 100 m lower during the glacial periods because of the ice sheets covering large parts of the NH continents. The present-day retreat of glaciers and ice caps is making a substantial contribution to sea level rise. This is expected to continue during the next 100 years. Their contribution should decrease in subsequent centuries as this store of freshwater diminishes.

The Greenland and Antarctic Ice Sheets contain much more ice and could make large contributions over many centuries. In recent years the Greenland Ice Sheet has experienced greater melting, which is projected to increase further. In a warmer climate, models suggest that the ice sheets could accumulate more snowfall, tending to lower sea level. However, in recent years any such tendency has probably been outweighed by accelerated ice flow and greater discharge observed in some marginal areas of the ice sheets. The processes of accelerated ice flow are not yet completely understood but could result in overall net sea level rise from ice sheets in the future.

The greatest climate- and weather-related impacts of sea level are due to extremes on time scales of days and hours, associated with tropical cyclones and mid-latitude storms. Low atmospheric pressure and high winds produce large local sea level excursions called 'storm surges', which are especially serious when they coincide with high tide. Changes in the frequency of occurrence of these extreme sea levels are affected both by changes in mean sea level and in the meteorological phenomena causing the extremes. {5.5}

TS.3.4 Consistency Among Observations

In this section, variability and trends within and across different climate variables including the atmosphere, cryosphere and oceans are examined for consistency based upon conceptual understanding of physical relationships between the variables. For example, increases in temperature will enhance the moisture-holding capacity of the atmosphere. Changes in temperature and/or precipitation should be consistent with those evident in glaciers. Consistency between independent observations using different techniques and variables provides a key test of understanding, and hence enhances confidence. {3.9}

Changes in the atmosphere, cryosphere and ocean show unequivocally that the world is warming. {3.2, 3.9, 4.2, 4.4–4.8, 5.2, 5.5}

Both land surface air temperatures and SSTs show warming. In both hemispheres, land regions have warmed at a faster rate than the oceans in the past few decades, consistent with the much greater thermal inertia of the oceans. {3.2}

The warming of the climate is consistent with observed increases in the number of daily warm extremes, reductions in the number of daily cold extremes and reductions in the number of frost days at mid-latitudes. {3.2, 3.8}

Surface air temperature trends since 1979 are now consistent with those at higher altitudes. It is likely that there is slightly greater warming in the troposphere than at the surface, and a higher tropopause, consistent with expectations from basic physical processes and observed increases in greenhouse gases together with depletion of stratospheric ozone. {3.4, 9.4}

Changes in temperature are broadly consistent with the observed nearly worldwide shrinkage of the cryosphere. There have been widespread reductions in mountain glacier mass and extent. Changes in climate consistent with warming are also indicated by decreases in snow cover, snow depth, arctic sea ice extent, permafrost thickness and temperature, the extent of seasonally frozen ground and the length of the freeze season of river and lake ice. {3.2, 3.9, 4.2–4.5, 4.7}

Observations of sea level rise since 1993 are consistent with observed changes in ocean heat content and the cryosphere. Sea level rose by $3.1 \pm 0.7 \text{ mm yr}^{-1}$ from 1993 to 2003, the period of availability of global altimetry measurements. During this time, a near balance was observed between observed total sea level rise and contributions from glacier, ice cap and ice sheet retreat together with increases in ocean heat content and associated ocean expansion. This balance gives increased

Table TS.4. Recent trends, assessment of human influence on trends, and projections of extreme weather and climate events for which there is evidence of an observed late 20th-century trend. An asterisk in the column headed ‘D’ indicates that formal detection and attribution studies were used, along with expert judgement, to assess the likelihood of a discernible human influence. Where this is not available, assessments of likelihood of human influence are based on attribution results for changes in the mean of a variable or changes in physically related variables and/or on the qualitative similarity of observed and simulated changes, combined with expert judgement. {3.8, 5.5, 9.7, 11.2–11.9; Tables 3.7, 3.8, 9.4}

Phenomenon ^a and direction of trend	Likelihood that trend occurred in late 20th century (typically post-1960)	Likelihood of a human contribution to observed trend	D	Likelihood of future trend based on projections for 21st century using SRES ^b scenarios
Warmer and fewer cold days and nights over most land areas	<i>Very likely^c</i>	<i>Likely^e</i>	*	<i>Virtually certain^e</i>
Warmer and more frequent hot days and nights over most land areas	<i>Very likely^d</i>	<i>Likely (nights)^e</i>	*	<i>Virtually certain^e</i>
Warm spells / heat waves: Frequency increases over most land areas	<i>Likely</i>	<i>More likely than not</i>		<i>Very likely</i>
Heavy precipitation events. Frequency (or proportion of total rainfall from heavy falls) increases over most areas	<i>Likely</i>	<i>More likely than not</i>		<i>Very likely</i>
Area affected by droughts increases	<i>Likely in many regions since 1970s</i>	<i>More likely than not</i>	*	<i>Likely</i>
Intense tropical cyclone activity increases	<i>Likely in some regions since 1970</i>	<i>More likely than not</i>		<i>Likely</i>
Increased incidence of extreme high sea level (excludes tsunamis)^f	<i>Likely</i>	<i>More likely than not^g</i>		<i>Likely^h</i>

Notes:

^a See Table 3.7 for further details regarding definitions.

^b SRES refers to the IPCC Special Report on Emission Scenarios. The SRES scenario families and illustrative cases are summarised in a box at the end of the Summary for Policymakers.

^c Decreased frequency of cold days and nights (coldest 10%)

^d Increased frequency of hot days and nights (hottest 10%)

^e Warming of the most extreme days/nights each year

^f Extreme high sea level depends on average sea level and on regional weather systems. It is defined here as the highest 1% of hourly values of observed sea level at a station for a given reference period.

^g Changes in observed extreme high sea level closely follow the changes in average sea level {5.5.2.6}. It is *very likely* that anthropogenic activity contributed to a rise in average sea level. {9.5.2}

^h In all scenarios, the projected global average sea level at 2100 is higher than in the reference period {10.6}. The effect of changes in regional weather systems on sea level extremes has not been assessed.

confidence that the observed sea level rise is a strong indicator of warming. However, the sea level budget is not balanced for the longer period 1961 to 2003. {5.5, 3.9}

Observations are consistent with physical understanding regarding the expected linkage between water vapour and temperature, and with intensification of precipitation events in a warmer world. Column and upper-tropospheric water vapour have increased, providing important support for the

hypothesis of simple physical models that specific humidity increases in a warming world and represents an important positive feedback to climate change. Consistent with rising amounts of water vapour in the atmosphere, there are widespread increases in the numbers of heavy precipitation events and increased likelihood of flooding events in many land regions, even those where there has been a reduction in total precipitation. Observations of changes in ocean salinity independently support the view

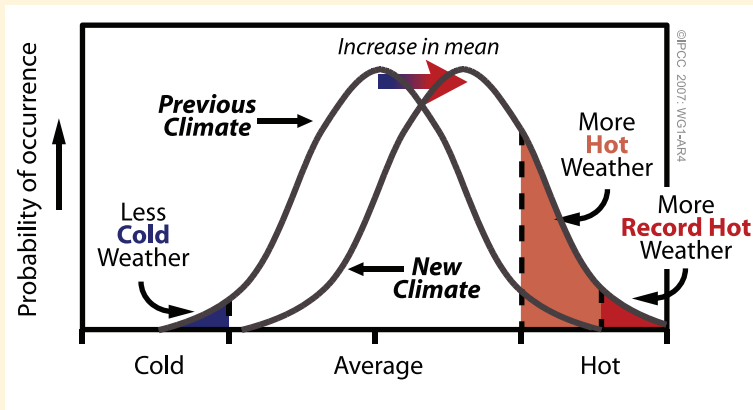
Box TS.5: Extreme Weather Events

People affected by an extreme weather event (e.g., the extremely hot summer in Europe in 2003, or the heavy rainfall in Mumbai, India in July 2005) often ask whether human influences on the climate are responsible for the event. A wide range of extreme weather events is expected in most regions even with an unchanging climate, so it is difficult to attribute any individual event to a change in the climate. In most regions, instrumental records of variability typically extend only over about 150 years, so there is limited information to characterise how extreme rare climatic events could be. Further, several factors usually need to combine to produce an extreme event, so linking a particular extreme event to a single, specific cause is problematic. In some cases, it may be possible to estimate the anthropogenic contribution to such changes in the probability of occurrence of extremes.

However, simple statistical reasoning indicates that substantial changes in the frequency of extreme events (and in the maximum feasible extreme, e.g., the maximum possible 24-hour rainfall at a specific location) can result from a relatively small shift of the distribution of a weather or climate variable.

Extremes are the infrequent events at the high and low end of the range of values of a particular variable. The probability of occurrence of values in this range is called a probability distribution function (PDF) that for some variables is shaped similarly to a 'Normal' or 'Gaussian' curve (the familiar 'bell' curve). Box TS.5, Figure 1 shows a schematic of a such a PDF and illustrates the effect a small shift (corresponding to a small change in the average or centre of the distribution) can have on the frequency of extremes at either end of the distribution. An increase in the frequency of one extreme (e.g., the number of hot days) will often be accompanied by a decline in the opposite extreme (in this case the number of cold days such as frosts). Changes in the variability or shape of the distribution can complicate this simple picture.

The IPCC Second Assessment Report noted that data and analyses of extremes related to climate change were sparse. By the time of the TAR, improved monitoring and data for changes in extremes was available, and climate models were being analysed to provide projections of extremes. Since the TAR, the observational basis of analyses of extremes has increased substantially, so that some extremes have now been examined over most land areas (e.g., daily temperature and rainfall extremes). More models have been used in the simulation and projection of extremes, and multiple integrations of models with different starting conditions (ensembles) now provide more robust information about PDFs and extremes. Since the TAR, some climate change detection and attribution studies focussed on changes in the global statistics of extremes have become available (Table TS.4). For some extremes (e.g., tropical cyclone intensity), there are still data concerns and/or inadequate models. Some assessments still rely on simple reasoning about how extremes might be expected to change with global warming (e.g., warming could be expected to lead to more heat waves). Others rely on qualitative similarity between observed and simulated changes. The assessed likelihood of anthropogenic contributions to trends is lower for variables where the assessment is based on indirect evidence.



Box TS.5, Figure 1. Schematic showing the effect on extreme temperatures when the mean temperature increases, for a normal temperature distribution.

that the Earth's hydrologic cycle has changed, in a manner consistent with observations showing greater precipitation and river runoff outside the tropics and subtropics, and increased transfer of freshwater from the ocean to the atmosphere at lower latitudes. {3.3, 3.4, 3.9, 5.2}

Although precipitation has increased in many areas of the globe, the area under drought has also increased. Drought duration and intensity has also increased. While regional droughts have occurred in the past, the widespread spatial extent of current droughts is broadly consistent with expected changes in the hydrologic cycle under warming. Water vapour increases with increasing global temperature, due to increased evaporation where surface moisture is available, and this tends to increase precipitation. However, increased continental temperatures are expected to lead to greater evaporation and drying, which is particularly important in dry regions where surface moisture is limited. Changes in snowpack, snow cover and in atmospheric circulation patterns and storm tracks can also reduce available seasonal moisture, and contribute to droughts. Changes in SSTs and associated changes in the atmospheric circulation and precipitation have contributed to changes in drought, particularly at low latitudes. The result is that drought has become more common, especially in the tropics and subtropics, since the 1970s. In Australia and Europe, direct links to global warming have been inferred through the extremes in high temperatures and heat waves accompanying recent droughts. {3.3, 3.8, 9.5}

TS.3.5 A Palaeoclimatic Perspective

Palaeoclimatic studies make use of measurements of past change derived from borehole temperatures, ocean sediment pore-water change and glacier extent changes, as well as proxy measurements involving the changes in chemical, physical and biological parameters that reflect past changes in the environment where the proxy grew or existed. Palaeoclimatic studies rely on multiple proxies so that results can be cross-verified and uncertainties better understood. It is now well accepted and verified that many biological organisms (e.g., trees, corals, plankton, animals) alter their growth and/or population dynamics in response to changing climate, and that these climate-induced changes are well recorded in past growth in living and dead (fossil) specimens or assemblages of organisms. Networks of tree ring width and tree ring density chronologies are used to infer past temperature changes based on calibration with temporally overlapping instrumental data. While these methods are heavily used, there are concerns regarding the distributions of available

measurements, how well these sample the globe, and such issues as the degree to which the methods have spatial and seasonal biases or apparent divergence in the relationship with recent climate change. {6.2}

It is very likely that average NH temperatures during the second half of the 20th century were warmer than any other 50-year period in the last 500 years and likely the warmest in at least the past 1300 years. The data supporting these conclusions are most extensive over summer extratropical land areas (particularly for the longer time period; see Figure TS.20). These conclusions are based upon proxy data such as the width and density of a tree ring, the isotopic composition of various elements in ice or the chemical composition of a growth band in corals, requiring analysis to derive temperature information and associated uncertainties. Among the key uncertainties are that temperature and precipitation are difficult to separate in some cases, or are representative of particular seasons rather than full years. There are now improved and expanded data since the TAR, including, for example, measurements at a larger number of sites, improved analysis of borehole temperature data and more extensive analyses of glaciers, corals and sediments. However, palaeoclimatic data are more limited than the instrumental record since 1850 in both space and time, so that statistical methods are employed to construct global averages, and these are subject to uncertainties as well. Current data are too limited to allow a similar evaluation of the SH temperatures prior to the period of instrumental data. {6.6, 6.7}

Some post-TAR studies indicate greater multi-centennial NH variability than was shown in the TAR, due to the particular proxies used and the specific statistical methods of processing and/or scaling them to represent past temperatures. The additional variability implies cooler conditions, predominantly during the 12th to 14th, the 17th and the 19th centuries; these are likely linked to natural forcings due to volcanic eruptions and/or solar activity. For example, reconstructions suggest decreased solar activity and increased volcanic activity in the 17th century as compared to current conditions. One reconstruction suggests slightly warmer conditions in the 11th century than those indicated in the TAR, but within the uncertainties quoted in the TAR. {6.6}

The ice core CO₂ record over the past millennium provides an additional constraint on natural climate variability. The amplitudes of the pre-industrial, decadal-scale NH temperature changes from the proxy-based reconstructions (<1°C) are broadly consistent with the ice core CO₂ record and understanding of the strength

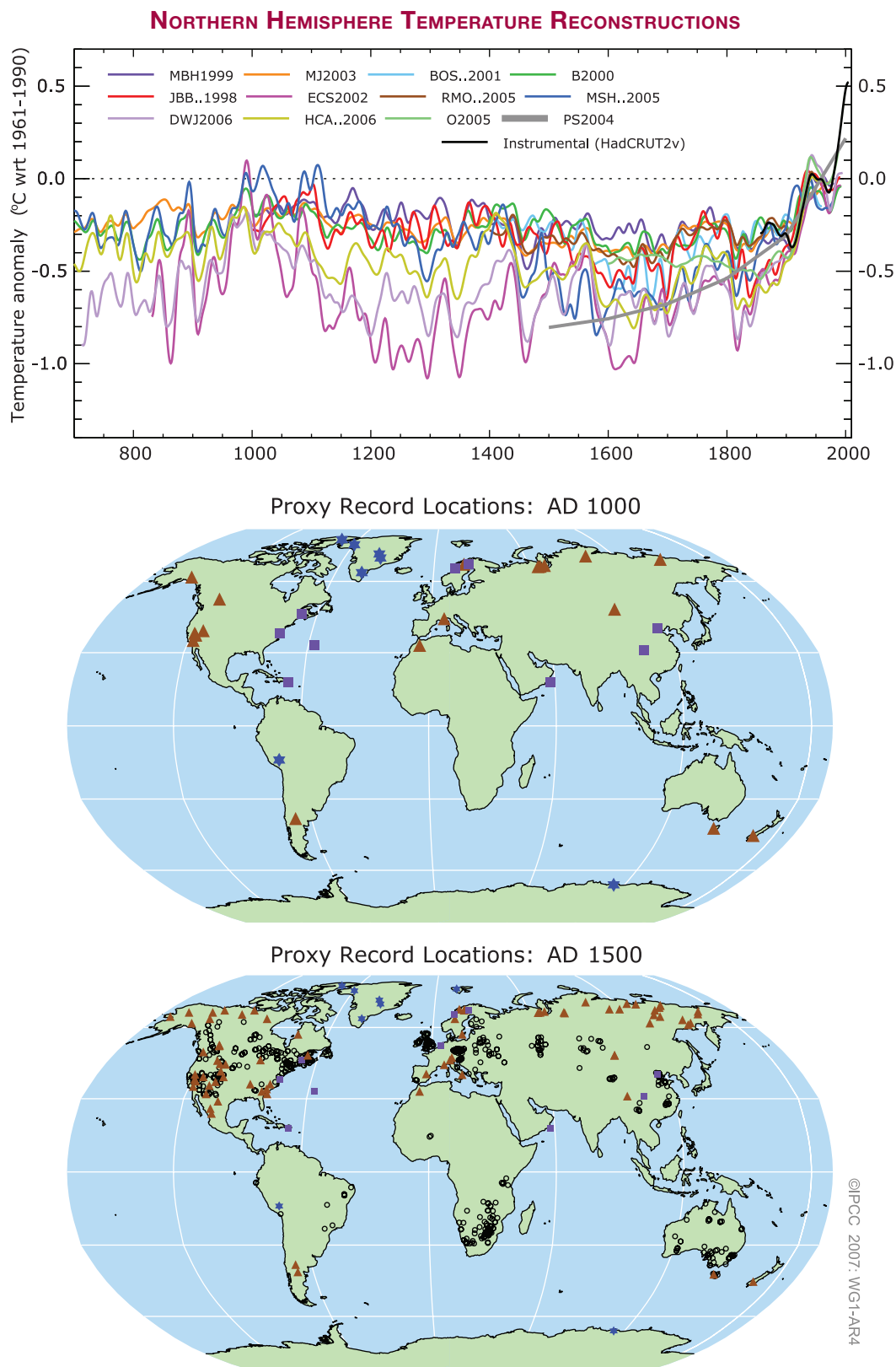


Figure TS.20. (Top) Records of Northern Hemisphere temperature variation during the last 1300 years with 12 reconstructions using multiple climate proxy records shown in colour and instrumental records shown in black. (Middle and Bottom) Locations of temperature-sensitive proxy records with data back to AD 1000 and AD 1500 (tree rings: brown triangles; boreholes: black circles; ice core/ice boreholes: blue stars; other records including low-resolution records: purple squares). Data sources are given in Table 6.1, Figure 6.10 and are discussed in Chapter 6. {Figures 6.10 and 6.11}

Box TS.6: Orbital Forcing

It is well known from astronomical calculations that periodic changes in characteristics of the Earth's orbit around the Sun control the seasonal and latitudinal distribution of incoming solar radiation at the top of the atmosphere (hereafter called 'insolation'). Past and future changes in insolation can be calculated over several millions of years with a high degree of confidence. {6.4}

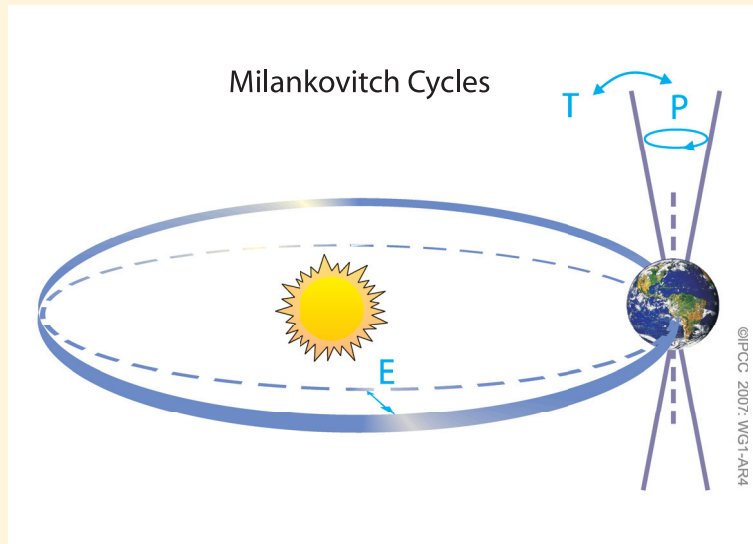
Precession refers to changes in the time of the year when the Earth is closest to the Sun, with quasi-periodicities of about 19,000 and 23,000 years. As a result, changes in the position and duration of the seasons on the orbit strongly modulate the latitudinal and seasonal distribution of insolation. Seasonal changes in insolation are much larger than annual mean changes and can reach 60 W m^{-2} (Box TS.6, Figure 1).

The obliquity (tilt) of the Earth's axis varies between about 22° and 24.5° with two neighbouring quasi-periodicities of around 41,000 years. Changes in obliquity modulate seasonal contrasts as well as annual mean insolation changes with opposite effects at low vs. high latitudes (and therefore no effect on global average insolation) {6.4}.

The eccentricity of the Earth's orbit around the Sun has longer quasi-periodicities at 400,000 years and around 100,000 years. Changes in eccentricity alone have limited impacts on insolation, due to the resulting very small changes in the distance between the Sun and the Earth. However, changes in eccentricity interact with seasonal effects induced by obliquity and precession of the equinoxes. During periods of low eccentricity, such as about 400,000 years ago and during the next 100,000 years, seasonal insolation changes induced by precession are not as large as during periods of larger eccentricity (Box TS.6, Figure 1). {6.4}

The Milankovitch, or 'orbital' theory of the ice ages is now well developed. Ice ages are generally triggered by minima in high-latitude NH summer insolation, enabling winter snowfall to persist through the year and therefore accumulate to build NH glacial ice sheets. Similarly, times with especially intense high-latitude NH summer insolation, determined by orbital changes, are thought to trigger rapid deglaciations, associated climate change and sea level rise. These orbital forcings determine the pacing of climatic changes, while the large responses appear to be determined by strong feedback processes that amplify the orbital forcing. Over multi-millennial time scales, orbital forcing also exerts a major influence on key climate systems such as the Earth's major monsoons, global ocean circulation and the greenhouse gas content of the atmosphere. {6.4}

Available evidence indicates that the current warming will not be mitigated by a natural cooling trend towards glacial conditions. Understanding of the Earth's response to orbital forcing indicates that the Earth would not naturally enter another ice age for at least 30,000 years. {6.4, FAQ 6.1}



Box TS.6, Figure 1. Schematic of the Earth's orbital changes (Milankovitch cycles) that drive the ice age cycles. 'T' denotes changes in the tilt (or obliquity) of the Earth's axis, 'E' denotes changes in the eccentricity of the orbit and 'P' denotes precession, that is, changes in the direction of the axis tilt at a given point of the orbit. {FAQ 6.1, Figure 1}

of the carbon cycle-climate feedback. Atmospheric CO₂ and temperature in Antarctica co-varied over the past 650,000 years. Available data suggest that CO₂ acts as an amplifying feedback. {6.4, 6.6}

Changes in glaciers are evident in Holocene data, but these changes were caused by different processes than the late 20th-century retreat. Glaciers of several mountain regions in the NH retreated in response to orbitally forced regional warmth between 11,000 and 5000 years ago, and were smaller than at the end of the 20th century (or even absent) at times prior to 5000 years ago. The current near-global retreat of mountain glaciers cannot be due to the same causes, because decreased summer insolation during the past few thousand years in the NH should be favourable to the growth of glaciers. {6.5}

Palaeoclimatic data provide evidence for changes in many regional climates. The strength and frequency of ENSO events have varied in past climates. There is evidence that the strength of the Asian monsoon, and hence precipitation amount, can change abruptly. The palaeoclimatic records of northern and eastern Africa

and of North America indicate that droughts lasting decades to centuries are a recurrent feature of climate in these regions, so that recent droughts in North America and northern Africa are not unprecedented. Individual decadal-resolution palaeoclimatic data sets support the existence of regional quasi-periodic climate variability, but it is *unlikely* that these regional signals were coherent at the global scale. {6.5, 6.6}

Strong evidence from ocean sediment data and from modelling links abrupt climate changes during the last glacial period and glacial-interglacial transition to changes in the Atlantic Ocean circulation. Current understanding suggests that the ocean circulation can become unstable and change rapidly when critical thresholds are crossed. These events have affected temperature by up to 16°C in Greenland and have influenced tropical rainfall patterns. They were probably associated with a redistribution of heat between the NH and SH rather than with large changes in global mean temperature. Such events have not been observed during the past 8000 years. {6.4}

THE ARCTIC AND THE LAST INTERGLACIAL

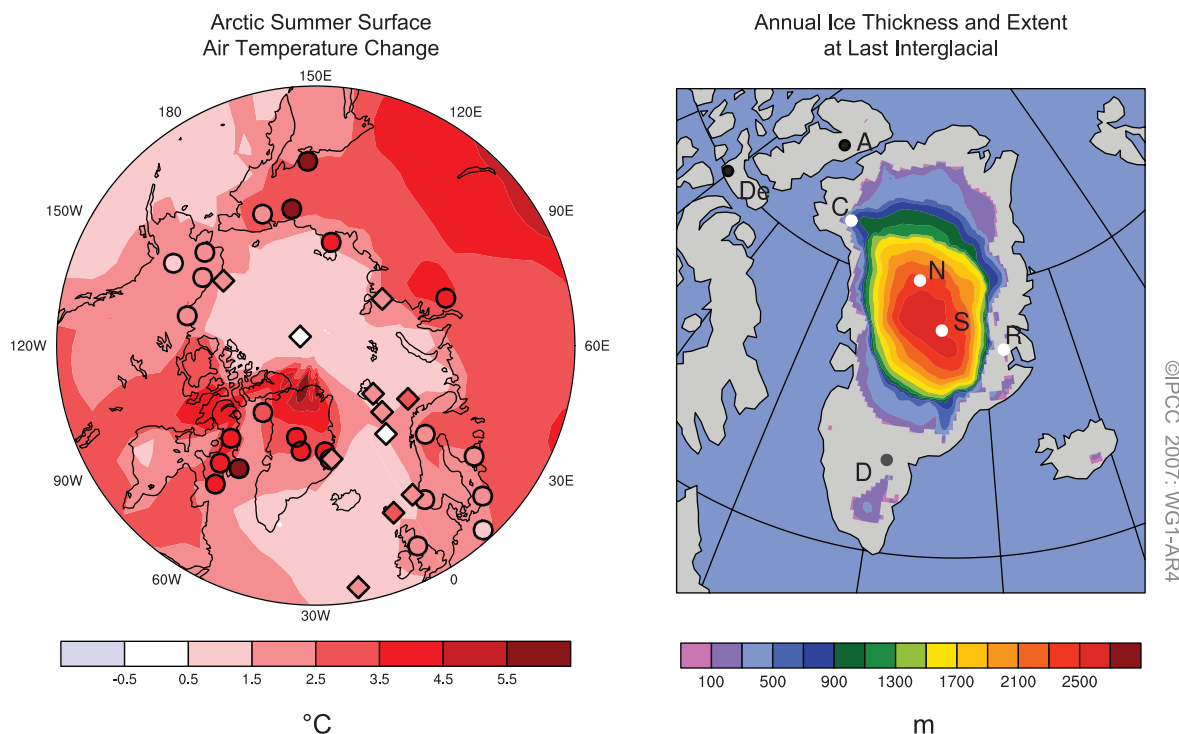


Figure TS.21. Summer surface air temperature change relative to the present over the Arctic (left) and ice thickness and extent for Greenland and western arctic glaciers (right) for the last interglacial, approximately 125,000 years ago, from a multi-model and multi-proxy synthesis. (Left) A multi-model simulation of summer warming during the last interglacial is overlain by proxy estimates of maximum summer warming from terrestrial (circles) and marine (diamonds) sites. (Right) Extents and thicknesses of the Greenland Ice Sheet and western Canadian and Iceland glaciers at their minimum extent during the last interglacial, shown as a multi-model average from three ice models. Ice core observations indicate ice during the last interglacial at sites (white dots), Renland (R), North Greenland Ice Core Project (N), Summit (S, GRIP and GISP2) and possibly Camp Century (C), but no ice at sites (black dots): Devon (De) and Agassiz (A). Evidence for LIG ice at Dye-3 (D, grey dot) is equivocal. {Figure 6.6}

Confidence in the understanding of past climate change and changes in orbital forcing is strengthened by the improved ability of current models to simulate past climate conditions.

The Last Glacial Maximum (LGM; the last ‘ice age’ about 21,000 years ago) and the mid-Holocene (6000 years ago) were different from the current climate not because of random variability, but because of altered seasonal and global forcing linked to known differences in the Earth’s orbit (see Box TS.6). Biogeochemical and biogeophysical feedbacks amplified the response to orbital forcings. Comparisons between simulated and reconstructed conditions in the LGM demonstrate that models capture the broad features of inferred changes in the temperature and precipitation patterns. For the mid-Holocene, coupled climate models are able to simulate mid-latitude warming and enhanced monsoons, with little change in global mean temperature (<0.4°C), consistent with our understanding of orbital forcing. {6.2, 6.4, 6.5, 9.3}

Global average sea level was likely between 4 and 6 m higher during the last interglacial period, about 125,000 years ago, than during the 20th century, mainly due to the retreat of polar ice (Figure TS.21). Ice core data suggest that the Greenland Summit region was ice-covered during this period, but reductions in the ice sheet extent are indicated in parts of southern Greenland. Ice core data also indicate that average polar temperatures at that time were 3°C to 5°C warmer than the 20th century because of differences in the Earth’s orbit. The Greenland Ice Sheet and other arctic ice fields likely contributed no more than 4 m of the observed sea level rise, implying that there may also have been a contribution from Antarctica. {6.4}

TS.4 Understanding and Attributing Climate Change

Attribution evaluates whether observed changes are consistent with quantitative responses to different forcings obtained in well-tested models, and are not consistent with alternative physically plausible explanations. The first IPCC Assessment Report (FAR) contained little observational evidence of a detectable anthropogenic influence on climate. Six years later, the IPCC Second Assessment Report (SAR) concluded that the balance of evidence suggested a discernible human influence on the climate of the 20th century. The TAR concluded that ‘most of the observed warming over the last 50 years

is likely to have been due to the increase in greenhouse gas concentrations’. Confidence in the assessment of the human contributions to recent climate change has increased considerably since the TAR, in part because of stronger signals obtained from longer records, and an expanded and improved range of observations allowing attribution of warming to be more fully addressed jointly with other changes in the climate system. Some apparent inconsistencies in the observational record (e.g., in the vertical profile of temperature changes) have been largely resolved. There have been improvements in the simulation of many aspects of present mean climate and its variability on seasonal to inter-decadal time scales, although uncertainties remain (see Box TS.7). Models now employ more detailed representations of processes related to aerosol and other forcings. Simulations of 20th-century climate change have used many more models and much more complete anthropogenic and natural forcings than were available for the TAR. Available multi-model ensembles increase confidence in attribution results by providing an improved representation of model uncertainty. An anthropogenic signal has now more clearly emerged in formal attribution studies of aspects of the climate system beyond global-scale atmospheric temperature, including changes in global ocean heat content, continental-scale temperature trends, temperature extremes, circulation and arctic sea ice extent. {9.1}

TS.4.1 Advances in Attribution of Changes in Global-Scale Temperature in the Instrumental Period: Atmosphere, Ocean and Ice

Anthropogenic warming of the climate system is widespread and can be detected in temperature observations taken at the surface, in the free atmosphere and in the oceans. {3.2, 3.4, 9.4}

Evidence of the effect of external influences, both anthropogenic and natural, on the climate system has continued to accumulate since the TAR. Model and data improvements, ensemble simulations and improved representations of aerosol and greenhouse gas forcing along with other influences lead to greater confidence that most current models reproduce large-scale forced variability of the atmosphere on decadal and inter-decadal time scales quite well. These advances confirm that past climate variations at large spatial scales have been strongly influenced by external forcings. However, uncertainties still exist in the magnitude and temporal evolution of estimated contributions from individual forcings other than well-mixed greenhouse gases, due, for

Box TS.7: Evaluation of Atmosphere-Ocean General Circulation Models

Atmosphere-ocean general circulation models (AOGCMs) are the primary tool used for understanding and attribution of past climate variations, and for future projections. Since there are no historical perturbations to radiative forcing that are fully analogous to the human-induced perturbations expected over the 21st century, confidence in the models must be built from a number of indirect methods, described below. In each of these areas there have been substantial advances since the TAR, increasing overall confidence in models. {8.1}

Enhanced scrutiny and analysis of model behaviour has been facilitated by internationally coordinated efforts to collect and disseminate output from model experiments performed under common conditions. This has encouraged a more comprehensive and open evaluation of models, encompassing a diversity of perspectives. {8.1}

Projections for different scales and different periods using global climate models. Climate models project the climate for several decades or longer into the future. Since the details of individual weather systems are not being tracked and forecast, the initial atmospheric conditions are much less important than for weather forecast models. For climate projections, the forcings are of much greater importance. These forcings include the amount of solar energy reaching the Earth, the amount of particulate matter from volcanic eruptions in the atmosphere, and the concentrations of anthropogenic gases and particles in the atmosphere. As the area of interest moves from global to regional to local, or the time scale of interest shortens, the amplitude of variability linked to weather increases relative to the signal of long-term climate change. This makes detection of the climate change signal more difficult at smaller scales. Conditions in the oceans are important as well, especially for interannual and decadal time scales. {FAQ 1.2, 9.4, 11.1}

Model formulation. The formulation of AOGCMs has developed through improved spatial resolution and improvements to numerical schemes and parametrizations (e.g., sea ice, atmospheric boundary layer, ocean mixing). More processes have been included in many models, including a number of key processes important for forcing (e.g., aerosols are now modelled interactively in many models). Most models now maintain a stable climate without use of flux adjustments, although some long-term trends remain in AOGCM control integrations, for example, due to slow processes in the ocean. {8.2, 8.3}

Simulation of present climate. As a result of improvements in model formulation, there have been improvements in the simulation of many aspects of present mean climate. Simulations of precipitation, sea level pressure and surface temperature have each improved overall, but deficiencies remain, notably in tropical precipitation. While significant deficiencies remain in the simulation of clouds (and corresponding feedbacks affecting climate sensitivity), some models have demonstrated improvements in the simulation of certain cloud regimes (notably marine stratocumulus). Simulation of extreme events (especially extreme temperature) has improved, but models generally simulate too little precipitation in the most extreme events. Simulation of extratropical cyclones has improved. Some models used for projections of tropical cyclone changes can simulate successfully the observed frequency and distribution of tropical cyclones. Improved simulations have been achieved for ocean water mass structure, the meridional overturning circulation and ocean heat transport. However most models show some biases in their simulation of the Southern Ocean, leading to some uncertainty in modelled ocean heat uptake when climate changes. {8.3, 8.5, 8.6}

Simulation of modes of climate variability. Models simulate dominant modes of extratropical climate variability that resemble the observed ones (NAM/SAM, PNA, PDO) but they still have problems in representing aspects of them. Some models can now simulate important aspects of ENSO, while simulation of the Madden-Julian Oscillation remains generally unsatisfactory. {8.4}

Simulation of past climate variations. Advances have been made in the simulation of past climate variations. Independently of any attribution of those changes, the ability of climate models to provide a physically self-consistent explanation of observed climate variations on various time scales builds confidence that the models are capturing many key processes for the evolution of 21st-century climate. Recent advances include success in modelling observed changes in a wider range of climate variables over the 20th century (e.g., continental-scale surface temperatures and extremes, sea ice extent, ocean heat content trends and land precipitation). There has also been progress in the ability to model many of the general features of past, very different climate states such as the mid-Holocene and the LGM using identical or related models to those used for studying current climate. Information on factors treated as boundary conditions in palaeoclimate calculations include the different states of ice sheets in those periods. The broad predictions of earlier climate models, of increasing global temperatures in response to increasing greenhouse gases, have been borne out by subsequent observations. This strengthens confidence in near-term climate projections and understanding of related climate change commitments. {6.4, 6.5, 8.1, 9.3–9.5}

(continued)

Weather and seasonal prediction using climate models. A few climate models have been tested for (and shown) capability in initial value prediction, on time scales from weather forecasting (a few days) to seasonal climate variations, when initialised with appropriate observations. While the predictive capability of models in this mode of operation does not necessarily imply that they will show the correct response to changes in climate forcing agents such as greenhouse gases, it does increase confidence that they are adequately representing some key processes and teleconnections in the climate system. {8.4}

Measures of model projection accuracy. The possibility of developing model capability measures ('metrics'), based on the above evaluation methods, that can be used to narrow uncertainty by providing quantitative constraints on model climate projections, has been explored for the first time using model ensembles. While these methods show promise, a proven set of measures has yet to be established. {8.1, 9.6, 10.5}

example, to uncertainties in model responses to forcing. Some potentially important forcings such as black carbon aerosols have not yet been considered in most formal detection and attribution studies. Uncertainties remain in estimates of natural internal climate variability. For example, there are discrepancies between estimates of ocean heat content variability from models and observations, although poor sampling of parts of the world ocean may explain this discrepancy. In addition, internal variability is difficult to estimate from available observational records since these are influenced by external forcing, and because records are not long enough in the case of instrumental data, or precise enough in the case of proxy reconstructions, to provide complete descriptions of variability on decadal and longer time scales (see Figure TS.22 and Box TS.7). {8.2–8.4, 8.6, 9.2–9.4}

It is extremely unlikely (<5%) that the global pattern of warming observed during the past half century can be explained without external forcing. These changes took place over a time period when non-anthropogenic forcing factors (i.e., the sum of solar and volcanic forcing) would be *likely* to have produced cooling, not warming (see Figure TS.23). Attribution studies show that it is *very likely* that these natural forcing factors alone cannot account for the observed warming (see Figure TS.23). There is also increased confidence that natural internal variability cannot account for the observed changes, due in part to improved studies demonstrating that the warming occurred in both oceans and atmosphere, together with observed ice mass losses. {2.9, 3.2, 5.2, 9.4, 9.5, 9.7}

It is very likely that anthropogenic greenhouse gas increases caused most of the observed increase in global average temperatures since the mid-20th century. Without the cooling effect of atmospheric aerosols, it is likely that greenhouse gases alone would have caused a greater global mean temperature rise than that observed during the last 50 years. A key

factor in identifying the aerosol fingerprint, and therefore the amount of cooling counteracting greenhouse warming, is the temperature change through time (see Figure TS.23), as well as the hemispheric warming contrast. The conclusion that greenhouse gas forcing has been dominant takes into account observational and forcing uncertainties, and is robust to the use of different climate models, different methods for estimating the responses to external forcing and different analysis techniques. It also allows for possible amplification of the response to solar forcing. {2.9, 6.6, 9.1, 9.2, 9.4}

Widespread warming has been detected in ocean temperatures. Formal attribution studies now suggest that it is *likely* that anthropogenic forcing has contributed to the observed warming of the upper several hundred metres of the global ocean during the latter half of the 20th century. {5.2, 9.5}

Anthropogenic forcing has likely contributed to recent decreases in arctic sea ice extent. Changes in arctic sea ice are expected given the observed enhanced arctic warming. Attribution studies and improvements in the modelled representation of sea ice and ocean heat transport strengthen the confidence in this conclusion. {3.3, 4.4, 8.2, 8.3, 9.5}

It is very likely that the response to anthropogenic forcing contributed to sea level rise during the latter half of the 20th century, but decadal variability in sea level rise remains poorly understood. Modelled estimates of the contribution to sea level rise from thermal expansion are in good agreement with estimates based on observations during 1961 to 2003, although the budget for sea level rise over that interval is not closed. The observed increase in the rate of loss of mass from glaciers and ice caps is proportional to the global average temperature rise, as expected qualitatively from physical considerations (see Table TS.3). The greater rate of sea level rise in 1993 to 2003 than in 1961 to 2003 may be linked to increasing anthropogenic forcing, which has

GLOBAL AND CONTINENTAL TEMPERATURE CHANGE

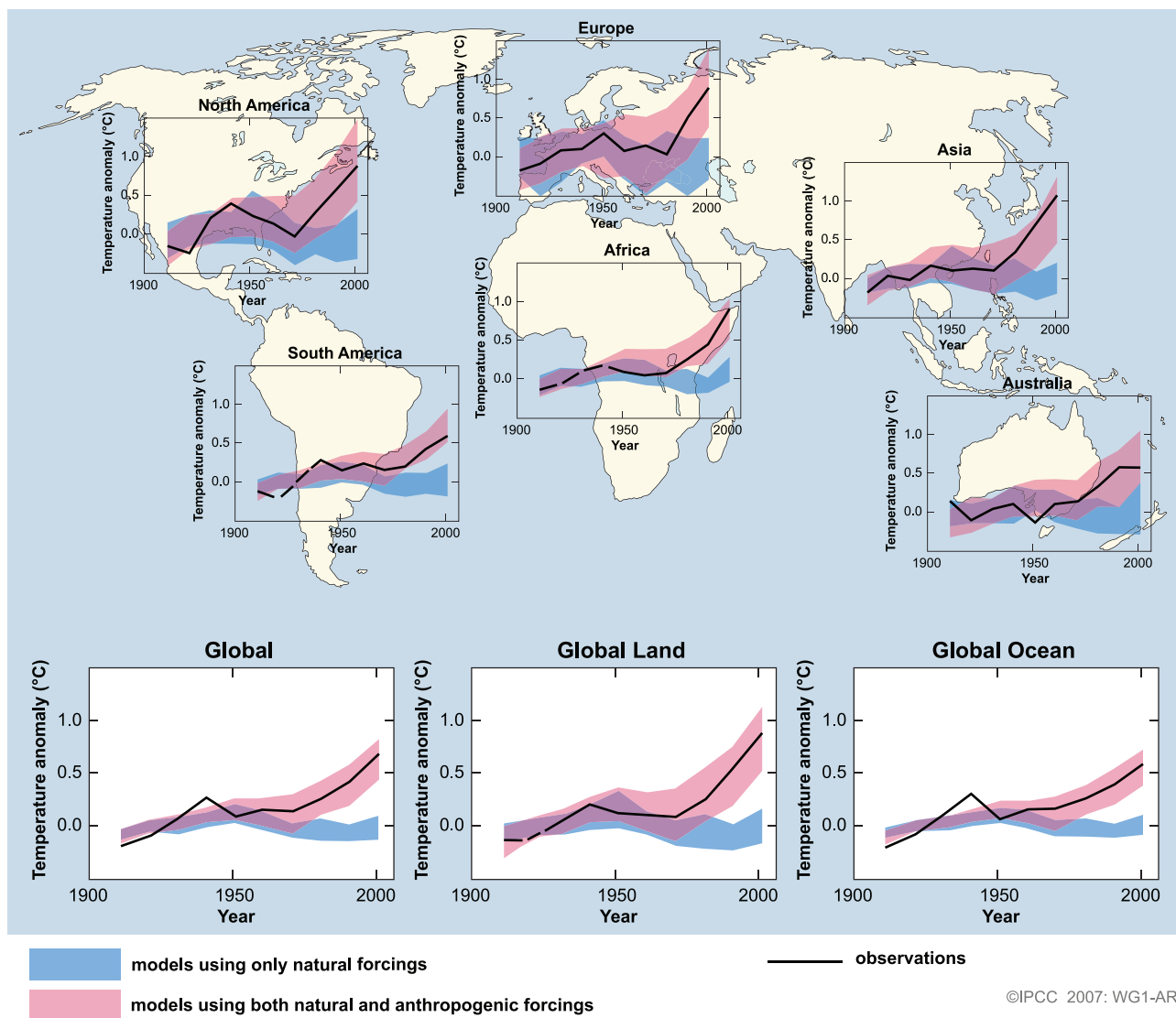


Figure TS.22. Comparison of observed continental- and global-scale changes in surface temperature with results simulated by climate models using natural and anthropogenic forcings. Decadal averages of observations are shown for the period 1906 to 2005 (black line) plotted against the centre of the decade and relative to the corresponding average for 1901 to 1950. Lines are dashed where spatial coverage is less than 50%. Blue shaded bands show the 5% to 95% range for 19 simulations from 5 climate models using only the natural forcings due to solar activity and volcanoes. Red shaded bands show the 5% to 95% range for 58 simulations from 14 climate models using both natural and anthropogenic forcings. Data sources and models used are described in Section 9.4, FAQ 9.2, Table 8.1 and the supplementary information for Chapter 9. {FAQ 9.2, Figure 1}

likely contributed to the observed warming of the upper ocean and widespread glacier retreat. On the other hand, the tide gauge record of global mean sea level suggests that similarly large rates may have occurred in previous 10-year periods since 1950, implying that natural internal variability could also be a factor in the high rates for 1993 to 2003 period. Observed decadal variability in the tide gauge record is larger than can be explained by variability in observationally based estimates of thermal expansion

and land ice changes. Further, the observed decadal variability in thermal expansion is larger than simulated by models for the 20th century. Thus, the physical causes of the variability seen in the tide gauge record are uncertain. These unresolved issues relating to sea level change and its decadal variability during 1961 to 2003 make it unclear how much of the higher rate of sea level rise in 1993 to 2003 is due to natural internal variability and how much to anthropogenic climate change. {5.5, 9.5}

TS.4.2 Attribution of Spatial and Temporal Changes in Temperature

The observed pattern of tropospheric warming and stratospheric cooling is *very likely* due to the influence of anthropogenic forcing, particularly that due to greenhouse gas increases and stratospheric ozone depletion. New analyses since the TAR show that this pattern corresponds to an increase in the height of the tropopause that is *likely* due largely to greenhouse gas and stratospheric ozone changes. Significant uncertainty remains in the estimation of tropospheric temperature trends, particularly from the radiosonde record. {3.2, 3.4, 9.4}

It is *likely* that there has been a substantial anthropogenic contribution to surface temperature increases averaged over every continent except Antarctica since the middle of the 20th century. Antarctica has insufficient observational coverage to make an assessment. Anthropogenic warming has also been identified in some sub-continental land areas. The ability of coupled climate models to simulate the temperature evolution on each of six continents provides stronger evidence of human influence on the global climate than was available in the TAR. No coupled global climate model that has used natural forcing only has reproduced the observed global mean warming trend, or the continental mean warming trends in individual

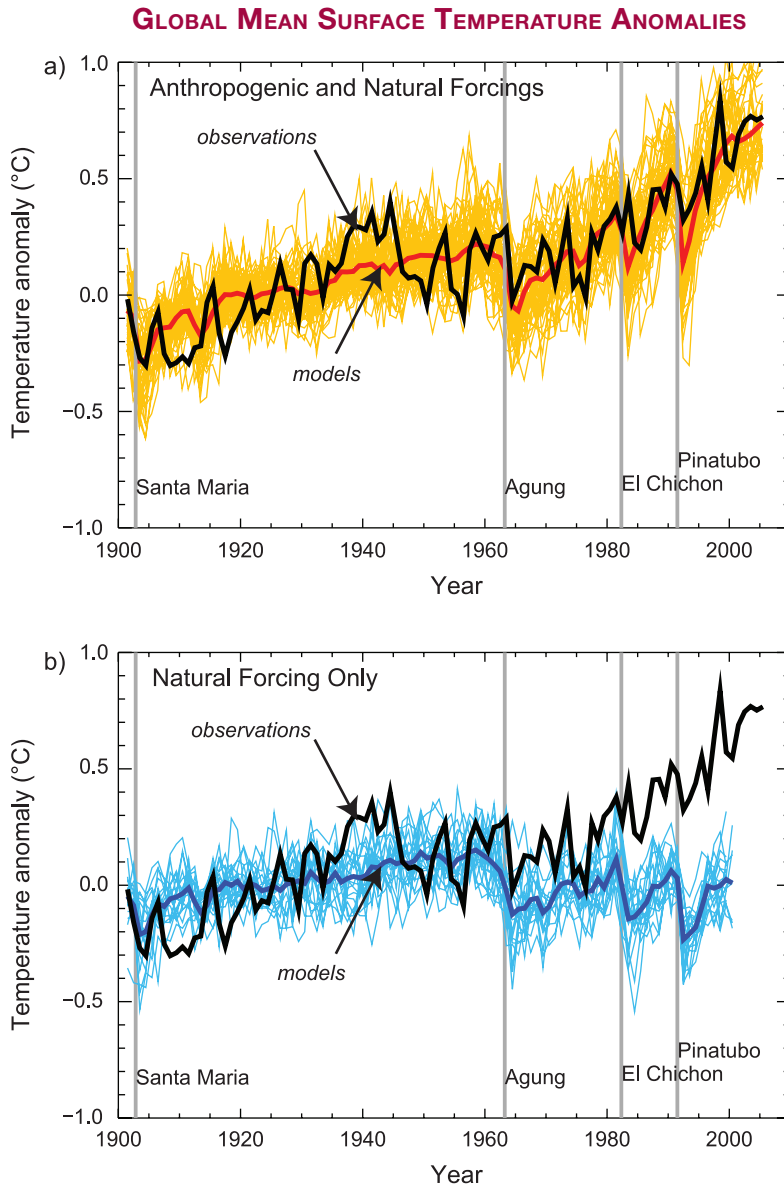


Figure TS.23. (a) Global mean surface temperature anomalies relative to the period 1901 to 1950, as observed (black line) and as obtained from simulations with both anthropogenic and natural forcings. The thick red curve shows the multi-model ensemble mean and the thin yellow curves show the individual simulations. Vertical grey lines indicate the timing of major volcanic events. (b) As in (a), except that the simulated global mean temperature anomalies are for natural forcings only. The thick blue curve shows the multi-model ensemble mean and the thin lighter blue curves show individual simulations. Each simulation was sampled so that coverage corresponds to that of the observations. {Figure 9.5}

continents (except Antarctica) over the second half of the 20th century. {9.4}

Difficulties remain in attributing temperature changes at smaller than continental scales and over time scales of less than 50 years. Attribution results at these scales have, with limited exceptions, not been established. Averaging over smaller regions reduces the natural variability less than does averaging over large regions, making it more difficult to distinguish between changes expected from external forcing and variability. In addition, temperature changes associated with some modes of variability are poorly simulated by models in some regions and seasons. Furthermore, the small-scale

details of external forcing and the response simulated by models are less credible than large-scale features. {8.3, 9.4}

Surface temperature extremes have likely been affected by anthropogenic forcing. Many indicators of extremes, including the annual numbers and most extreme values of warm and cold days and nights, as well as numbers of frost days, show changes that are consistent with warming. Anthropogenic influence has been detected in some of these indices, and there is evidence that anthropogenic forcing may have substantially increased the risk of extremely warm summer conditions regionally, such as the 2003 European heat wave. {9.4}

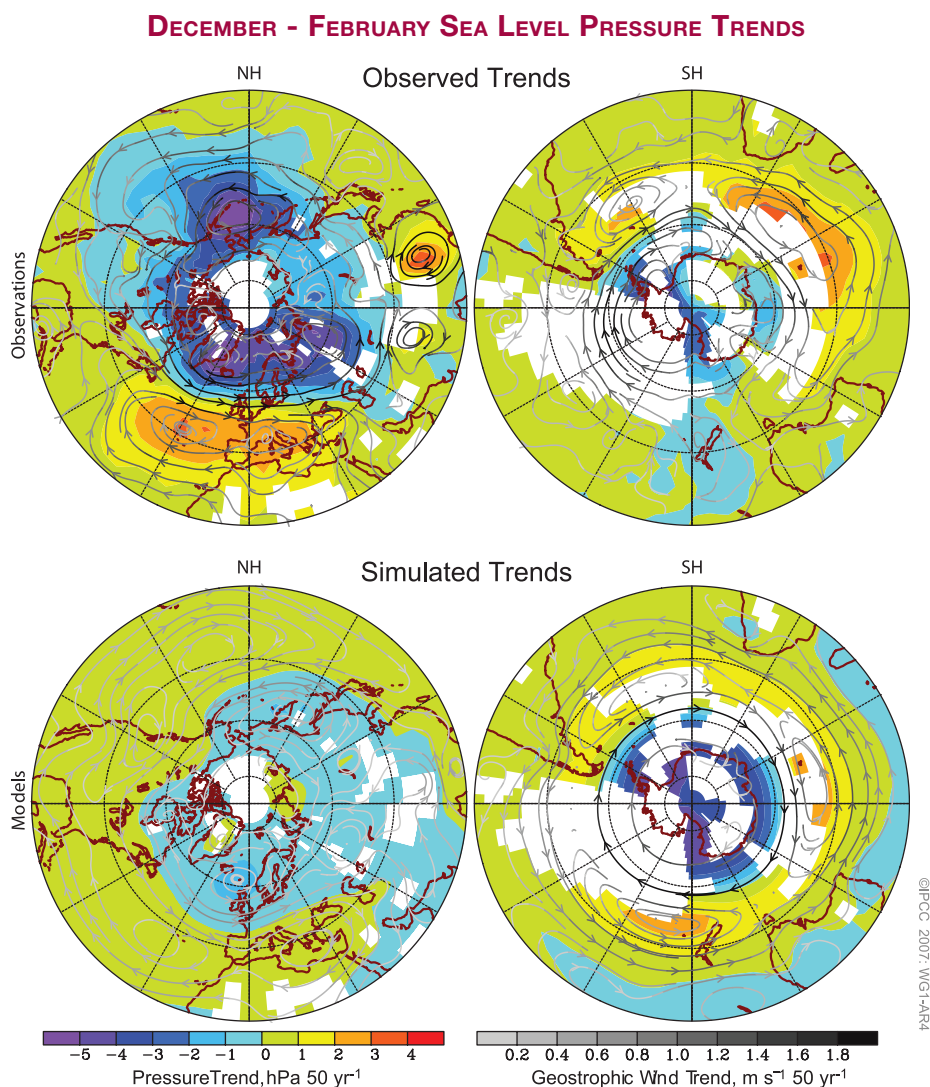


Figure TS.24. December through February sea level pressure trends based on decadal means for the period 1955 to 2005. (Top) Trends estimated from an observational data set and displayed in regions where there is observational coverage. (Bottom) Mean trends simulated in response to natural and anthropogenic forcing changes in eight coupled models. The model-simulated trends are displayed only where observationally based trends are displayed. Streamlines, which are not masked, indicate the direction of the trends in the geostrophic wind derived from the trends in sea level pressure, and the shading of the streamlines indicates the magnitude of the change, with darker streamlines corresponding to larger changes in geostrophic wind. Data sources and models are described in Chapter 9 and its supplementary material, and Table 8.1 provides model details. {Figure 9.16}

TS.4.3 Attribution of Changes in Circulation, Precipitation and Other Climate Variables

Trends in the Northern and Southern Annular Modes over recent decades, which correspond to sea level pressure reductions over the poles and related changes in atmospheric circulation, are likely related in part to human activity (see Figure TS.24). Models reproduce the sign of the NAM trend, but the simulated response is smaller than observed. Models including both greenhouse gas and stratospheric ozone changes simulate a realistic trend in the SAM, leading to a detectable human influence on global sea level pressure that is also consistent with the observed cooling trend in surface climate over parts of Antarctica. These changes in hemispheric circulation and their attribution to human activity imply that anthropogenic effects have *likely* contributed to changes in mid- and high-latitude patterns of circulation and temperature, as well as changes in winds and storm tracks. However, quantitative effects are uncertain because simulated responses to 20th century forcing change for the NH agree only qualitatively and not quantitatively with observations of these variables. {3.6, 9.5, 10.3}

There is some evidence of the impact of external influences on the hydrological cycle. The observed large-scale pattern of changes in land precipitation over the 20th century is qualitatively consistent with simulations, suggestive of a human influence. An observed global trend towards increases in drought in the second half of the 20th century has been reproduced with a model by taking anthropogenic and natural forcing into account. A number of studies have now demonstrated that changes in land use, due for example to overgrazing and conversion of woodland to agriculture, are *unlikely* to have been the primary cause of Sahelian and Australian droughts. Comparisons between observations and models suggest that changes in monsoons, storm intensities and Sahelian rainfall are related at least in part to changes in observed SSTs. Changes in global SSTs are expected to be affected by anthropogenic forcing, but an association of regional SST changes with forcing has not been established. Changes in rainfall depend not just upon SSTs but also upon changes in the spatial and temporal SST patterns and regional changes in atmospheric circulation, making attribution to human influences difficult. {3.3, 9.5, 10.3, 11.2}

TS.4.4 Palaeoclimate Studies of Attribution

It is very likely that climate changes of at least the seven centuries prior to 1950 were not due to unforced variability alone. Detection and attribution studies indicate that a substantial fraction of pre-industrial NH inter-decadal temperature variability contained in reconstructions for those centuries is *very likely* attributable to natural external forcing. Such forcing includes episodic cooling due to known volcanic eruptions, a number of which were larger than those of the 20th century (based on evidence such as ice cores), and long-term variations in solar irradiance, such as reduced radiation during the Maunder Minimum. Further, it is *likely* that anthropogenic forcing contributed to the early 20th-century warming evident in these records. Uncertainties are unlikely to lead to a spurious agreement between temperature reconstructions and forcing reconstructions as they are derived from independent proxies. Insufficient data are available to make a similar SH evaluation. {6.6, 9.3}

TS.4.5 Climate Response to Radiative Forcing

Specification of a likely range and a most likely value for equilibrium climate sensitivity⁸ in this report represents significant progress in quantifying the climate system response to radiative forcing since the TAR and an advance in challenges to understanding that have persisted for over 30 years. A range for equilibrium climate sensitivity – the equilibrium global average warming expected if CO₂ concentrations were to be sustained at double their pre-industrial values (about 550 ppm) – was given in the TAR as between 1.5°C and 4.5°C. It has not been possible previously to provide a best estimate or to estimate the probability that climate sensitivity might fall outside that quoted range. Several approaches are used in this assessment to constrain climate sensitivity, including the use of AOGCMs, examination of the transient evolution of temperature (surface, upper air and ocean) over the last 150 years and examination of the rapid response of the global climate system to changes in the forcing caused by volcanic eruptions (see Figure TS.25). These are complemented by estimates based upon palaeoclimate studies such as reconstructions of the NH temperature record of the past millennium and the LGM. Large ensembles of climate model simulations have shown that the ability of models to simulate present climate has value in constraining climate sensitivity. {8.1, 8.6, 9.6, Box 10.2}

⁸ See the Glossary for a detailed definition of climate sensitivity.

Analysis of models together with constraints from observations suggest that the equilibrium climate sensitivity is *likely* to be in the range 2°C to 4.5°C, with a best estimate value of about 3°C. It is *very unlikely* to be less than 1.5°C. Values substantially higher than 4.5°C cannot be excluded, but agreement with observations is not as good for those values. Probability density functions derived from different information and approaches generally tend to have a long tail towards high values exceeding 4.5°C. Analysis of climate and forcing evolution over previous centuries and model ensemble studies do not rule out climate sensitivity being as high as 6°C or more. One factor in this is the possibility of small net radiative forcing over the 20th century if aerosol indirect cooling effects were at the upper end of their uncertainty range, thus cancelling most of the positive forcing due to greenhouse gases. However, there is no well-established way of estimating a single probability distribution function from individual results taking account of the different assumptions in each study. The lack of strong constraints limiting high climate sensitivities prevents the specification of a 95th percentile bound or a very likely range for climate sensitivity. {Box 10.2}

There is now increased confidence in the understanding of key climate processes that are important to climate sensitivity due to improved analyses and comparisons of models to one another and to observations. Water vapour changes dominate the feedbacks affecting climate sensitivity and are now better understood. New observational and modelling evidence strongly favours a combined water vapour-lapse rate⁹ feedback of around the strength found in General Circulation Models (GCMs), that is, approximately 1 W m⁻² per degree global temperature increase, corresponding to about a 50% amplification of global mean warming. Such GCMs have demonstrated an ability to simulate seasonal to inter-decadal humidity variations in the upper troposphere over land and ocean, and have successfully simulated the observed surface temperature and humidity changes associated with volcanic eruptions. Cloud feedbacks (particularly from low clouds) remain the largest source of uncertainty. Cryospheric feedbacks such as changes in snow cover have been shown to contribute less to the spread in model estimates of climate sensitivity than cloud or water vapour feedbacks, but they

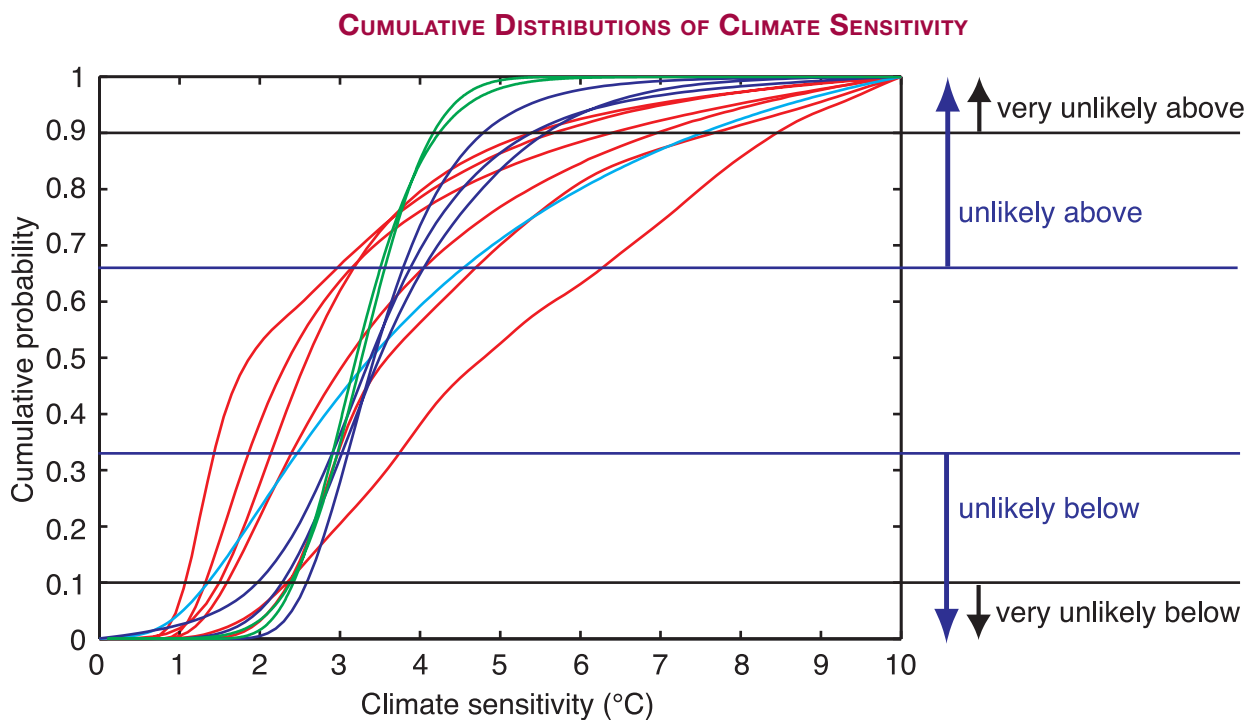


Figure TS.25. Cumulative distributions of climate sensitivity derived from observed 20th-century warming (red), model climatology (blue), proxy evidence (cyan) and from climate sensitivities of AOGCMs (green). Horizontal lines and arrows mark the boundaries of the likelihood estimates defined in the IPCC Fourth Assessment Uncertainty Guidance Note (see Box TS.1). {Box 10.2, Figures 1 and 2}

⁹ The rate at which air temperature decreases with altitude.

can be important for regional climate responses at mid- and high latitudes. A new model intercomparison suggests that differences in radiative transfer formulations also contribute to the range. {3.4, 8.6, 9.3, 9.4, 9.6, 10.2, Box 10.2}

Improved quantification of climate sensitivity allows estimation of best estimate equilibrium temperatures and ranges that could be expected if concentrations of CO₂ were to be stabilised at various levels based on global energy balance considerations (see Table TS.5). As in the estimate of climate sensitivity, a very likely upper bound cannot be established. Limitations to the concept of radiative forcing and climate sensitivity should be noted. Only a few AOGCMs have been run to equilibrium under elevated CO₂ concentrations, and some results show that climate feedbacks may change over long time scales, resulting in substantial deviations from estimates of warming based on equilibrium climate sensitivity inferred from mixed layer ocean models and past climate change. {10.7}

Agreement among models for projected transient climate change has also improved since the TAR. The range of transient climate responses (defined as the global average surface air temperature averaged over a 20-year period centred at the time of CO₂ doubling in a 1% yr⁻¹ increase experiment) among models is smaller than the range in the equilibrium climate sensitivity. This parameter is now better constrained by multi-model ensembles and comparisons with observations; it is *very likely* to be greater than 1°C and *very unlikely* to be greater than 3°C. The transient climate response

Table TS.5. Best estimate, likely ranges and very likely lower bounds of global mean equilibrium surface temperature increase (°C) over pre-industrial temperatures for different levels of CO₂-equivalent radiative forcing, as derived from the climate sensitivity.

Equilibrium CO ₂ -eq (ppm)	Temperature Increase (°C)		
	Best Estimate	Very Likely Above	Likely in the Range
350	1.0	0.5	0.6–1.4
450	2.1	1.0	1.4–3.1
550	2.9	1.5	1.9–4.4
650	3.6	1.8	2.4–5.5
750	4.3	2.1	2.8–6.4
1000	5.5	2.8	3.7–8.3
1200	6.3	3.1	4.2–9.4

is related to sensitivity in a nonlinear way such that high sensitivities are not immediately manifested in the short-term response. Transient climate response is strongly affected by the rate of ocean heat uptake. Although the ocean models have improved, systematic model biases and limited ocean temperature data to evaluate transient ocean heat uptake affect the accuracy of current estimates. {8.3, 8.6, 9.4, 9.6, 10.5}

TS.5 Projections of Future Changes in Climate

Since the TAR, there have been many important advances in the science of climate change projections. An unprecedented effort has been initiated to make new model results available for prompt scrutiny by researchers outside of the modelling centres. A set of coordinated, standard experiments was performed by 14 AOGCM modelling groups from 10 countries using 23 models. The resulting multi-model database of outputs, analysed by hundreds of researchers worldwide, forms the basis for much of this assessment of model results. Many advances have come from the use of multi-member ensembles from single models (e.g., to test the sensitivity of response to initial conditions) and from multi-model ensembles. These two different types of ensembles allow more robust studies of the range of model results and more quantitative model evaluation against observations, and provide new information on simulated statistical variability. {8.1, 8.3, 9.4, 9.5, 10.1}

A number of methods for providing probabilistic climate change projections, both for global means and geographical depictions, have emerged since the TAR and are a focus of this report. These include methods based on results of AOGCM ensembles without formal application of observational constraints as well as methods based on detection algorithms and on large model ensembles that provide projections consistent with observations of climate change and their uncertainties. Some methods now explicitly account for key uncertainty sources such as climate feedbacks, ocean heat uptake, radiative forcing and the carbon cycle. Short-term projections are similarly constrained by observations of recent trends. Some studies have probed additional probabilistic issues, such as the likelihood of future changes in extremes such as heat waves that could occur due to human influences. Advances have also occurred since the TAR through broader ranges

of studies of committed climate change and of carbon-climate feedbacks. {8.6, 9.6, 10.1, 10.3, 10.5}

These advances in the science of climate change modelling provide a probabilistic basis for distinguishing projections of climate change for different SRES marker scenarios. This is in contrast to the TAR where ranges for different marker scenarios could not be given in probabilistic terms. As a result, this assessment identifies and quantifies the difference in character between uncertainties that arise in climate modelling and those that arise from a lack of prior knowledge of decisions that will affect greenhouse gas emissions. A loss of policy-relevant information would result from combining probabilistic projections. For these reasons, projections for different emission scenarios are not combined in this report.

Model simulations used here consider the response of the physical climate system to a range of possible future conditions through use of idealised emissions or concentration assumptions. These include experiments with greenhouse gases and aerosols held constant at year

2000 levels, CO₂ doubling and quadrupling experiments, SRES marker scenarios for the 2000 to 2100 period, and experiments with greenhouse gases and aerosols held constant after 2100, providing new information on the physical aspects of long-term climate change and stabilisation. The SRES scenarios did not include climate initiatives. This Working Group I assessment does not evaluate the plausibility or likelihood of any specific emission scenario. {10.1, 10.3}

A new multi-model data set using Earth System Models of Intermediate Complexity (EMICs) complements AOGCM experiments to extend the time horizon for several more centuries in the future. This provides a more comprehensive range of model responses in this assessment as well as new information on climate change over long time scales when greenhouse gas and aerosol concentrations are held constant. Some AOGCMs and EMICs contain prognostic carbon cycle components, which permit estimation of the likely effects and associated uncertainties of carbon cycle feedbacks. {10.1}

Box TS.8: Hierarchy of Global Climate Models

Estimates of change in global mean temperature and sea level rise due to thermal expansion can be made using Simple Climate Models (SCMs) that represent the ocean-atmosphere system as a set of global or hemispheric boxes, and predict global surface temperature using an energy balance equation, a prescribed value of climate sensitivity and a basic representation of ocean heat uptake. Such models can also be coupled to simplified models of biogeochemical cycles and allow rapid estimation of the climate response to a wide range of emission scenarios. {8.8, 10.5}

Earth System Models of Intermediate Complexity (EMICs) include some dynamics of the atmospheric and oceanic circulations, or parametrizations thereof, and often include representations of biogeochemical cycles, but they commonly have reduced spatial resolution. These models can be used to investigate continental-scale climate change and long-term, large-scale effects of coupling between Earth system components using large ensembles of model runs or runs over many centuries. For both SCMs and EMICs it is computationally feasible to sample parameter spaces thoroughly, taking account of parameter uncertainties derived from tuning to more comprehensive climate models, matching observations and use of expert judgment. Thus, both types of model are well suited to the generation of probabilistic projections of future climate and allow a comparison of the 'response uncertainty' arising from uncertainty in climate model parameters with the 'scenario range' arising from the range of emission scenarios being considered. Earth System Models of Intermediate Complexity have been evaluated in greater depth than previously and intercomparison exercises have demonstrated that they are useful for studying questions involving long time scales or requiring large ensembles of simulations. {8.8, 10.5, 10.7}

The most comprehensive climate models are the AOGCMs. They include dynamical components describing atmospheric, oceanic and land surface processes, as well as sea ice and other components. Much progress has been made since the TAR (see Box TS.7), and there are over 20 models from different centres available for climate simulations. Although the large-scale dynamics of these models are comprehensive, parametrizations are still used to represent unresolved physical processes such as the formation of clouds and precipitation, ocean mixing due to wave processes and the formation of water masses, etc. Uncertainty in parametrizations is the primary reason why climate projections differ between different AOGCMs. While the resolution of AOGCMs is rapidly improving, it is often insufficient to capture the fine-scale structure of climatic variables in many regions. In such cases, the output from AOGCMs can be used to drive limited-area (or regional climate) models that combine the comprehensiveness of process representations comparable to AOGCMs with much higher spatial resolution. {8.2}

TS.5.1 Understanding Near-Term Climate Change

Knowledge of the climate system together with model simulations confirm that past changes in greenhouse gas concentrations will lead to a committed warming (see Box TS.9 for a definition) and future climate change. New model results for experiments in which concentrations of all forcing agents were held constant provide better estimates of the committed changes in atmospheric variables that would follow because of the long response time of the climate system, particularly the oceans. {10.3, 10.7}

Previous IPCC projections of future climate changes can now be compared to recent observations, increasing confidence in short-term projections and the underlying physical understanding of committed climate change over a few decades. Projections for 1990 to 2005 carried out for the FAR and the SAR suggested global mean temperature increases of about 0.3°C and 0.15°C per decade, respectively.¹⁰ The difference between the two was due primarily to the inclusion of aerosol cooling effects in the SAR, whereas there was no quantitative basis for doing so in the FAR. Projections given in the TAR were similar to those of the SAR. These results are comparable to observed values of about 0.2°C per decade, as shown in Figure TS.26, providing broad confidence in such short-term projections. Some of this warming is the committed effect of changes in the concentrations of greenhouse gases prior to the times of those earlier assessments. {1.2, 3.2}

Committed climate change (see Box TS.9) due to atmospheric composition in the year 2000 corresponds to a warming trend of about 0.1°C per decade over the next two decades, in the absence of large changes in volcanic or solar forcing. About twice as much warming (0.2°C per decade) would be expected if emissions were to fall within the range of the SRES marker scenarios. This result is insensitive to the choice among the SRES marker scenarios, none of which considered climate initiatives. By 2050, the range of expected warming shows limited sensitivity to the choice among SRES scenarios (1.3°C to 1.7°C relative to 1980–1999) with about a quarter being due to the committed climate change if all radiative forcing agents were stabilised today. {10.3, 10.5, 10.7}

Sea level is expected to continue to rise over the next several decades. During 2000 to 2020 under the SRES A1B scenario in the ensemble of AOGCMs, the rate of thermal expansion is projected to be $1.3 \pm 0.7 \text{ mm yr}^{-1}$, and is not significantly different under the A2 or B1 scenarios. These projected rates are within the uncertainty of the observed contribution of thermal expansion for 1993 to 2003 of $1.6 \pm 0.6 \text{ mm yr}^{-1}$. The ratio of committed thermal expansion, caused by constant atmospheric composition at year 2000 values, to total thermal expansion (that is the ratio of expansion occurring after year 2000 to that occurring before and after) is larger than the corresponding ratio for global average surface temperature. {10.6, 10.7}

Box TS.9: Committed Climate Change

If the concentrations of greenhouse gases and aerosols were held fixed after a period of change, the climate system would continue to respond due to the thermal inertia of the oceans and ice sheets and their long time scales for adjustment. ‘Committed warming’ is defined here as the further change in global mean temperature after atmospheric composition, and hence radiative forcing, is held constant. Committed change also involves other aspects of the climate system, in particular sea level. Note that holding concentrations of radiatively active species constant would imply that ongoing emissions match natural removal rates, which for most species would be equivalent to a large reduction in emissions, although the corresponding model experiments are not intended to be considered as emission scenarios. {FAQ 10.3}

The troposphere adjusts to changes in its boundary conditions over time scales shorter than a month or so. The upper ocean responds over time scales of several years to decades, and the deep ocean and ice sheet response time scales are from centuries to millennia. When the radiative forcing changes, internal properties of the atmosphere tend to adjust quickly. However, because the atmosphere is strongly coupled to the oceanic mixed layer, which in turn is coupled to the deeper oceanic layer, it takes a very long time for the atmospheric variables to come to an equilibrium. During the long periods where the surface climate is changing very slowly, one can consider that the atmosphere is in a quasi-equilibrium state, and most energy is being absorbed by the ocean, so that ocean heat uptake is a key measure of climate change. {10.7}

¹⁰ See IPCC First Assessment Report, Policymakers Summary, and Second Assessment Report, Technical Summary, Figure 18.

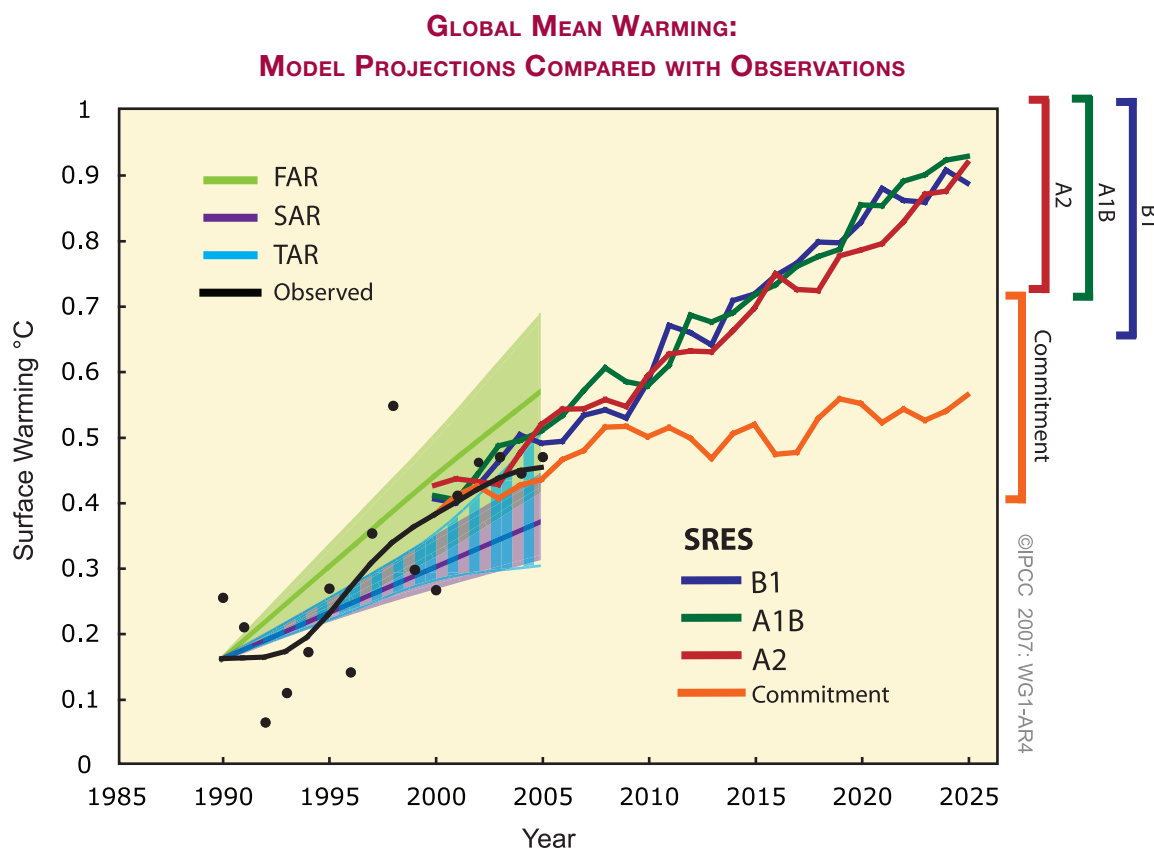


Figure TS.26. Model projections of global mean warming compared to observed warming. Observed temperature anomalies, as in Figure TS.6, are shown as annual (black dots) and decadal average values (black line). Projected trends and their ranges from the IPCC First (FAR) and Second (SAR) Assessment Reports are shown as green and magenta solid lines and shaded areas, and the projected range from the TAR is shown by vertical blue bars. These projections were adjusted to start at the observed decadal average value in 1990. Multi-model mean projections from this report for the SRES B1, A1B and A2 scenarios, as in Figure TS.32, are shown for the period 2000 to 2025 as blue, green and red curves with uncertainty ranges indicated against the right-hand axis. The orange curve shows model projections of warming if greenhouse gas and aerosol concentrations were held constant from the year 2000 – that is, the committed warming. {Figures 1.1 and 10.4}

TS.5.2 Large-Scale Projections for the 21st Century

This section covers advances in understanding global-scale climate projections and the processes that will influence their large-scale patterns in the 21st century. More specific discussion of regional-scale changes follows in TS.5.3.

Projected global average surface warming for the end of the 21st century (2090–2099) is scenario-dependent and the actual warming will be significantly affected by the actual emissions that occur. Warmings compared to 1980 to 1999 for six SRES scenarios¹¹ and for constant year 2000 concentrations, given as best estimates and corresponding *likely* ranges,

are shown in Table TS.6. These results are based on AOGCMs, observational constraints and other methods to quantify the range of model response (see Figure TS.27). The combination of multiple lines of evidence allows likelihoods to be assigned to the resulting ranges, representing an important advance since the TAR. {10.5}

Assessed uncertainty ranges are larger than those given in the TAR because they consider a more complete range of models and climate-carbon cycle feedbacks. Warming tends to reduce land and ocean uptake of atmospheric CO₂, increasing the fraction of anthropogenic emissions that remains in the atmosphere. For the A2 scenario for example, the CO₂ feedback increases the corresponding global average warming in 2100 by more than 1°C. {7.3, 10.5}

¹¹ Approximate CO₂ equivalent concentrations corresponding to the computed radiative forcing due to anthropogenic greenhouse gases and aerosols in 2100 (see p. 823 of the TAR) for the SRES B1, A1T, B2, A1B, A2 and A1FI illustrative marker scenarios are about 600, 700, 800, 850, 1,250 and 1,550 ppm respectively. Constant emission at year 2000 levels would lead to a concentration for CO₂ alone of about 520 ppm by 2100.

Table TS.6. Projected global average surface warming and sea level rise at the end of the 21st century. {10.5, 10.6, Table 10.7}

Case	Temperature Change (°C at 2090-2099 relative to 1980-1999) ^a		Sea Level Rise (m at 2090-2099 relative to 1980-1999)
	Best estimate	Likely range	Model-based range excluding future rapid dynamical changes in ice flow
Constant Year 2000 concentrations^b	0.6	0.3 – 0.9	NA
B1 scenario	1.8	1.1 – 2.9	0.18 – 0.38
A1T scenario	2.4	1.4 – 3.8	0.20 – 0.45
B2 scenario	2.4	1.4 – 3.8	0.20 – 0.43
A1B scenario	2.8	1.7 – 4.4	0.21 – 0.48
A2 scenario	3.4	2.0 – 5.4	0.23 – 0.51
A1FI scenario	4.0	2.4 – 6.4	0.26 – 0.59

Notes:

^a These estimates are assessed from a hierarchy of models that encompass a simple climate model, several Earth Models of Intermediate Complexity (EMICs), and a large number of Atmosphere-Ocean Global Circulation Models (AOGCMs).

^b Year 2000 constant composition is derived from AOGCMs only.

Projected global-average sea level rise at the end of the 21st century (2090 to 2099), relative to 1980 to 1999 for the six SRES marker scenarios, given as 5% to 95% ranges based on the spread of model results, are shown in Table TS.6. Thermal expansion contributes 70 to 75% to the best estimate for each scenario. An improvement since the TAR is the use of AOGCMs to evaluate ocean heat uptake and thermal expansion. This has also reduced the projections as compared to the simple model used in the TAR. In all the SRES marker scenarios except B1, the average rate of sea level rise during the 21st century *very likely* exceeds the 1961–2003 average rate ($1.8 \pm 0.5 \text{ mm yr}^{-1}$). For an average model, the scenario spread in sea level rise is only 0.02 m by the middle of the century, but by the end of the century it is 0.15 m. These ranges do not include uncertainties in carbon-cycle feedbacks or ice flow processes because a basis in published literature is lacking. {10.6, 10.7}

For each scenario, the midpoint of the range given here is within 10% of the TAR model average for 2090–2099, noting that the TAR projections were given for 2100, whereas projections in this report are for 2090–2099. The uncertainty in these projections is less than in the TAR for several reasons: uncertainty in land ice models is assumed independent of uncertainty in temperature and expansion projections; improved observations of recent mass loss from glaciers provide a better observational constraint; and the present report gives uncertainties as 5% to 95% ranges, equivalent to ± 1.65 standard deviations, whereas the TAR gave

uncertainty ranges of ± 2 standard deviations. The TAR would have had similar ranges for sea level projections to those in this report if it had treated the uncertainties in the same way. {10.6, 10.7}

Changes in the cryosphere will continue to affect sea level rise during the 21st century. Glaciers, ice caps and the Greenland Ice Sheet are projected to lose mass in the 21st century because increased melting will exceed increased snowfall. Current models suggest that the Antarctic Ice Sheet will remain too cold for widespread melting and may gain mass in future through increased snowfall, acting to reduce sea level rise. However, changes in ice dynamics could increase the contributions of both Greenland and Antarctica to 21st-century sea level rise. Recent observations of some Greenland outlet glaciers give strong evidence for enhanced flow when ice shelves are removed. The observations in west-central Greenland of seasonal variation in ice flow rate and of a correlation with summer temperature variation suggest that surface melt water may join a sub-glacially routed drainage system lubricating the ice flow. By both of these mechanisms, greater surface melting during the 21st century could cause acceleration of ice flow and discharge and increase the sea level contribution. In some parts of West Antarctica, large accelerations of ice flow have recently occurred, which may have been caused by thinning of ice shelves due to ocean warming. Although this has not been formally attributed to anthropogenic climate change due to greenhouse gases, it suggests that future warming could cause faster mass loss and greater

PROJECTED WARMING IN 2090–2099

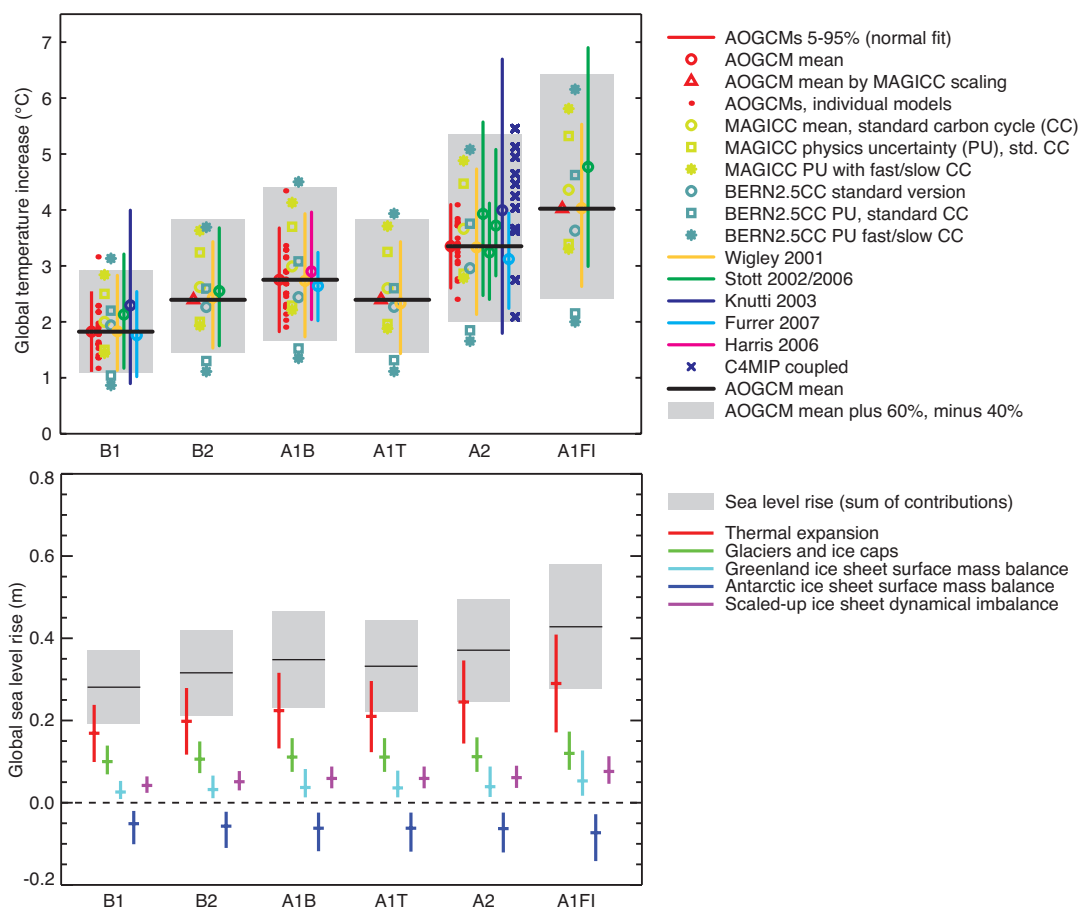


Figure TS.27. (Top) Projected global mean temperature change in 2090 to 2099 relative to 1980 to 1999 for the six SRES marker scenarios based on results from different and independent models. The multi-model AOGCM mean and the range of the mean minus 40% to the mean plus 60% are shown as black horizontal solid lines and grey bars, respectively. Carbon cycle uncertainties are estimated for scenario A2 based on Coupled Carbon Cycle Climate Model Intercomparison Project (C⁴MIP) models (dark blue crosses), and for all marker scenarios using an EMIC (pale blue symbols). Other symbols represent individual studies (see Figure 10.29 for details of specific models). (Bottom) Projected global average sea level rise and its components in 2090 to 2099 (relative to 1980–1999) for the six SRES marker scenarios. The uncertainties denote 5 to 95% ranges, based on the spread of model results, and not including carbon cycle uncertainties. The contributions are derived by scaling AOGCM results and estimating land ice changes from temperature changes (see Appendix 10.A for details). Individual contributions are added to give the total sea level rise, which does not include the contribution shown for ice sheet dynamical imbalance, for which the current level of understanding prevents a best estimate from being given. {Figures 10.29 and 10.33}

sea level rise. Quantitative projections of this effect cannot be made with confidence. If recently observed increases in ice discharge rates from the Greenland and Antarctic Ice Sheets were to increase linearly with global average temperature change, that would add 0.1 to 0.2 m to the upper bound of sea level rise. Understanding of these effects is too limited to assess their likelihood or to give a best estimate. {4.6, 10.6}

Many of the global and regional patterns of temperature and precipitation seen in the TAR projections remain in the new generation of models and across ensemble results (see Figure TS.28). Confidence

in the robustness of these patterns is increased by the fact that they have remained largely unchanged while overall model simulations have improved (Box TS.7). This adds to confidence that these patterns reflect basic physical constraints on the climate system as it warms. {8.3–8.5, 10.3, 11.2–11.9}

The projected 21st-century temperature change is positive everywhere. It is greatest over land and at most high latitudes in the NH during winter, and increases going from the coasts into the continental interiors. In otherwise geographically similar areas, warming is typically larger in arid than in moist regions. {10.3, 11.2–11.9}

In contrast, warming is least over the southern oceans and parts of the North Atlantic Ocean. Temperatures are projected to increase, including over the North Atlantic and Europe, despite a projected slowdown of the meridional overturning circulation (MOC) in most models, due to the much larger influence of the increase in greenhouse gases. The projected pattern of zonal mean temperature change in the atmosphere displays a maximum warming in the upper tropical troposphere and cooling in the stratosphere. Further zonal mean warming in the ocean is expected to occur first near the surface and in the northern mid-latitudes, with the warming gradually reaching the ocean interior, most evident at high latitudes where vertical mixing is greatest. The projected pattern of change is very similar among the late-century cases irrespective of the scenario. Zonally averaged fields normalised by the mean warming are very similar for the scenarios examined (see Figure TS.28). {10.3}

It is *very likely* that the Atlantic MOC will slow down over the course of the 21st century. The multi-model average reduction by 2100 is 25% (range from zero to about 50%) for SRES emission scenario A1B. Temperatures in the Atlantic region are projected to increase despite such changes due to the much larger warming associated with projected increases of greenhouse gases. The projected reduction of the Atlantic MOC is due to the combined effects of an increase in high latitude temperatures and precipitation, which reduce the density of the surface waters in the North Atlantic. This could lead to a significant reduction in Labrador Sea Water formation. Very few AOGCM studies have included the impact of additional freshwater from melting of the Greenland Ice Sheet, but those that have do not suggest that this will lead to a complete MOC shutdown. Taken together, it is *very likely* that the MOC will reduce, but very *unlikely* that the MOC will undergo a large abrupt transition during the course of the 21st century. Longer-term changes in the MOC cannot be assessed with confidence. {8.7, 10.3}

PROJECTIONS OF SURFACE TEMPERATURES

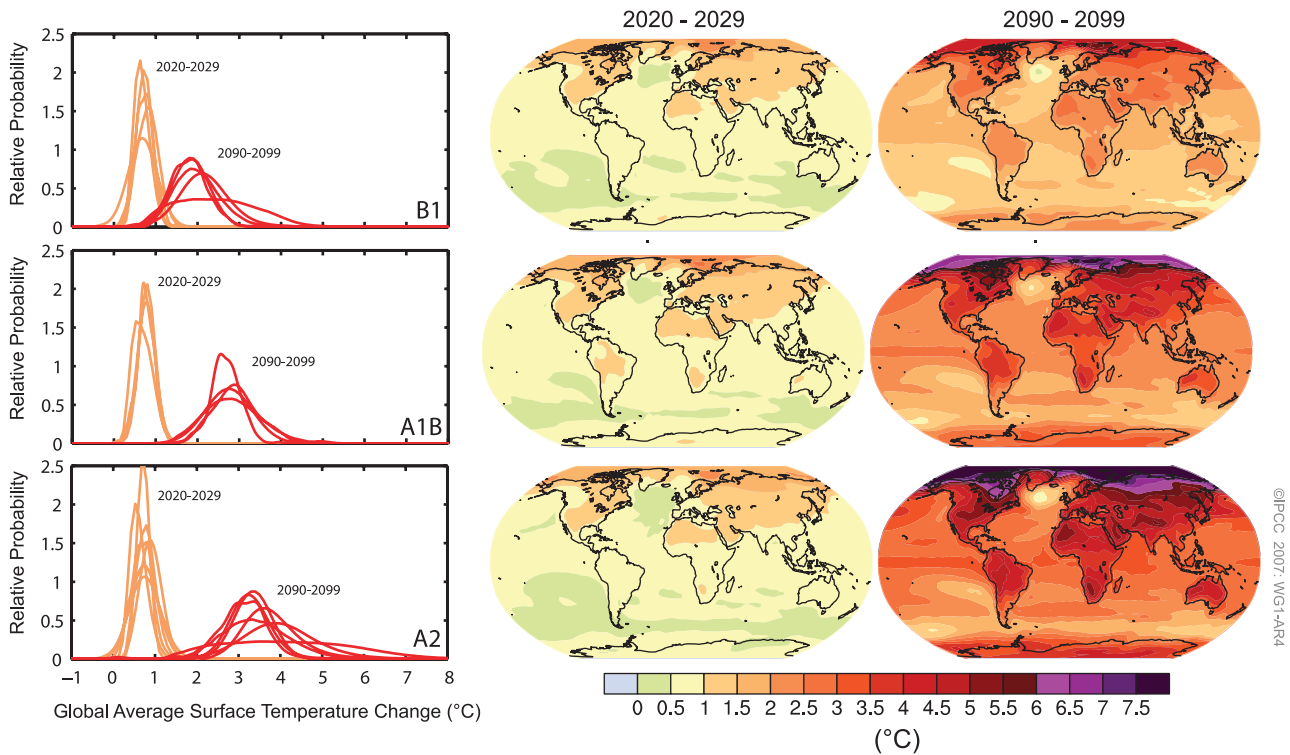


Figure TS.28. Projected surface temperature changes for the early and late 21st century relative to the period 1980 to 1999. The central and right panels show the AOGCM multi-model average projections (°C) for the B1 (top), A1B (middle) and A2 (bottom) SRES scenarios averaged over the decades 2020 to 2029 (centre) and 2090 to 2099 (right). The left panel shows corresponding uncertainties as the relative probabilities of estimated global average warming from several different AOGCM and EMIC studies for the same periods. Some studies present results only for a subset of the SRES scenarios, or for various model versions. Therefore the difference in the number of curves, shown in the left-hand panels, is due only to differences in the availability of results. {Adapted from Figures 10.8 and 10.28}

Models indicate that sea level rise during the 21st century will not be geographically uniform. Under scenario A1B for 2070 to 2099, AOGCMs give a median spatial standard deviation of 0.08 m, which is about 25% of the central estimate of the global average sea level rise. The geographic patterns of future sea level change arise mainly from changes in the distribution of heat and salinity in the ocean and consequent changes in ocean circulation. Projected patterns display more similarity across models than those analysed in the TAR. Common features are a smaller than average sea level rise in the Southern Ocean, larger than average sea level rise in the Arctic and a narrow band of pronounced sea level rise stretching across the southern Atlantic and Indian Oceans. {10.6}

Projections of changes in extremes such as the frequency of heat waves are better quantified than in the TAR, due to improved models and a better assessment of model spread based on multi-model ensembles. The TAR concluded that there was a risk of increased temperature extremes, with more extreme heat episodes in a future climate. This result has been confirmed and expanded in more recent studies. Future increases in temperature extremes are projected to follow increases in mean temperature over most of the world except where surface properties (e.g., snow cover or soil moisture) change. A multi-model analysis, based on simulations of 14 models for three scenarios, investigated changes in extreme seasonal (DJF and JJA) temperatures where ‘extreme’ is defined as lying above the 95th percentile of the simulated temperature distribution for the 20th century. By the end of the 21st century, the projected probability of extreme warm seasons rises above 90% in many tropical areas, and reaches around 40% elsewhere. Several recent studies have addressed possible future changes in heat waves, and found that, in a future climate, heat waves are expected to be more intense, longer lasting and more frequent. Based on an eight-member multi-model ensemble, heat waves are simulated to have been increasing for the latter part of the 20th century, and are projected to increase globally and over most regions. {8.5, 10.3}

For a future warmer climate, models project a 50 to 100% decline in the frequency of cold air outbreaks relative to the present in NH winters in most areas. Results from a nine-member multi-model ensemble show simulated decreases in frost days for the 20th century continuing into the 21st century globally and in most regions. Growing season length is related to frost days and is projected to increase in future climates. {10.3, FAQ 10.1}

Snow cover is projected to decrease. Widespread increases in thaw depth are projected to occur over most permafrost regions. {10.3}

Under several different scenarios (SRES A1B, A2 and B1), large parts of the Arctic Ocean are expected to no longer have year-round ice cover by the end of the 21st century. Arctic sea ice responds sensitively to warming. While projected changes in winter sea ice extent are moderate, late-summer sea ice is projected to disappear almost completely towards the end of the 21st century under the A2 scenario in some models. The reduction is accelerated by a number of positive feedbacks in the climate system. The ice-albedo feedback allows open water to receive more heat from the Sun during summer, the insulating effect of sea ice is reduced and the increase in ocean heat transport to the Arctic further reduces ice cover. Model simulations indicate that the late-summer sea ice cover decreases substantially and generally evolves over the same time scale as global warming. Antarctic sea ice extent is also projected to decrease in the 21st century. {8.6, 10.3, Box 10.1}

Sea level pressure is projected to increase over the subtropics and mid-latitudes, and decrease over high latitudes associated with an expansion of the Hadley Circulation and annular mode changes (NAM/NAO and SAM, see Box TS.2). A positive trend in the NAM/NAO as well as the SAM index is projected by many models. The magnitude of the projected increase is generally greater for the SAM, and there is considerable spread among the models. As a result of these changes, storm tracks are projected to move poleward, with consequent changes in wind, precipitation and temperature patterns outside the tropics, continuing the broad pattern of observed trends over the last half century. Some studies suggest fewer storms in mid-latitude regions. There are also indications of changes in extreme wave height associated with changing storm tracks and circulation. {3.6, 10.3}

In most models, the central and eastern equatorial Pacific SSTs warm more than those in the western equatorial Pacific, with a corresponding mean eastward shift in precipitation. ENSO interannual variability is projected to continue in all models, although changes differ from model to model. Large inter-model differences in projected changes in El Niño amplitude, and the inherent centennial time-scale variability of El Niño in the models, preclude a definitive projection of trends in ENSO variability. {10.3}

Recent studies with improved global models, ranging in resolution from about 100 to 20 km, suggest future changes in the number and intensity of future tropical cyclones (typhoons and hurricanes).

A synthesis of the model results to date indicates, for a warmer future climate, increased peak wind intensities and increased mean and peak precipitation intensities in future tropical cyclones, with the possibility of a decrease in the number of relatively weak hurricanes, and increased numbers of intense hurricanes. However, the total number of tropical cyclones globally is projected to decrease. The apparent observed increase in the proportion of very intense hurricanes since 1970 in some regions is in the same direction but much larger than predicted by theoretical models. {10.3, 8.5, 3.8}

Since the TAR, there is an improving understanding of projected patterns of precipitation. Increases in the amount of precipitation are *very likely* at high latitudes while decreases are *likely* in most subtropical land regions (by as much as about 20% in the A1B scenario in 2100). Poleward of 50°, mean precipitation is projected to increase due to the increase in water vapour in the atmosphere and the resulting increase in vapour transport from lower latitudes. Moving equatorward, there is a transition to mostly decreasing precipitation in the subtropics (20°–40° latitude). Due to increased water vapour transport out of the subtropics and a poleward expansion of the subtropical high-pressure systems, the drying tendency is especially pronounced at the higher-latitude margins of the subtropics (see Figure TS.30). {8.3, 10.3, 11.2–11.9}

Models suggest that changes in mean precipitation amount, even where robust, will rise above natural variability more slowly than the temperature signal. {10.3, 11.1}

Available research indicates a tendency for an increase in heavy daily rainfall events in many regions, including some in which the mean rainfall is projected to decrease. In the latter cases, the rainfall decrease is often attributable to a reduction in the number of rain days rather than the intensity of rain when it occurs. {11.2–11.9}

TS.5.3 Regional-Scale Projections

For each of the continental regions, the projected warming over 2000 to 2050 resulting from the SRES emissions scenarios is greater than the global average and greater than the observed warming over the past century. The warming projected for the next few decades of the 21st century, when averaged over the continents individually, would substantially exceed estimated 20th-century natural forced and unforced variability in all cases except Antarctica (Figure TS.29). Model best-estimate projections indicate that decadal average warming over each continent except Antarctica by 2030 is *very likely* to be at least twice as large as the corresponding model-estimated natural variability during the 20th century. The simulated warming over this period is not very sensitive to the choice of scenarios across the SRES set as is illustrated in Figure TS.32. Over longer time scales, the choice of scenario is more important, as shown in Figure TS.28. The projected warming in the SRES scenarios over 2000 to 2050 also exceeds estimates of natural variability when averaged over most sub-continental regions. {11.1}

Box TS.10. Regional Downscaling

Simulation of regional climates has improved in AOGCMs and, as a consequence, in nested regional climate models and in empirical downscaling techniques. Both dynamic and empirical downscaling methodologies show improving skill in simulating local features in present-day climates when the observed state of the atmosphere at scales resolved by current AOGCMs is used as input. The availability of downscaling and other regionally focused studies remains uneven geographically, causing unevenness in the assessments that can be provided, particularly for extreme weather events. Downscaling studies demonstrate that local precipitation changes can vary significantly from those expected from the large-scale hydrological response pattern, particularly in areas of complex topography. {11.10}

There remain a number of important sources of uncertainty limiting the ability to project regional climate change. While hydrological responses are relatively robust in certain core subpolar and subtropical regions, there is uncertainty in the precise location of these boundaries between increasing and decreasing precipitation. There are some important climate processes that have a significant effect on regional climate, but for which the climate change response is still poorly known. These include ENSO, the NAO, blocking, the thermohaline circulation and changes in tropical cyclone distribution. For those regions that have strong topographical controls on their climatic patterns, there is often insufficient climate change information at the fine spatial resolution of the topography. In some regions there has been only very limited research on extreme weather events. Further, the projected climate change signal becomes comparable to larger internal variability at smaller spatial and temporal scales, making it more difficult to utilise recent trends to evaluate model performance. {Box 11.1, 11.2–11.9}

CONTINENTAL SURFACE TEMPERATURE ANOMALIES: OBSERVATIONS AND PROJECTIONS

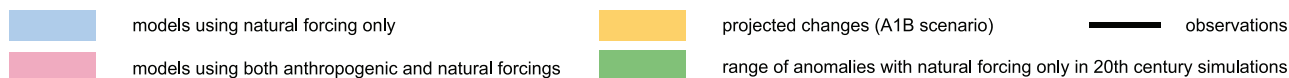
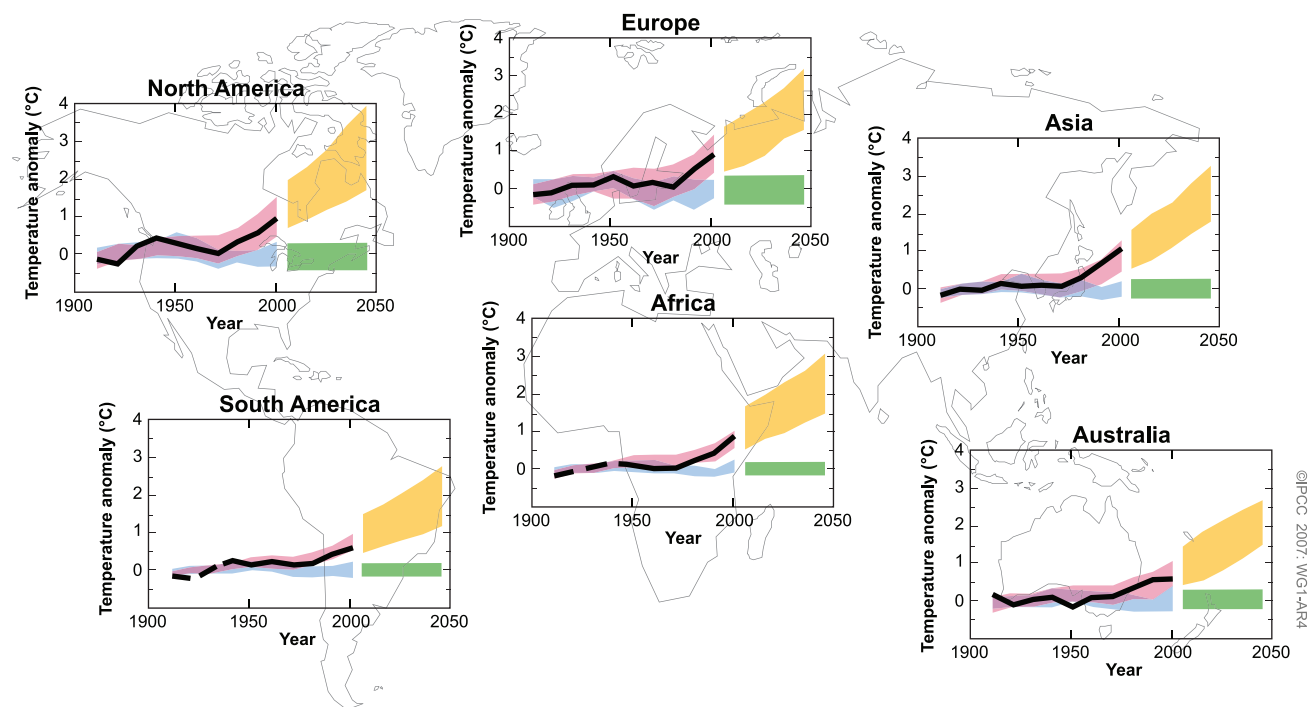


Figure TS.29. Decadal mean continental surface temperature anomalies ($^{\circ}\text{C}$) in observations and simulations for the period 1906 to 2005 and in projections for 2001 to 2050. Anomalies are calculated from the 1901 to 1950 average. The black lines represent the observations and the red and blue bands show simulated average temperature anomalies as in Figure TS.22 for the 20th century (i.e., red includes anthropogenic and natural forcings and blue includes only natural forcings). The yellow shading represents the 5th to 95th percentile range of projected changes according to the SRES A1B emissions scenario. The green bar denotes the 5th to 95th percentile range of decadal mean anomalies from the 20th-century simulations with only natural forcings (i.e., a measure of the natural decadal variability). For the observed part of these graphs, the decadal averages are centred on calendar decade boundaries (i.e., the last point is at 2000 for 1996 to 2005), whereas for the future period they are centred on calendar decade mid-points (i.e., the first point is at 2005 for 2001 to 2010). To construct the ranges, all simulations from the set of models involved were considered independent realisations of the possible evolution of the climate given the forcings applied. This involved 58 simulations from 14 models for the red curve, 19 simulations from 5 models (a subset of the 14) for the blue curve and green bar and 47 simulations from 18 models for the yellow curve. {FAQ 9.2.1, Figure 1 and Box 11.1, Figure 1}

In the NH a robust pattern of increased subpolar and decreased subtropical precipitation dominates the projected precipitation pattern for the 21st century over North America and Europe, while subtropical drying is less evident over Asia (see Figure TS.30). Nearly all models project increased precipitation over most of northern North America and decreased precipitation over Central America, with much of the continental USA and northern Mexico in a more uncertain transition zone that moves north and south following the seasons. Decreased

precipitation is confidently projected for southern Europe and Mediterranean Africa, with a transition to increased precipitation in northern Europe. In both continents, summer drying is extensive due both to the poleward movement of this transition zone in summer and to increased evaporation. Subpolar increases in precipitation are projected over much of northern Asia but with the subtropical drying spreading from the Mediterranean displaced by distinctive monsoonal signatures as one moves from central Asia eastward. {11.2–11.5}

SEASONAL MEAN PRECIPITATION RATES

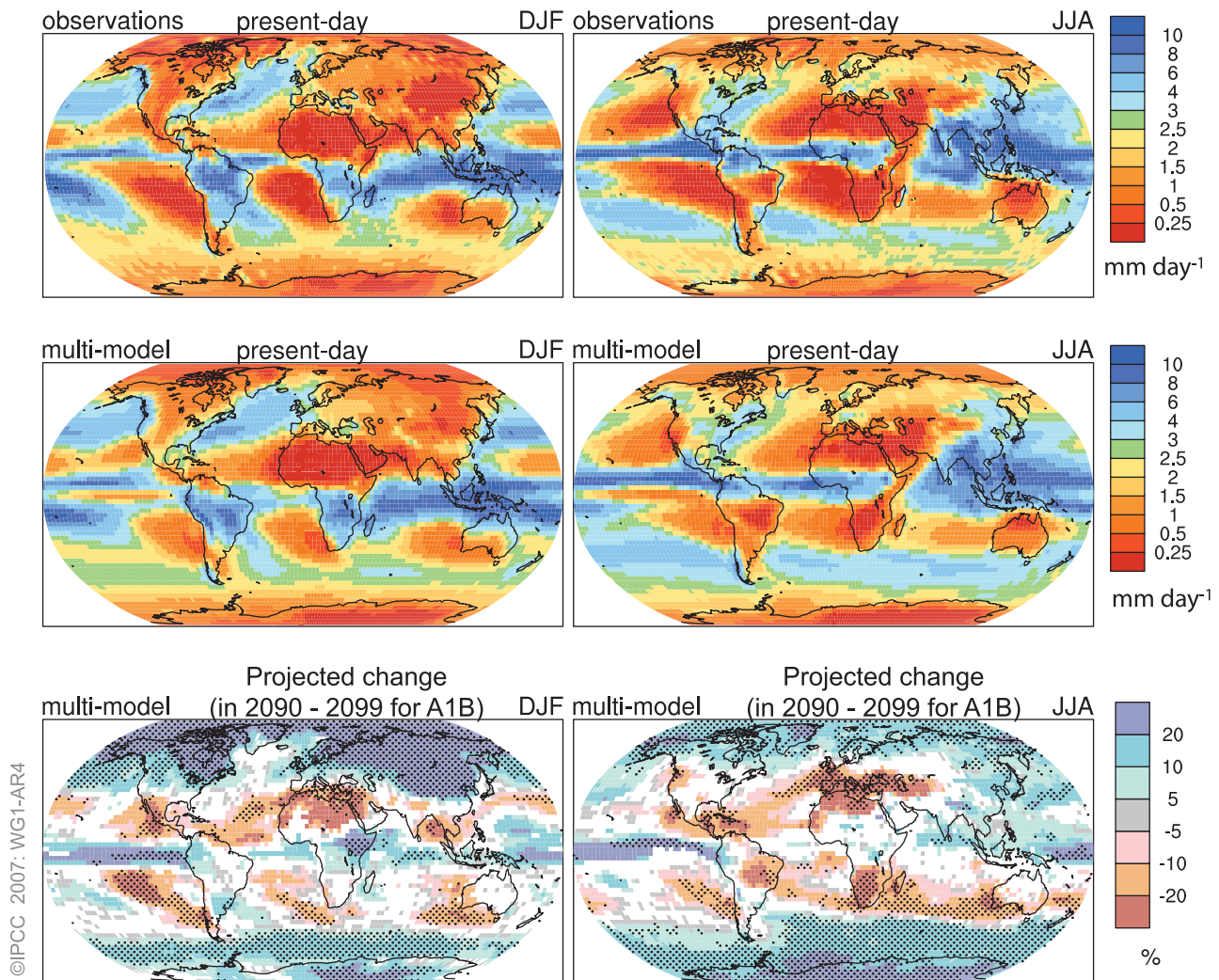


Figure TS.30. Spatial patterns of observed (top row) and multi-model mean (middle row) seasonal mean precipitation rate (mm day^{-1}) for the period 1979 to 1993 and the multi-model mean for changes by the period 2090 to 2099 relative to 1980 to 1999 (% change) based on the SRES A1B scenario (bottom row). December to February means are in the left column, June to August means in the right column. In the bottom panel, changes are plotted only where more than 66% of the models agree on the sign of the change. The stippling indicates areas where more than 90% of the models agree on the sign of the change. {Based on same datasets as shown in Figures 8.5 and 10.9}

In the SH, there are few land areas in the zone of projected subpolar moistening during the 21st century, with the subtropical drying more prominent (see Figure TS.30). The South Island of New Zealand and Tierra del Fuego fall within the subpolar precipitation increase zone, with southernmost Africa, the southern Andes in South America and southern Australia experiencing the drying tendency typical of the subtropics. {11.2, 11.6, 11.7}

Projections of precipitation over tropical land regions are more uncertain than those at higher latitudes, but, despite significant inadequacies in

modelling tropical convection and atmosphere-ocean interactions, and the added uncertainty associated with tropical cyclones, some robust features emerge in models. Rainfall in the summer monsoon season of South and Southeast Asia increases in most models, as does rainfall in East Africa. The sign of the precipitation response is considered less certain over both the Amazon and the African Sahel. These are regions in which there is added uncertainty due to potential vegetation-climate links, and there is less robustness across models even when vegetation feedbacks are not included. {8.3, 11.2, 11.4, 11.6}

TS.5.4 Coupling Between Climate Change and Changes in Biogeochemical Cycles

All models that treat the coupling of the carbon cycle to climate change indicate a positive feedback effect with warming acting to suppress land and ocean uptake of CO₂, leading to larger atmospheric CO₂ increases and greater climate change for a given emissions scenario, but the strength of this feedback effect varies markedly among models. Since the TAR, several new projections based on fully coupled carbon cycle-climate models have been performed and compared. For the SRES A2 scenario, and based on a range of model results, the projected increase in atmospheric CO₂ concentration over the 21st century is *likely* between 10 and 25% higher than projections without this feedback, adding more than 1°C to projected mean warming by 2100 for higher emission SRES scenarios. Correspondingly, the reduced CO₂ uptake caused by this effect reduces the CO₂ emissions that are consistent with a target stabilisation level. However, there are still significant uncertainties due, for example, to limitations in the understanding of the dynamics of land ecosystems and soils. {7.3, 10.4}

Increasing atmospheric CO₂ concentrations lead directly to increasing acidification of the surface ocean. Projections based on SRES scenarios give reductions in pH of between 0.14 and 0.35 units in the 21st century (depending on scenario), extending the present decrease of 0.1 units from pre-industrial times. Ocean acidification would lead to dissolution of shallow-water carbonate sediments. Southern Ocean surface waters are projected to exhibit undersaturation with regard to calcium carbonate (CaCO₃) for CO₂ concentrations higher than 600 ppm, a level exceeded during the second half of the 21st century in most of the SRES scenarios. Low-latitude regions and the deep ocean will be affected as well. These changes could affect marine organisms that form their exoskeletons out of CaCO₃, but the net effect on the biological cycling of carbon in the oceans is not well understood. {Box 7.3, 10.4}

Committed climate change due to past emissions varies considerably for different forcing agents because of differing lifetimes in the Earth's atmosphere (see Box TS.9). The committed climate change due to past emissions takes account of both (i) the time lags in the responses of the climate system to changes in radiative forcing; and (ii) the time scales over which different forcing agents persist in the atmosphere after their emission because of their differing lifetimes.

Typically the committed climate change due to past emissions includes an initial period of further increase in temperature, for the reasons discussed above, followed by a long-term decrease as radiative forcing decreases. Some greenhouse gases have relatively short atmospheric lifetimes (decades or less), such as CH₄ and carbon monoxide, while others such as N₂O have lifetimes of the order of a century, and some have lifetimes of millennia, such as SF₆ and PFCs. Atmospheric concentrations of CO₂ do not decay with a single well-defined lifetime if emissions are stopped. Removal of CO₂ emitted to the atmosphere occurs over multiple time scales, but some CO₂ will stay in the atmosphere for many thousands of years, so that emissions lead to a very long commitment to climate change. The slow long-term buffering of the ocean, including CaCO₃-sediment feedback, requires 30,000 to 35,000 years for atmospheric CO₂ concentrations to reach equilibrium. Using coupled carbon cycle components, EMICs show that the committed climate change due to past CO₂ emissions persists for more than 1000 years, so that even over these very long time scales, temperature and sea level do not return to pre-industrial values. An indication of the long time scales of committed climate change is obtained by prescribing anthropogenic CO₂ emissions following a path towards stabilisation at 750 ppm, but arbitrarily setting emissions to zero at year 2100. In this test case, it takes about 100 to 400 years in the different models for the atmospheric CO₂ concentration to drop from the maximum (ranges between 650 to 700 ppm) to below the level of two times the pre-industrial CO₂ concentration (about 560 ppm), owing to a continuous but slow transfer of carbon from the atmosphere and terrestrial reservoirs to the ocean (see Figure TS.31). {7.3, 10.7}

Future concentrations of many non-CO₂ greenhouse gases and their precursors are expected to be coupled to future climate change. Insufficient understanding of the causes of recent variations in the CH₄ growth rate suggests large uncertainties in future projections for this gas in particular. Emissions of CH₄ from wetlands are *likely* to increase in a warmer and wetter climate and to decrease in a warmer and drier climate. Observations also suggest increases in CH₄ released from northern peatlands that are experiencing permafrost melt, although the large-scale magnitude of this effect is not well quantified. Changes in temperature, humidity and clouds could also affect biogenic emissions of ozone precursors, such as volatile organic compounds. Climate change is also expected to affect tropospheric ozone through changes in chemistry and transport. Climate change could induce changes in OH through changes in humidity, and could alter stratospheric ozone concentrations and hence solar ultraviolet radiation in the troposphere. {7.4, 4.7}

CLIMATE CHANGE COMMITMENT

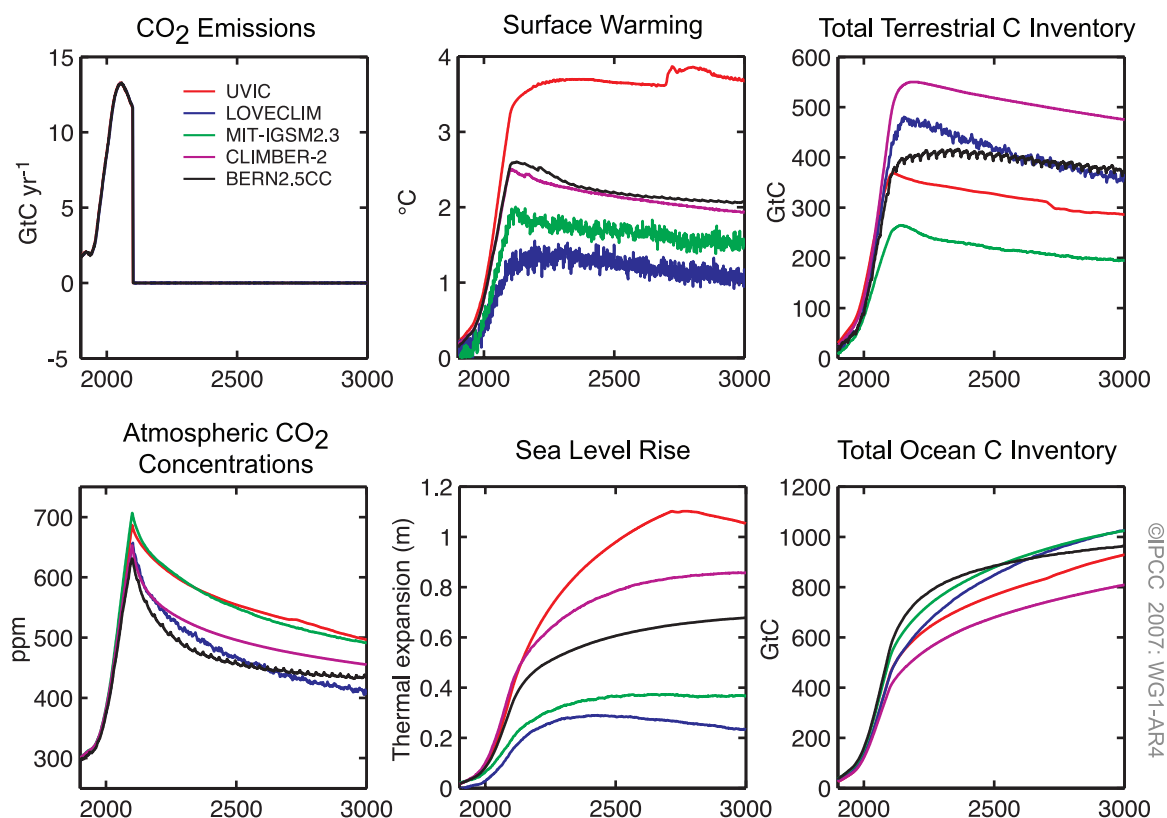


Figure TS.31. Calculation of climate change commitment due to past emissions for five different EMICs and an idealised scenario where emissions follow a pathway leading to stabilisation of atmospheric CO₂ at 750 ppm, but before reaching this target, emissions are reduced to zero instantly at year 2100. (Left) CO₂ emissions and atmospheric CO₂ concentrations; (centre) surface warming and sea level rise due to thermal expansion; (right) change in total terrestrial and oceanic carbon inventory since the pre-industrial era. {Figure 10.35}

Future emissions of many aerosols and their precursors are expected to be affected by climate change. Estimates of future changes in dust emissions under several climate and land use scenarios suggest that the effects of climate change are more important in controlling future dust emissions than changes in land use. Results from one study suggest that meteorology and climate have a greater influence on future Asian dust emissions and associated Asian dust storm occurrences than desertification. The biogenic emission of volatile organic compounds, a significant source of secondary organic aerosols, is known to be highly sensitive to (and increase with) temperature. However, aerosol yields decrease with temperature and the effects of changing precipitation and physiological adaptation are uncertain. Thus, change in biogenic secondary organic aerosol production in a warmer climate could be considerably lower than the response of biogenic volatile organic carbon emissions. Climate change may affect fluxes from the ocean of dimethyl sulphide (which is a precursor for

some sulphate aerosols) and sea salt aerosols, however, the effects on temperature and precipitation remain very uncertain. {7.5}

While the warming effect of CO₂ represents a commitment over many centuries, aerosols are removed from the atmosphere over time scales of only a few days, so that the negative radiative forcing due to aerosols could change rapidly in response to any changes in emissions of aerosols or aerosol precursors. Because sulphate aerosols are *very likely* exerting a substantial negative radiative forcing at present, future net forcing is very sensitive to changes in sulphate emissions. One study suggests that the hypothetical removal from the atmosphere of the entire current burden of anthropogenic sulphate aerosol particles would produce a rapid increase in global mean temperature of about 0.8°C within a decade or two. Changes in aerosols are also likely to influence precipitation. Thus, the effect of environmental strategies aimed at mitigating climate change requires consideration of changes in both greenhouse gas and aerosol emissions.

Changes in aerosol emissions may result from measures implemented to improve air quality which may therefore have consequences for climate change. {Box 7.4, 7.6, 10.7}

Climate change would modify a number of chemical and physical processes that control air quality and the net effects are likely to vary from one region to another. Climate change can affect air quality by modifying the rates at which pollutants are dispersed, the rate at which aerosols and soluble species are removed from the atmosphere, the general chemical environment for pollutant generation and the strength of emissions from the biosphere, fires and dust. Climate change is also expected to decrease the global ozone background. Overall, the net effect of climate change on air quality is highly uncertain. {Box 7.4}

TS.5.5 Implications of Climate Processes and their Time Scales for Long-Term Projections

The commitments to climate change after stabilisation of radiative forcing are expected to be

about 0.5 to 0.6°C, mostly within the following century.

The multi-model average when stabilising concentrations of greenhouse gases and aerosols at year 2000 values after a 20th-century climate simulation, and running an additional 100 years, is about 0.6°C of warming (relative to 1980–1999) at year 2100 (see Figure TS.32). If the B1 or A1B scenarios were to characterise 21st-century emissions followed by stabilisation at those levels, the additional warming after stabilisation is similar, about 0.5°C, mostly in the subsequent hundred years. {10.3, 10.7}

The magnitude of the positive feedback between climate change and the carbon cycle is uncertain. This leads to uncertainty in the trajectory of CO₂ emissions required to achieve a particular stabilization level of atmospheric CO₂ concentration. Based upon current understanding of climate-carbon cycle feedback, model studies suggest that, in order to stabilise CO₂ at 450 ppm, cumulative emissions in the 21st century could be reduced from a model average of approximately 670 [630 to 710] GtC to approximately 490 [375 to 600] GtC. Similarly, to stabilise CO₂ at 1000 ppm, the cumulative emissions could be reduced by this feedback from a model average of

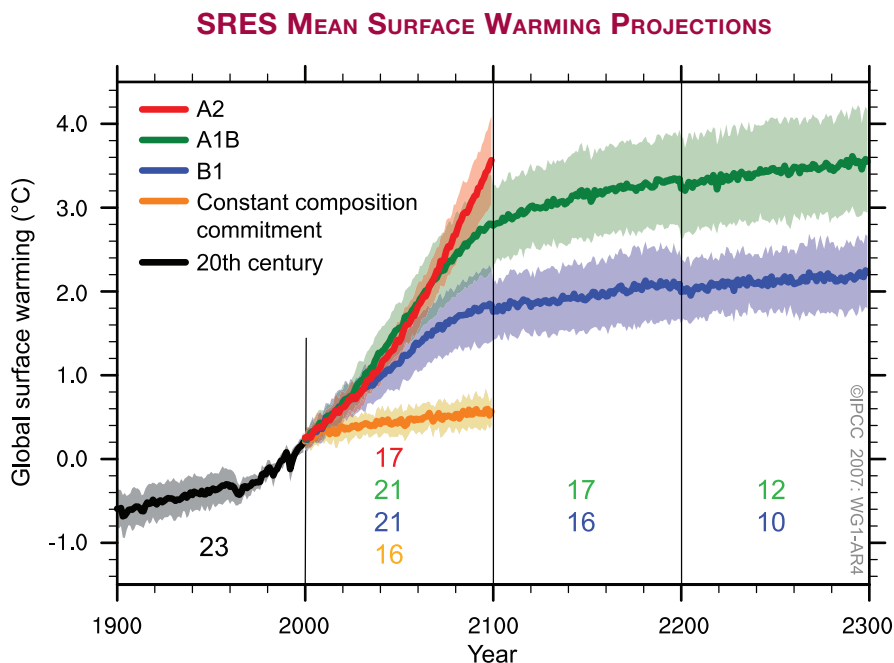


Figure TS.32. Multi-model means of surface warming (compared to the 1980–1999 base period) for the SRES scenarios A2 (red), A1B (green) and B1 (blue), shown as continuations of the 20th-century simulation. The latter two scenarios are continued beyond the year 2100 with forcing kept constant (committed climate change as it is defined in Box TS.9). An additional experiment, in which the forcing is kept at the year 2000 level is also shown (orange). Linear trends from the corresponding control runs have been removed from these time series. Lines show the multi-model means, shading denotes the ± 1 standard deviation range. Discontinuities between different periods have no physical meaning and are caused by the fact that the number of models that have run a given scenario is different for each period and scenario (numbers indicated in figure). For the same reason, uncertainty across scenarios should not be interpreted from this figure (see Section 10.5 for uncertainty estimates). {Figure 10.4}

approximately 1415 [1340 to 1490] GtC to approximately 1100 [980 to 1250] GtC. {7.3, 10.4}

If radiative forcing were to be stabilised in 2100 at A1B concentrations, thermal expansion alone would lead to 0.3 to 0.8 m of sea level rise by 2300 (relative to 1980–1999) and would continue at decreasing rates for many centuries, due to slow processes that mix heat into the deep ocean. {10.7}

Contraction of the Greenland Ice Sheet is projected to continue to contribute to sea level rise after 2100. For stabilisation at A1B concentrations in 2100, a rate of 0.03 to 0.21 m per century due to thermal expansion is projected. If a global average warming of 1.9°C to 4.6°C relative to pre-industrial temperatures were maintained for millennia, the Greenland Ice Sheet would largely be eliminated except for remnant glaciers in the mountains. This would raise sea level by about 7 m and could be irreversible. These temperatures are comparable to those inferred for the last interglacial period 125,000 years ago, when palaeoclimatic information suggests reductions of polar ice extent and 4 to 6 m of sea level rise. {6.4, 10.7}

Dynamical processes not included in current models but suggested by recent observations could increase the vulnerability of the ice sheets to warming, increasing future sea level rise. Understanding of these processes is limited and there is no consensus on their likely magnitude. {4.6, 10.7}

Current global model studies project that the Antarctic Ice Sheet will remain too cold for widespread surface melting and will gain in mass due to increased snowfall. However, net loss of ice mass could occur if dynamical ice discharge dominates the ice sheet mass balance. {10.7}

While no models run for this assessment suggest an abrupt MOC shutdown during the 21st century, some models of reduced complexity suggest MOC shutdown as a possible long-term response to sufficiently strong warming. However, the likelihood of this occurring cannot be evaluated with confidence. The few available simulations with models of different complexity rather suggest a centennial-scale slowdown. Recovery of the MOC is *likely* if the radiative forcing is stabilised but would take several centuries. Systematic model comparison studies have helped establish some key processes that are responsible for variations between models in the response of the ocean to climate change (especially ocean heat uptake). {8.7, FAQ 10.2, 10.3}

TS.6 Robust Findings and Key Uncertainties

TS.6.1 Changes in Human and Natural Drivers of Climate

Robust Findings:

Current atmospheric concentrations of CO₂ and CH₄, and their associated positive radiative forcing, far exceed those determined from ice core measurements spanning the last 650,000 years. {6.4}

Fossil fuel use, agriculture and land use have been the dominant cause of increases in greenhouse gases over the last 250 years. {2.3, 7.3, 7.4}

Annual emissions of CO₂ from fossil fuel burning, cement production and gas flaring increased from a mean of 6.4 ± 0.4 GtC yr⁻¹ in the 1990s to 7.2 ± 0.3 GtC yr⁻¹ for 2000 to 2005. {7.3}

The sustained rate of increase in radiative forcing from CO₂, CH₄ and N₂O over the past 40 years is larger than at any time during at least the past 2000 years. {6.4}

Natural processes of CO₂ uptake by the oceans and terrestrial biosphere remove about 50 to 60% of

anthropogenic emissions (i.e., fossil CO₂ emissions and land use change flux). Uptake by the oceans and the terrestrial biosphere are similar in magnitude over recent decades but that by the terrestrial biosphere is more variable. {7.3}

It is *virtually certain* that anthropogenic aerosols produce a net negative radiative forcing (cooling influence) with a greater magnitude in the NH than in the SH. {2.9, 9.2}

From new estimates of the combined anthropogenic forcing due to greenhouse gases, aerosols and land surface changes, it is *extremely likely* that human activities have exerted a substantial net warming influence on climate since 1750. {2.9}

Solar irradiance contributions to global average radiative forcing are considerably smaller than the contribution of increases in greenhouse gases over the industrial period. {2.5, 2.7}

Key Uncertainties:

The full range of processes leading to modification of cloud properties by aerosols is not well understood and the magnitudes of associated indirect radiative effects are poorly determined. {2.4, 7.5}

The causes of, and radiative forcing due to stratospheric water vapour changes are not well quantified. {2.3}

The geographical distribution and time evolution of the radiative forcing due to changes in aerosols during the 20th century are not well characterised. {2.4}

The causes of recent changes in the growth rate of atmospheric CH₄ are not well understood. {7.4}

The roles of different factors increasing tropospheric ozone concentrations since pre-industrial times are not well characterised. {2.3}

Land surface properties and land-atmosphere interactions that lead to radiative forcing are not well quantified. {2.5}

Knowledge of the contribution of past solar changes to radiative forcing on the time scale of centuries is not based upon direct measurements and is hence strongly dependent upon physical understanding. {2.7}

TS.6.2 Observations of Changes in Climate

TS.6.2.1 Atmosphere and Surface

Robust Findings:

Global mean surface temperatures continue to rise. Eleven of the last 12 years rank among the 12 warmest years on record since 1850. {3.2}

Rates of surface warming increased in the mid-1970s and the global land surface has been warming at about double the rate of ocean surface warming since then. {3.2}

Changes in surface temperature extremes are consistent with warming of the climate. {3.8}

Estimates of mid- and lower-tropospheric temperature trends have substantially improved. Lower-tropospheric temperatures have slightly greater warming rates than the surface from 1958 to 2005. {3.4}

Long-term trends from 1900 to 2005 have been observed in precipitation amount in many large regions. {3.3}

Increases have occurred in the number of heavy precipitation events. {3.8}

Droughts have become more common, especially in the tropics and subtropics, since the 1970s. {3.3}

Tropospheric water vapour has increased, at least since the 1980s. {3.4}

Key Uncertainties:

Radiosonde records are much less complete spatially than surface records and evidence suggests a number of radiosonde records are unreliable, especially in the tropics. It is likely that all records of tropospheric temperature trends still contain residual errors. {3.4}

While changes in large-scale atmospheric circulation are apparent, the quality of analyses is best only after 1979, making analysis of, and discrimination between, change and variability difficult. {3.5, 3.6}

Surface and satellite observations disagree on total and low-level cloud changes over the ocean. {3.4}

Multi-decadal changes in DTR are not well understood, in part because of limited observations of changes in cloudiness and aerosols. {3.2}

Difficulties in the measurement of precipitation remain an area of concern in quantifying trends in global and regional precipitation. {3.3}

Records of soil moisture and streamflow are often very short, and are available for only a few regions, which impedes complete analyses of changes in droughts. {3.3}

The availability of observational data restricts the types of extremes that can be analysed. The rarer the event, the more difficult it is to identify long-term changes because there are fewer cases available. {3.8}

Information on hurricane frequency and intensity is limited prior to the satellite era. There are questions about the interpretation of the satellite record. {3.8}

There is insufficient evidence to determine whether trends exist in tornadoes, hail, lightning and dust storms at small spatial scales. {3.8}

TS.6.2.2 Snow, Ice and Frozen Ground

Robust Findings:

The amount of ice on the Earth is decreasing. There has been widespread retreat of mountain glaciers since the end of the 19th century. The rate of mass loss from glaciers and the Greenland Ice Sheet is increasing. {4.5, 4.6}

The extent of NH snow cover has declined. Seasonal river and lake ice duration has decreased over the past 150 years. {4.2, 4.3}

Since 1978, annual mean arctic sea ice extent has been declining and summer minimum arctic ice extent has decreased. {4.4}

Ice thinning occurred in the Antarctic Peninsula and Amundsen shelf ice during the 1990s. Tributary glaciers have accelerated and complete breakup of the Larsen B Ice Shelf occurred in 2002. {4.6}

Temperature at the top of the permafrost layer has increased by up to 3°C since the 1980s in the Arctic. The maximum extent of seasonally frozen ground has decreased by about 7% in the NH since 1900, and its maximum depth has decreased by about 0.3 m in Eurasia since the mid-20th century. {4.7}

Key Uncertainties:

There is no global compilation of *in situ* snow data prior to 1960. Well-calibrated snow water equivalent data are not available for the satellite era. {4.2}

There are insufficient data to draw any conclusions about trends in the thickness of antarctic sea ice. {4.4}

Uncertainties in estimates of glacier mass loss arise from limited global inventory data, incomplete area-volume relationships and imbalance in geographic coverage. {4.5}

Mass balance estimates for ice shelves and ice sheets, especially for Antarctica, are limited by calibration and validation of changes detected by satellite altimetry and gravity measurements. {4.6}

Limited knowledge of basal processes and of ice shelf dynamics leads to large uncertainties in the understanding of ice flow processes and ice sheet stability. {4.6}

TS.6.2.3 Oceans and Sea Level

Robust Findings:

The global temperature (or heat content) of the oceans has increased since 1955. {5.2}

Large-scale regionally coherent trends in salinity have been observed over recent decades with freshening in subpolar regions and increased salinity in the shallower parts of the tropics and subtropics. These trends are consistent with changes in precipitation and inferred larger water transport in the atmosphere from low latitudes to high latitudes and from the Atlantic to the Pacific. {5.2}

Global average sea level rose during the 20th century. There is high confidence that the rate of sea level rise increased between the mid-19th and mid-20th centuries. During 1993 to 2003, sea level rose more rapidly than during 1961 to 2003. {5.5}

Thermal expansion of the ocean and loss of mass from glaciers and ice caps made substantial contributions to the observed sea level rise. {5.5}

The observed rate of sea level rise from 1993 to 2003 is consistent with the sum of observed contributions from thermal expansion and loss of land ice. {5.5}

The rate of sea level change over recent decades has not been geographically uniform. {5.5}

As a result of uptake of anthropogenic CO₂ since 1750, the acidity of the surface ocean has increased. {5.4, 7.3}

Key Uncertainties:

Limitations in ocean sampling imply that decadal variability in global heat content, salinity and sea level changes can only be evaluated with moderate confidence. {5.2, 5.5}

There is low confidence in observations of trends in the MOC. {Box 5.1}

Global average sea level rise from 1961 to 2003 appears to be larger than can be explained by thermal expansion and land ice melting. {5.5}

TS.6.2.4 Palaeoclimate

Robust Findings:

During the last interglacial, about 125,000 years ago, global sea level was *likely* 4 to 6 m higher than present, due primarily to retreat of polar ice. {6.4}

A number of past abrupt climate changes were *very likely* linked to changes in Atlantic Ocean circulation and affected the climate broadly across the NH. {6.4}

It is *very unlikely* that the Earth would naturally enter another ice age for at least 30,000 years. {6.4}

Biogeochemical and biogeophysical feedbacks have amplified climatic changes in the past. {6.4}

It is *very likely* that average NH temperatures during the second half of the 20th century were warmer than in any other 50-year period in the last 500 years and *likely* that this was also the warmest 50-year period in the past 1300 years. {6.6}

Palaeoclimate records indicate with high confidence that droughts lasting decades or longer were a recurrent feature of climate in several regions over the last 2000 years. {6.6}

Key Uncertainties:

Mechanisms of onset and evolution of past abrupt climate change and associated climate thresholds are not well understood. This limits confidence in the ability of climate models to simulate realistic abrupt change. {6.4}

The degree to which ice sheets retreated in the past, the rates of such change and the processes involved are not well known. {6.4}

Knowledge of climate variability over more than the last few hundred years in the SH and tropics is limited by the lack of palaeoclimatic records. {6.6}

Differing amplitudes and variability observed in available millennial-length NH temperature reconstructions, as well as the relation of these differences to choice of proxy data and statistical calibration methods, still need to be reconciled. {6.6}

The lack of extensive networks of proxy data for temperature in the last 20 years limits understanding of how such proxies respond to rapid global warming and of the influence of other environmental changes. {6.6}

TS.6.3 Understanding and Attributing Climate Change

Robust Findings:

Greenhouse gas forcing has *very likely* caused most of the observed global warming over the last 50 years. Greenhouse gas forcing alone during the past half century would *likely* have resulted in greater than the observed warming if there had not been an offsetting cooling effect from aerosol and other forcings. {9.4}

It is *extremely unlikely* (<5%) that the global pattern of warming during the past half century can be explained without external forcing, and *very unlikely* that it is due to known natural external causes alone. The warming occurred in both the ocean and the atmosphere and took place at a time when natural external forcing factors would *likely* have produced cooling. {9.4, 9.7}

Key Uncertainties:

Confidence in attributing some climate change phenomena to anthropogenic influences is currently limited by uncertainties in radiative forcing, as well as uncertainties in feedbacks and in observations. {9.4, 9.5}

Attribution at scales smaller than continental and over time scales of less than 50 years is limited by larger climate variability on smaller scales, by uncertainties in the small-scale details of external forcing and the response simulated by models, as well as uncertainties in simulation of internal variability on small scales, including in relation to modes of variability. {9.4}

There is less confidence in understanding of forced changes in precipitation and surface pressure than there is of temperature. {9.5}

The range of attribution statements is limited by the absence of formal detection and attribution studies, or their very limited number, for some phenomena (e.g., some types of extreme events). {9.5}

It is *likely* that anthropogenic forcing has contributed to the general warming observed in the upper several hundred metres of the ocean during the latter half of the 20th century. Anthropogenic forcing, resulting in thermal expansion from ocean warming and glacier mass loss, has *very likely* contributed to sea level rise during the latter half of the 20th century. {9.5}

A substantial fraction of the reconstructed NH inter-decadal temperature variability of the past seven centuries is *very likely* attributable to natural external forcing (volcanic eruptions and solar variability). {9.3}

Incomplete global data sets for extremes analysis and model uncertainties still restrict the regions and types of detection studies of extremes that can be performed. {9.4, 9.5}

Despite improved understanding, uncertainties in model-simulated internal climate variability limit some aspects of attribution studies. For example, there are apparent discrepancies between estimates of ocean heat content variability from models and observations. {5.2, 9.5}

Lack of studies quantifying the contributions of anthropogenic forcing to ocean heat content increase or glacier melting together with the open part of the sea level budget for 1961 to 2003 are among the uncertainties in quantifying the anthropogenic contribution to sea level rise. {9.5}

TS.6.4 Projections of Future Changes in Climate

TS.6.4.1 Model Evaluation

Robust Findings:

Climate models are based on well-established physical principles and have been demonstrated to reproduce observed features of recent climate and past climate changes. There is considerable confidence that AOGCMs provide credible quantitative estimates of future climate change, particularly at continental scales and above. Confidence in these estimates is higher for some climate variables (e.g., temperature) than for others (e.g., precipitation). {FAQ 8.1}

Confidence in models has increased due to:

- improvements in the simulation of many aspects of present climate, including important modes of climate variability and extreme hot and cold spells;
- improved model resolution, computational methods and parametrizations and inclusion of additional processes;
- more comprehensive diagnostic tests, including tests of model ability to forecast on time scales from days to a year when initialised with observed conditions; and
- enhanced scrutiny of models and expanded diagnostic analysis of model behaviour facilitated by internationally coordinated efforts to collect and disseminate output from model experiments performed under common conditions. {8.4}

Key Uncertainties:

A proven set of model metrics comparing simulations with observations, that might be used to narrow the range of plausible climate projections, has yet to be developed. {8.2}

Most models continue to have difficulty controlling climate drift, particularly in the deep ocean. This drift must be accounted for when assessing change in many oceanic variables. {8.2}

Models differ considerably in their estimates of the strength of different feedbacks in the climate system. {8.6}

Problems remain in the simulation of some modes of variability, notably the Madden-Julian Oscillation, recurrent atmospheric blocking and extreme precipitation. {8.4}

Systematic biases have been found in most models' simulations of the Southern Ocean that are linked to uncertainty in transient climate response. {8.3}

Climate models remain limited by the spatial resolution that can be achieved with present computer resources, by the need for more extensive ensemble runs and by the need to include some additional processes. {8.1–8.5}

TS.6.4.2 Equilibrium and Transient Climate Sensitivity

Robust Findings:

Equilibrium climate sensitivity is *likely* to be in the range 2°C to 4.5°C with a most likely value of about 3°C, based upon multiple observational and modelling constraints. It is *very unlikely* to be less than 1.5°C. {8.6, 9.6, Box 10.2}

The transient climate response is better constrained than the equilibrium climate sensitivity. It is *very likely* larger than 1°C and *very unlikely* greater than 3°C. {10.5}

There is a good understanding of the origin of differences in equilibrium climate sensitivity found in different models. Cloud feedbacks are the primary source of inter-model differences in equilibrium climate sensitivity, with low cloud being the largest contributor. {8.6}

New observational and modelling evidence strongly supports a combined water vapour-lapse rate feedback of a strength comparable to that found in AOGCMs. {8.6}

Key Uncertainties:

Large uncertainties remain about how clouds might respond to global climate change. {8.6}

TS.6.4.3 Global Projections

Robust Findings:

Even if concentrations of radiative forcing agents were to be stabilised, further committed warming and related climate changes would be expected to occur, largely because of time lags associated with processes in the oceans. {10.7}

Near-term warming projections are little affected by different scenario assumptions or different model sensitivities, and are consistent with that observed for the past few decades. The multi-model mean warming, averaged over 2011 to 2030 relative to 1980 to 1999 for all AOGCMs considered here, lies in a narrow range of 0.64°C to 0.69°C for the three different SRES emission scenarios B1, A1B and A2. {10.3}

Geographic patterns of projected warming show the greatest temperature increases at high northern latitudes and over land, with less warming over the southern oceans and North Atlantic. {10.3}

Changes in precipitation show robust large-scale patterns: precipitation generally increases in the tropical precipitation maxima, decreases in the subtropics and increases at high latitudes as a consequence of a general intensification of the global hydrological cycle. {10.3}

As the climate warms, snow cover and sea ice extent decrease; glaciers and ice caps lose mass and contribute to sea level rise. Sea ice extent decreases in the 21st century

in both the Arctic and Antarctic. Snow cover reduction is accelerated in the Arctic by positive feedbacks and widespread increases in thaw depth occur over much of the permafrost regions. {10.3}

Based on current simulations, it is *very likely* that the Atlantic Ocean MOC will slow down by 2100. However, it is *very unlikely* that the MOC will undergo a large abrupt transition during the course of the 21st century. {10.3}

Heat waves become more frequent and longer lasting in a future warmer climate. Decreases in frost days are projected to occur almost everywhere in the mid- and high latitudes, with an increase in growing season length. There is a tendency for summer drying of the mid-continental areas during summer, indicating a greater risk of droughts in those regions. {10.3, FAQ 10.1}

Future warming would tend to reduce the capacity of the Earth system (land and ocean) to absorb anthropogenic CO₂. As a result, an increasingly large fraction of anthropogenic CO₂ would stay in the atmosphere under a warmer climate. This feedback requires reductions in the cumulative emissions consistent with stabilisation at a given atmospheric CO₂ level compared to the hypothetical case of no such feedback. The higher the stabilisation scenario, the larger the amount of climate change and the larger the required reductions. {7.3, 10.4}

Key Uncertainties:

The likelihood of a large abrupt change in the MOC beyond the end of the 21st century cannot yet be assessed reliably. For low and medium emission scenarios with atmospheric greenhouse gas concentrations stabilised beyond 2100, the MOC recovers from initial weakening within one to several centuries. A permanent reduction in the MOC cannot be excluded if the forcing is strong and long enough. {10.7}

The model projections for extremes of precipitation show larger ranges in amplitude and geographical locations than for temperature. {10.3, 11.1}

The response of some major modes of climate variability such as ENSO still differs from model to model, which may

be associated with differences in the spatial and temporal representation of present-day conditions. {10.3}

The robustness of many model responses of tropical cyclones to climate change is still limited by the resolution of typical climate models. {10.3}

Changes in key processes that drive some global and regional climate changes are poorly known (e.g., ENSO, NAO, blocking, MOC, land surface feedbacks, tropical cyclone distribution). {11.2–11.9}

The magnitude of future carbon cycle feedbacks is still poorly determined. {7.3, 10.4}

TS.6.4.4 Sea Level

Robust Findings:

Sea level will continue to rise in the 21st century because of thermal expansion and loss of land ice. Sea level rise was not geographically uniform in the past and will not be in the future. {10.6}

Projected warming due to emission of greenhouse gases during the 21st century will continue to contribute to sea level rise for many centuries. {10.7}

Sea level rise due to thermal expansion and loss of mass from ice sheets would continue for centuries or millennia even if radiative forcing were to be stabilised. {10.7}

Key Uncertainties:

Models do not yet exist that address key processes that could contribute to large rapid dynamical changes in the Antarctic and Greenland Ice Sheets that could increase the discharge of ice into the ocean. {10.6}

The sensitivity of ice sheet surface mass balance (melting and precipitation) to global climate change is not well constrained by observations and has a large spread in models. There is consequently a large uncertainty in the magnitude of global warming that, if sustained, would lead to the elimination of the Greenland Ice Sheet. {10.7}

TS.6.4.5 Regional Projections

Robust Findings:

Temperatures averaged over all habitable continents and over many sub-continental land regions will *very likely* rise at greater than the global average rate in the next 50 years and by an amount substantially in excess of natural variability. {10.3, 11.2–11.9}

Precipitation is *likely* to increase in most subpolar and polar regions. The increase is considered especially robust, and *very likely* to occur, in annual precipitation in most of northern Europe, Canada, the northeast USA and the Arctic, and in winter precipitation in northern Asia and the Tibetan Plateau. {11.2–11.9}

Precipitation is *likely* to decrease in many subtropical regions, especially at the poleward margins of the subtropics. The decrease is considered especially robust, and *very likely* to occur, in annual precipitation in European and African regions bordering the Mediterranean and in winter rainfall in south-western Australia. {11.2–11.9}

Extremes of daily precipitation are *likely* to increase in many regions. The increase is considered as *very likely* in northern Europe, south Asia, East Asia, Australia and New Zealand – this list in part reflecting uneven geographic coverage in existing published research. {11.2–11.9}

Key Uncertainties:

In some regions there has been only very limited study of key aspects of regional climate change, particularly with regard to extreme events. {11.2–11.9}

Atmosphere-Ocean General Circulation Models show no consistency in simulated regional precipitation change in some key regions (e.g., northern South America, northern Australia and the Sahel). {10.3, 11.2–11.9}

In many regions where fine spatial scales in climate are generated by topography, there is insufficient information on how climate change will be expressed at these scales. {11.2–11.9}

**From the report accepted by Working Group I
of the Intergovernmental Panel on Climate Change
but not approved in detail**

Frequently Asked Questions

FAQ Citation:

These Frequently Asked Questions have been taken directly from the chapters of the underlying report and are collected here. When referencing specific FAQs, please reference the corresponding chapter in the report from whence the FAQ originated.

When referencing the group of FAQs, please cite as:

IPCC, 2007: *Climate Change 2007: The Physical Science Basis. Contribution of Working Group I to the Fourth Assessment Report of the Intergovernmental Panel on Climate Change* [Solomon, S., D. Qin, M. Manning, Z. Chen, M. Marquis, K.B. Averyt, M. Tignor and H.L. Miller (eds.)]. Cambridge University Press, Cambridge, United Kingdom and New York, NY, USA.

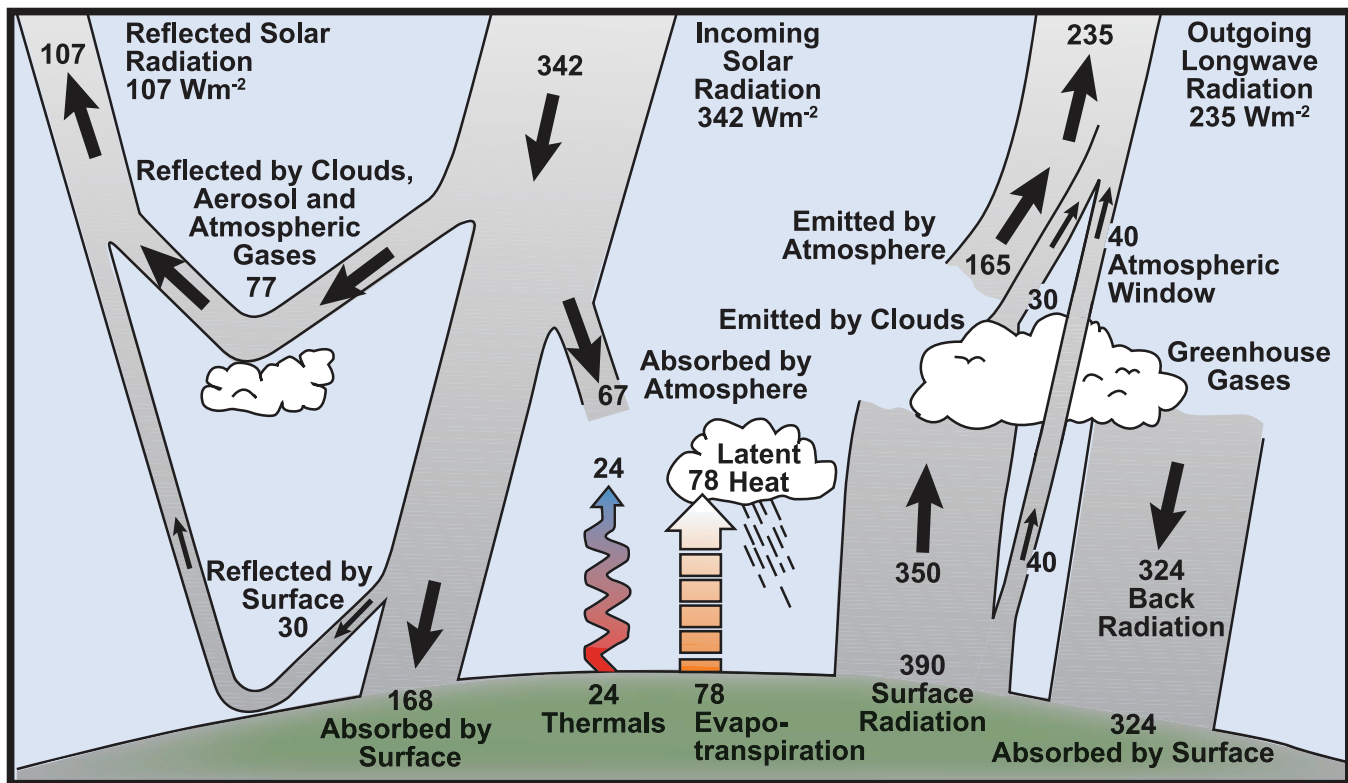
Frequently Asked Question 1.1 What Factors Determine Earth's Climate?

The climate system is a complex, interactive system consisting of the atmosphere, land surface, snow and ice, oceans and other bodies of water, and living things. The atmospheric component of the climate system most obviously characterises climate; climate is often defined as 'average weather'. Climate is usually described in terms of the mean and variability of temperature, precipitation and wind over a period of time, ranging from months to millions of years (the classical period is 30 years). The climate system evolves in time under the influence of its own internal dynamics and due to changes in external factors that affect climate (called 'forcings'). External forcings include natural phenomena such as volcanic eruptions and solar variations, as well as human-induced changes in atmospheric composition. Solar radiation powers the climate system. There are three fundamental ways to change the radiation balance of the Earth: 1) by changing the incoming solar radiation (e.g., by changes in Earth's orbit or in the Sun itself); 2) by changing the fraction of solar radiation that is reflected (called

'albedo'; e.g., by changes in cloud cover, atmospheric particles or vegetation); and 3) by altering the longwave radiation from Earth back towards space (e.g., by changing greenhouse gas concentrations). Climate, in turn, responds directly to such changes, as well as indirectly, through a variety of feedback mechanisms.

The amount of energy reaching the top of Earth's atmosphere each second on a surface area of one square metre facing the Sun during daytime is about 1,370 Watts, and the amount of energy per square metre per second averaged over the entire planet is one-quarter of this (see Figure 1). About 30% of the sunlight that reaches the top of the atmosphere is reflected back to space. Roughly two-thirds of this reflectivity is due to clouds and small particles in the atmosphere known as 'aerosols'. Light-coloured areas of Earth's surface – mainly snow, ice and deserts – reflect the remaining one-third of the sunlight. The most dramatic change in aerosol-produced reflectivity comes when major volcanic eruptions eject material very high into the atmosphere. Rain typically

(continued)



FAQ 1.1, Figure 1. Estimate of the Earth's annual and global mean energy balance. Over the long term, the amount of incoming solar radiation absorbed by the Earth and atmosphere is balanced by the Earth and atmosphere releasing the same amount of outgoing longwave radiation. About half of the incoming solar radiation is absorbed by the Earth's surface. This energy is transferred to the atmosphere by warming the air in contact with the surface (thermals), by evapotranspiration and by longwave radiation that is absorbed by clouds and greenhouse gases. The atmosphere in turn radiates longwave energy back to Earth as well as out to space. Source: Kiehl and Trenberth (1997).

clears aerosols out of the atmosphere in a week or two, but when material from a violent volcanic eruption is projected far above the highest cloud, these aerosols typically influence the climate for about a year or two before falling into the troposphere and being carried to the surface by precipitation. Major volcanic eruptions can thus cause a drop in mean global surface temperature of about half a degree celsius that can last for months or even years. Some man-made aerosols also significantly reflect sunlight.

The energy that is not reflected back to space is absorbed by the Earth's surface and atmosphere. This amount is approximately 240 Watts per square metre (W m^{-2}). To balance the incoming energy, the Earth itself must radiate, on average, the same amount of energy back to space. The Earth does this by emitting outgoing longwave radiation. Everything on Earth emits longwave radiation continuously. That is the heat energy one feels radiating out from a fire; the warmer an object, the more heat energy it radiates. To emit 240 W m^{-2} , a surface would have to have a temperature of around -19°C . This is much colder than the conditions that actually exist at the Earth's surface (the global mean surface temperature is about 14°C). Instead, the necessary -19°C is found at an altitude about 5 km above the surface.

The reason the Earth's surface is this warm is the presence of greenhouse gases, which act as a partial blanket for the longwave radiation coming from the surface. This blanketing is known as the natural greenhouse effect. The most important greenhouse gases are water vapour and carbon dioxide. The two most abundant constituents of the atmosphere – nitrogen and oxygen – have no such effect. Clouds, on the other hand, do exert a blanketing effect similar to that of the greenhouse gases; however, this effect is offset by their reflectivity, such that on average, clouds tend to have a cooling effect on climate (although locally one can feel the warming effect: cloudy nights tend to remain warmer than clear nights because the clouds radiate longwave energy back down to the surface). Human activities intensify the blanketing effect through the release of greenhouse gases. For instance, the amount of carbon dioxide in the atmosphere has increased by about 35% in the industrial era, and this increase is known to be due to human activities, primarily the combustion of fossil fuels and removal of forests. Thus, humankind has dramatically altered the chemical composition of the global atmosphere with substantial implications for climate.

Because the Earth is a sphere, more solar energy arrives for a given surface area in the tropics than at higher latitudes, where

sunlight strikes the atmosphere at a lower angle. Energy is transported from the equatorial areas to higher latitudes via atmospheric and oceanic circulations, including storm systems. Energy is also required to evaporate water from the sea or land surface, and this energy, called latent heat, is released when water vapour condenses in clouds (see Figure 1). Atmospheric circulation is primarily driven by the release of this latent heat. Atmospheric circulation in turn drives much of the ocean circulation through the action of winds on the surface waters of the ocean, and through changes in the ocean's surface temperature and salinity through precipitation and evaporation.

Due to the rotation of the Earth, the atmospheric circulation patterns tend to be more east-west than north-south. Embedded in the mid-latitude westerly winds are large-scale weather systems that act to transport heat toward the poles. These weather systems are the familiar migrating low- and high-pressure systems and their associated cold and warm fronts. Because of land-ocean temperature contrasts and obstacles such as mountain ranges and ice sheets, the circulation system's planetary-scale atmospheric waves tend to be geographically anchored by continents and mountains although their amplitude can change with time. Because of the wave patterns, a particularly cold winter over North America may be associated with a particularly warm winter elsewhere in the hemisphere. Changes in various aspects of the climate system, such as the size of ice sheets, the type and distribution of vegetation or the temperature of the atmosphere or ocean will influence the large-scale circulation features of the atmosphere and oceans.

There are many feedback mechanisms in the climate system that can either amplify ('positive feedback') or diminish ('negative feedback') the effects of a change in climate forcing. For example, as rising concentrations of greenhouse gases warm Earth's climate, snow and ice begin to melt. This melting reveals darker land and water surfaces that were beneath the snow and ice, and these darker surfaces absorb more of the Sun's heat, causing more warming, which causes more melting, and so on, in a self-reinforcing cycle. This feedback loop, known as the 'ice-albedo feedback', amplifies the initial warming caused by rising levels of greenhouse gases. Detecting, understanding and accurately quantifying climate feedbacks have been the focus of a great deal of research by scientists unravelling the complexities of Earth's climate.

Frequently Asked Question 1.2

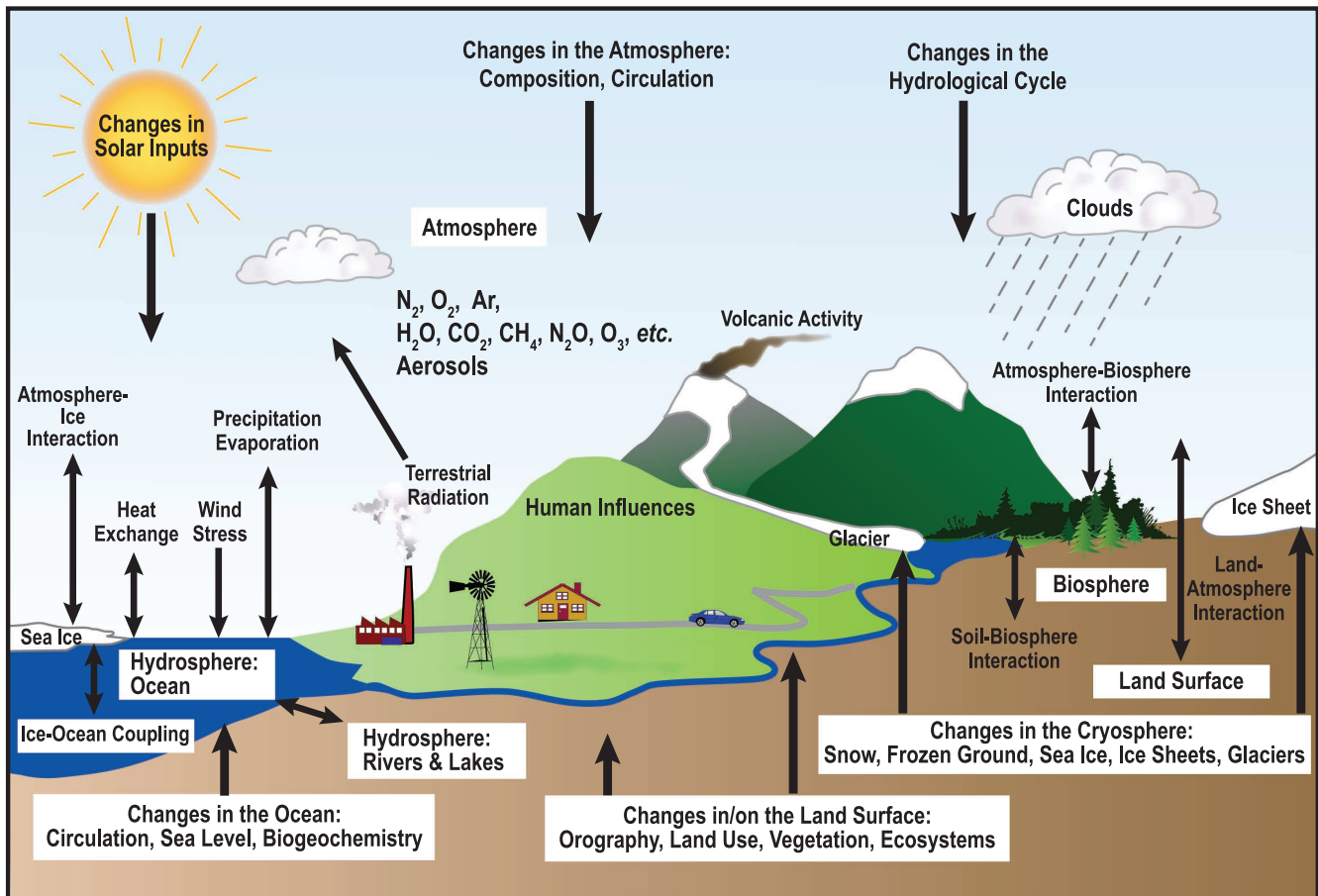
What is the Relationship between Climate Change and Weather?

Climate is generally defined as average weather, and as such, climate change and weather are intertwined. Observations can show that there have been changes in weather, and it is the statistics of changes in weather over time that identify climate change. While weather and climate are closely related, there are important differences. A common confusion between weather and climate arises when scientists are asked how they can predict climate 50 years from now when they cannot predict the weather a few weeks from now. The chaotic nature of weather makes it unpredictable beyond a few days. Projecting changes in climate (i.e., long-term average weather) due to changes in atmospheric composition or other factors is a very different and much more manageable issue. As an analogy, while it is impossible to predict the age at which any particular man will die, we can say with high confidence that the average age of death for men in industrialised countries is about 75. Another common confusion of these issues is thinking

that a cold winter or a cooling spot on the globe is evidence against global warming. There are always extremes of hot and cold, although their frequency and intensity change as climate changes. But when weather is averaged over space and time, the fact that the globe is warming emerges clearly from the data.

Meteorologists put a great deal of effort into observing, understanding and predicting the day-to-day evolution of weather systems. Using physics-based concepts that govern how the atmosphere moves, warms, cools, rains, snows, and evaporates water, meteorologists are typically able to predict the weather successfully several days into the future. A major limiting factor to the predictability of weather beyond several days is a fundamental dynamical property of the atmosphere. In the 1960s, meteorologist Edward Lorenz discovered that very slight differences in initial conditions can produce very different forecast results.

(continued)



FAQ 1.2, Figure 1. Schematic view of the components of the climate system, their processes and interactions.

This is the so-called butterfly effect: a butterfly flapping its wings (or some other small phenomenon) in one place can, in principle, alter the subsequent weather pattern in a distant place. At the core of this effect is chaos theory, which deals with how small changes in certain variables can cause apparent randomness in complex systems.

Nevertheless, chaos theory does not imply a total lack of order. For example, slightly different conditions early in its history might alter the day a storm system would arrive or the exact path it would take, but the average temperature and precipitation (that is, climate) would still be about the same for that region and that period of time. Because a significant problem facing weather forecasting is knowing all the conditions at the start of the forecast period, it can be useful to think of climate as dealing with the background conditions for weather. More precisely, climate can be viewed as concerning the status of the entire Earth system, including the atmosphere, land, oceans, snow, ice and living things (see Figure 1) that serve as the global background conditions that determine weather patterns. An example of this would be an El Niño affecting the weather in coastal Peru. The El Niño sets limits on the probable evolution of weather patterns that random effects can produce. A La Niña would set different limits.

Another example is found in the familiar contrast between summer and winter. The march of the seasons is due to changes in the geographical patterns of energy absorbed and radiated away by the Earth system. Likewise, projections of future climate are

shaped by fundamental changes in heat energy in the Earth system, in particular the increasing intensity of the greenhouse effect that traps heat near Earth's surface, determined by the amount of carbon dioxide and other greenhouse gases in the atmosphere. Projecting changes in climate due to changes in greenhouse gases 50 years from now is a very different and much more easily solved problem than forecasting weather patterns just weeks from now. To put it another way, long-term variations brought about by changes in the composition of the atmosphere are much more predictable than individual weather events. As an example, while we cannot predict the outcome of a single coin toss or roll of the dice, we can predict the statistical behaviour of a large number of such trials.

While many factors continue to influence climate, scientists have determined that human activities have become a dominant force, and are responsible for most of the warming observed over the past 50 years. Human-caused climate change has resulted primarily from changes in the amounts of greenhouse gases in the atmosphere, but also from changes in small particles (aerosols), as well as from changes in land use, for example. As climate changes, the probabilities of certain types of weather events are affected. For example, as Earth's average temperature has increased, some weather phenomena have become more frequent and intense (e.g., heat waves and heavy downpours), while others have become less frequent and intense (e.g., extreme cold events).

Frequently Asked Question 1.3

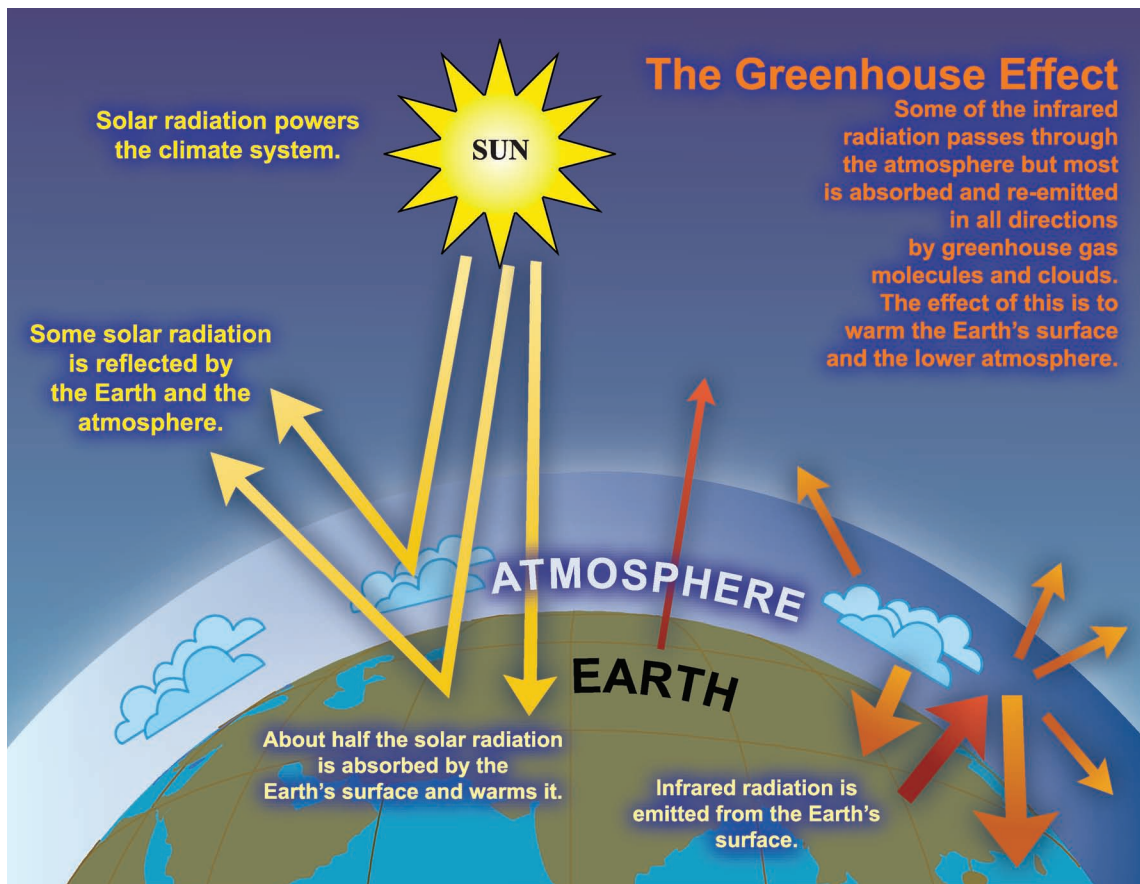
What is the Greenhouse Effect?

The Sun powers Earth's climate, radiating energy at very short wavelengths, predominately in the visible or near-visible (e.g., ultraviolet) part of the spectrum. Roughly one-third of the solar energy that reaches the top of Earth's atmosphere is reflected directly back to space. The remaining two-thirds is absorbed by the surface and, to a lesser extent, by the atmosphere. To balance the absorbed incoming energy, the Earth must, on average, radiate the same amount of energy back to space. Because the Earth is much colder than the Sun, it radiates at much longer wavelengths, primarily in the infrared part of the spectrum (see Figure 1). Much of this thermal radiation emitted by the land and ocean is absorbed by the atmosphere, including clouds, and reradiated back to Earth. This is called the greenhouse effect. The glass walls in a greenhouse reduce airflow and increase the temperature of the air inside. Analogously, but through a different physical process, the Earth's greenhouse effect warms the surface of the planet. Without the natural greenhouse effect, the average temperature at Earth's surface would be below the freezing point of water. Thus,

Earth's natural greenhouse effect makes life as we know it possible. However, human activities, primarily the burning of fossil fuels and clearing of forests, have greatly intensified the natural greenhouse effect, causing global warming.

The two most abundant gases in the atmosphere, nitrogen (comprising 78% of the dry atmosphere) and oxygen (comprising 21%), exert almost no greenhouse effect. Instead, the greenhouse effect comes from molecules that are more complex and much less common. Water vapour is the most important greenhouse gas, and carbon dioxide (CO₂) is the second-most important one. Methane, nitrous oxide, ozone and several other gases present in the atmosphere in small amounts also contribute to the greenhouse effect. In the humid equatorial regions, where there is so much water vapour in the air that the greenhouse effect is very large, adding a small additional amount of CO₂ or water vapour has only a small direct impact on downward infrared radiation. However, in the cold, dry polar regions, the effect of a small increase in CO₂ or

(continued)



FAQ 1.3, Figure 1. An idealised model of the natural greenhouse effect. See text for explanation.

water vapour is much greater. The same is true for the cold, dry upper atmosphere where a small increase in water vapour has a greater influence on the greenhouse effect than the same change in water vapour would have near the surface.

Several components of the climate system, notably the oceans and living things, affect atmospheric concentrations of greenhouse gases. A prime example of this is plants taking CO₂ out of the atmosphere and converting it (and water) into carbohydrates via photosynthesis. In the industrial era, human activities have added greenhouse gases to the atmosphere, primarily through the burning of fossil fuels and clearing of forests.

Adding more of a greenhouse gas, such as CO₂, to the atmosphere intensifies the greenhouse effect, thus warming Earth's climate. The amount of warming depends on various feedback mechanisms. For example, as the atmosphere warms due to rising levels of greenhouse gases, its concentration of water vapour

increases, further intensifying the greenhouse effect. This in turn causes more warming, which causes an additional increase in water vapour, in a self-reinforcing cycle. This water vapour feedback may be strong enough to approximately double the increase in the greenhouse effect due to the added CO₂ alone.

Additional important feedback mechanisms involve clouds. Clouds are effective at absorbing infrared radiation and therefore exert a large greenhouse effect, thus warming the Earth. Clouds are also effective at reflecting away incoming solar radiation, thus cooling the Earth. A change in almost any aspect of clouds, such as their type, location, water content, cloud altitude, particle size and shape, or lifetimes, affects the degree to which clouds warm or cool the Earth. Some changes amplify warming while others diminish it. Much research is in progress to better understand how clouds change in response to climate warming, and how these changes affect climate through various feedback mechanisms.

Frequently Asked Question 2.1

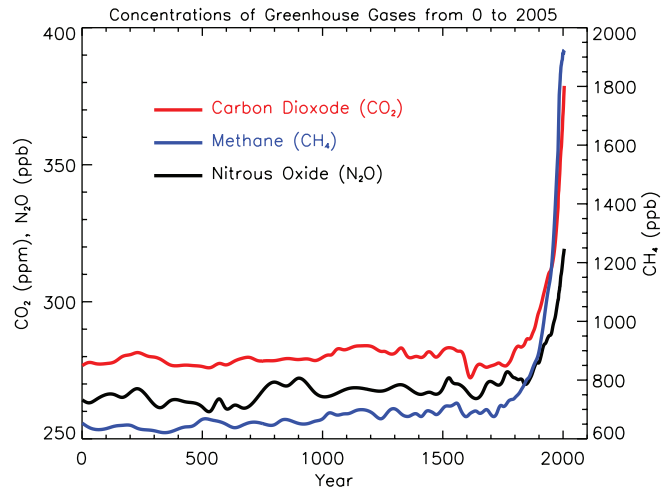
How do Human Activities Contribute to Climate Change and How do They Compare with Natural Influences?

Human activities contribute to climate change by causing changes in Earth's atmosphere in the amounts of greenhouse gases, aerosols (small particles), and cloudiness. The largest known contribution comes from the burning of fossil fuels, which releases carbon dioxide gas to the atmosphere. Greenhouse gases and aerosols affect climate by altering incoming solar radiation and outgoing infrared (thermal) radiation that are part of Earth's energy balance. Changing the atmospheric abundance or properties of these gases and particles can lead to a warming or cooling of the climate system. Since the start of the industrial era (about 1750), the overall effect of human activities on climate has been a warming influence. The human impact on climate during this era greatly exceeds that due to known changes in natural processes, such as solar changes and volcanic eruptions.

Greenhouse Gases

Human activities result in emissions of four principal greenhouse gases: carbon dioxide (CO₂), methane (CH₄), nitrous oxide (N₂O) and the halocarbons (a group of gases containing fluorine, chlorine and bromine). These gases accumulate in the atmosphere, causing concentrations to increase with time. Significant increases in all of these gases have occurred in the industrial era (see Figure 1). All of these increases are attributable to human activities.

- Carbon dioxide has increased from fossil fuel use in transportation, building heating and cooling and the manufacture of cement and other goods. Deforestation releases CO₂ and reduces its uptake by plants. Carbon dioxide is also released in natural processes such as the decay of plant matter.
- Methane has increased as a result of human activities related to agriculture, natural gas distribution and landfills. Methane is also released from natural processes that occur, for example, in wetlands. Methane concentrations are not currently increasing in the atmosphere because growth rates decreased over the last two decades.
- Nitrous oxide is also emitted by human activities such as fertilizer use and fossil fuel burning. Natural processes in soils and the oceans also release N₂O.
- Halocarbon gas concentrations have increased primarily due to human activities. Natural processes are also a small source. Principal halocarbons include the chlorofluorocarbons (e.g., CFC-11 and CFC-12), which were used extensively as refrigeration agents and in other industrial processes before their presence in the atmosphere was found to cause stratospheric ozone depletion. The abundance of chlorofluorocarbon gases is decreasing as a result of international regulations designed to protect the ozone layer.



FAQ 2.1, Figure 1. Atmospheric concentrations of important long-lived greenhouse gases over the last 2,000 years. Increases since about 1750 are attributed to human activities in the industrial era. Concentration units are parts per million (ppm) or parts per billion (ppb), indicating the number of molecules of the greenhouse gas per million or billion air molecules, respectively, in an atmospheric sample. (Data combined and simplified from Chapters 6 and 2 of this report.)

- Ozone is a greenhouse gas that is continually produced and destroyed in the atmosphere by chemical reactions. In the troposphere, human activities have increased ozone through the release of gases such as carbon monoxide, hydrocarbons and nitrogen oxide, which chemically react to produce ozone. As mentioned above, halocarbons released by human activities destroy ozone in the stratosphere and have caused the ozone hole over Antarctica.
- Water vapour is the most abundant and important greenhouse gas in the atmosphere. However, human activities have only a small direct influence on the amount of atmospheric water vapour. Indirectly, humans have the potential to affect water vapour substantially by changing climate. For example, a warmer atmosphere contains more water vapour. Human activities also influence water vapour through CH₄ emissions, because CH₄ undergoes chemical destruction in the stratosphere, producing a small amount of water vapour.
- Aerosols are small particles present in the atmosphere with widely varying size, concentration and chemical composition. Some aerosols are emitted directly into the atmosphere while others are formed from emitted compounds. Aerosols contain both naturally occurring compounds and those emitted as a result of human activities. Fossil fuel and biomass burning have increased aerosols containing sulphur compounds, organic compounds and black carbon (soot). Human activities such as

(continued)

surface mining and industrial processes have increased dust in the atmosphere. Natural aerosols include mineral dust released from the surface, sea salt aerosols, biogenic emissions from the land and oceans and sulphate and dust aerosols produced by volcanic eruptions.

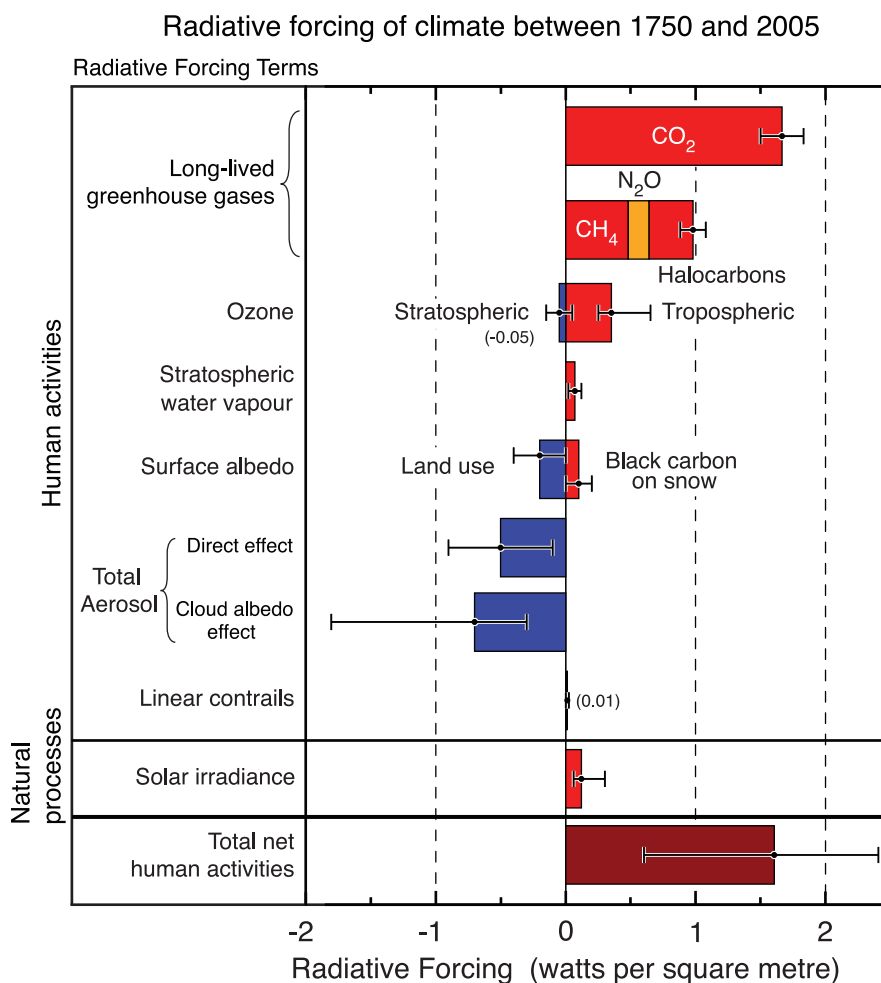
Radiative Forcing of Factors Affected by Human Activities

The contributions to radiative forcing from some of the factors influenced by human activities are shown in Figure 2. The values reflect the total forcing relative to the start of the industrial era (about 1750). The forcings for all greenhouse gas increases, which are the best understood of those due to human activities, are positive because each gas absorbs outgoing infrared radiation in the atmosphere. Among the greenhouse gases, CO₂ increases have caused the largest forcing over this period. Tropospheric ozone increases have also contributed to warming, while stratospheric ozone decreases have contributed to cooling.

Aerosol particles influence radiative forcing directly through reflection and absorption of solar and infrared radiation in the atmosphere. Some aerosols cause a positive forcing while others cause a negative forcing. The direct radiative forcing summed over all aerosol types is negative. Aerosols also cause a negative radiative forcing indirectly through the changes they cause in cloud properties.

Human activities since the industrial era have altered the nature of land cover over the globe, principally through changes in

(continued)



FAQ 2.1, Figure 2. Summary of the principal components of the radiative forcing of climate change. All these radiative forcings result from one or more factors that affect climate and are associated with human activities or natural processes as discussed in the text. The values represent the forcings in 2005 relative to the start of the industrial era (about 1750). Human activities cause significant changes in long-lived gases, ozone, water vapour, surface albedo, aerosols and contrails. The only increase in natural forcing of any significance between 1750 and 2005 occurred in solar irradiance. Positive forcings lead to warming of climate and negative forcings lead to a cooling. The thin black line attached to each coloured bar represents the range of uncertainty for the respective value. (Figure adapted from Figure 2.20 of this report.)

FAQ 2.1, Box 1: What is Radiative Forcing?

What is radiative forcing? The influence of a factor that can cause climate change, such as a greenhouse gas, is often evaluated in terms of its radiative forcing. Radiative forcing is a measure of how the energy balance of the Earth-atmosphere system is influenced when factors that affect climate are altered. The word radiative arises because these factors change the balance between incoming solar radiation and outgoing infrared radiation within the Earth's atmosphere. This radiative balance controls the Earth's surface temperature. The term forcing is used to indicate that Earth's radiative balance is being pushed away from its normal state.

Radiative forcing is usually quantified as the 'rate of energy change per unit area of the globe as measured at the top of the atmosphere', and is expressed in units of 'Watts per square metre' (see Figure 2). When radiative forcing from a factor or group of factors is evaluated as positive, the energy of the Earth-atmosphere system will ultimately increase, leading to a warming of the system. In contrast, for a negative radiative forcing, the energy will ultimately decrease, leading to a cooling of the system. Important challenges for climate scientists are to identify all the factors that affect climate and the mechanisms by which they exert a forcing, to quantify the radiative forcing of each factor and to evaluate the total radiative forcing from the group of factors.

croplands, pastures and forests. They have also modified the reflective properties of ice and snow. Overall, it is likely that more solar radiation is now being reflected from Earth's surface as a result of human activities. This change results in a negative forcing.

Aircraft produce persistent linear trails of condensation ('contrails') in regions that have suitably low temperatures and high humidity. Contrails are a form of cirrus cloud that reflect solar radiation and absorb infrared radiation. Linear contrails from global aircraft operations have increased Earth's cloudiness and are estimated to cause a small positive radiative forcing.

Radiative Forcing from Natural Changes

Natural forcings arise due to solar changes and explosive volcanic eruptions. Solar output has increased gradually in the industrial era, causing a small positive radiative forcing (see Figure 2). This is in addition to the cyclic changes in solar radiation that

follow an 11-year cycle. Solar energy directly heats the climate system and can also affect the atmospheric abundance of some greenhouse gases, such as stratospheric ozone. Explosive volcanic eruptions can create a short-lived (2 to 3 years) negative forcing through the temporary increases that occur in sulphate aerosol in the stratosphere. The stratosphere is currently free of volcanic aerosol, since the last major eruption was in 1991 (Mt. Pinatubo).

The differences in radiative forcing estimates between the present day and the start of the industrial era for solar irradiance changes and volcanoes are both very small compared to the differences in radiative forcing estimated to have resulted from human activities. As a result, in today's atmosphere, the radiative forcing from human activities is much more important for current and future climate change than the estimated radiative forcing from changes in natural processes.

Frequently Asked Question 3.1

How are Temperatures on Earth Changing?

Instrumental observations over the past 157 years show that temperatures at the surface have risen globally, with important regional variations. For the global average, warming in the last century has occurred in two phases, from the 1910s to the 1940s (0.35°C), and more strongly from the 1970s to the present (0.55°C). An increasing rate of warming has taken place over the last 25 years, and 11 of the 12 warmest years on record have occurred in the past 12 years. Above the surface, global observations since the late 1950s show that the troposphere (up to about 10 km) has warmed at a slightly greater rate than the surface, while the stratosphere (about 10–30 km) has cooled markedly since 1979. This is in accord with physical expectations and most model results. Confirmation of global warming comes from warming of the oceans, rising sea levels, glaciers melting, sea ice retreating in the Arctic and diminished snow cover in the Northern Hemisphere.

There is no single thermometer measuring the global temperature. Instead, individual thermometer measurements taken every day at several thousand stations over the land areas of the world are combined with thousands more measurements of sea surface temperature taken from ships moving over the oceans to produce an estimate of global average temperature every month. To obtain consistent changes over time, the main analysis is actually of anomalies (departures from the climatological mean at each site) as these are more robust to changes in data availability. It is now possible to use these measurements from 1850 to the present, although coverage is much less than global in the second half of the 19th century, is much better after 1957 when measurements began in Antarctica, and best after about 1980, when satellite measurements began.

Expressed as a global average, surface temperatures have increased by about 0.74°C over the past hundred years (between 1906 and 2005; see Figure 1). However, the warming has been neither steady nor the same in different seasons or in different locations. There was not much overall change from 1850 to about 1915, aside from ups and downs associated with natural variability but which may have also partly arisen from poor sampling. An increase (0.35°C) occurred in the global average temperature from the 1910s to the 1940s, followed by a slight cooling (0.1°C), and then a rapid warming (0.55°C) up to the end of 2006 (Figure 1). The warmest years of the series are 1998 and 2005 (which are statistically indistinguishable), and 11 of the 12 warmest years have occurred in the last 12 years (1995 to 2006). Warming, particularly since the 1970s, has generally been greater over land than over the oceans. Seasonally, warming has been slightly greater in the winter hemisphere. Additional warming occurs in cities and urban areas (often referred to as the urban heat island effect), but is confined in spatial extent, and its effects are allowed for both by excluding as many of the affected sites as possible from the global temperature data and by increasing the error range (the blue band in the figure).

A few areas have cooled since 1901, most notably the northern North Atlantic near southern Greenland. Warming during this time has been strongest over the continental interiors of Asia and northern North America. However, as these are areas with large year-to-year variability, the most evident warming signal has occurred in parts of the middle and lower latitudes, particularly the tropical oceans. In the lower left panel of Figure 1, which shows temperature trends since 1979, the pattern in the Pacific Ocean features warming and cooling regions related to El Niño.

Analysis of long-term changes in daily temperature extremes has recently become possible for many regions of the world (parts of North America and southern South America, Europe, northern and eastern Asia, southern Africa and Australasia). Especially since the 1950s, these records show a decrease in the number of very cold days and nights and an increase in the number of extremely hot days and warm nights (see FAQ 3.3). The length of the frost-free season has increased in most mid- and high-latitude regions of both hemispheres. In the Northern Hemisphere, this is mostly manifest as an earlier start to spring.

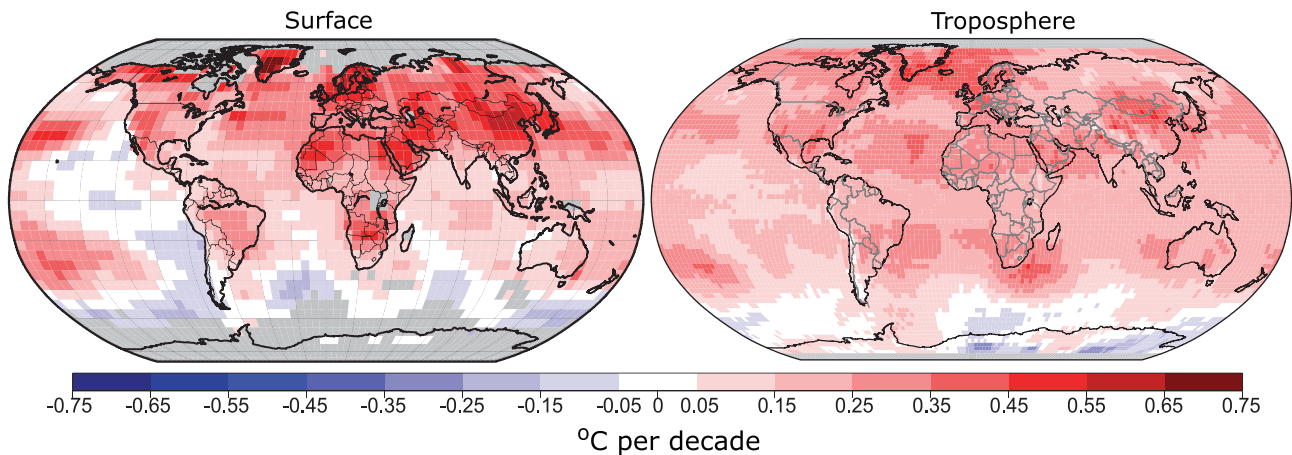
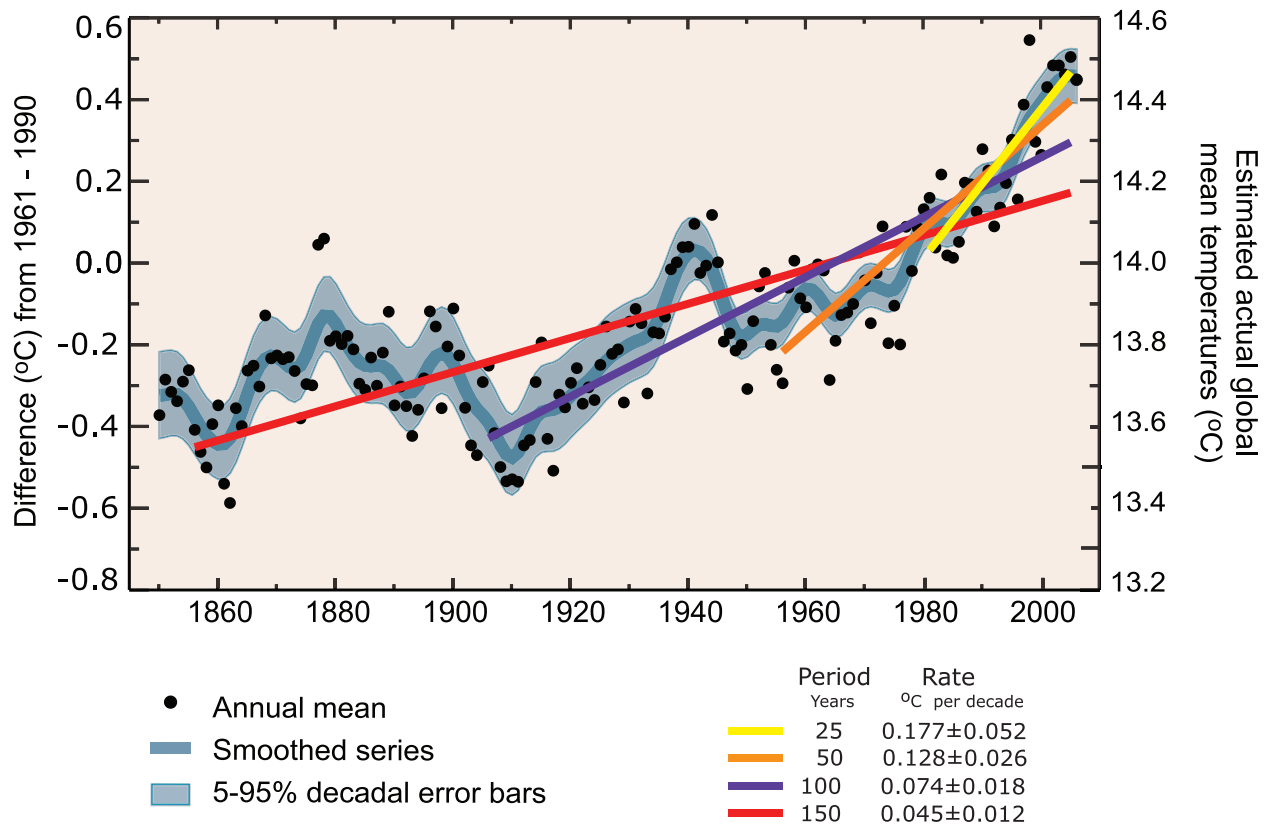
In addition to the surface data described above, measurements of temperature above the surface have been made with weather balloons, with reasonable coverage over land since 1958, and from satellite data since 1979. All data are adjusted for changes in instruments and observing practices where necessary. Microwave satellite data have been used to create a 'satellite temperature record' for thick layers of the atmosphere including the troposphere (from the surface up to about 10 km) and the lower stratosphere (about 10 to 30 km). Despite several new analyses with improved cross-calibration of the 13 instruments on different satellites used since 1979 and compensation for changes in observing time and satellite altitude, some uncertainties remain in trends.

For global observations since the late 1950s, the most recent versions of all available data sets show that the troposphere has warmed at a slightly greater rate than the surface, while the stratosphere has cooled markedly since 1979. This is in accord with physical expectations and most model results, which demonstrate the role of increasing greenhouse gases in tropospheric warming and stratospheric cooling; ozone depletion also contributes substantially to stratospheric cooling.

Consistent with observed increases in surface temperature, there have been decreases in the length of river and lake ice seasons. Further, there has been an almost worldwide reduction in glacial mass and extent in the 20th century; melting of the Greenland Ice Sheet has recently become apparent; snow cover has decreased in many Northern Hemisphere regions; sea ice thickness and extent have decreased in the Arctic in all seasons, most dramatically in spring and summer; the oceans are warming; and sea level is rising due to thermal expansion of the oceans and melting of land ice.

(continued)

Global Mean Temperature



FAQ 3.1, Figure 1. (Top) Annual global mean observed temperatures¹ (black dots) along with simple fits to the data. The left hand axis shows anomalies relative to the 1961 to 1990 average and the right hand axis shows the estimated actual temperature (°C). Linear trend fits to the last 25 (yellow), 50 (orange), 100 (purple) and 150 years (red) are shown, and correspond to 1981 to 2005, 1956 to 2005, 1906 to 2005, and 1856 to 2005, respectively. Note that for shorter recent periods, the slope is greater, indicating accelerated warming. The blue curve is a smoothed depiction to capture the decadal variations. To give an idea of whether the fluctuations are meaningful, decadal 5% to 95% (light blue) error ranges about that line are given (accordingly, annual values do exceed those limits). Results from climate models driven by estimated radiative forcings for the 20th century (Chapter 9) suggest that there was little change prior to about 1915, and that a substantial fraction of the early 20th-century change was contributed by naturally occurring influences including solar radiation changes, volcanism and natural variability. From about 1940 to 1970 the increasing industrialisation following World War II increased pollution in the Northern Hemisphere, contributing to cooling, and increases in carbon dioxide and other greenhouse gases dominate the observed warming after the mid-1970s. (Bottom) Patterns of linear global temperature trends from 1979 to 2005 estimated at the surface (left), and for the troposphere (right) from the surface to about 10 km altitude, from satellite records. Grey areas indicate incomplete data. Note the more spatially uniform warming in the satellite tropospheric record while the surface temperature changes more clearly relate to land and ocean.

¹ From the HadCRUT3 data set.

Frequently Asked Question 3.2

How is Precipitation Changing?

Observations show that changes are occurring in the amount, intensity, frequency and type of precipitation. These aspects of precipitation generally exhibit large natural variability, and El Niño and changes in atmospheric circulation patterns such as the North Atlantic Oscillation have a substantial influence. Pronounced long-term trends from 1900 to 2005 have been observed in precipitation amount in some places: significantly wetter in eastern North and South America, northern Europe and northern and central Asia, but drier in the Sahel, southern Africa, the Mediterranean and southern Asia. More precipitation now falls as rain rather than snow in northern regions. Widespread increases in heavy precipitation events have been observed, even in places where total amounts have decreased. These changes are associated with increased water vapour in the atmosphere arising from the warming of the world's oceans, especially at lower latitudes. There are also increases in some regions in the occurrences of both droughts and floods.

Precipitation is the general term for rainfall, snowfall and other forms of frozen or liquid water falling from clouds. Precipitation is intermittent, and the character of the precipitation when it occurs depends greatly on temperature and the weather situation. The latter determines the supply of moisture through winds and surface evaporation, and how it is gathered together in storms as clouds. Precipitation forms as water vapour condenses, usually in rising air that expands and hence cools. The upward motion comes from air rising over mountains, warm air riding over cooler air (warm front), colder air pushing under warmer air (cold front), convection from local heating of the surface, and other weather and cloud systems. Hence, changes in any of these aspects alter precipitation. As precipitation maps tend to be spotty, overall trends in precipitation are indicated by the Palmer Drought Severity Index (see Figure 1), which is a measure of soil moisture using precipitation and crude estimates of changes in evaporation.

A consequence of increased heating from the human-induced enhanced greenhouse effect is increased evaporation, provided that adequate surface moisture is available (as it always is over the oceans and other wet surfaces). Hence, surface moisture effectively acts as an 'air conditioner', as heat used for evaporation acts to moisten the air rather than warm it. An observed consequence of this is that summers often tend to be either warm and dry or cool and wet. In the areas of eastern North and South America where it has become wetter (Figure 1), temperatures have therefore increased less than elsewhere (see FAQ 3.3, Figure 1 for changes in warm days). Over northern continents in winter, however, more precipitation is associated with higher temperatures, as the water holding capacity of the atmosphere increases in the warmer conditions. However, in these regions, where precipitation has generally increased somewhat, increases in temperatures (FAQ 3.1) have increased drying, making the precipitation changes less evident in Figure 1.

As climate changes, several direct influences alter precipitation amount, intensity, frequency and type. Warming accelerates land surface drying and increases the potential incidence and severity of droughts, which has been observed in many places worldwide (Figure 1). However, a well-established physical law (the Clausius-Clapeyron relation) determines that the water-holding capacity of the atmosphere increases by about 7% for every 1°C rise in temperature. Observations of trends in relative humidity are uncertain but suggest that it has remained about the same overall, from the surface throughout the troposphere, and hence increased temperatures will have resulted in increased water vapour. Over the 20th century, based on changes in sea surface temperatures, it is estimated that atmospheric water vapour increased by about 5% in the atmosphere over the oceans. Because precipitation comes mainly from weather systems that feed on the water vapour stored in the atmosphere, this has generally increased precipitation intensity and the risk of heavy rain and snow events. Basic theory, climate model simulations and empirical evidence all confirm that warmer climates, owing to increased water vapour, lead to more intense precipitation events even when the total annual precipitation is reduced slightly, and with prospects for even stronger events when the overall precipitation amounts increase. The warmer climate therefore increases risks of both drought – where it is not raining – and floods – where it is – but at different times and/or places. For instance, the summer of 2002 in Europe brought widespread floods but was followed a year later in 2003 by record-breaking heat waves and drought. The distribution and timing of floods and droughts is most profoundly affected by the cycle of El Niño events, particularly in the tropics and over much of the mid-latitudes of Pacific-rim countries.

In areas where aerosol pollution masks the ground from direct sunlight, decreases in evaporation reduce the overall moisture supply to the atmosphere. Hence, even as the potential for heavier precipitation results from increased water vapour amounts, the duration and frequency of events may be curtailed, as it takes longer to recharge the atmosphere with water vapour.

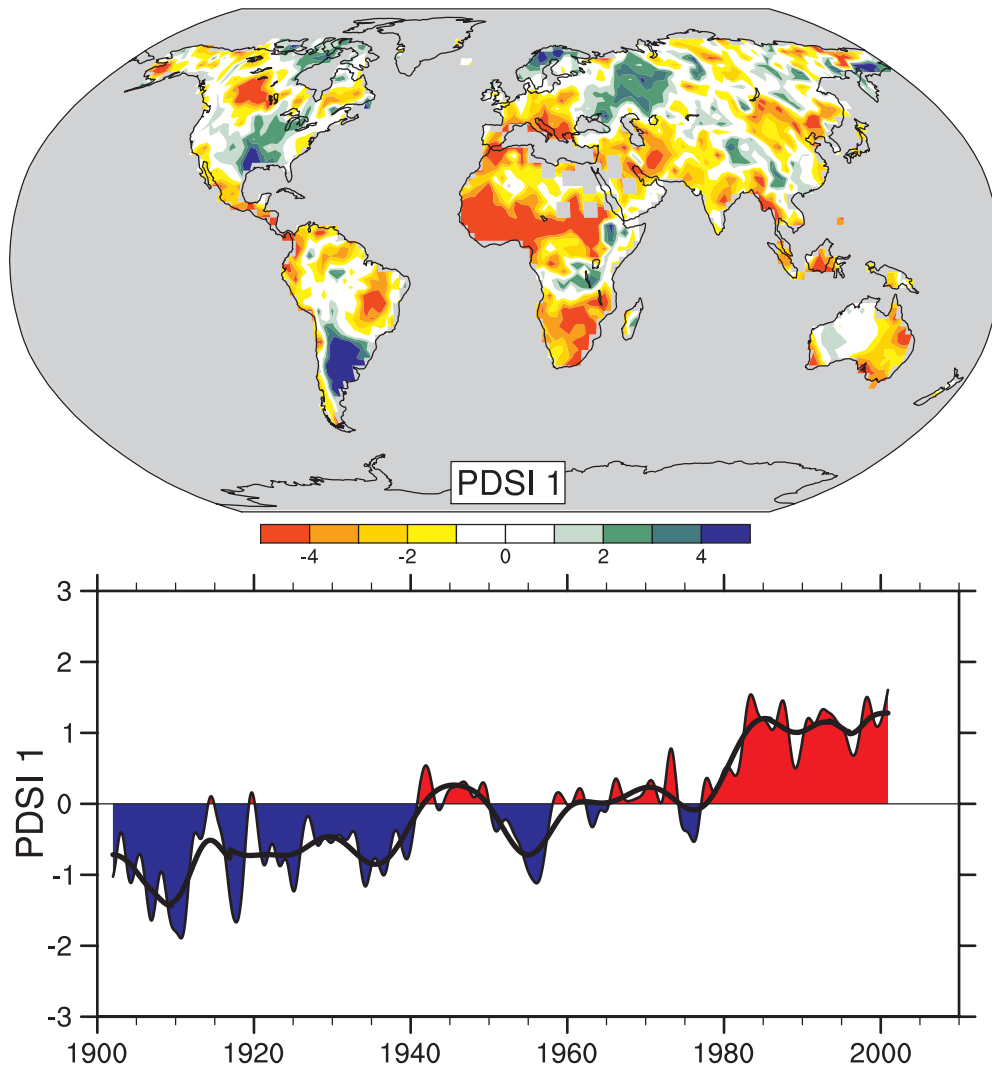
Local and regional changes in the character of precipitation also depend a great deal on atmospheric circulation patterns determined by El Niño, the North Atlantic Oscillation (NAO; a measure of westerly wind strength over the North Atlantic in winter) and other patterns of variability. Some of these observed circulation changes are associated with climate change. An associated shift in the storm track makes some regions wetter and some – often nearby – drier, making for complex patterns of change. For instance, in the European sector a more positive NAO in the 1990s led to wetter conditions in northern Europe and drier conditions over the Mediterranean and northern African regions (Figure 1). The prolonged drought in the Sahel (see Figure 1), which was pronounced from the late 1960s to the late 1980s,

(continued)

continues although it is not quite as intense as it was; it has been linked, through changes in atmospheric circulation, to changes in tropical sea surface temperature patterns in the Pacific, Indian and Atlantic Basins. Drought has become widespread throughout much of Africa and more common in the tropics and subtropics.

As temperatures rise, the likelihood of precipitation falling as rain rather than snow increases, especially in autumn and spring at the beginning and end of the snow season, and in areas where temperatures are near freezing. Such changes are observed in many places, especially over land in middle and high latitudes of

the Northern Hemisphere, leading to increased rains but reduced snowpacks, and consequently diminished water resources in summer, when they are most needed. Nevertheless, the often spotty and intermittent nature of precipitation means observed patterns of change are complex. The long-term record emphasizes that patterns of precipitation vary somewhat from year to year, and even prolonged multi-year droughts are usually punctuated by a year of heavy rains; for instance as El Niño influences are felt. An example may be the wet winter of 2004-2005 in the southwestern USA following a six-year drought and below-normal snowpack.



FAQ 3.2, Figure 1. The most important spatial pattern (top) of the monthly Palmer Drought Severity Index (PDSI) for 1900 to 2002. The PDSI is a prominent index of drought and measures the cumulative deficit (relative to local mean conditions) in surface land moisture by incorporating previous precipitation and estimates of moisture drawn into the atmosphere (based on atmospheric temperatures) into a hydrological accounting system. The lower panel shows how the sign and strength of this pattern has changed since 1900. Red and orange areas are drier (wetter) than average and blue and green areas are wetter (drier) than average when the values shown in the lower plot are positive (negative). The smooth black curve shows decadal variations. The time series approximately corresponds to a trend, and this pattern and its variations account for 67% of the linear trend of PDSI from 1900 to 2002 over the global land area. It therefore features widespread increasing African drought, especially in the Sahel, for instance. Note also the wetter areas, especially in eastern North and South America and northern Eurasia. Adapted from Dai et al. (2004b).

Frequently Asked Question 3.3

Has there been a Change in Extreme Events like Heat Waves, Droughts, Floods and Hurricanes?

Since 1950, the number of heat waves has increased and widespread increases have occurred in the numbers of warm nights. The extent of regions affected by droughts has also increased as precipitation over land has marginally decreased while evaporation has increased due to warmer conditions. Generally, numbers of heavy daily precipitation events that lead to flooding have increased, but not everywhere. Tropical storm and hurricane frequencies vary considerably from year to year, but evidence suggests substantial increases in intensity and duration since the 1970s. In the extratropics, variations in tracks and intensity of storms reflect variations in major features of the atmospheric circulation, such as the North Atlantic Oscillation.

In several regions of the world, indications of changes in various types of extreme climate events have been found. The extremes are commonly considered to be the values exceeded 1, 5 and 10% of the time (at one extreme) or 90, 95 and 99% of the time (at the other extreme). The warm nights or hot days (discussed below) are those exceeding the 90th percentile of temperature, while cold nights or days are those falling below the 10th percentile. Heavy precipitation is defined as daily amounts greater than the 95th (or for 'very heavy', the 99th) percentile.

In the last 50 years for the land areas sampled, there has been a significant decrease in the annual occurrence of cold nights and a significant increase in the annual occurrence of warm nights (Figure 1). Decreases in the occurrence of cold days and increases in hot days, while widespread, are generally less marked. The distributions of minimum and maximum temperatures have not only shifted to higher values, consistent with overall warming, but the cold extremes have warmed more than the warm extremes over the last 50 years (Figure 1). More warm extremes imply an increased frequency of heat waves. Further supporting indications include the observed trend towards fewer frost days associated with the average warming in most mid-latitude regions.

A prominent indication of a change in extremes is the observed evidence of increases in heavy precipitation events over the mid-latitudes in the last 50 years, even in places where mean precipitation amounts are not increasing (see also FAQ 3.2). For very heavy precipitation events, increasing trends are reported as well, but results are available for few areas.

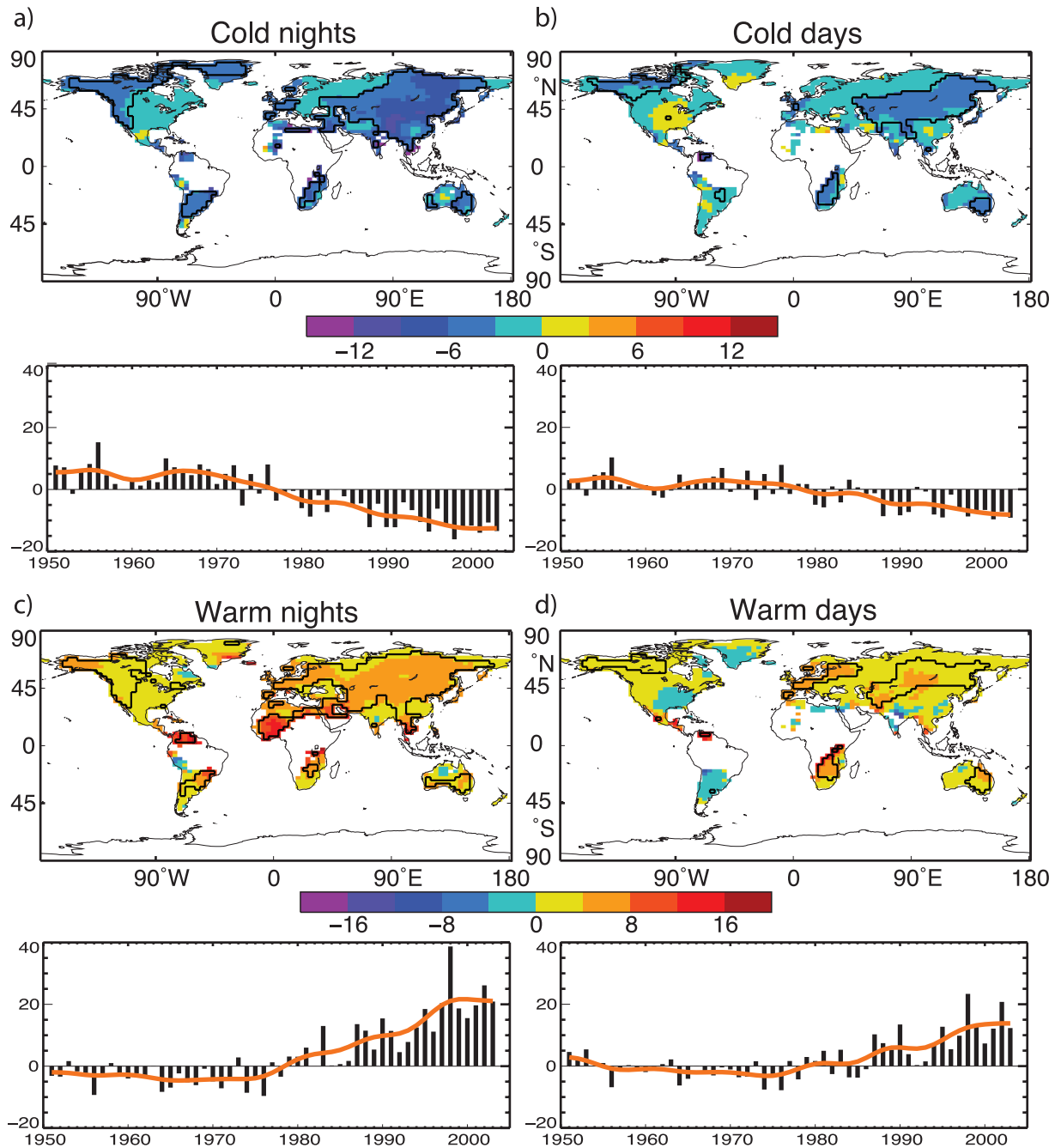
Drought is easier to measure because of its long duration. While there are numerous indices and metrics of drought, many studies use monthly precipitation totals and temperature averages combined into a measure called the Palmer Drought Severity Index (PDSI). The PDSI calculated from the middle of the 20th century shows a large drying trend over many Northern Hemisphere land areas since the mid-1950s, with widespread drying over much of southern Eurasia, northern Africa, Canada and Alaska

(FAQ 3.2, Figure 1), and an opposite trend in eastern North and South America. In the Southern Hemisphere, land surfaces were wet in the 1970s and relatively dry in the 1960s and 1990s, and there was a drying trend from 1974 to 1998. Longer-duration records for Europe for the whole of the 20th century indicate few significant trends. Decreases in precipitation over land since the 1950s are the likely main cause for the drying trends, although large surface warming during the last two to three decades has also likely contributed to the drying. One study shows that very dry land areas across the globe (defined as areas with a PDSI of less than -3.0) have more than doubled in extent since the 1970s, associated with an initial precipitation decrease over land related to the El Niño-Southern Oscillation and with subsequent increases primarily due to surface warming.

Changes in tropical storm and hurricane frequency and intensity are masked by large natural variability. The El Niño-Southern Oscillation greatly affects the location and activity of tropical storms around the world. Globally, estimates of the potential destructiveness of hurricanes show a substantial upward trend since the mid-1970s, with a trend towards longer storm duration and greater storm intensity, and the activity is strongly correlated with tropical sea surface temperature. These relationships have been reinforced by findings of a large increase in numbers and proportion of strong hurricanes globally since 1970 even as total numbers of cyclones and cyclone days decreased slightly in most basins. Specifically, the number of category 4 and 5 hurricanes increased by about 75% since 1970. The largest increases were in the North Pacific, Indian and Southwest Pacific Oceans. However, numbers of hurricanes in the North Atlantic have also been above normal in 9 of the last 11 years, culminating in the record-breaking 2005 season.

Based on a variety of measures at the surface and in the upper troposphere, it is likely that there has been a poleward shift as well as an increase in Northern Hemisphere winter storm track activity over the second half of the 20th century. These changes are part of variations that have occurred related to the North Atlantic Oscillation. Observations from 1979 to the mid-1990s reveal a tendency towards a stronger December to February circumpolar westerly atmospheric circulation throughout the troposphere and lower stratosphere, together with poleward displacements of jet streams and increased storm track activity. Observational evidence for changes in small-scale severe weather phenomena (such as tornadoes, hail and thunderstorms) is mostly local and too scattered to draw general conclusions; increases in many areas arise because of increased public awareness and improved efforts to collect reports of these phenomena.

(continued)



FAQ 3.3, Figure 1. Observed trends (days per decade) for 1951 to 2003 in the frequency of extreme temperatures, defined based on 1961 to 1990 values, as maps for the 10th percentile: (a) cold nights and (b) cold days; and 90th percentile: (c) warm nights and (d) warm days. Trends were calculated only for grid boxes that had at least 40 years of data during this period and had data until at least 1999. Black lines enclose regions where trends are significant at the 5% level. Below each map are the global annual time series of anomalies (with respect to 1961 to 1990). The orange line shows decadal variations. Trends are significant at the 5% level for all the global indices shown. Adapted from Alexander et al. (2006).

Frequently Asked Question 4.1

Is the Amount of Snow and Ice on the Earth Decreasing?

Yes. Observations show a global-scale decline of snow and ice over many years, especially since 1980 and increasing during the past decade, despite growth in some places and little change in others (Figure 1). Most mountain glaciers are getting smaller. Snow cover is retreating earlier in the spring. Sea ice in the Arctic is shrinking in all seasons, most dramatically in summer. Reductions are reported in permafrost, seasonally frozen ground and river and lake ice. Important coastal regions of the ice sheets on Greenland and West Antarctica, and the glaciers of the Antarctic Peninsula, are thinning and contributing to sea level rise. The total contribution of glacier, ice cap and ice sheet melt to sea level rise is estimated as $1.2 \pm 0.4 \text{ mm yr}^{-1}$ for the period 1993 to 2003.

Continuous satellite measurements capture most of the Earth's seasonal snow cover on land, and reveal that Northern Hemisphere spring snow cover has declined by about 2% per decade since 1966, although there is little change in autumn or early winter. In many places, the spring decrease has occurred despite increases in precipitation.

Satellite data do not yet allow similarly reliable measurement of ice conditions on lakes and rivers, or in seasonally or permanently frozen ground. However, numerous local and regional reports have been published, and generally seem to indicate warming of permafrost, an increase in thickness of the summer thawed layer over permafrost, a decrease in winter freeze depth in seasonally frozen areas, a decrease in areal extent of permafrost and a decrease in duration of seasonal river and lake ice.

Since 1978, satellite data have provided continuous coverage of sea ice extent in both polar regions. For the Arctic, average annual sea ice extent has decreased by $2.7 \pm 0.6\%$ per decade, while summer sea ice extent has decreased by $7.4 \pm 2.4\%$ per decade. The antarctic sea ice extent exhibits no significant trend. Thickness data, especially from submarines, are available but restricted to the central Arctic, where they indicate thinning of approximately 40% between the period 1958 to 1977 and the 1990s. This is likely an overestimate of the thinning over the entire arctic region however.

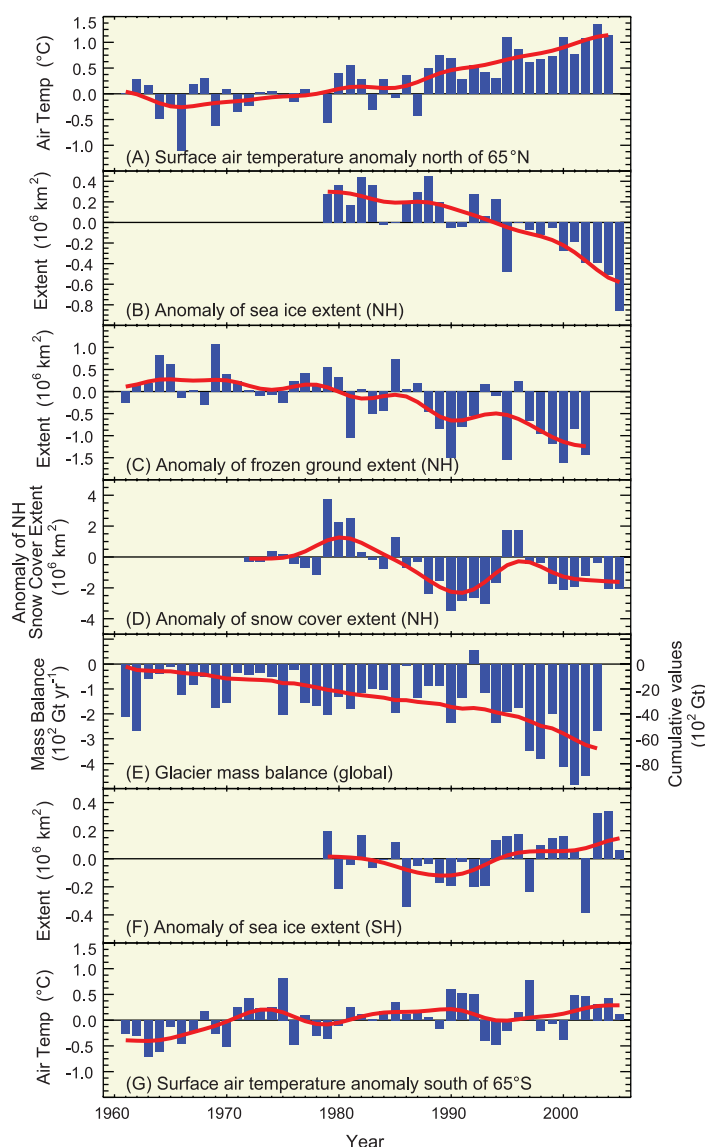
Most mountain glaciers and ice caps have been shrinking, with the retreat probably having started about 1850. Although many Northern Hemisphere glaciers had a few years of near-balance around 1970, this was followed by increased shrinkage. Melting of glaciers and ice caps contributed $0.77 \pm 0.22 \text{ mm yr}^{-1}$ to sea level rise between 1991 and 2004

Taken together, the ice sheets of Greenland and Antarctica are very likely shrinking, with Greenland contributing about $0.2 \pm 0.1 \text{ mm yr}^{-1}$ and Antarctica contributing $0.2 \pm 0.35 \text{ mm yr}^{-1}$ to sea level rise over the period 1993 to 2003. There is evidence of accelerated loss through 2005. Thickening of high-altitude, cold regions of Greenland and East Antarctica, perhaps from increased snowfall, has been more than offset by thinning in

coastal regions of Greenland and West Antarctica in response to increased ice outflow and increased Greenland surface melting.

Ice interacts with the surrounding climate in complex ways, so the causes of specific changes are not always clear. Nonetheless, it is an unavoidable fact that ice melts when the local temperature is

(continued)



FAQ 4.1, Figure 1. Anomaly time series (departure from the long-term mean) of polar surface air temperature (A, G), arctic and antarctic sea ice extent (B, F), Northern Hemisphere (NH) frozen ground extent (C), NH snow cover extent (D) and global glacier mass balance (E). The solid red line in E denotes the cumulative global glacier mass balance; in the other panels it shows decadal variations (see Appendix 3.A).

above the freezing point. Reductions in snow cover and in mountain glaciers have occurred despite increased snowfall in many cases, implicating increased air temperatures. Similarly, although snow cover changes affect frozen ground and lake and river ice, this does not seem sufficient to explain the observed changes, suggesting that increased local air temperatures have been important. Observed arctic sea ice reductions can be simulated fairly well in

models driven by historical circulation and temperature changes. The observed increases in snowfall on ice sheets in some cold central regions, surface melting in coastal regions and sub-ice-shelf melting along many coasts are all consistent with warming. The geographically widespread nature of these snow and ice changes suggests that widespread warming is the cause of the Earth's overall loss of ice.

Frequently Asked Question 5.1

Is Sea Level Rising?

Yes, there is strong evidence that global sea level gradually rose in the 20th century and is currently rising at an increased rate, after a period of little change between AD 0 and AD 1900. Sea level is projected to rise at an even greater rate in this century. The two major causes of global sea level rise are thermal expansion of the oceans (water expands as it warms) and the loss of land-based ice due to increased melting.

Global sea level rose by about 120 m during the several millennia that followed the end of the last ice age (approximately 21,000 years ago), and stabilised between 3,000 and 2,000 years ago. Sea level indicators suggest that global sea level did not change significantly from then until the late 19th century. The instrumental record of modern sea level change shows evidence for onset of sea level rise during the 19th century. Estimates for the 20th century show that global average sea level rose at a rate of about 1.7 mm yr⁻¹.

Satellite observations available since the early 1990s provide more accurate sea level data with nearly global coverage. This decade-long satellite altimetry data set shows that since 1993, sea level has been rising at a rate of around 3 mm yr⁻¹, significantly higher than the average during the previous half century. Coastal tide gauge measurements confirm this observation, and indicate that similar rates have occurred in some earlier decades.

In agreement with climate models, satellite data and hydrographic observations show that sea level is not rising uniformly around the world. In some regions, rates are up to several times the global mean rise, while in other regions sea level is falling. Substantial spatial variation in rates of sea level change is also inferred from hydrographic observations. Spatial variability of the rates of sea level rise is mostly due to non-uniform changes in temperature and salinity and related to changes in the ocean circulation.

Near-global ocean temperature data sets made available in recent years allow a direct calculation of thermal expansion. It is believed that on average, over the period from 1961 to 2003, thermal expansion contributed about one-quarter of the observed sea level rise, while melting of land ice accounted for less than half. Thus, the full magnitude of the observed sea level rise during that period was not satisfactorily explained by those data sets, as reported in the IPCC Third Assessment Report.

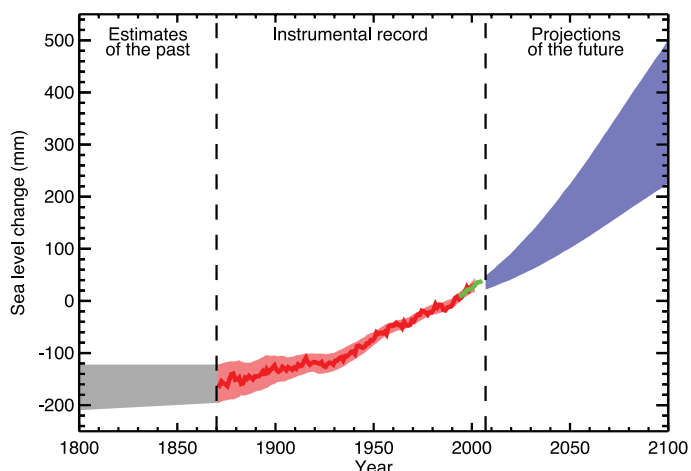
During recent years (1993–2003), for which the observing system is much better, thermal expansion and melting of land ice each account for about half of the observed sea level rise, although there is some uncertainty in the estimates.

The reasonable agreement in recent years between the observed rate of sea level rise and the sum of thermal expansion and loss of land ice suggests an upper limit for the magnitude of change in land-based water storage, which is relatively poorly known. Model results suggest no net trend in the storage of water over land due to climate-driven changes but there are large interannual and decadal fluctuations. However, for the recent period 1993 to 2003,

the small discrepancy between observed sea level rise and the sum of known contributions might be due to unquantified human-induced processes (e.g., groundwater extraction, impoundment in reservoirs, wetland drainage and deforestation).

Global sea level is projected to rise during the 21st century at a greater rate than during 1961 to 2003. Under the IPCC Special Report on Emission Scenarios (SRES) A1B scenario by the mid-2090s, for instance, global sea level reaches 0.22 to 0.44 m above 1990 levels, and is rising at about 4 mm yr⁻¹. As in the past, sea level change in the future will not be geographically uniform, with regional sea level change varying within about ±0.15 m of the mean in a typical model projection. Thermal expansion is projected to contribute more than half of the average rise, but land ice will lose mass increasingly rapidly as the century progresses. An important uncertainty relates to whether discharge of ice from the ice sheets will continue to increase as a consequence of accelerated ice flow, as has been observed in recent years. This would add to the amount of sea level rise, but quantitative projections of how much it would add cannot be made with confidence, owing to limited understanding of the relevant processes.

Figure 1 shows the evolution of global mean sea level in the past and as projected for the 21st century for the SRES A1B scenario.



FAQ 5.1, Figure 1. Time series of global mean sea level (deviation from the 1980–1999 mean) in the past and as projected for the future. For the period before 1870, global measurements of sea level are not available. The grey shading shows the uncertainty in the estimated long-term rate of sea level change (Section 6.4.3). The red line is a reconstruction of global mean sea level from tide gauges (Section 5.5.2.1), and the red shading denotes the range of variations from a smooth curve. The green line shows global mean sea level observed from satellite altimetry. The blue shading represents the range of model projections for the SRES A1B scenario for the 21st century, relative to the 1980 to 1999 mean, and has been calculated independently from the observations. Beyond 2100, the projections are increasingly dependent on the emissions scenario (see Chapter 10 for a discussion of sea level rise projections for other scenarios considered in this report). Over many centuries or millennia, sea level could rise by several metres (Section 10.7.4).

Frequently Asked Question 6.1

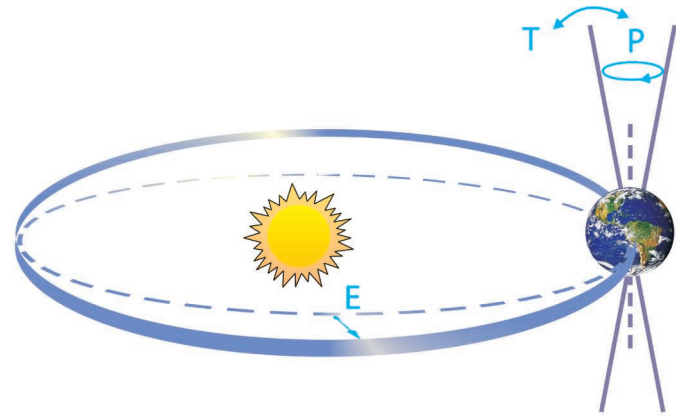
What Caused the Ice Ages and Other Important Climate Changes Before the Industrial Era?

Climate on Earth has changed on all time scales, including long before human activity could have played a role. Great progress has been made in understanding the causes and mechanisms of these climate changes. Changes in Earth's radiation balance were the principal driver of past climate changes, but the causes of such changes are varied. For each case – be it the Ice Ages, the warmth at the time of the dinosaurs or the fluctuations of the past millennium – the specific causes must be established individually. In many cases, this can now be done with good confidence, and many past climate changes can be reproduced with quantitative models.

Global climate is determined by the radiation balance of the planet (see FAQ 1.1). There are three fundamental ways the Earth's radiation balance can change, thereby causing a climate change: (1) changing the incoming solar radiation (e.g., by changes in the Earth's orbit or in the Sun itself), (2) changing the fraction of solar radiation that is reflected (this fraction is called the albedo – it can be changed, for example, by changes in cloud cover, small particles called aerosols or land cover), and (3) altering the long-wave energy radiated back to space (e.g., by changes in greenhouse gas concentrations). In addition, local climate also depends on how heat is distributed by winds and ocean currents. All of these factors have played a role in past climate changes.

Starting with the ice ages that have come and gone in regular cycles for the past nearly three million years, there is strong evidence that these are linked to regular variations in the Earth's orbit around the Sun, the so-called Milankovitch cycles (Figure 1). These cycles change the amount of solar radiation received at each latitude in each season (but hardly affect the global annual mean), and they can be calculated with astronomical precision. There is still some discussion about how exactly this starts and ends ice ages, but many studies suggest that the amount of summer sunshine on northern continents is crucial: if it drops below a critical value, snow from the past winter does not melt away in summer and an ice sheet starts to grow as more and more snow accumulates. Climate model simulations confirm that an Ice Age can indeed be started in this way, while simple conceptual models have been used to successfully 'hindcast' the onset of past glaciations based on the orbital changes. The next large reduction in northern summer insolation, similar to those that started past Ice Ages, is due to begin in 30,000 years.

Although it is not their primary cause, atmospheric carbon dioxide (CO₂) also plays an important role in the ice ages. Antarctic ice core data show that CO₂ concentration is low in the cold glacial times (~190 ppm), and high in the warm interglacials (~280 ppm); atmospheric CO₂ follows temperature changes in Antarctica with a lag of some hundreds of years. Because the climate changes at the beginning and end of ice ages take several thousand years,



FAQ 6.1, Figure 1. Schematic of the Earth's orbital changes (Milankovitch cycles) that drive the ice age cycles. 'T' denotes changes in the tilt (or obliquity) of the Earth's axis, 'E' denotes changes in the eccentricity of the orbit (due to variations in the minor axis of the ellipse), and 'P' denotes precession, that is, changes in the direction of the axis tilt at a given point of the orbit. Source: Rahmstorf and Schellnhuber (2006).

most of these changes are affected by a positive CO₂ feedback; that is, a small initial cooling due to the Milankovitch cycles is subsequently amplified as the CO₂ concentration falls. Model simulations of ice age climate (see discussion in Section 6.4.1) yield realistic results only if the role of CO₂ is accounted for.

During the last ice age, over 20 abrupt and dramatic climate shifts occurred that are particularly prominent in records around the northern Atlantic (see Section 6.4). These differ from the glacial-interglacial cycles in that they probably do not involve large changes in global mean temperature: changes are not synchronous in Greenland and Antarctica, and they are in the opposite direction in the South and North Atlantic. This means that a major change in global radiation balance would not have been needed to cause these shifts; a redistribution of heat within the climate system would have sufficed. There is indeed strong evidence that changes in ocean circulation and heat transport can explain many features of these abrupt events; sediment data and model simulations show that some of these changes could have been triggered by instabilities in the ice sheets surrounding the Atlantic at the time, and the associated freshwater release into the ocean.

Much warmer times have also occurred in climate history – during most of the past 500 million years, Earth was probably completely free of ice sheets (geologists can tell from the marks ice leaves on rock), unlike today, when Greenland and Antarctica are ice-covered. Data on greenhouse gas abundances going back beyond a million years, that is, beyond the reach of antarctic ice cores, are still rather uncertain, but analysis of geological

(continued)

samples suggests that the warm ice-free periods coincide with high atmospheric CO₂ levels. On million-year time scales, CO₂ levels change due to tectonic activity, which affects the rates of CO₂ exchange of ocean and atmosphere with the solid Earth. See Section 6.3 for more about these ancient climates.

Another likely cause of past climatic changes is variations in the energy output of the Sun. Measurements over recent decades show that the solar output varies slightly (by close to 0.1%) in an 11-year cycle. Sunspot observations (going back to the 17th century), as well as data from isotopes generated by cosmic radiation, provide evidence for longer-term changes in solar activity. Data correlation and model simulations indicate that solar variability

and volcanic activity are likely to be leading reasons for climate variations during the past millennium, before the start of the industrial era.

These examples illustrate that different climate changes in the past had different causes. The fact that natural factors caused climate changes in the past does not mean that the current climate change is natural. By analogy, the fact that forest fires have long been caused naturally by lightning strikes does not mean that fires cannot also be caused by a careless camper. FAQ 2.1 addresses the question of how human influences compare with natural ones in their contributions to recent climate change.

Frequently Asked Question 6.2

Is the Current Climate Change Unusual Compared to Earlier Changes in Earth's History?

Climate has changed on all time scales throughout Earth's history. Some aspects of the current climate change are not unusual, but others are. The concentration of CO₂ in the atmosphere has reached a record high relative to more than the past half-million years, and has done so at an exceptionally fast rate. Current global temperatures are warmer than they have ever been during at least the past five centuries, probably even for more than a millennium. If warming continues unabated, the resulting climate change within this century would be extremely unusual in geological terms. Another unusual aspect of recent climate change is its cause: past climate changes were natural in origin (see FAQ 6.1), whereas most of the warming of the past 50 years is attributable to human activities.

When comparing the current climate change to earlier, natural ones, three distinctions must be made. First, it must be clear which variable is being compared: is it greenhouse gas concentration or temperature (or some other climate parameter), and is it their absolute value or their rate of change? Second, local changes must not be confused with global changes. Local climate changes are often much larger than global ones, since local factors (e.g., changes in oceanic or atmospheric circulation) can shift the delivery of heat or moisture from one place to another and local feedbacks operate (e.g., sea ice feedback). Large changes in global mean temperature, in contrast, require some global forcing (such as a change in greenhouse gas concentration or solar activity). Third, it is necessary to distinguish between time scales. Climate changes over millions of years can be much larger and have different causes (e.g., continental drift) compared to climate changes on a centennial time scale.

The main reason for the current concern about climate change is the rise in atmospheric carbon dioxide (CO₂) concentration (and some other greenhouse gases), which is very unusual for the Quaternary (about the last two million years). The concentration of CO₂ is now known accurately for the past 650,000 years from antarctic ice cores. During this time, CO₂ concentration varied between a low of 180 ppm during cold glacial times and a high of 300 ppm during warm interglacials. Over the past century, it rapidly increased well out of this range, and is now 379 ppm (see Chapter 2). For comparison, the approximately 80-ppm rise in CO₂ concentration at the end of the past ice ages generally took over 5,000 years. Higher values than at present have only occurred many millions of years ago (see FAQ 6.1).

Temperature is a more difficult variable to reconstruct than CO₂ (a globally well-mixed gas), as it does not have the same value all over the globe, so that a single record (e.g., an ice core) is only of limited value. Local temperature fluctuations, even those over just a few decades, can be several degrees celsius, which is larger than the global warming signal of the past century of about 0.7°C.

More meaningful for global changes is an analysis of large-scale (global or hemispheric) averages, where much of the local varia-

tion averages out and variability is smaller. Sufficient coverage of instrumental records goes back only about 150 years. Further back in time, compilations of proxy data from tree rings, ice cores, etc., go back more than a thousand years with decreasing spatial coverage for earlier periods (see Section 6.5). While there are differences among those reconstructions and significant uncertainties remain, all published reconstructions find that temperatures were warm during medieval times, cooled to low values in the 17th, 18th and 19th centuries, and warmed rapidly after that. The medieval level of warmth is uncertain, but may have been reached again in the mid-20th century, only to have likely been exceeded since then. These conclusions are supported by climate modelling as well. Before 2,000 years ago, temperature variations have not been systematically compiled into large-scale averages, but they do not provide evidence for warmer-than-present global annual mean temperatures going back through the Holocene (the last 11,600 years; see Section 6.4). There are strong indications that a warmer climate, with greatly reduced global ice cover and higher sea level, prevailed until around 3 million years ago. Hence, current warmth appears unusual in the context of the past millennia, but not unusual on longer time scales for which changes in tectonic activity (which can drive natural, slow variations in greenhouse gas concentration) become relevant (see Box 6.1).

A different matter is the current rate of warming. Are more rapid global climate changes recorded in proxy data? The largest temperature changes of the past million years are the glacial cycles, during which the global mean temperature changed by 4°C to 7°C between ice ages and warm interglacial periods (local changes were much larger, for example near the continental ice sheets). However, the data indicate that the global warming at the end of an ice age was a gradual process taking about 5,000 years (see Section 6.3). It is thus clear that the current rate of global climate change is much more rapid and very unusual in the context of past changes. The much-discussed abrupt climate shifts during glacial times (see Section 6.3) are not counter-examples, since they were probably due to changes in ocean heat transport, which would be unlikely to affect the global mean temperature.

Further back in time, beyond ice core data, the time resolution of sediment cores and other archives does not resolve changes as rapid as the present warming. Hence, although large climate changes have occurred in the past, there is no evidence that these took place at a faster rate than present warming. If projections of approximately 5°C warming in this century (the upper end of the range) are realised, then the Earth will have experienced about the same amount of global mean warming as it did at the end of the last ice age; there is no evidence that this rate of possible future global change was matched by any comparable global temperature increase of the last 50 million years.

Frequently Asked Question 7.1

Are the Increases in Atmospheric Carbon Dioxide and Other Greenhouse Gases During the Industrial Era Caused by Human Activities?

Yes, the increases in atmospheric carbon dioxide (CO₂) and other greenhouse gases during the industrial era are caused by human activities. In fact, the observed increase in atmospheric CO₂ concentrations does not reveal the full extent of human emissions in that it accounts for only 55% of the CO₂ released by human activity since 1959. The rest has been taken up by plants on land and by the oceans. In all cases, atmospheric concentrations of greenhouse gases, and their increases, are determined by the balance between sources (emissions of the gas from human activities and natural systems) and sinks (the removal of the gas from the atmosphere by conversion to a different chemical compound). Fossil fuel combustion (plus a smaller contribution from cement manufacture) is responsible for more than 75% of human-caused CO₂ emissions. Land use change (primarily deforestation) is responsible for the remainder. For methane, another important greenhouse gas, emissions generated by human activities exceeded natural emissions over the last 25 years. For nitrous oxide, emissions generated by human activities are equal to natural emissions to the atmosphere. Most of the long-lived halogen-containing gases (such as chlorofluorocarbons) are manufactured by humans, and were not present in the atmosphere before the industrial era. On average, present-day tropospheric ozone has increased 38% since pre-industrial times, and the increase results from atmospheric reactions of short-lived pollutants emitted by human activity. The concentration of CO₂ is now 379 parts per million (ppm) and methane is greater than 1,774 parts per billion (ppb), both very likely much higher than any time in at least 650 kyr (during which CO₂ remained between 180 and 300 ppm and methane between 320 and 790 ppb). The recent rate of change is dramatic and unprecedented; increases in CO₂ never exceeded 30 ppm in 1 kyr – yet now CO₂ has risen by 30 ppm in just the last 17 years.

Carbon Dioxide

Emissions of CO₂ (Figure 1a) from fossil fuel combustion, with contributions from cement manufacture, are responsible for more than 75% of the increase in atmospheric CO₂ concentration since pre-industrial times. The remainder of the increase comes from land use changes dominated by deforestation (and associated biomass burning) with contributions from changing agricultural practices. All these increases are caused by human activity. The natural carbon cycle cannot explain the observed atmospheric increase of 3.2 to 4.1 GtC yr⁻¹ in the form of CO₂ over the last 25 years. (One GtC equals 10¹⁵ grams of carbon, i.e., one billion tonnes.)

Natural processes such as photosynthesis, respiration, decay and sea surface gas exchange lead to massive exchanges, sources and sinks of CO₂ between the land and atmosphere (estimated at

~120 GtC yr⁻¹) and the ocean and atmosphere (estimated at ~90 GtC yr⁻¹; see figure 7.3). The natural sinks of carbon produce a small net uptake of CO₂ of approximately 3.3 GtC yr⁻¹ over the last 15 years, partially offsetting the human-caused emissions. Were it not for the natural sinks taking up nearly half the human-produced CO₂ over the past 15 years, atmospheric concentrations would have grown even more dramatically.

The increase in atmospheric CO₂ concentration is known to be caused by human activities because the character of CO₂ in the atmosphere, in particular the ratio of its heavy to light carbon atoms, has changed in a way that can be attributed to addition of fossil fuel carbon. In addition, the ratio of oxygen to nitrogen in the atmosphere has declined as CO₂ has increased; this is as expected because oxygen is depleted when fossil fuels are burned. A heavy form of carbon, the carbon-13 isotope, is less abundant in vegetation and in fossil fuels that were formed from past vegetation, and is more abundant in carbon in the oceans and in volcanic or geothermal emissions. The relative amount of the carbon-13 isotope in the atmosphere has been declining, showing that the added carbon comes from fossil fuels and vegetation. Carbon also has a rare radioactive isotope, carbon-14, which is present in atmospheric CO₂ but absent in fossil fuels. Prior to atmospheric testing of nuclear weapons, decreases in the relative amount of carbon-14 showed that fossil fuel carbon was being added to the atmosphere.

Halogen-Containing Gases

Human activities are responsible for the bulk of long-lived atmospheric halogen-containing gas concentrations. Before industrialisation, there were only a few naturally occurring halogen-containing gases, for example, methyl bromide and methyl chloride. The development of new techniques for chemical synthesis resulted in a proliferation of chemically manufactured halogen-containing gases during the last 50 years of the 20th century. Emissions of key halogen-containing gases produced by humans are shown in Figure 1b. Atmospheric lifetimes range from 45 to 100 years for the chlorofluorocarbons (CFCs) plotted here, from 1 to 18 years for the hydrochlorofluorocarbons (HCFCs), and from 1 to 270 years for the hydrofluorocarbons (HFCs). The perfluorocarbons (PFCs, not plotted) persist in the atmosphere for thousands of years. Concentrations of several important halogen-containing gases, including CFCs, are now stabilising or decreasing at the Earth's surface as a result of the Montreal Protocol on Substances that Deplete the Ozone Layer and its Amendments. Concentrations of HCFCs, production of which is to be phased out by 2030, and of the Kyoto Protocol gases HFCs and PFCs, are currently increasing. *(continued)*

Methane

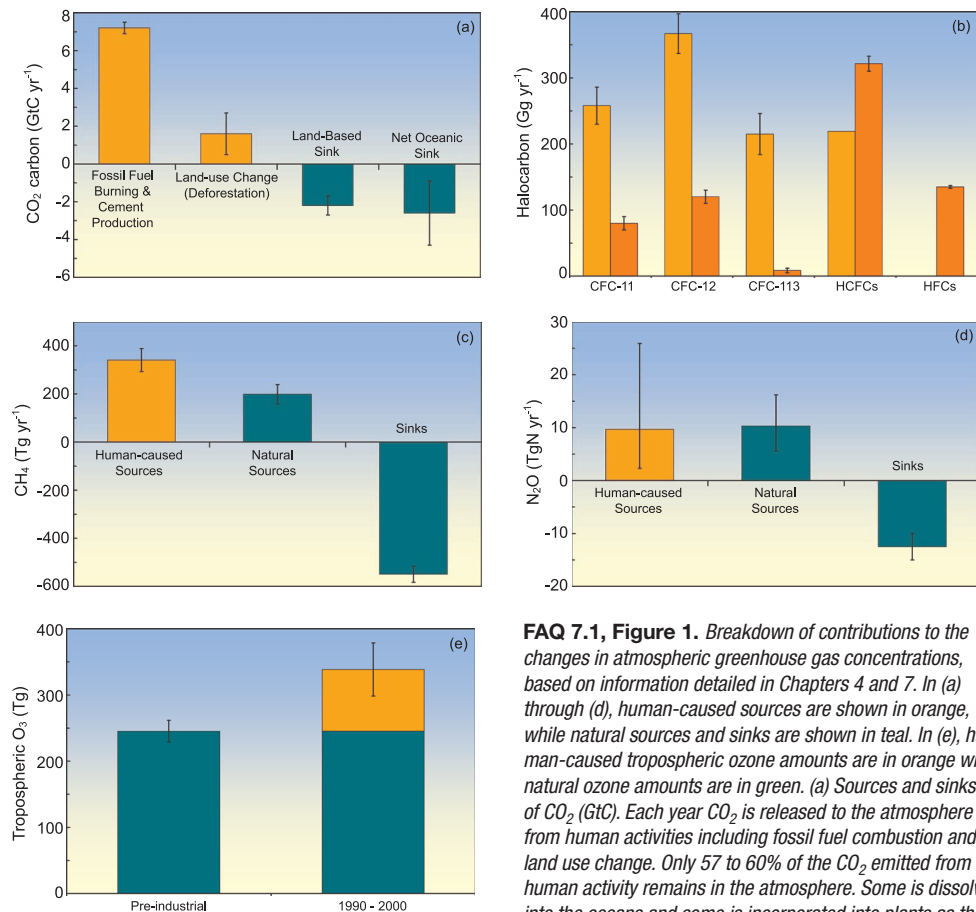
Methane (CH_4) sources to the atmosphere generated by human activities exceed CH_4 sources from natural systems (Figure 1c). Between 1960 and 1999, CH_4 concentrations grew an average of at least six times faster than over any 40-year period of the two millennia before 1800, despite a near-zero growth rate since 1980. The main natural source of CH_4 to the atmosphere is wetlands. Additional natural sources include termites, oceans, vegetation and CH_4 hydrates. The human activities that produce CH_4 include energy production from coal and natural gas, waste disposal in landfills, raising ruminant animals (e.g., cattle and sheep), rice agriculture and biomass burning. Once emitted, CH_4 remains in the atmosphere for approximately 8.4 years before removal, mainly by chemical oxidation in the troposphere. Minor sinks for CH_4 include uptake by soils and eventual destruction in the stratosphere.

Nitrous Oxide

Nitrous oxide (N_2O) sources to the atmosphere from human activities are approximately equal to N_2O sources from natural systems (Figure 1d). Between 1960 and 1999, N_2O concentrations grew an average of at least two times faster than over any 40-year period of the two millennia before 1800. Natural sources of N_2O include oceans, chemical oxidation of ammonia in the atmosphere, and soils. Tropical soils are a particularly important source of N_2O to the atmosphere. Human activities that emit N_2O include transformation of fertilizer nitrogen into N_2O and its subsequent emission from agricultural soils, biomass burning, raising cattle and some industrial activities, including nylon manufacture. Once emitted, N_2O remains in the atmosphere for approximately 114 years before removal, mainly by destruction in the stratosphere.

Tropospheric Ozone

Tropospheric ozone is produced by photochemical reactions in the atmosphere involving forerunner chemicals such as carbon monoxide, CH_4 , volatile organic compounds and nitrogen oxides. These chemicals are emitted by natural biological processes and by human activities including land use change and fuel combustion. Because tropospheric ozone is relatively short-lived, lasting for a few days to weeks in the atmosphere, its distributions are highly variable and tied to the abundance of its forerunner compounds, water vapour and sunlight.



FAQ 7.1, Figure 1. Breakdown of contributions to the changes in atmospheric greenhouse gas concentrations, based on information detailed in Chapters 4 and 7. In (a) through (d), human-caused sources are shown in orange, while natural sources and sinks are shown in teal. In (e), human-caused tropospheric ozone amounts are in orange while natural ozone amounts are in green. (a) Sources and sinks of CO_2 (GtC). Each year CO_2 is released to the atmosphere from human activities including fossil fuel combustion and land use change. Only 57 to 60% of the CO_2 emitted from human activity remains in the atmosphere. Some is dissolved into the oceans and some is incorporated into plants as they grow. Land-related fluxes are for the 1990s; fossil fuel and cement fluxes and net ocean uptake are for the period 2000 to 2005. All values and uncertainty ranges are from Table 7.1. (b) Global emissions of CFCs and other halogen-containing compounds for 1990 (light orange) and 2002 (dark orange). These chemicals are exclusively human-produced. Here, 'HCFCs' comprise HCFC-22, -141b and -142b, while 'HFCs' comprise HFC-23, -125, -134a and -152a. One Gg = 10^9 g (1,000 tonnes). Most data are from reports listed in Chapter 2. (c) Sources and sinks of CH_4 for the period 1983 to 2004. Human-caused sources of CH_4 include energy production, landfills, ruminant animals (e.g., cattle and sheep), rice agriculture and biomass burning. One Tg = 10^{12} g (1 million tonnes). Values and uncertainties are the means and standard deviations for CH_4 of the corresponding aggregate values from Table 7.6. (d) Sources and sinks of N_2O . Human-caused sources of N_2O include the transformation of fertilizer nitrogen into N_2O and its subsequent emission from agricultural soils, biomass burning, cattle and some industrial activities including nylon manufacture. Source values and uncertainties are the midpoints and range limits from Table 7.7. N_2O losses are from Chapter 7.4. (e) Tropospheric ozone in the 19th and early 20th centuries and the 1990 to 2000 period. The increase in tropospheric ozone formation is human-induced, resulting from atmospheric chemical reactions of pollutants emitted by burning of fossil fuels or biofuels. The pre-industrial value and uncertainty range are from Table 4.9 of the IPCC Third Assessment Report (TAR), estimated from reconstructed observations. The present-day total and its uncertainty range are the average and standard deviation of model results quoted in Table 7.9 of this report, excluding those from the TAR.

Tropospheric ozone concentrations are significantly higher in urban air, downwind of urban areas and in regions of biomass burning. The increase of 38% (20–50%) in tropospheric ozone since the pre-industrial era (Figure 1e) is human-caused.

It is very likely that the increase in the combined radiative forcing from CO_2 , CH_4 and N_2O was at least six times faster between 1960 and 1999 than over any 40-year period during the two millennia prior to the year 1800.

Frequently Asked Question 8.1

How Reliable Are the Models Used to Make Projections of Future Climate Change?

There is considerable confidence that climate models provide credible quantitative estimates of future climate change, particularly at continental scales and above. This confidence comes from the foundation of the models in accepted physical principles and from their ability to reproduce observed features of current climate and past climate changes. Confidence in model estimates is higher for some climate variables (e.g., temperature) than for others (e.g., precipitation). Over several decades of development, models have consistently provided a robust and unambiguous picture of significant climate warming in response to increasing greenhouse gases.

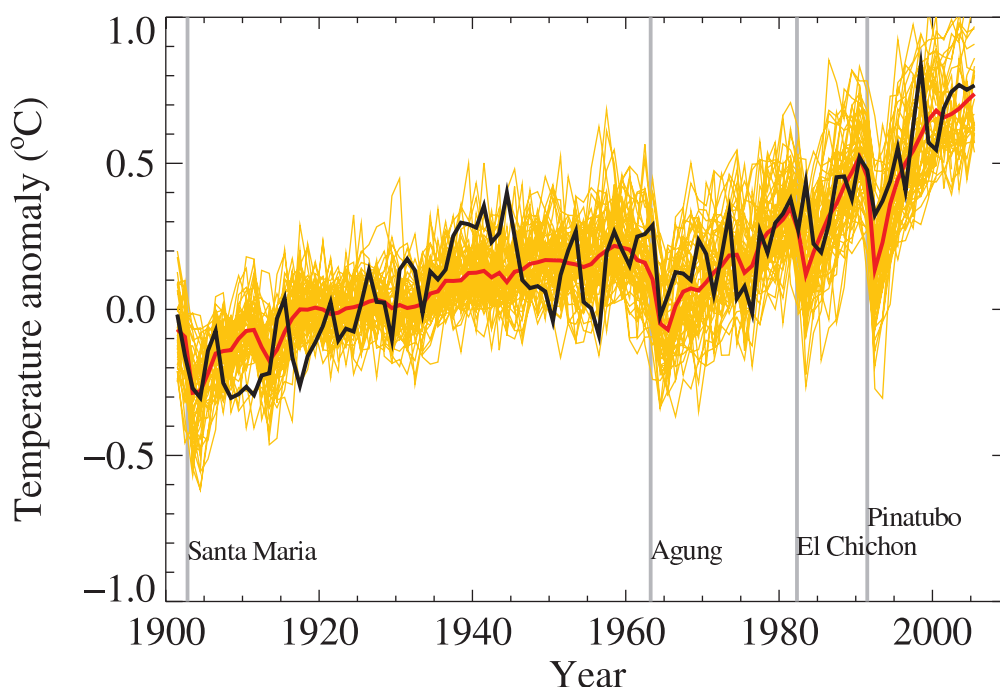
Climate models are mathematical representations of the climate system, expressed as computer codes and run on powerful computers. One source of confidence in models comes from the fact that model fundamentals are based on established physical laws, such as conservation of mass, energy and momentum, along with a wealth of observations.

A second source of confidence comes from the ability of models to simulate important aspects of the current climate. Models are routinely and extensively assessed by comparing their simulations with observations of the atmosphere, ocean, cryosphere and land surface. Unprecedented levels of evaluation have taken place over the last decade in the form of organised multi-model ‘intercomparisons’. Models show significant and

increasing skill in representing many important mean climate features, such as the large-scale distributions of atmospheric temperature, precipitation, radiation and wind, and of oceanic temperatures, currents and sea ice cover. Models can also simulate essential aspects of many of the patterns of climate variability observed across a range of time scales. Examples include the advance and retreat of the major monsoon systems, the seasonal shifts of temperatures, storm tracks and rain belts, and the hemispheric-scale seesawing of extratropical surface pressures (the Northern and Southern ‘annular modes’). Some climate models, or closely related variants, have also been tested by using them to predict weather and make seasonal forecasts. These models demonstrate skill in such forecasts, showing they can represent important features of the general circulation across shorter time scales, as well as aspects of seasonal and interannual variability. Models’ ability to represent these and other important climate features increases our confidence that they represent the essential physical processes important for the simulation of future climate change. (Note that the limitations in climate models’ ability to forecast weather beyond a few days do not limit their ability to predict long-term climate changes, as these are very different types of prediction – see FAQ 1.2.)

(continued)

FAQ 8.1, Figure 1. Global mean near-surface temperatures over the 20th century from observations (black) and as obtained from 58 simulations produced by 14 different climate models driven by both natural and human-caused factors that influence climate (yellow). The mean of all these runs is also shown (thick red line). Temperature anomalies are shown relative to the 1901 to 1950 mean. Vertical grey lines indicate the timing of major volcanic eruptions. (Figure adapted from Chapter 9, Figure 9.5. Refer to corresponding caption for further details.)



A third source of confidence comes from the ability of models to reproduce features of past climates and climate changes. Models have been used to simulate ancient climates, such as the warm mid-Holocene of 6,000 years ago or the last glacial maximum of 21,000 years ago (see Chapter 6). They can reproduce many features (allowing for uncertainties in reconstructing past climates) such as the magnitude and broad-scale pattern of oceanic cooling during the last ice age. Models can also simulate many observed aspects of climate change over the instrumental record. One example is that the global temperature trend over the past century (shown in Figure 1) can be modelled with high skill when both human and natural factors that influence climate are included. Models also reproduce other observed changes, such as the faster increase in nighttime than in daytime temperatures, the larger degree of warming in the Arctic and the small, short-term global cooling (and subsequent recovery) which has followed major volcanic eruptions, such as that of Mt. Pinatubo in 1991 (see FAQ 8.1, Figure 1). Model global temperature projections made over the last two decades have also been in overall agreement with subsequent observations over that period (Chapter 1).

Nevertheless, models still show significant errors. Although these are generally greater at smaller scales, important large-scale problems also remain. For example, deficiencies remain in the simulation of tropical precipitation, the El Niño-Southern Oscillation and the Madden-Julian Oscillation (an observed variation in tropical winds and rainfall with a time scale of 30 to 90 days). The ultimate source of most such errors is that many important small-scale processes cannot be represented explicitly in models, and so must be included in approximate form as they interact with larger-scale features. This is partly due to limitations in computing power, but also results from limitations in scientific understanding or in the availability of detailed observations of some physical processes. Significant uncertainties, in particular, are associated with the representation of clouds, and in the resulting cloud responses to climate change. Consequently, models continue to display a substantial range of global temperature change in response to specified greenhouse gas forcing (see Chapter 10). Despite such uncertainties, however, models are unanimous in their predic-

tion of substantial climate warming under greenhouse gas increases, and this warming is of a magnitude consistent with independent estimates derived from other sources, such as from observed climate changes and past climate reconstructions.

Since confidence in the changes projected by global models decreases at smaller scales, other techniques, such as the use of regional climate models, or downscaling methods, have been specifically developed for the study of regional- and local-scale climate change (see FAQ 11.1). However, as global models continue to develop, and their resolution continues to improve, they are becoming increasingly useful for investigating important smaller-scale features, such as changes in extreme weather events, and further improvements in regional-scale representation are expected with increased computing power. Models are also becoming more comprehensive in their treatment of the climate system, thus explicitly representing more physical and biophysical processes and interactions considered potentially important for climate change, particularly at longer time scales. Examples are the recent inclusion of plant responses, ocean biological and chemical interactions, and ice sheet dynamics in some global climate models.

In summary, confidence in models comes from their physical basis, and their skill in representing observed climate and past climate changes. Models have proven to be extremely important tools for simulating and understanding climate, and there is considerable confidence that they are able to provide credible quantitative estimates of future climate change, particularly at larger scales. Models continue to have significant limitations, such as in their representation of clouds, which lead to uncertainties in the magnitude and timing, as well as regional details, of predicted climate change. Nevertheless, over several decades of model development, they have consistently provided a robust and unambiguous picture of significant climate warming in response to increasing greenhouse gases.

Frequently Asked Question 9.1

Can Individual Extreme Events be Explained by Greenhouse Warming?

Changes in climate extremes are expected as the climate warms in response to increasing atmospheric greenhouse gases resulting from human activities, such as the use of fossil fuels. However, determining whether a specific, single extreme event is due to a specific cause, such as increasing greenhouse gases, is difficult, if not impossible, for two reasons: 1) extreme events are usually caused by a combination of factors and 2) a wide range of extreme events is a normal occurrence even in an unchanging climate. Nevertheless, analysis of the warming observed over the past century suggests that the likelihood of some extreme events, such as heat waves, has increased due to greenhouse warming, and that the likelihood of others, such as frost or extremely cold nights, has decreased. For example, a recent study estimates that human influences have more than doubled the risk of a very hot European summer like that of 2003.

People affected by an extreme weather event often ask whether human influences on the climate could be held to some extent responsible. Recent years have seen many extreme events that some commentators have linked to increasing greenhouse gases. These include the prolonged drought in Australia, the extremely hot summer in Europe in 2003 (see Figure 1), the intense North Atlantic hurricane seasons of 2004 and 2005 and the extreme rainfall events in Mumbai, India in July 2005. Could a human influence such as increased concentrations of greenhouse gases in the atmosphere have ‘caused’ any of these events?

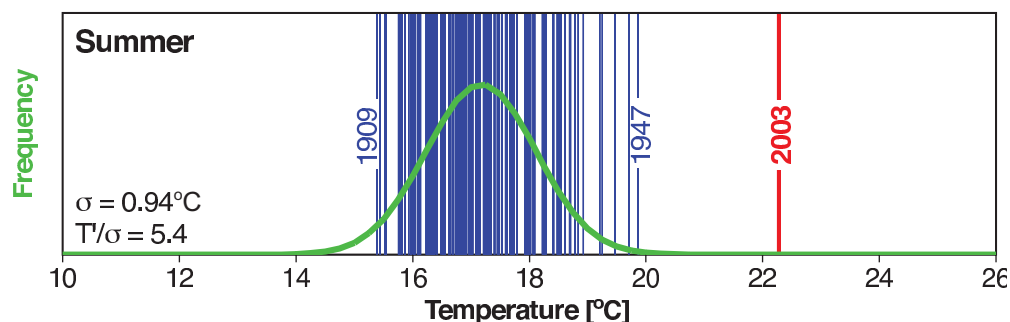
Extreme events usually result from a combination of factors. For example, several factors contributed to the extremely hot European summer of 2003, including a persistent high-pressure system that was associated with very clear skies and dry soil, which left more solar energy available to heat the land because less energy was consumed to evaporate moisture from the soil. Similarly, the formation of a hurricane requires warm sea surface temperatures and specific atmospheric circulation conditions. Because some factors may be strongly affected by human activities, such as sea surface temperatures, but others may not, it is not simple to detect a human influence on a single, specific extreme event.

Nevertheless, it may be possible to use climate models to determine whether human influences have changed the likelihood of certain types of extreme

events. For example, in the case of the 2003 European heat wave, a climate model was run including only historical changes in natural factors that affect the climate, such as volcanic activity and changes in solar output. Next, the model was run again including both human and natural factors, which produced a simulation of the evolution of the European climate that was much closer to that which had actually occurred. Based on these experiments, it was estimated that over the 20th century, human influences more than doubled the risk of having a summer in Europe as hot as that of 2003, and that in the absence of human influences, the risk would probably have been one in many hundred years. More detailed modelling work will be required to estimate the change in risk for specific high-impact events, such as the occurrence of a series of very warm nights in an urban area such as Paris.

The value of such a probability-based approach – ‘Does human influence change the likelihood of an event?’ – is that it can be used to estimate the influence of external factors, such as increases in greenhouse gases, on the frequency of specific types of events, such as heat waves or frost. Nevertheless, careful statistical analyses are required, since the likelihood of individual extremes, such as a late-spring frost, could change due to changes in climate variability as well as changes in average climate conditions. Such analyses rely on climate-model based estimates of climate variability, and thus the climate models used should adequately represent that variability.

The same likelihood-based approach can be used to examine changes in the frequency of heavy rainfall or floods. Climate models predict that human influences will cause an increase in many types of extreme events, including extreme rainfall. There is already evidence that, in recent decades, extreme rainfall has increased in some regions, leading to an increase in flooding.



FAQ 9.1, Figure 1. Summer temperatures in Switzerland from 1864 to 2003 are, on average, about 17°C, as shown by the green curve. During the extremely hot summer of 2003, average temperatures exceeded 22°C, as indicated by the red bar (a vertical line is shown for each year in the 137-year record). The fitted Gaussian distribution is indicated in green. The years 1909, 1947 and 2003 are labelled because they represent extreme years in the record. The values in the lower left corner indicate the standard deviation (σ) and the 2003 anomaly normalised by the 1864 to 2000 standard deviation (T'/σ). From Schär et al. (2004).

Frequently Asked Question 9.2

Can the Warming of the 20th Century be Explained by Natural Variability?

It is very unlikely that the 20th-century warming can be explained by natural causes. The late 20th century has been unusually warm. Palaeoclimatic reconstructions show that the second half of the 20th century was likely the warmest 50-year period in the Northern Hemisphere in the last 1300 years. This rapid warming is consistent with the scientific understanding of how the climate should respond to a rapid increase in greenhouse gases like that which has occurred over the past century, and the warming is inconsistent with the scientific understanding of how the climate should respond to natural external factors such as variability in solar output and volcanic activity. Climate models provide a suitable tool to study the various influences on the Earth's climate. When the effects of increasing levels of greenhouse gases are included in the models, as well as natural external factors, the models produce good simulations of the warming that has occurred over the past century. The models fail to reproduce the observed warming when run using only natural factors. When human factors are included, the models also simulate a geographic pattern of temperature change around the globe similar to that which has occurred in recent decades. This spatial pattern, which has features such as a greater warming at high northern latitudes, differs from the most important patterns of natural climate variability that are associated with internal climate processes, such as El Niño.

Variations in the Earth's climate over time are caused by natural internal processes, such as El Niño, as well as changes in external influences. These external influences can be natural in origin, such as volcanic activity and variations in solar output, or caused by human activity, such as greenhouse gas emissions, human-sourced aerosols, ozone depletion and land use change. The role of natural internal processes can be estimated by studying observed variations in climate and by running climate models without changing any of the external factors that affect climate. The effect of external influences can be estimated with models by changing these factors, and by using physical understanding of the processes involved. The combined effects of natural internal variability and natural external factors can also be estimated from climate information recorded in tree rings, ice cores and other types of natural 'thermometers' prior to the industrial age.

The natural external factors that affect climate include volcanic activity and variations in solar output. Explosive volcanic eruptions occasionally eject large amounts of dust and sulphate aerosol high into the atmosphere, temporarily shielding the Earth and reflecting sunlight back to space. Solar output has an 11-year cycle and may also have longer-term variations. Human activities over the last 100 years, particularly the burning of fossil fuels, have caused a rapid increase in carbon dioxide and other greenhouse gases in the atmosphere. Before

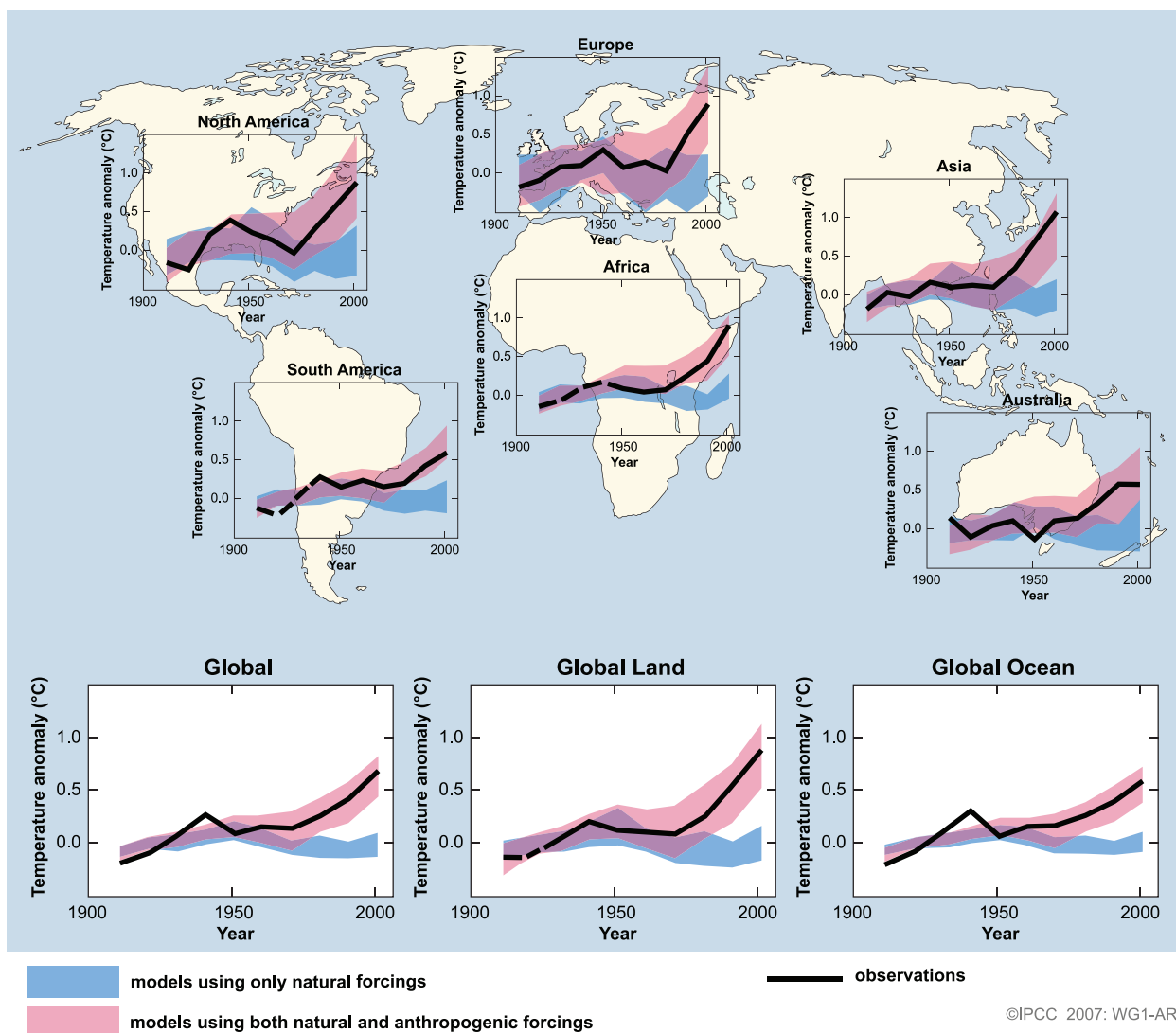
the industrial age, these gases had remained at near stable concentrations for thousands of years. Human activities have also caused increased concentrations of fine reflective particles, or 'aerosols', in the atmosphere, particularly during the 1950s and 1960s.

Although natural internal climate processes, such as El Niño, can cause variations in global mean temperature for relatively short periods, analysis indicates that a large portion is due to external factors. Brief periods of global cooling have followed major volcanic eruptions, such as Mt. Pinatubo in 1991. In the early part of the 20th century, global average temperature rose, during which time greenhouse gas concentrations started to rise, solar output was probably increasing and there was little volcanic activity. During the 1950s and 1960s, average global temperatures levelled off, as increases in aerosols from fossil fuels and other sources cooled the planet. The eruption of Mt. Agung in 1963 also put large quantities of reflective dust into the upper atmosphere. The rapid warming observed since the 1970s has occurred in a period when the increase in greenhouse gases has dominated over all other factors.

Numerous experiments have been conducted using climate models to determine the likely causes of the 20th-century climate change. These experiments indicate that models cannot reproduce the rapid warming observed in recent decades when they only take into account variations in solar output and volcanic activity. However, as shown in Figure 1, models are able to simulate the observed 20th-century changes in temperature when they include all of the most important external factors, including human influences from sources such as greenhouse gases and natural external factors. The model-estimated responses to these external factors are detectable in the 20th-century climate globally and in each individual continent except Antarctica, where there are insufficient observations. The human influence on climate very likely dominates over all other causes of change in global average surface temperature during the past half century.

An important source of uncertainty arises from the incomplete knowledge of some external factors, such as human-sourced aerosols. In addition, the climate models themselves are imperfect. Nevertheless, all models simulate a pattern of response to greenhouse gas increases from human activities that is similar to the observed pattern of change. This pattern includes more warming over land than over the oceans. This pattern of change, which differs from the principal patterns of temperature change associated with natural internal variability, such as El Niño, helps to distinguish the response to greenhouse gases from that of natural external factors. Models and observations also both show warming in the lower part of

(continued)



FAQ 9.2, Figure 1. Temperature changes relative to the corresponding average for 1901-1950 (°C) from decade to decade from 1906 to 2005 over the Earth's continents, as well as the entire globe, global land area and the global ocean (lower graphs). The black line indicates observed temperature change, while the coloured bands show the combined range covered by 90% of recent model simulations. Red indicates simulations that include natural and human factors, while blue indicates simulations that include only natural factors. Dashed black lines indicate decades and continental regions for which there are substantially fewer observations. Detailed descriptions of this figure and the methodology used in its production are given in the Supplementary Material, Appendix 9.C.

the atmosphere (the troposphere) and cooling higher up in the stratosphere. This is another 'fingerprint' of change that reveals the effect of human influence on the climate. If, for example, an increase in solar output had been responsible for the recent climate warming, both the troposphere and the stratosphere would have warmed. In addition, differences in the timing of the human and natural external influences help to distinguish the climate responses to these factors. Such considerations increase confidence that human rather than natural factors were the dominant cause of the global warming observed over the last 50 years.

Estimates of Northern Hemisphere temperatures over the last one to two millennia, based on natural 'thermometers' such as tree rings that vary in width or density as temperatures change, and historical weather records, provide additional evidence that

the 20th-century warming cannot be explained by only natural internal variability and natural external forcing factors. Confidence in these estimates is increased because prior to the industrial era, much of the variation they show in Northern Hemisphere average temperatures can be explained by episodic cooling caused by large volcanic eruptions and by changes in the Sun's output. The remaining variation is generally consistent with the variability simulated by climate models in the absence of natural and human-induced external factors. While there is uncertainty in the estimates of past temperatures, they show that it is likely that the second half of the 20th century was the warmest 50-year period in the last 1300 years. The estimated climate variability caused by natural factors is small compared to the strong 20th-century warming.

Frequently Asked Question 10.1

Are Extreme Events, Like Heat Waves, Droughts or Floods, Expected to Change as the Earth's Climate Changes?

Yes; the type, frequency and intensity of extreme events are expected to change as Earth's climate changes, and these changes could occur even with relatively small mean climate changes. Changes in some types of extreme events have already been observed, for example, increases in the frequency and intensity of heat waves and heavy precipitation events (see FAQ 3.3).

In a warmer future climate, there will be an increased risk of more intense, more frequent and longer-lasting heat waves. The European heat wave of 2003 is an example of the type of extreme heat event lasting from several days to over a week that is likely to become more common in a warmer future climate. A related aspect of temperature extremes is that there is likely to be a decrease in the daily (diurnal) temperature range in most regions. It is also likely that a warmer future climate would have fewer frost days (i.e., nights where the temperature dips below freezing). Growing season length is related to number of frost days, and has been projected to increase as climate warms. There is likely to be a decline in the frequency of cold air outbreaks (i.e., periods of extreme cold lasting from several days to over a week) in NH winter in most areas. Exceptions could occur in areas with the smallest reductions of extreme cold in western North America, the North Atlantic and southern Europe and Asia due to atmospheric circulation changes.

In a warmer future climate, most Atmosphere–Ocean General Circulation Models project increased summer dryness and winter wetness in most parts of the northern middle and high latitudes. Summer dryness indicates a greater risk of drought. Along with the risk of drying, there is an increased chance of intense precipitation and flooding due to the greater water-holding capacity of a warmer atmosphere. This has already been observed and is projected to continue because in a warmer world, precipitation tends to be concentrated into more intense events, with longer periods of little precipitation in between. Therefore, intense and heavy downpours would be interspersed with longer relatively dry periods. Another aspect of these projected changes is that wet extremes are projected to become more severe in many areas

where mean precipitation is expected to increase, and dry extremes are projected to become more severe in areas where mean precipitation is projected to decrease.

In concert with the results for increased extremes of intense precipitation, even if the wind strength of storms in a future climate did not change, there would be an increase in extreme rainfall intensity. In particular, over NH land, an increase in the likelihood of very wet winters is projected over much of central and northern Europe due to the increase in intense precipitation during storm events, suggesting an increased chance of flooding over Europe and other mid-latitude regions due to more intense rainfall and snowfall events producing more runoff. Similar results apply for summer precipitation, with implications for more flooding in the Asian monsoon region and other tropical areas. The increased risk of floods in a number of major river basins in a future warmer climate has been related to an increase in river discharge with an increased risk of future intense storm-related precipitation events and flooding. Some of these changes would be extensions of trends already underway.

There is evidence from modelling studies that future tropical cyclones could become more severe, with greater wind speeds and more intense precipitation. Studies suggest that such changes may already be underway; there are indications that the average number of Category 4 and 5 hurricanes per year has increased over the past 30 years. Some modelling studies have projected a decrease in the number of tropical cyclones globally due to the increased stability of the tropical troposphere in a warmer climate, characterised by fewer weak storms and greater numbers of intense storms. A number of modelling studies have also projected a general tendency for more intense but fewer storms outside the tropics, with a tendency towards more extreme wind events and higher ocean waves in several regions in association with those deepened cyclones. Models also project a poleward shift of storm tracks in both hemispheres by several degrees of latitude.

Frequently Asked Question 10.2

How Likely are Major or Abrupt Climate Changes, such as Loss of Ice Sheets or Changes in Global Ocean Circulation?

Abrupt climate changes, such as the collapse of the West Antarctic Ice Sheet, the rapid loss of the Greenland Ice Sheet or large-scale changes of ocean circulation systems, are not considered likely to occur in the 21st century, based on currently available model results. However, the occurrence of such changes becomes increasingly more likely as the perturbation of the climate system progresses.

Physical, chemical and biological analyses from Greenland ice cores, marine sediments from the North Atlantic and elsewhere and many other archives of past climate have demonstrated that local temperatures, wind regimes and water cycles can change rapidly within just a few years. The comparison of results from records in different locations of the world shows that in the past major changes of hemispheric to global extent occurred. This has led to the notion of an unstable past climate that underwent phases of abrupt change. Therefore, an important concern is that the continued growth of greenhouse gas concentrations in the atmosphere may constitute a perturbation sufficiently strong to trigger abrupt changes in the climate system. Such interference with the climate system could be considered dangerous, because it would have major global consequences.

Before discussing a few examples of such changes, it is useful to define the terms ‘abrupt’ and ‘major’. ‘Abrupt’ conveys the meaning that the changes occur much faster than the perturbation inducing the change; in other words, the response is nonlinear. A ‘major’ climate change is one that involves changes that exceed the range of current natural variability and have a spatial extent ranging from several thousand kilometres to global. At local to regional scales, abrupt changes are a common characteristic of natural climate variability. Here, isolated, short-lived events that are more appropriately referred to as ‘extreme events’ are not considered, but rather large-scale changes that evolve rapidly and persist for several years to decades. For instance, the mid-1970s shift in sea surface temperatures in the Eastern Pacific, or the salinity reduction in the upper 1,000 m of the Labrador Sea since the mid-1980s, are examples of abrupt events with local to regional consequences, as opposed to the larger-scale, longer-term events that are the focus here.

One example is the potential collapse, or shut-down of the Gulf Stream, which has received broad public attention. The Gulf Stream is a primarily horizontal current in the north-western Atlantic Ocean driven by winds. Although a stable feature of the general circulation of the ocean, its northern extension, which feeds deep-water formation in the Greenland-Norwegian-Iceland Seas and thereby delivers substantial amounts of heat to these seas and nearby land areas, is influenced strongly by changes in the density of the surface waters in these areas. This current

constitutes the northern end of a basin-scale meridional overturning circulation (MOC) that is established along the western boundary of the Atlantic basin. A consistent result from climate model simulations is that if the density of the surface waters in the North Atlantic decreases due to warming or a reduction in salinity, the strength of the MOC is decreased, and with it, the delivery of heat into these areas. Strong sustained reductions in salinity could induce even more substantial reduction, or complete shut-down of the MOC in all climate model projections. Such changes have indeed happened in the distant past.

The issue now is whether the increasing human influence on the atmosphere constitutes a strong enough perturbation to the MOC that such a change might be induced. The increase in greenhouse gases in the atmosphere leads to warming and an intensification of the hydrological cycle, with the latter making the surface waters in the North Atlantic less salty as increased rain leads to more freshwater runoff to the ocean from the region’s rivers. Warming also causes land ice to melt, adding more freshwater and further reducing the salinity of ocean surface waters. Both effects would reduce the density of the surface waters (which must be dense and heavy enough to sink in order to drive the MOC), leading to a reduction in the MOC in the 21st century. This reduction is predicted to proceed in lockstep with the warming: none of the current models simulates an abrupt (nonlinear) reduction or a complete shut-down in this century. There is still a large spread among the models’ simulated reduction in the MOC, ranging from virtually no response to a reduction of over 50% by the end of the 21st century. This cross-model variation is due to differences in the strengths of atmosphere and ocean feedbacks simulated in these models.

Uncertainty also exists about the long-term fate of the MOC. Many models show a recovery of the MOC once climate is stabilised. But some models have thresholds for the MOC, and they are passed when the forcing is strong enough and lasts long enough. Such simulations then show a gradual reduction of the MOC that continues even after climate is stabilised. A quantification of the likelihood of this occurring is not possible at this stage. Nevertheless, even if this were to occur, Europe would still experience warming, since the radiative forcing caused by increasing greenhouse gases would overwhelm the cooling associated with the MOC reduction. Catastrophic scenarios suggesting the beginning of an ice age triggered by a shutdown of the MOC are thus mere speculations, and no climate model has produced such an outcome. In fact, the processes leading to an ice age are sufficiently well understood and so completely different from those discussed here, that we can confidently exclude this scenario.

(continued)

Irrespective of the long-term evolution of the MOC, model simulations agree that the warming and resulting decline in salinity will significantly reduce deep and intermediate water formation in the Labrador Sea during the next few decades. This will alter the characteristics of the intermediate water masses in the North Atlantic and eventually affect the deep ocean. The long-term effects of such a change are unknown.

Other widely discussed examples of abrupt climate changes are the rapid disintegration of the Greenland Ice Sheet, or the sudden collapse of the West Antarctic Ice Sheet. Model simulations and observations indicate that warming in the high latitudes of the Northern Hemisphere is accelerating the melting of the Greenland Ice Sheet, and that increased snowfall due to the intensified hydrological cycle is unable to compensate for this melting. As a consequence, the Greenland Ice Sheet may shrink substantially in the coming centuries. Moreover, results suggest that there is a critical temperature threshold beyond which the Greenland Ice Sheet would be committed to disappearing completely, and that threshold could be crossed in this century. However, the total melting of the Greenland Ice Sheet, which

would raise global sea level by about seven metres, is a slow process that would take many hundreds of years to complete.

Recent satellite and *in situ* observations of ice streams behind disintegrating ice shelves highlight some rapid reactions of ice sheet systems. This raises new concern about the overall stability of the West Antarctic Ice Sheet, the collapse of which would trigger another five to six metres of sea level rise. While these streams appear buttressed by the shelves in front of them, it is currently unknown whether a reduction or failure of this buttressing of relatively limited areas of the ice sheet could actually trigger a widespread discharge of many ice streams and hence a destabilisation of the entire West Antarctic Ice Sheet. Ice sheet models are only beginning to capture such small-scale dynamical processes that involve complicated interactions with the glacier bed and the ocean at the perimeter of the ice sheet. Therefore, no quantitative information is available from the current generation of ice sheet models as to the likelihood or timing of such an event.

Frequently Asked Question 10.3

If Emissions of Greenhouse Gases are Reduced, How Quickly do Their Concentrations in the Atmosphere Decrease?

The adjustment of greenhouse gas concentrations in the atmosphere to reductions in emissions depends on the chemical and physical processes that remove each gas from the atmosphere. Concentrations of some greenhouse gases decrease almost immediately in response to emission reduction, while others can actually continue to increase for centuries even with reduced emissions.

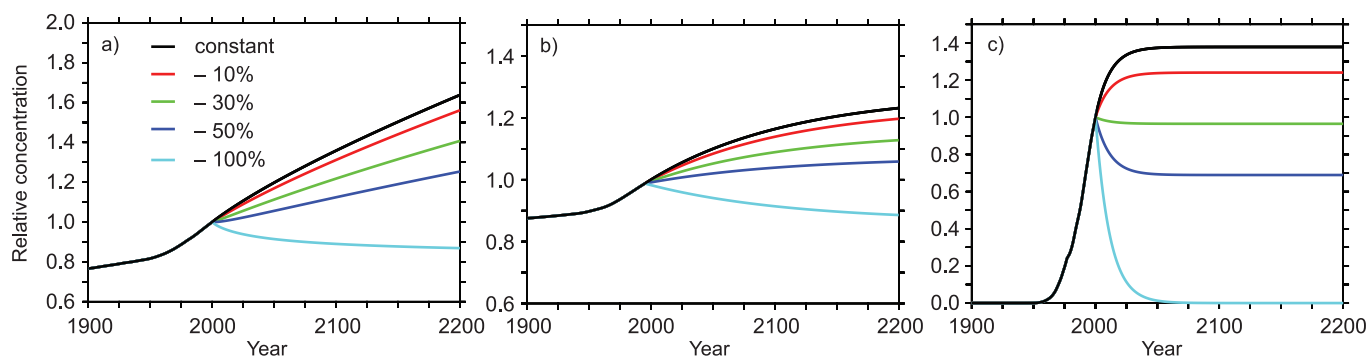
The concentration of a greenhouse gas in the atmosphere depends on the competition between the rates of emission of the gas into the atmosphere and the rates of processes that remove it from the atmosphere. For example, carbon dioxide (CO_2) is exchanged between the atmosphere, the ocean and the land through processes such as atmosphere-ocean gas transfer and chemical (e.g., weathering) and biological (e.g., photosynthesis) processes. While more than half of the CO_2 emitted is currently removed from the atmosphere within a century, some fraction (about 20%) of emitted CO_2 remains in the atmosphere for many millennia. Because of slow removal processes, atmospheric CO_2 will continue to increase in the long term even if its emission is substantially reduced from present levels. Methane (CH_4) is removed by chemical processes in the atmosphere, while nitrous oxide (N_2O) and some halocarbons are destroyed in the upper atmosphere by solar radiation. These processes each operate at different time scales ranging from years to millennia. A measure for this is the lifetime of a gas in the atmosphere, defined as the time it takes for a perturbation to be reduced to 37% of its initial amount. While for CH_4 , N_2O , and other trace gases such as hydrochlorofluorocarbon-22 (HCFC-22), a refrigerant fluid, such lifetimes can be reasonably determined (for CH_4 it is about 12 yr, for N_2O about 110 yr and for HCFC-22 about 12 yr), a lifetime for CO_2 cannot be defined.

The change in concentration of any trace gas depends in part on how its emissions evolve over time. If emissions increase with time, the atmospheric concentration will also increase with time, regardless of the atmospheric lifetime of the gas. However, if actions are taken to reduce the emissions, the fate of the trace gas concentration will depend on the relative changes not only of emissions but also of its removal processes. Here we show how the lifetimes and removal processes of different gases dictate the evolution of concentrations when emissions are reduced.

As examples, FAQ 10.3, Figure 1 shows test cases illustrating how the future concentration of three trace gases would respond to illustrative changes in emissions (represented here as a response to an imposed pulse change in emission). We consider CO_2 , which has no specific lifetime, as well as a trace gas with a well-defined long lifetime on the order of a century (e.g., N_2O), and a trace gas with a well-defined short lifetime on the order of decade (such as CH_4 , HCFC-22 or other halocarbons). For each gas, five illustrative cases of future emissions are presented: stabilisation of emissions at present-day levels, and immediate emission reduction by 10%, 30%, 50% and 100%.

The behaviour of CO_2 (Figure 1a) is completely different from the trace gases with well-defined lifetimes. Stabilisation of CO_2 emissions at current levels would result in a continuous increase of atmospheric CO_2 over the 21st century and beyond, whereas for a gas with a lifetime on the order of a century (Figure 1b) or a decade (Figure 1c), stabilisation of emissions at current levels would lead to a stabilisation of its concentration at a level higher than today within a couple of centuries, or decades, respectively. In fact, only in the case of essentially complete elimination of

(continued)



FAQ 10.3, Figure 1. (a) Simulated changes in atmospheric CO_2 concentration relative to the present-day for emissions stabilised at the current level (black), or at 10% (red), 30% (green), 50% (dark blue) and 100% (light blue) lower than the current level; (b) as in (a) for a trace gas with a lifetime of 120 years, driven by natural and anthropogenic fluxes; and (c) as in (a) for a trace gas with a lifetime of 12 years, driven by only anthropogenic fluxes.

emissions can the atmospheric concentration of CO₂ ultimately be stabilised at a constant level. All other cases of moderate CO₂ emission reductions show increasing concentrations because of the characteristic exchange processes associated with the cycling of carbon in the climate system.

More specifically, the rate of emission of CO₂ currently greatly exceeds its rate of removal, and the slow and incomplete removal implies that small to moderate reductions in its emissions would not result in stabilisation of CO₂ concentrations, but rather would only reduce the rate of its growth in coming decades. A 10% reduction in CO₂ emissions would be expected to reduce the growth rate by 10%, while a 30% reduction in emissions would similarly reduce the growth rate of atmospheric CO₂ concentrations by 30%. A 50% reduction would stabilise atmospheric CO₂, but only for less than a decade. After that, atmospheric CO₂ would be expected to rise again as the land and ocean sinks decline owing to well-known chemical and biological adjustments. Complete elimination of CO₂ emissions is estimated to lead to a slow decrease in atmospheric CO₂ of about 40 ppm over the 21st century.

The situation is completely different for the trace gases with a well-defined lifetime. For the illustrative trace gas with a lifetime of the order of a century (e.g., N₂O), emission reduction of more than 50% is required to stabilise the concentrations close to present-day values (Figure 1b). Constant emission leads to a stabilisation of the concentration within a few centuries.

In the case of the illustrative gas with the short lifetime, the present-day loss is around 70% of the emissions. A reduction in emissions of less than 30% would still produce a short-term increase in concentration in this case, but, in contrast to CO₂, would lead to stabilisation of its concentration within a couple of decades (Figure 1c). The decrease in the level at which the concentration of such a gas would stabilise is directly proportional to the emission reduction. Thus, in this illustrative example, a reduction in emissions of this trace gas larger than 30% would be required to stabilise concentrations at levels significantly below those at present. A complete cut-off of the emissions would lead to a return to pre-industrial concentrations within less than a century for a trace gas with a lifetime of the order of a decade.

Frequently Asked Question 11.1

Do Projected Changes in Climate Vary from Region to Region?

Climate varies from region to region. This variation is driven by the uneven distribution of solar heating, the individual responses of the atmosphere, oceans and land surface, the interactions between these, and the physical characteristics of the regions. The perturbations of the atmospheric constituents that lead to global changes affect certain aspects of these complex interactions. Some human-induced factors that affect climate ('forcings') are global in nature, while others differ from one region to another. For example, carbon dioxide, which causes warming, is distributed evenly around the globe, regardless of where the emissions originate, whereas sulphate aerosols (small particles) that offset some of the warming tend to be regional in their distribution. Furthermore, the response to forcings is partly governed by feedback processes that may operate in different regions from those in which the forcing is greatest. Thus, the projected changes in climate will also vary from region to region.

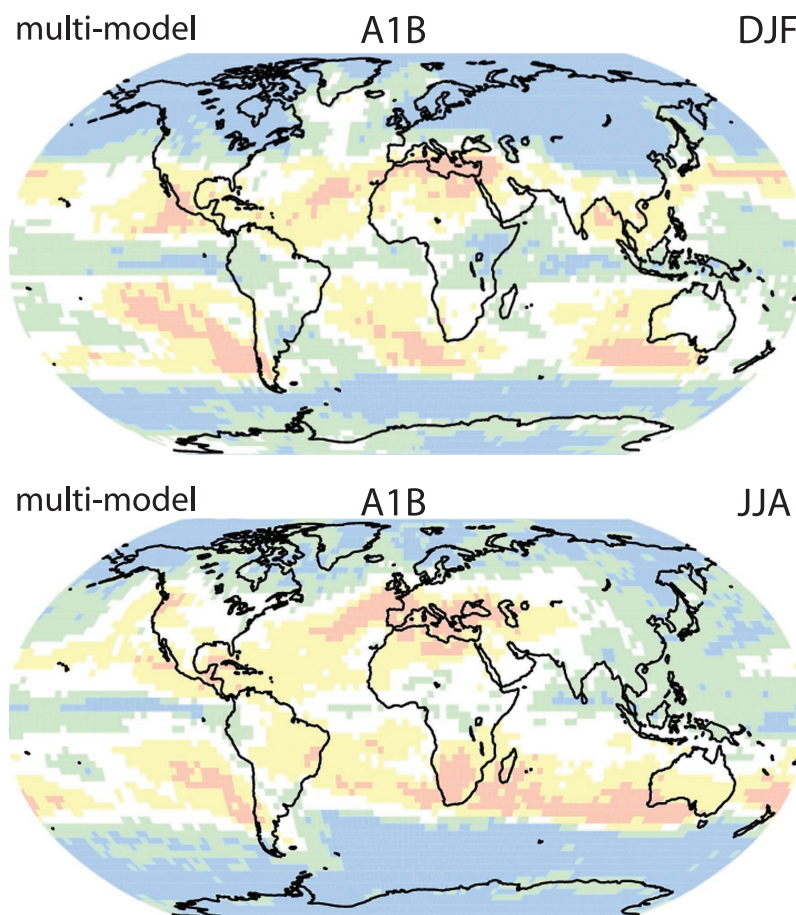
Latitude is a good starting point for considering how changes in climate will affect a region. For example, while warming is expected everywhere on Earth, the amount of projected warming generally increases from the tropics to the poles in the Northern Hemisphere. Precipitation is more complex, but also has some latitude-dependent features. At latitudes adjacent to the polar regions, precipitation is projected to increase, while decreases are projected in many regions adjacent to the tropics (see Figure 1). Increases in tropical precipitation are projected during rainy seasons (e.g., monsoons), and over the tropical Pacific in particular.

Location with respect to oceans and mountain ranges is also an important factor. Generally, the interiors of continents are projected to warm more than the coastal areas. Precipitation responses are especially sensitive not only to the continental geometry, but to the shape of nearby mountain ranges and wind flow direction. Monsoons, extratropical cyclones and hurricanes/typhoons are all influenced in different ways by these region-specific features.

Some of the most difficult aspects of understanding and projecting changes in regional climate relate to possible changes in the circulation of the atmosphere and oceans, and their patterns of variability. Although general statements covering a variety of regions with

qualitatively similar climates can be made in some cases, nearly every region is idiosyncratic in some ways. This is true whether it is the coastal zones surrounding the subtropical Mediterranean Sea, the extreme weather in the North American interior that depends on moisture transport from the Gulf of Mexico, or the interactions between vegetation distribution, oceanic temperatures and atmospheric circulation that help control the southern limit of the Sahara Desert.

While developing an understanding of the correct balance of global and regional factors remains a challenge, the understanding of these factors is steadily growing, increasing our confidence in regional projections.



FAQ 11.1, Figure 1. Blue and green areas on the map are by the end of the century projected to experience increases in precipitation, while areas in yellow and pink are projected to have decreases. The top panel shows projections for the period covering December, January and February, while the bottom panel shows projections for the period covering June, July and August.

Annex I

Glossary

Editor: A.P.M. Baede (Netherlands)

Notes: This glossary defines some specific terms as the lead authors intend them to be interpreted in the context of this report. Red, italicised words indicate that the term is defined in the Glossary.

8.2ka event Following the last post-glacial warming, a rapid *climate* oscillation with a cooling lasting about 400 years occurred about 8.2 ka. This event is also referred to as the *8.2kyr event*.

Abrupt climate change The *nonlinearity* of the *climate system* may lead to abrupt climate change, sometimes called *rapid climate change*, *abrupt events* or *even surprises*. The term *abrupt* often refers to time scales faster than the typical time scale of the responsible forcing. However, not all abrupt climate changes need be *externally forced*. Some possible abrupt events that have been proposed include a dramatic reorganisation of the *thermohaline circulation*, rapid deglaciation and massive melting of *permafrost* or increases in soil *respiration* leading to fast changes in the *carbon cycle*. Others may be truly unexpected, resulting from a strong, rapidly changing forcing of a nonlinear system.

Active layer The layer of ground that is subject to annual thawing and freezing in areas underlain by *permafrost* (Van Everdingen, 1998).

Adiabatic process An adiabatic process is a process in which no external heat is gained or lost by the system. The opposite is called a *diabatic process*.

Adjustment time See *Lifetime*; see also *Response time*.

Advection Transport of water or air along with its properties (e.g., temperature, chemical tracers) by the motion of the fluid. Regarding the general distinction between advection and *convection*, the former describes the predominantly horizontal, large-scale motions of the *atmosphere* or ocean, while convection describes the predominantly vertical, locally induced motions.

Aerosols A collection of airborne solid or liquid particles, with a typical size between 0.01 and 10 μm that reside in the *atmosphere* for at least several hours. Aerosols may be of either natural or *anthropogenic* origin. Aerosols may influence *climate* in several ways: directly through scattering and absorbing radiation, and indirectly by acting as *cloud condensation nuclei* or modifying the optical properties and lifetime of clouds (see *Indirect aerosol effect*).

Afforestation Planting of new forests on lands that historically have not contained forests. For a discussion of the term *forest* and related terms such as afforestation, *reforestation* and *deforestation*, see the IPCC Special Report on Land Use, Land-Use Change and Forestry (IPCC, 2000). See also the report on Definitions and Methodological Options to Inventory Emissions from Direct Human-induced Degradation of Forests and Devegetation of Other Vegetation Types (IPCC, 2003).

Air mass A widespread body of air, the approximately homogeneous properties of which (1) have been established while that air was situated over a particular *region* of the Earth's surface, and (2) undergo specific modifications while in transit away from the source region (AMS, 2000).

Albedo The fraction of *solar radiation* reflected by a surface or object, often expressed as a percentage. Snow-covered surfaces have a high albedo, the surface albedo of soils ranges from high to low, and vegetation-covered surfaces and oceans have a low albedo. The Earth's planetary albedo varies mainly through varying cloudiness, snow, ice, leaf area and land cover changes.

Albedo feedback A *climate feedback* involving changes in the Earth's *albedo*. It usually refers to changes in the *cryosphere*, which has an albedo much larger (~ 0.8) than the average planetary albedo (~ 0.3). In a warming *climate*, it is anticipated that the cryosphere would shrink, the Earth's overall albedo would decrease and more *solar radiation* would be absorbed to warm the Earth still further.

Alkalinity A measure of the capacity of a solution to neutralize acids.

Altimetry A technique for measuring the height of the sea, lake or river, land or ice surface with respect to the centre of the Earth within a defined terrestrial reference frame. More conventionally, the height is with respect to a standard *reference ellipsoid* approximating the Earth's oblateness, and can be measured from space by using radar or laser with centimetric precision at present. Altimetry has the advantages of being a geocentric measurement, rather than a measurement relative to the Earth's crust as for a *tide gauge*, and of affording quasi-global coverage.

Annular modes Preferred patterns of change in atmospheric circulation corresponding to changes in the zonally averaged mid-latitude westerlies. The *Northern Annular Mode* has a bias to the North Atlantic and has a large correlation with the *North Atlantic Oscillation*. The *Southern Annular Mode* occurs in the Southern Hemisphere. The variability of the mid-latitude westerlies has also been known as *zonal flow* (or *wind*) vacillation, and defined through a *zonal index*. For the corresponding circulation indices, see Box 3.4.

Anthropogenic Resulting from or produced by human beings.

Atlantic Multi-decadal Oscillation (AMO) A multi-decadal (65 to 75 year) fluctuation in the North Atlantic, in which *sea surface temperatures* showed warm phases during roughly 1860 to 1880 and 1930 to 1960 and cool phases during 1905 to 1925 and 1970 to 1990 with a range of order 0.4°C.

Atmosphere The gaseous envelope surrounding the Earth. The dry atmosphere consists almost entirely of nitrogen (78.1% *volume mixing ratio*) and oxygen (20.9% volume mixing ratio), together with a number of trace gases, such as argon (0.93% volume mixing ratio), helium and radiatively active *greenhouse gases* such as *carbon dioxide* (0.035% volume mixing ratio) and *ozone*. In addition, the atmosphere contains the greenhouse gas water vapour, whose amounts are highly variable but typically around 1% volume mixing ratio. The atmosphere also contains clouds and *aerosols*.

Atmospheric boundary layer The atmospheric layer adjacent to the Earth's surface that is affected by friction against that boundary

surface, and possibly by transport of heat and other variables across that surface (AMS, 2000). The lowest 10 metres or so of the boundary layer, where mechanical generation of turbulence is dominant, is called the *surface boundary layer* or *surface layer*.

Atmospheric lifetime See *Lifetime*.

Attribution See *Detection and attribution*.

Autotrophic respiration *Respiration* by *photosynthetic* organisms (plants).

Bayesian method A Bayesian method is a method by which a statistical analysis of an unknown or uncertain quantity is carried out in two steps. First, a prior probability distribution is formulated on the basis of existing knowledge (either by eliciting expert opinion or by using existing data and studies). At this first stage, an element of subjectivity may influence the choice, but in many cases, the prior probability distribution is chosen as neutrally as possible, in order not to influence the final outcome of the analysis. In the second step, newly acquired data are introduced, using a theorem formulated by and named after the British mathematician Bayes (1702–1761), to update the prior distribution into a posterior distribution.

Biomass The total mass of living organisms in a given area or volume; dead plant material can be included as dead biomass.

Biome A biome is a major and distinct regional element of the *biosphere*, typically consisting of several *ecosystems* (e.g. *forests*, rivers, ponds, swamps within a *region*). Biomes are characterised by typical communities of plants and animals.

Biosphere (terrestrial and marine) The part of the Earth system comprising all *ecosystems* and living organisms, in the *atmosphere*, on land (*terrestrial biosphere*) or in the oceans (*marine biosphere*), including derived dead organic matter, such as litter, soil organic matter and oceanic detritus.

Black carbon (BC) Operationally defined *aerosol* species based on measurement of light absorption and chemical reactivity and/or thermal stability; consists of *soot*, *charcoal* and/or possible light-absorbing refractory organic matter (Charlson and Heintzenberg, 1995, p. 401).

Blocking anticyclone An anticyclone that remains nearly stationary for a week or more at middle to high latitudes, so that it blocks the normal eastward progression of high- and low-pressure systems.

Bowen ratio The ratio of *sensible* to *latent heat fluxes* from the Earth's surface up into the *atmosphere*. Values are low (order 0.1) for wet surfaces like the ocean, and greater than 2 for deserts and *drought* regions.

Burden The total mass of a gaseous substance of concern in the *atmosphere*.

¹³C Stable isotope of carbon having an atomic weight of approximately 13. Measurements of the ratio of ¹³C/¹²C in *carbon dioxide* molecules are used to infer the importance of different *carbon cycle* and *climate* processes and the size of the terrestrial carbon *reservoir*.

¹⁴C Unstable isotope of carbon having an atomic weight of approximately 14, and a half-life of about 5,700 years. It is often used for dating purposes going back some 40 kyr. Its variation in time is affected by the magnetic fields of the Sun and Earth,

which influence its production from cosmic rays (see *Cosmogenic isotopes*).

C3 plants Plants that produce a three-carbon compound during *photosynthesis*, including most trees and agricultural crops such as rice, wheat, soybeans, potatoes and vegetables.

C4 plants Plants that produce a four-carbon compound during *photosynthesis*, mainly of tropical origin, including grasses and the agriculturally important crops maize, sugar cane, millet and sorghum.

Carbonaceous aerosol *Aerosol* consisting predominantly of organic substances and various forms of *black carbon* (Charlson and Heintzenberg, 1995, p. 401).

Carbon cycle The term used to describe the flow of carbon (in various forms, e.g., as *carbon dioxide*) through the *atmosphere*, ocean, terrestrial *biosphere* and *lithosphere*.

Carbon dioxide (CO₂) A naturally occurring gas, also a by-product of burning fossil fuels from fossil carbon deposits, such as oil, gas and coal, of burning *biomass* and of *land use* changes and other industrial processes. It is the principal *anthropogenic greenhouse gas* that affects the Earth's radiative balance. It is the reference gas against which other greenhouse gases are measured and therefore has a *Global Warming Potential* of 1.

Carbon dioxide (CO₂) fertilization The enhancement of the growth of plants as a result of increased atmospheric *carbon dioxide* (CO₂) concentration. Depending on their mechanism of *photosynthesis*, certain types of plants are more sensitive to changes in atmospheric CO₂ concentration. In particular, *C3 plants* generally show a larger response to CO₂ than *C4 plants*.

CFC See *Halocarbons*.

Chaos A *dynamical system* such as the *climate system*, governed by nonlinear deterministic equations (see *Nonlinearity*), may exhibit erratic or chaotic behaviour in the sense that very small changes in the initial state of the system in time lead to large and apparently unpredictable changes in its temporal evolution. Such chaotic behaviour may limit the *predictability* of nonlinear dynamical systems.

Charcoal Material resulting from charring of *biomass*, usually retaining some of the microscopic texture typical of plant tissues; chemically it consists mainly of carbon with a disturbed graphitic structure, with lesser amounts of oxygen and hydrogen (Charlson and Heintzenberg, 1995, p. 402). See *Black carbon*; *Soot*.

Chronology Arrangement of events according to dates or times of occurrence.

Clathrate (methane) A partly frozen slushy mix of methane gas and ice, usually found in sediments.

Climate Climate in a narrow sense is usually defined as the average weather, or more rigorously, as the statistical description in terms of the mean and variability of relevant quantities over a period of time ranging from months to thousands or millions of years. The classical period for averaging these variables is 30 years, as defined by the World Meteorological Organization. The relevant quantities are most often surface variables such as temperature, precipitation and wind. Climate in a wider sense is the state, including a statistical description, of the *climate system*. In various chapters in this report different averaging periods, such as a period of 20 years, are also used.

Climate change Climate change refers to a change in the state of the *climate* that can be identified (e.g., by using statistical tests) by changes in the mean and/or the variability of its properties, and that persists for an extended period, typically decades or longer. Climate change may be due to natural internal processes or *external forcings*, or to persistent *anthropogenic* changes in the composition of the *atmosphere* or in *land use*. Note that the *Framework Convention on Climate Change* (UNFCCC), in its Article 1, defines *climate change* as: ‘a change of climate which is attributed directly or indirectly to human activity that alters the composition of the global atmosphere and which is in addition to natural climate variability observed over comparable time periods’. The UNFCCC thus makes a distinction between climate change attributable to human activities altering the atmospheric composition, and *climate variability* attributable to natural causes. See also *Climate variability; Detection and Attribution*.

Climate change commitment Due to the thermal inertia of the ocean and slow processes in the *biosphere*, the *cryosphere* and land surfaces, the *climate* would continue to change even if the atmospheric composition were held fixed at today’s values. Past change in atmospheric composition leads to a *committed climate change*, which continues for as long as a radiative imbalance persists and until all components of the *climate system* have adjusted to a new state. The further change in temperature after the composition of the *atmosphere* is held constant is referred to as the *constant composition temperature commitment* or simply *committed warming* or *warming commitment*. Climate change commitment includes other future changes, for example in the hydrological cycle, in *extreme weather* and climate events, and in *sea level change*.

Climate feedback An interaction mechanism between processes in the *climate system* is called a climate feedback when the result of an initial process triggers changes in a second process that in turn influences the initial one. A positive feedback intensifies the original process, and a negative feedback reduces it.

Climate Feedback Parameter A way to quantify the radiative response of the *climate system* to a *global surface temperature* change induced by a *radiative forcing* (units: $\text{W m}^{-2} \text{ } ^\circ\text{C}^{-1}$). It varies as the inverse of the effective *climate sensitivity*. Formally, the Climate Feedback Parameter (Λ) is defined as: $\Lambda = (\Delta Q - \Delta F) / \Delta T$, where Q is the global mean radiative forcing, T is the global mean air surface temperature, F is the heat flux into the ocean and Δ represents a change with respect to an unperturbed *climate*.

Climate model (spectrum or hierarchy) A numerical representation of the *climate system* based on the physical, chemical and biological properties of its components, their interactions and *feedback* processes, and accounting for all or some of its known properties. The climate system can be represented by models of varying complexity, that is, for any one component or combination of components a *spectrum* or *hierarchy* of models can be identified, differing in such aspects as the number of spatial dimensions, the extent to which physical, chemical or biological processes are explicitly represented, or the level at which empirical *parametrizations* are involved. Coupled Atmosphere–Ocean General Circulation Models (AOGCMs) provide a representation of the climate system that is near the most comprehensive end of the spectrum currently available. There is an evolution towards more complex models with interactive chemistry and biology (see Chapter 8). Climate models are applied as a research tool to study and simulate the climate, and for operational purposes, including monthly, seasonal and interannual *climate predictions*.

Climate prediction A climate prediction or *climate forecast* is the result of an attempt to produce an estimate of the actual evolution

of the *climate* in the future, for example, at seasonal, interannual or long-term time scales. Since the future evolution of the *climate system* may be highly sensitive to initial conditions, such predictions are usually probabilistic in nature. See also *Climate projection; Climate scenario; Predictability*.

Climate projection A *projection* of the response of the *climate system* to *emission or concentration scenarios* of *greenhouse gases* and *aerosols*, or *radiative forcing* scenarios, often based upon simulations by *climate models*. Climate projections are distinguished from *climate predictions* in order to emphasize that climate projections depend upon the emission/concentration/radiative forcing scenario used, which are based on assumptions concerning, for example, future socioeconomic and technological developments that may or may not be realised and are therefore subject to substantial *uncertainty*.

Climate response
See *Climate sensitivity*.

Climate scenario A plausible and often simplified representation of the future *climate*, based on an internally consistent set of climatological relationships that has been constructed for explicit use in investigating the potential consequences of *anthropogenic climate change*, often serving as input to impact models. *Climate projections* often serve as the raw material for constructing climate scenarios, but climate scenarios usually require additional information such as about the observed current climate. A *climate change scenario* is the difference between a climate scenario and the current climate.

Climate sensitivity In IPCC reports, *equilibrium climate sensitivity* refers to the equilibrium change in the annual mean *global surface temperature* following a doubling of the atmospheric *equivalent carbon dioxide concentration*. Due to computational constraints, the equilibrium climate sensitivity in a *climate model* is usually estimated by running an atmospheric general circulation model coupled to a mixed-layer ocean model, because equilibrium climate sensitivity is largely determined by atmospheric processes. Efficient models can be run to equilibrium with a dynamic ocean.

The *effective climate sensitivity* is a related measure that circumvents the requirement of equilibrium. It is evaluated from model output for evolving non-equilibrium conditions. It is a measure of the strengths of the *climate feedbacks* at a particular time and may vary with forcing history and *climate* state. The climate sensitivity parameter (units: $^\circ\text{C} (\text{W m}^{-2})^{-1}$) refers to the equilibrium change in the annual mean *global surface temperature* following a unit change in *radiative forcing*.

The *transient climate response* is the change in the global surface temperature, averaged over a 20-year period, centred at the time of atmospheric carbon dioxide doubling, that is, at year 70 in a 1% yr^{-1} compound carbon dioxide increase experiment with a global coupled climate model. It is a measure of the strength and rapidity of the surface temperature response to *greenhouse gas* forcing.

Climate shift or climate regime shift An abrupt shift or jump in mean values signalling a change in *regime*. Most widely used in conjunction with the 1976/1977 climate shift that seems to correspond to a change in *El Niño–Southern Oscillation* behavior.

Climate system The climate system is the highly complex system consisting of five major components: the *atmosphere*, the *hydrosphere*, the *cryosphere*, the land surface and the *biosphere*, and the interactions between them. The climate system evolves in time under the influence of its own internal dynamics and because of *external forcings* such as volcanic eruptions, solar variations and

anthropogenic forcings such as the changing composition of the atmosphere and *land use change*.

Climate variability Climate variability refers to variations in the mean state and other statistics (such as standard deviations, the occurrence of extremes, etc.) of the *climate* on all *spatial and temporal scales* beyond that of individual weather events. Variability may be due to natural internal processes within the *climate system* (*internal variability*), or to variations in natural or *anthropogenic external forcing* (*external variability*). See also *Climate change*.

Cloud condensation nuclei (CCN) Airborne particles that serve as an initial site for the condensation of liquid water, which can lead to the formation of cloud droplets. See also *Aerosols*.

Cloud feedback A *climate feedback* involving changes in any of the properties of clouds as a response to other atmospheric changes. Understanding cloud feedbacks and determining their magnitude and sign require an understanding of how a change in *climate* may affect the spectrum of cloud types, the cloud fraction and height, and the radiative properties of clouds, and an estimate of the impact of these changes on the Earth's radiation budget. At present, cloud feedbacks remain the largest source of *uncertainty in climate sensitivity* estimates. See also *Cloud radiative forcing*; *Radiative forcing*.

Cloud radiative forcing Cloud radiative forcing is the difference between the all-sky Earth's radiation budget and the clear-sky Earth's radiation budget (units: $W\ m^{-2}$).

CO₂-equivalent See *Equivalent carbon dioxide*.

Confidence The *level of confidence* in the correctness of a result is expressed in this report, using a standard terminology defined in Box 1.1. See also *Likelihood*; *Uncertainty*.

Convection Vertical motion driven by buoyancy forces arising from static instability, usually caused by near-surface cooling or increases in salinity in the case of the ocean and near-surface warming in the case of the *atmosphere*. At the location of convection, the horizontal scale is approximately the same as the vertical scale, as opposed to the large contrast between these scales in the *general circulation*. The net vertical mass transport is usually much smaller than the upward and downward exchange.

Cosmogenic isotopes Rare isotopes that are created when a high-energy cosmic ray interacts with the nucleus of an *in situ* atom. They are often used as indications of solar magnetic activity (which can shield cosmic rays) or as tracers of atmospheric transport, and are also called *cosmogenic nuclides*.

Cryosphere The component of the *climate system* consisting of all snow, ice and *frozen ground* (including *permafrost*) on and beneath the surface of the Earth and ocean. See also *Glacier*; *Ice sheet*.

Dansgaard-Oeschger events Abrupt warming events followed by gradual cooling. The abrupt warming and gradual cooling is primarily seen in Greenland *ice cores* and in *palaeoclimate* records from the nearby North Atlantic, while a more general warming followed by a gradual cooling has been observed in other areas as well, at intervals of 1.5 to 7 kyr during glacial times.

Deforestation Conversion of forest to non-forest. For a discussion of the term *forest* and related terms such as *afforestation*, *reforestation*, and deforestation see the IPCC Special Report on Land Use, Land-Use Change and Forestry (IPCC, 2000). See also the report on Definitions and Methodological Options to Inventory

Emissions from Direct Human-induced Degradation of Forests and Devegetation of Other Vegetation Types (IPCC, 2003).

Desertification Land degradation in arid, semi-arid, and dry sub-humid areas resulting from various factors, including climatic variations and human activities. The United Nations Convention to Combat Desertification defines land degradation as a reduction or loss in arid, semi-arid, and dry sub-humid areas, of the biological or economic productivity and complexity of rain-fed cropland, irrigated cropland, or range, pasture, *forest*, and woodlands resulting from *land uses* or from a process or combination of processes, including processes arising from human activities and habitation patterns, such as (i) soil erosion caused by wind and/or water; (ii) deterioration of the physical, chemical and biological or economic properties of soil; and (iii) long-term loss of natural vegetation.

Detection and attribution *Climate* varies continually on all time scales. *Detection of climate change* is the process of demonstrating that climate has changed in some defined statistical sense, without providing a reason for that change. *Attribution* of causes of climate change is the process of establishing the most likely causes for the detected change with some defined level of *confidence*.

Diatoms Silt-sized algae that live in surface waters of lakes, rivers and oceans and form shells of opal. Their species distribution in ocean cores is often related to past *sea surface temperatures*.

Diurnal temperature range The difference between the maximum and minimum temperature during a 24-hour period.

Dobson unit (DU) A unit to measure the total amount of *ozone* in a vertical column above the Earth's surface (*total column ozone*). The number of Dobson units is the thickness in units of 10^{-5} m that the ozone column would occupy if compressed into a layer of uniform density at a pressure of 1,013 hPa and a temperature of 0°C. One DU corresponds to a column of ozone containing $2.69 \times 1,020$ molecules per square metre. A typical value for the amount of ozone in a column of the Earth's atmosphere, although very variable, is 300 DU.

Downscaling Downscaling is a method that derives local- to regional-scale (10 to 100 km) information from larger-scale models or data analyses. Two main methods are distinguished: *dynamical downscaling* and *empirical/statistical downscaling*. The dynamical method uses the output of regional *climate models*, global models with variable spatial resolution or high-resolution global models. The empirical/statistical methods develop statistical relationships that link the large-scale atmospheric variables with local/regional climate variables. In all cases, the quality of the downscaled product depends on the quality of the driving model.

Drought In general terms, drought is a 'prolonged absence or marked deficiency of precipitation', a 'deficiency that results in water shortage for some activity or for some group', or a 'period of abnormally dry weather sufficiently prolonged for the lack of precipitation to cause a serious hydrological imbalance' (Heim, 2002). Drought has been defined in a number of ways. *Agricultural drought* relates to moisture deficits in the topmost 1 metre or so of soil (the root zone) that affect crops, *meteorological drought* is mainly a prolonged deficit of precipitation, and *hydrologic drought* is related to below-normal streamflow, lake and groundwater levels. A *megadrought* is a long-drawn out and pervasive drought, lasting much longer than normal, usually a decade or more. For further information, see Box 3.1.

Dynamical system A process or set of processes whose evolution in time is governed by a set of deterministic physical laws. The *climate system* is a dynamical system. See *Abrupt climate change*; *Chaos*; *Nonlinearity*; *Predictability*.

Ecosystem A system of living organisms interacting with each other and their physical environment. The boundaries of what could be called an ecosystem are somewhat arbitrary, depending on the focus of interest or study. Thus, the extent of an ecosystem may range from very small spatial scales to, ultimately, the entire Earth.

Efficacy A measure of how effective a *radiative forcing* from a given *anthropogenic* or natural mechanism is at changing the equilibrium *global surface temperature* compared to an equivalent *radiative forcing* from *carbon dioxide*. A carbon dioxide increase by definition has an efficacy of 1.0.

Ekman pumping Frictional stress at the surface between two fluids (*atmosphere* and ocean) or between a fluid and the adjacent solid surface (Earth's surface) forces a circulation. When the resulting mass transport is converging, mass conservation requires a vertical flow away from the surface. This is called Ekman pumping. The opposite effect, in case of divergence, is called *Ekman suction*. The effect is important in both the *atmosphere* and the ocean.

Ekman transport The total transport resulting from a balance between the Coriolis force and the frictional stress due to the action of the wind on the ocean surface. See also *Ekman pumping*.

El Niño-Southern Oscillation (ENSO) The term *El Niño* was initially used to describe a warm-water current that periodically flows along the coast of Ecuador and Perú, disrupting the local fishery. It has since become identified with a basin-wide warming of the tropical Pacific Ocean east of the dateline. This oceanic event is associated with a fluctuation of a global-scale tropical and subtropical surface pressure pattern called the Southern Oscillation. This coupled *atmosphere*-ocean phenomenon, with preferred time scales of two to about seven years, is collectively known as the El Niño-Southern Oscillation (ENSO). It is often measured by the surface pressure anomaly difference between Darwin and Tahiti and the *sea surface temperatures* in the central and eastern equatorial Pacific. During an ENSO event, the prevailing trade winds weaken, reducing upwelling and altering ocean currents such that the sea surface temperatures warm, further weakening the trade winds. This event has a great impact on the wind, sea surface temperature and precipitation patterns in the tropical Pacific. It has climatic effects throughout the Pacific *region* and in many other parts of the world, through global *teleconnections*. The cold phase of ENSO is called *La Niña*.

Emission scenario A plausible representation of the future development of emissions of substances that are potentially radiatively active (e.g., *greenhouse gases*, *aerosols*), based on a coherent and internally consistent set of assumptions about driving forces (such as demographic and socioeconomic development, technological change) and their key relationships. *Concentration scenarios*, derived from emission scenarios, are used as input to a *climate model* to compute *climate projections*. In IPCC (1992) a set of emission scenarios was presented which were used as a basis for the climate projections in IPCC (1996). These emission scenarios are referred to as the IS92 scenarios. In the IPCC Special Report on Emission Scenarios (Nakićenović and Swart, 2000) new emission scenarios, the so-called SRES scenarios, were published, some of which were used, among others, as a basis for the climate projections presented in Chapters 9 to 11 of IPCC (2001) and Chapters 10 and 11 of this report. For the meaning of some terms related to these scenarios, see *SRES scenarios*.

Energy balance The difference between the total incoming and total outgoing energy. If this balance is positive, warming occurs; if it is negative, cooling occurs. Averaged over the globe and over long time periods, this balance must be zero. Because the *climate system* derives virtually all its energy from the Sun, zero balance

implies that, globally, the amount of incoming *solar radiation* on average must be equal to the sum of the outgoing reflected solar radiation and the outgoing *thermal infrared radiation* emitted by the climate system. A perturbation of this global radiation balance, be it *anthropogenic* or natural, is called *radiative forcing*.

Ensemble A group of parallel model simulations used for *climate projections*. Variation of the results across the ensemble members gives an estimate of *uncertainty*. Ensembles made with the same model but different initial conditions only characterise the uncertainty associated with internal *climate variability*, whereas multi-model ensembles including simulations by several models also include the impact of model differences. Perturbed-parameter ensembles, in which model parameters are varied in a systematic manner, aim to produce a more objective estimate of modelling uncertainty than is possible with traditional multi-model ensembles.

Equilibrium and transient climate experiment An *equilibrium climate experiment* is an experiment in which a *climate model* is allowed to fully adjust to a change in *radiative forcing*. Such experiments provide information on the difference between the initial and final states of the model, but not on the time-dependent response. If the forcing is allowed to evolve gradually according to a prescribed *emission scenario*, the time-dependent response of a climate model may be analysed. Such an experiment is called a *transient climate experiment*. See *Climate projection*.

Equilibrium line The boundary between the region on a *glacier* where there is a net annual loss of ice mass (ablation area) and that where there is a net annual gain (accumulation area). The altitude of this boundary is referred to as *equilibrium line altitude*.

Equivalent carbon dioxide (CO₂) concentration

The concentration of *carbon dioxide* that would cause the same amount of *radiative forcing* as a given mixture of carbon dioxide and other *greenhouse gases*.

Equivalent carbon dioxide (CO₂) emission The amount of *carbon dioxide* emission that would cause the same integrated *radiative forcing*, over a given time horizon, as an emitted amount of a well mixed *greenhouse gas* or a mixture of well mixed greenhouse gases. The equivalent carbon dioxide emission is obtained by multiplying the emission of a well mixed greenhouse gas by its *Global Warming Potential* for the given time horizon. For a mix of greenhouse gases it is obtained by summing the equivalent carbon dioxide emissions of each gas. Equivalent carbon dioxide emission is a standard and useful *metric* for comparing emissions of different greenhouse gases but does not imply exact equivalence of the corresponding *climate change* responses (see Section 2.10).

Evapotranspiration The combined process of evaporation from the Earth's surface and transpiration from vegetation.

External forcing External forcing refers to a forcing agent outside the *climate system* causing a change in the climate system. Volcanic eruptions, solar variations and *anthropogenic* changes in the composition of the *atmosphere* and *land use change* are external forcings.

Extreme weather event An extreme weather event is an event that is rare at a particular place and time of year. Definitions of *rare* vary, but an extreme weather event would normally be as rare as or rarer than the 10th or 90th *percentile* of the observed *probability density function*. By definition, the characteristics of what is called *extreme weather* may vary from place to place in an absolute sense. Single extreme events cannot be simply and directly attributed to

anthropogenic climate change, as there is always a finite chance the event in question might have occurred naturally. When a pattern of extreme weather persists for some time, such as a season, it may be classed as an *extreme climate event*, especially if it yields an average or total that is itself extreme (e.g., *drought* or heavy rainfall over a season).

Faculae Bright patches on the Sun. The area covered by faculae is greater during periods of high *solar activity*.

Feedback See *Climate feedback*.

Fingerprint The *climate* response pattern in space and/or time to a specific forcing is commonly referred to as a fingerprint. Fingerprints are used to detect the presence of this response in observations and are typically estimated using forced *climate model* simulations.

Flux adjustment To avoid the problem of coupled *Atmosphere-Ocean General Circulation Models* (AOGCMs) drifting into some unrealistic *climate* state, adjustment terms can be applied to the atmosphere-ocean fluxes of heat and moisture (and sometimes the surface stresses resulting from the effect of the wind on the ocean surface) before these fluxes are imposed on the model ocean and atmosphere. Because these adjustments are pre-computed and therefore independent of the coupled model integration, they are uncorrelated with the anomalies that develop during the integration. Chapter 8 of this report concludes that most models used in this report (Fourth Assessment Report AOGCMs) do not use flux adjustments, and that in general, fewer models use them.

Forest A vegetation type dominated by trees. Many definitions of the term *forest* are in use throughout the world, reflecting wide differences in biogeophysical conditions, social structure and economics. For a discussion of the term *forest* and related terms such as *afforestation*, *reforestation* and *deforestation* see the IPCC Report on Land Use, Land-Use Change and Forestry (IPCC, 2000). See also the Report on Definitions and Methodological Options to Inventory Emissions from Direct Human-induced Degradation of Forests and Devegetation of Other Vegetation Types (IPCC, 2003).

Fossil fuel emissions Emissions of *greenhouse gases* (in particular *carbon dioxide*) resulting from the combustion of fuels from fossil carbon deposits such as oil, gas and coal.

Framework Convention on Climate Change See *United Nations Framework Convention on Climate Change* (UNFCCC).

Free atmosphere

The atmospheric layer that is negligibly affected by friction against the Earth's surface, and which is above the *atmospheric boundary layer*.

Frozen ground Soil or rock in which part or all of the *pore water* is frozen (Van Everdingen, 1998). Frozen ground includes *permafrost*. Ground that freezes and thaws annually is called *seasonally frozen ground*.

General circulation The large-scale motions of the *atmosphere* and the ocean as a consequence of differential heating on a rotating Earth, which tend to restore the *energy balance* of the system through transport of heat and momentum.

General Circulation Model (GCM) See *Climate model*.

Geoid The equipotential surface (i.e., having the same gravity potential at each point) that best fits the mean sea level (see *relative sea level*) in the absence of astronomical tides; ocean circulations;

hydrological, cryospheric and atmospheric effects; Earth rotation variations and polar motion; nutation and precession; tectonics and other effects such as *post-glacial rebound*. The geoid is global and extends over continents, oceans and *ice sheets*, and at present includes the effect of the permanent tides (zero-frequency gravitational effect from the Sun and the Moon). It is the surface of reference for astronomical observations, geodetic levelling, and for ocean, hydrological, glaciological and climate modelling. In practice, there exist various operational definitions of the geoid, depending on the way the time-variable effects mentioned above are modelled.

Geostrophic winds or currents A wind or current that is in balance with the horizontal pressure gradient and the Coriolis force, and thus is outside of the influence of friction. Thus, the wind or current is directly parallel to isobars and its speed is inversely proportional to the spacing of the isobaric contours.

Glacial isostatic adjustment See *Post-glacial rebound*.

Glacier A mass of land ice that flows downhill under gravity (through internal deformation and/or sliding at the base) and is constrained by internal stress and friction at the base and sides. A glacier is maintained by accumulation of snow at high altitudes, balanced by melting at low altitudes or discharge into the sea. See *Equilibrium line*; *Mass balance*.

Global dimming Global dimming refers to perceived widespread reduction of *solar radiation* received at the surface of the Earth from about the year 1961 to around 1990.

Global surface temperature The global surface temperature is an estimate of the global mean surface air temperature. However, for changes over time, only anomalies, as departures from a climatology, are used, most commonly based on the area-weighted global average of the *sea surface temperature* anomaly and *land surface air temperature* anomaly.

Global Warming Potential (GWP) An index, based upon radiative properties of well-mixed *greenhouse gases*, measuring the *radiative forcing* of a unit mass of a given well-mixed greenhouse gas in the present-day *atmosphere* integrated over a chosen time horizon, relative to that of *carbon dioxide*. The GWP represents the combined effect of the differing times these gases remain in the atmosphere and their relative effectiveness in absorbing outgoing *thermal infrared radiation*. The *Kyoto Protocol* is based on GWPs from pulse emissions over a 100-year time frame.

Greenhouse effect *Greenhouse gases* effectively absorb *thermal infrared radiation*, emitted by the Earth's surface, by the *atmosphere* itself due to the same gases, and by clouds. Atmospheric radiation is emitted to all sides, including downward to the Earth's surface. Thus, greenhouse gases trap heat within the surface-*troposphere* system. This is called the *greenhouse effect*. Thermal infrared radiation in the troposphere is strongly coupled to the temperature of the atmosphere at the altitude at which it is emitted. In the troposphere, the temperature generally decreases with height. Effectively, infrared radiation emitted to space originates from an altitude with a temperature of, on average, -19°C , in balance with the net incoming *solar radiation*, whereas the Earth's surface is kept at a much higher temperature of, on average, $+14^{\circ}\text{C}$. An increase in the concentration of greenhouse gases leads to an increased infrared opacity of the atmosphere, and therefore to an effective radiation into space from a higher altitude at a lower temperature. This causes a *radiative forcing* that leads to an enhancement of the greenhouse effect, the so-called *enhanced greenhouse effect*.

Greenhouse gas (GHG) Greenhouse gases are those gaseous constituents of the *atmosphere*, both natural and *anthropogenic*, that absorb and emit radiation at specific wavelengths within the spectrum of *thermal infrared radiation* emitted by the Earth's surface, the atmosphere itself, and by clouds. This property causes the *greenhouse effect*. Water vapour (H₂O), *carbon dioxide* (CO₂), nitrous oxide (N₂O), methane (CH₄) and *ozone* (O₃) are the primary greenhouse gases in the Earth's atmosphere. Moreover, there are a number of entirely human-made greenhouse gases in the atmosphere, such as the *halocarbons* and other chlorine- and bromine-containing substances, dealt with under the *Montreal Protocol*. Beside CO₂, N₂O and CH₄, the *Kyoto Protocol* deals with the greenhouse gases sulphur hexafluoride (SF₆), hydrofluorocarbons (HFCs) and perfluorocarbons (PFCs).

Gross Primary Production (GPP) The amount of energy fixed from the *atmosphere* through *photosynthesis*.

Ground ice A general term referring to all types of ice contained in freezing and seasonally *frozen ground* and *permafrost* (Van Everdingen, 1998).

Ground temperature The temperature of the ground near the surface (often within the first 10 cm). It is often called *soil temperature*.

Grounding line/zone The junction between a *glacier* or *ice sheet* and *ice shelf*; the place where ice starts to float.

Gyre Basin-scale ocean horizontal circulation pattern with slow flow circulating around the ocean basin, closed by a strong and narrow (100–200 km wide) boundary current on the western side. The subtropical gyres in each ocean are associated with high pressure in the centre of the gyres; the subpolar gyres are associated with low pressure.

Hadley Circulation A direct, thermally driven overturning cell in the *atmosphere* consisting of poleward flow in the upper *troposphere*, subsiding air into the subtropical anticyclones, return flow as part of the trade winds near the surface, and with rising air near the equator in the so-called *Inter-Tropical Convergence Zone*.

Halocarbons A collective term for the group of partially halogenated organic species, including the chlorofluorocarbons (CFCs), hydrochlorofluorocarbons (HCFCs), hydrofluorocarbons (HFCs), halons, methyl chloride, methyl bromide, etc. Many of the halocarbons have large *Global Warming Potentials*. The chlorine- and bromine-containing halocarbons are also involved in the depletion of the *ozone layer*.

Halosteric See *Sea level change*.

HCFC See *Halocarbons*.

HFC See *Halocarbons*.

Heterotrophic respiration The conversion of organic matter to *carbon dioxide* by organisms other than plants.

Holocene The Holocene geological epoch is the latter of two *Quaternary* epochs, extending from about 11.6 ka to and including the present.

Hydrosphere The component of the *climate system* comprising liquid surface and subterranean water, such as oceans, seas, rivers, fresh water lakes, underground water, etc.

Ice age An ice age or *glacial period* is characterised by a long-term reduction in the temperature of the Earth's *climate*,

resulting in growth of continental *ice sheets* and mountain *glaciers* (*glaciation*).

Ice cap A dome shaped ice mass, usually covering a highland area, which is considerably smaller in extent than an *ice sheet*.

Ice core A cylinder of ice drilled out of a *glacier* or *ice sheet*.

Ice sheet A mass of land ice that is sufficiently deep to cover most of the underlying bedrock topography, so that its shape is mainly determined by its dynamics (the flow of the ice as it deforms internally and/or slides at its base). An ice sheet flows outward from a high central ice plateau with a small average surface slope. The margins usually slope more steeply, and most ice is discharged through fast-flowing *ice streams* or outlet *glaciers*, in some cases into the sea or into *ice shelves* floating on the sea. There are only three large ice sheets in the modern world, one on Greenland and two on Antarctica, the East and West Antarctic Ice Sheets, divided by the Transantarctic Mountains. During glacial periods there were others.

Ice shelf A floating slab of ice of considerable thickness extending from the coast (usually of great horizontal extent with a level or gently sloping surface), often filling embayments in the coastline of the *ice sheets*. Nearly all ice shelves are in Antarctica, where most of the ice discharged seaward flows into ice shelves.

Ice stream A stream of ice flowing faster than the surrounding *ice sheet*. It can be thought of as a *glacier* flowing between walls of slower-moving ice instead of rock.

Indirect aerosol effect *Aerosols* may lead to an indirect *radiative forcing* of the *climate system* through acting as *cloud condensation nuclei* or modifying the optical properties and lifetime of clouds. Two indirect effects are distinguished:

Cloud albedo effect A radiative forcing induced by an increase in *anthropogenic* aerosols that cause an initial increase in droplet concentration and a decrease in droplet size for fixed liquid water content, leading to an increase in cloud *albedo*. This effect is also known as the *first indirect effect* or *Twomey effect*.

Cloud lifetime effect A forcing induced by an increase in anthropogenic aerosols that cause a decrease in droplet size, reducing the precipitation efficiency, thereby modifying the liquid water content, cloud thickness and cloud life time. This effect is also known as the *second indirect effect* or *Albrecht effect*.

Apart from these indirect effects, aerosols may have a *semi-direct effect*. This refers to the absorption of *solar radiation* by absorbing aerosol, which heats the air and tends to increase the static stability relative to the surface. It may also cause evaporation of cloud droplets.

Industrial revolution A period of rapid industrial growth with far-reaching social and economic consequences, beginning in Britain during the second half of the eighteenth century and spreading to Europe and later to other countries including the United States. The invention of the steam engine was an important trigger of this development. The industrial revolution marks the beginning of a strong increase in the use of fossil fuels and emission of, in particular, fossil *carbon dioxide*. In this report the terms *pre-industrial* and *industrial* refer, somewhat arbitrarily, to the periods before and after 1750, respectively.

Infrared radiation See *Thermal infrared radiation*.

Insolation The amount of *solar radiation* reaching the Earth by latitude and by season. Usually *insolation* refers to the radiation arriving at the top of the *atmosphere*. Sometimes it is specified as referring to the radiation arriving at the Earth's surface. See also: *Total Solar Irradiance*.

Interglacials The warm periods between *ice age* glaciations. The previous interglacial, dated approximately from 129 to 116 ka, is referred to as the *Last Interglacial* (AMS, 2000)

Internal variability See *Climate variability*.

Inter-Tropical Convergence Zone (ITCZ) The Inter-Tropical Convergence Zone is an equatorial zonal belt of low pressure near the equator where the northeast trade winds meet the southeast trade winds. As these winds converge, moist air is forced upward, resulting in a band of heavy precipitation. This band moves seasonally.

Isostatic or Isostasy Isostasy refers to the way in which the *lithosphere* and mantle respond visco-elastically to changes in surface loads. When the loading of the lithosphere and/or the mantle is changed by alterations in land ice mass, ocean mass, sedimentation, erosion or mountain building, vertical isostatic adjustment results, in order to balance the new load.

Kyoto Protocol The Kyoto Protocol to the *United Nations Framework Convention on Climate Change* (UNFCCC) was adopted in 1997 in Kyoto, Japan, at the Third Session of the Conference of the Parties (COP) to the UNFCCC. It contains legally binding commitments, in addition to those included in the UNFCCC. Countries included in Annex B of the Protocol (most Organisation for Economic Cooperation and Development countries and countries with economies in transition) agreed to reduce their *anthropogenic greenhouse gas* emissions (*carbon dioxide*, methane, nitrous oxide, hydrofluorocarbons, perfluorocarbons, and sulphur hexafluoride) by at least 5% below 1990 levels in the commitment period 2008 to 2012. The Kyoto Protocol entered into force on 16 February 2005.

Land use and Land use change *Land use* refers to the total of arrangements, activities and inputs undertaken in a certain land cover type (a set of human actions). The term land use is also used in the sense of the social and economic purposes for which land is managed (e.g., grazing, timber extraction and conservation). *Land use change* refers to a change in the use or management of land by humans, which may lead to a change in land cover. Land cover and land use change may have an impact on the surface *albedo*, *evapotranspiration*, *sources* and *sinks* of *greenhouse gases*, or other properties of the *climate system* and may thus have a *radiative forcing* and/or other impacts on *climate*, locally or globally. See also the IPCC Report on Land Use, Land-Use Change, and Forestry (IPCC, 2000).

La Niña See *El Niño-Southern Oscillation*.

Land surface air temperature The surface air temperature as measured in well-ventilated screens over land at 1.5 m above the ground.

Lapse rate The rate of change of an atmospheric variable, usually temperature, with height. The lapse rate is considered positive when the variable decreases with height.

Last Glacial Maximum (LGM) The Last Glacial Maximum refers to the time of maximum extent of the *ice sheets* during the last glaciation, approximately 21 ka. This period has been widely studied because the *radiative forcings* and boundary conditions are relatively well known and because the global cooling during that period is comparable with the projected warming over the 21st century.

Last Interglacial (LIG) See *Interglacial*.

Latent heat flux The flux of heat from the Earth's surface to the *atmosphere* that is associated with evaporation or condensation of water vapour at the surface; a component of the surface energy budget.

Level of Scientific Understanding (LOSU) This is an index on a 5-step scale (high, medium, medium-low, low and very low) designed to characterise the degree of scientific understanding of the *radiative forcing* agents that affect *climate change*. For each agent, the index represents a subjective judgement about the evidence for the physical/chemical mechanisms determining the forcing and the consensus surrounding the quantitative estimate and its *uncertainty*.

Lifetime Lifetime is a general term used for various time scales characterising the rate of processes affecting the concentration of trace gases. The following lifetimes may be distinguished:

Turnover time (T) (also called *global atmospheric lifetime*) is the ratio of the mass *M* of a *reservoir* (e.g., a gaseous compound in the *atmosphere*) and the total rate of removal *S* from the reservoir: $T = M / S$. For each removal process, separate turnover times can be defined. In soil carbon biology, this is referred to as *Mean Residence Time*.

Adjustment time or *response time (T_a)* is the time scale characterising the decay of an instantaneous pulse input into the reservoir. The term adjustment time is also used to characterise the adjustment of the mass of a reservoir following a step change in the *source* strength. *Half-life* or *decay constant* is used to quantify a first-order exponential decay process. See *response time* for a different definition pertinent to *climate* variations.

The term *lifetime* is sometimes used, for simplicity, as a surrogate for *adjustment time*.

In simple cases, where the global removal of the compound is directly proportional to the total mass of the reservoir, the adjustment time equals the turnover time: $T = T_a$. An example is *CFC-11*, which is removed from the *atmosphere* only by photochemical processes in the *stratosphere*. In more complicated cases, where several reservoirs are involved or where the removal is not proportional to the total mass, the equality $T = T_a$ no longer holds. *Carbon dioxide* (CO_2) is an extreme example. Its turnover time is only about four years because of the rapid exchange between the atmosphere and the ocean and terrestrial biota. However, a large part of that CO_2 is returned to the atmosphere within a few years. Thus, the adjustment time of CO_2 in the atmosphere is actually determined by the rate of removal of carbon from the surface layer of the oceans into its deeper layers. Although an approximate value of 100 years may be given for the adjustment time of CO_2 in the atmosphere, the actual adjustment is faster initially and slower later on. In the case of methane (CH_4), the adjustment time is different from the turnover time because the removal is mainly through a chemical reaction with the hydroxyl radical OH, the concentration of which itself depends on the CH_4 concentration. Therefore, the CH_4 removal rate *S* is not proportional to its total mass *M*.

Likelihood The likelihood of an occurrence, an outcome or a result, where this can be estimated probabilistically, is expressed in this report using a standard terminology, defined in Box 1.1. See also *Uncertainty*; *Confidence*.

Lithosphere The upper layer of the solid Earth, both continental and oceanic, which comprises all crustal rocks and the cold, mainly elastic part of the uppermost mantle. Volcanic activity, although part of the lithosphere, is not considered as part of the *climate system*, but acts as an *external forcing* factor. See *Isostatic*.

Little Ice Age (LIA) An interval between approximately AD 1400 and 1900 when temperatures in the Northern Hemisphere were generally colder than today's, especially in Europe.

Mass balance (of glaciers, ice caps or ice sheets) The balance between the mass input to the ice body (accumulation) and the mass loss (ablation, iceberg calving). Mass balance terms include the following:

Specific mass balance: net mass loss or gain over a hydrological cycle at a point on the surface of a *glacier*.

Total mass balance (of the glacier): The specific mass balance spatially integrated over the entire glacier area; the total mass a glacier gains or loses over a hydrological cycle.

Mean specific mass balance: The total mass balance per unit area of the glacier. If *surface* is specified (*specific surface mass balance*, etc.) then ice flow contributions are not considered; otherwise, mass balance includes contributions from ice flow and iceberg calving. The specific surface mass balance is positive in the accumulation area and negative in the ablation area.

Mean sea level See *Relative sea level*.

Medieval Warm Period (MWP) An interval between AD 1000 and 1300 in which some Northern Hemisphere *regions* were warmer than during the *Little Ice Age* that followed.

Meridional Overturning Circulation (MOC) Meridional (north-south) overturning circulation in the ocean quantified by zonal (east-west) sums of mass transports in depth or density layers. In the North Atlantic, away from the subpolar *regions*, the MOC (which is in principle an observable quantity) is often identified with the *Thermohaline Circulation* (THC), which is a conceptual interpretation. However, it must be borne in mind that the MOC can also include shallower, wind-driven overturning cells such as occur in the upper ocean in the tropics and subtropics, in which warm (light) waters moving poleward are transformed to slightly denser waters and *subducted* equatorward at deeper levels.

Metadata Information about meteorological and climatological data concerning how and when they were measured, their quality, known problems and other characteristics.

Metric A consistent measurement of a characteristic of an object or activity that is otherwise difficult to quantify.

Mitigation A human intervention to reduce the *sources* or enhance the *sinks* of *greenhouse gases*.

Mixing ratio See *Mole fraction*.

Model hierarchy See *Climate model* (spectrum or hierarchy).

Modes of climate variability Natural variability of the *climate system*, in particular on seasonal and longer time scales, predominantly occurs with preferred spatial patterns and time scales, through the dynamical characteristics of the atmospheric circulation and through interactions with the land and ocean surfaces. Such patterns are often called *regimes*, *modes* or *teleconnections*. Examples are the *North Atlantic Oscillation* (NAO), the *Pacific-North American pattern* (PNA), the *El Niño-Southern Oscillation* (ENSO), the *Northern Annular Mode* (NAM; previously called Arctic Oscillation, AO) and the *Southern Annular Mode* (SAM; previously called the Antarctic Oscillation, AAO). Many of the prominent modes of climate variability are discussed in section 3.6. See also *Patterns of climate variability*.

Mole fraction Mole fraction, or *mixing ratio*, is the ratio of the number of moles of a constituent in a given volume to the total number of moles of all constituents in that volume. It is usually reported for dry air. Typical values for long-lived *greenhouse gases* are in the order of $\mu\text{mol mol}^{-1}$ (parts per million: *ppm*), nmol mol^{-1} (parts per billion: *ppb*), and fmol mol^{-1} (parts per trillion: *ppt*). Mole

fraction differs from *volume mixing ratio*, often expressed in ppmv etc., by the corrections for non-ideality of gases. This correction is significant relative to measurement precision for many greenhouse gases. (Schwartz and Warneck, 1995).

Monsoon A monsoon is a tropical and subtropical seasonal reversal in both the surface winds and associated precipitation, caused by differential heating between a continental-scale land mass and the adjacent ocean. Monsoon rains occur mainly over land in summer.

Montreal Protocol The Montreal Protocol on Substances that Deplete the Ozone Layer was adopted in Montreal in 1987, and subsequently adjusted and amended in London (1990), Copenhagen (1992), Vienna (1995), Montreal (1997) and Beijing (1999). It controls the consumption and production of chlorine- and bromine-containing chemicals that destroy stratospheric *ozone*, such as chlorofluorocarbons, methyl chloroform, carbon tetrachloride and many others.

Microwave Sounding Unit (MSU) A satellite-borne microwave sounder that estimates the temperature of thick layers of the *atmosphere* by measuring the thermal emission of oxygen molecules from a complex of emission lines near 60 GHz. A series of nine MSUs began making this kind of measurement in late 1978. Beginning in mid 1998, a follow-on series of instruments, the Advanced Microwave Sounding Units (AMSUs), began operation.

MSU See *Microwave Sounding Unit*.

Nonlinearity A process is called *nonlinear* when there is no simple proportional relation between cause and effect. The *climate system* contains many such nonlinear processes, resulting in a system with a potentially very complex behaviour. Such complexity may lead to *abrupt climate change*. See also *Chaos; Predictability*.

North Atlantic Oscillation (NAO) The North Atlantic Oscillation consists of opposing variations of barometric pressure near Iceland and near the Azores. It therefore corresponds to fluctuations in the strength of the main westerly winds across the Atlantic into Europe, and thus to fluctuations in the embedded cyclones with their associated frontal systems. See NAO Index, Box 3.4.

Northern Annular Mode (NAM) A winter fluctuation in the amplitude of a pattern characterised by low surface pressure in the Arctic and strong mid-latitude westerlies. The NAM has links with the northern polar vortex into the *stratosphere*. Its pattern has a bias to the North Atlantic and has a large correlation with the *North Atlantic Oscillation*. See NAM Index, Box 3.4.

Ocean acidification A decrease in the *pH* of sea water due to the *uptake* of *anthropogenic carbon dioxide*.

Ocean heat uptake efficiency This is a measure ($\text{W m}^{-2} \text{ } ^\circ\text{C}^{-1}$) of the rate at which heat storage by the global ocean increases as global surface temperature rises. It is a useful parameter for *climate change* experiments in which the *radiative forcing* is changing monotonically, when it can be compared with the climate sensitivity parameter to gauge the relative importance of climate response and ocean heat uptake in determining the rate of climate change. It can be estimated from a $1\% \text{ yr}^{-1}$ atmospheric *carbon dioxide* increase experiment as the ratio of the global average top-of-*atmosphere* net downward radiative flux to the *transient climate response* (see *climate sensitivity*).

Organic aerosol *Aerosol* particles consisting predominantly of organic compounds, mainly carbon, hydrogen, oxygen and lesser amounts of other elements. (Charlson and Heintzenberg, 1995, p. 405). See *Carbonaceous aerosol*.

Ozone Ozone, the triatomic form of oxygen (O₃), is a gaseous atmospheric constituent. In the *troposphere*, it is created both naturally and by photochemical reactions involving gases resulting from human activities (*smog*). Tropospheric ozone acts as a *greenhouse gas*. In the *stratosphere*, it is created by the interaction between solar ultraviolet radiation and molecular oxygen (O₂). Stratospheric ozone plays a dominant role in the stratospheric radiative balance. Its concentration is highest in the *ozone layer*.

Ozone hole See *Ozone layer*.

Ozone layer The *stratosphere* contains a layer in which the concentration of *ozone* is greatest, the so-called ozone layer. The layer extends from about 12 to 40 km above the Earth's surface. The ozone concentration reaches a maximum between about 20 and 25 km. This layer is being depleted by human emissions of chlorine and bromine compounds. Every year, during the Southern Hemisphere spring, a very strong depletion of the ozone layer takes place over the antarctic *region*, caused by *anthropogenic* chlorine and bromine compounds in combination with the specific meteorological conditions of that region. This phenomenon is called the *ozone hole*. See *Montreal Protocol*.

Pacific decadal variability Coupled decadal-to-inter-decadal variability of the atmospheric circulation and underlying ocean in the Pacific Basin. It is most prominent in the North Pacific, where fluctuations in the strength of the winter Aleutian Low pressure system co-vary with North Pacific *sea surface temperatures*, and are linked to decadal variations in atmospheric circulation, sea surface temperatures and ocean circulation throughout the whole Pacific Basin. Such fluctuations have the effect of modulating the *El Niño-Southern Oscillation* cycle. Key measures of Pacific decadal variability are the *North Pacific Index (NPI)*, the *Pacific Decadal Oscillation (PDO)* index and the *Inter-decadal Pacific Oscillation (IPO)* index, all defined in Box 3.4.

Pacific-North American (PNA) pattern An atmospheric large-scale wave pattern featuring a sequence of tropospheric high- and low-pressure anomalies stretching from the subtropical west Pacific to the east coast of North America. See PNA pattern index, Box 3.4.

Palaeoclimate *Climate* during periods prior to the development of measuring instruments, including historic and geologic time, for which only *proxy* climate records are available.

Parametrization In *climate models*, this term refers to the technique of representing processes that cannot be explicitly resolved at the spatial or temporal resolution of the model (sub-grid scale processes) by relationships between model-resolved larger-scale flow and the area- or time-averaged effect of such sub-grid scale processes.

Patterns of climate variability See *Modes of climate variability*.

Percentile A percentile is a value on a scale of one hundred that indicates the percentage of the data set values that is equal to or below it. The percentile is often used to estimate the extremes of a distribution. For example, the 90th (10th) percentile may be used to refer to the threshold for the upper (lower) extremes.

Permafrost Ground (soil or rock and included ice and organic material) that remains at or below 0°C for at least two consecutive years (Van Everdingen, 1998).

pH pH is a dimensionless measure of the acidity of water (or any solution) given by its concentration of hydrogen ions (H⁺). pH is measured on a logarithmic scale where

$\text{pH} = -\log_{10}(\text{H}^+)$. Thus, a pH decrease of 1 unit corresponds to a 10-fold increase in the concentration of H⁺, or acidity.

Photosynthesis The process by which plants take carbon dioxide from the air (or bicarbonate in water) to build carbohydrates, releasing oxygen in the process. There are several pathways of photosynthesis with different responses to atmospheric carbon dioxide concentrations. See Carbon dioxide fertilization; C3 plants; C4 plants.

Plankton Microorganisms living in the upper layers of aquatic systems. A distinction is made between *phytoplankton*, which depend on *photosynthesis* for their energy supply, and *zooplankton*, which feed on phytoplankton.

Pleistocene The earlier of two *Quaternary* epochs, extending from the end of the Pliocene, about 1.8 Ma, until the beginning of the *Holocene* about 11.6 ka.

Pollen analysis A technique of both relative dating and environmental *reconstruction*, consisting of the identification and counting of pollen types preserved in peat, lake sediments and other deposits. See *Proxy*.

Post-glacial rebound The vertical movement of the land and sea floor following the reduction of the load of an ice mass, for example, since the *Last Glacial Maximum* (21 ka). The rebound is an *isostatic* land movement.

Precipitable water The total amount of atmospheric water vapour in a vertical column of unit cross-sectional area. It is commonly expressed in terms of the height of the water if completely condensed and collected in a vessel of the same unit cross section.

Precursors Atmospheric compounds that are not *greenhouse gases* or *aerosols*, but that have an effect on greenhouse gas or aerosol concentrations by taking part in physical or chemical processes regulating their production or destruction rates.

Predictability The extent to which future states of a system may be predicted based on knowledge of current and past states of the system.

Since knowledge of the *climate system*'s past and current states is generally imperfect, as are the models that utilise this knowledge to produce a *climate prediction*, and since the climate system is inherently *nonlinear* and *chaotic*, predictability of the climate system is inherently limited. Even with arbitrarily accurate models and observations, there may still be limits to the predictability of such a nonlinear system (AMS, 2000)

Pre-industrial See *Industrial revolution*.

Probability Density Function (PDF) A probability density function is a function that indicates the relative chances of occurrence of different outcomes of a variable. The function integrates to unity over the domain for which it is defined and has the property that the integral over a sub-domain equals the probability that the outcome of the variable lies within that sub-domain. For example, the probability that a temperature anomaly defined in a particular way is greater than zero is obtained from its PDF by integrating the PDF over all possible temperature anomalies greater than zero. Probability density functions that describe two or more variables simultaneously are similarly defined.

Projection A projection is a potential future evolution of a quantity or set of quantities, often computed with the aid of a model.

Projections are distinguished from *predictions* in order to emphasize that projections involve assumptions concerning, for example, future socioeconomic and technological developments that may or may not be realised, and are therefore subject to substantial *uncertainty*. See also *Climate projection*; *Climate prediction*.

Proxy A proxy *climate* indicator is a local record that is interpreted, using physical and biophysical principles, to represent some combination of climate-related variations back in time. Climate-related data derived in this way are referred to as proxy data. Examples of proxies include *pollen analysis*, *tree ring* records, characteristics of corals and various data derived from *ice cores*.

Quaternary The period of geological time following the *Tertiary* (65 Ma to 1.8 Ma). Following the current definition (which is under revision at present) the Quaternary extends from 1.8 Ma until the present. It is formed of two epochs, the *Pleistocene* and the *Holocene*.

Radiative forcing Radiative forcing is the change in the net, downward minus upward, irradiance (expressed in W m^{-2}) at the *tropopause* due to a change in an external driver of *climate change*, such as, for example, a change in the concentration of *carbon dioxide* or the output of the Sun. Radiative forcing is computed with all tropospheric properties held fixed at their unperturbed values, and after allowing for stratospheric temperatures, if perturbed, to readjust to radiative-dynamical equilibrium. Radiative forcing is called *instantaneous* if no change in stratospheric temperature is accounted for. For the purposes of this report, radiative forcing is further defined as the change relative to the year 1750 and, unless otherwise noted, refers to a global and annual average value. Radiative forcing is not to be confused with *cloud radiative forcing*, a similar terminology for describing an unrelated measure of the impact of clouds on the irradiance at the top of the *atmosphere*.

Radiative forcing scenario A plausible representation of the future development of *radiative forcing* associated, for example, with changes in atmospheric composition or *land use change*, or with external factors such as variations in *solar activity*. Radiative forcing scenarios can be used as input into simplified *climate models* to compute *climate projections*.

Rapid climate change See *Abrupt climate change*.

Reanalysis Reanalyses are atmospheric and oceanic analyses of temperature, wind, current, and other meteorological and oceanographic quantities, created by processing past meteorological and oceanographic data using fixed state-of-the-art weather forecasting models and data assimilation techniques. Using fixed data assimilation avoids effects from the changing analysis system that occurs in operational analyses. Although continuity is improved, global reanalyses still suffer from changing coverage and biases in the observing systems.

Reconstruction The use of *climate* indicators to help determine (generally past) climates.

Reforestation Planting of forests on lands that have previously contained forests but that have been converted to some other use. For a discussion of the term *forest* and related terms such as *afforestation*, reforestation and *deforestation*, see the IPCC Report on Land Use, Land-Use Change and Forestry (IPCC, 2000). See also the Report on Definitions and Methodological Options to Inventory Emissions from Direct Human-induced Degradation of Forests and Devegetation of Other Vegetation Types (IPCC, 2003)

Regime A regime is preferred states of the *climate system*, often representing one phase of dominant patterns or *modes of climate variability*.

Region A region is a territory characterised by specific geographical and climatological features. The *climate* of a region is affected by regional and local scale forcings like topography, *land use* characteristics, lakes, etc., as well as remote influences from other regions. See *Teleconnection*.

Relative sea level Sea level measured by a *tide gauge* with respect to the land upon which it is situated. *Mean sea level* is normally defined as the average relative sea level over a period, such as a month or a year, long enough to average out transients such as waves and tides. See *Sea level change*.

Reservoir A component of the *climate system*, other than the *atmosphere*, which has the capacity to store, accumulate or release a substance of concern, for example, carbon, a *greenhouse gas* or a *precursor*. Oceans, soils and *forests* are examples of reservoirs of carbon. *Pool* is an equivalent term (note that the definition of pool often includes the atmosphere). The absolute quantity of the substance of concern held within a reservoir at a specified time is called the *stock*.

Respiration The process whereby living organisms convert organic matter to *carbon dioxide*, releasing energy and consuming molecular oxygen.

Response time The response time or *adjustment time* is the time needed for the *climate system* or its components to re-equilibrate to a new state, following a forcing resulting from external and internal processes or *feedbacks*. It is very different for various components of the climate system. The response time of the *troposphere* is relatively short, from days to weeks, whereas the *stratosphere* reaches equilibrium on a time scale of typically a few months. Due to their large heat capacity, the oceans have a much longer response time: typically decades, but up to centuries or millennia. The response time of the strongly coupled surface-troposphere system is, therefore, slow compared to that of the stratosphere, and mainly determined by the oceans. The *biosphere* may respond quickly (e.g., to *droughts*), but also very slowly to imposed changes. See *lifetime* for a different definition of response time pertinent to the rate of processes affecting the concentration of trace gases.

Return period The average time between occurrences of a defined event (AMS, 2000).

Return value The highest (or, alternatively, lowest) value of a given variable, on average occurring once in a given period of time (e.g., in 10 years).

Scenario A plausible and often simplified description of how the future may develop, based on a coherent and internally consistent set of assumptions about driving forces and key relationships. Scenarios may be derived from *projections*, but are often based on additional information from other sources, sometimes combined with a *narrative storyline*. See also *SRES scenarios*; *Climate scenario*; *Emission scenario*.

Sea ice Any form of ice found at sea that has originated from the freezing of seawater. Sea ice may be discontinuous pieces (ice floes) moved on the ocean surface by wind and currents (pack ice), or a motionless sheet attached to the coast (land-fast ice). Sea ice less than one year old is called *first-year ice*. *Multi-year ice* is sea ice that has survived at least one summer melt season.

Sea level change Sea level can change, both globally and locally, due to (i) changes in the shape of the ocean basins, (ii) changes in the total mass of water and (iii) changes in water density. Sea level changes induced by changes in water density are called *steric*. Density changes induced by temperature changes only are called *thermosteric*, while density changes induced by salinity changes are called *halosteric*. See also *Relative Sea Level*; *Thermal expansion*.

Sea level equivalent (SLE) The change in global average sea level that would occur if a given amount of water or ice were added to or removed from the oceans.

Seasonally frozen ground See *Frozen ground*.

Sea surface temperature (SST) The sea surface temperature is the temperature of the subsurface bulk temperature in the top few metres of the ocean, measured by ships, buoys and drifters. From ships, measurements of water samples in buckets were mostly switched in the 1940s to samples from engine intake water. Satellite measurements of *skin temperature* (uppermost layer; a fraction of a millimetre thick) in the infrared or the top centimetre or so in the microwave are also used, but must be adjusted to be compatible with the bulk temperature.

Sensible heat flux The flux of heat from the Earth's surface to the *atmosphere* that is not associated with phase changes of water; a component of the surface energy budget.

Sequestration See *Uptake*.

Significant wave height The average height of the highest one-third of the wave heights (sea and swell) occurring in a particular time period.

Sink Any process, activity or mechanism that removes a *greenhouse gas*, an *aerosol* or a *precursor* of a greenhouse gas or aerosol from the *atmosphere*.

Slab-ocean model A simplified presentation in a *climate model* of the ocean as a motionless layer of water with a depth of 50 to 100 m. Climate models with a slab ocean can only be used for estimating the equilibrium response of climate to a given forcing, not the transient evolution of climate. See *Equilibrium and transient climate experiment*.

Snow line The lower limit of permanent snow cover, below which snow does not accumulate.

Soil moisture Water stored in or at the land surface and available for evaporation.

Soil temperature See *Ground temperature*.

Solar activity The Sun exhibits periods of high activity observed in numbers of *sunspots*, as well as radiative output, magnetic activity and emission of high-energy particles. These variations take place on a range of time scales from millions of years to minutes. See *Solar cycle*.

Solar ('11 year') cycle A quasi-regular modulation of *solar activity* with varying amplitude and a period of between 9 and 13 years.

Solar radiation Electromagnetic radiation emitted by the Sun. It is also referred to as *shortwave radiation*. Solar radiation has a distinctive range of wavelengths (spectrum) determined by the temperature of the Sun, peaking in visible wavelengths. See also: *Thermal infrared radiation*, *Insolation*.

Soot Particles formed during the quenching of gases at the outer edge of flames of organic vapours, consisting predominantly of carbon, with lesser amounts of oxygen and hydrogen present as carboxyl and phenolic groups and exhibiting an imperfect graphitic structure. See *Black carbon*; *Charcoal* (Charlson and Heintzenberg, 1995, p. 406).

Source Any process, activity or mechanism that releases a *greenhouse gas*, an *aerosol* or a *precursor* of a greenhouse gas or aerosol into the *atmosphere*.

Southern Annular Mode (SAM) The fluctuation of a pattern like the *Northern Annular Mode*, but in the Southern Hemisphere. See SAM Index, Box 3.4.

Southern Oscillation See *El Niño-Southern Oscillation* (ENSO).

Spatial and temporal scales *Climate* may vary on a large range of spatial and temporal scales. Spatial scales may range from local (less than 100,000 km²), through regional (100,000 to 10 million km²) to continental (10 to 100 million km²). Temporal scales may range from seasonal to geological (up to hundreds of millions of years).

SRES scenarios SRES scenarios are *emission scenarios* developed by Nakićenović and Swart (2000) and used, among others, as a basis for some of the *climate projections* shown in Chapter 10 of this report. The following terms are relevant for a better understanding of the structure and use of the set of SRES scenarios:

Scenario family Scenarios that have a similar demographic, societal, economic and technical change storyline. Four scenario families comprise the SRES scenario set: A1, A2, B1 and B2.

Illustrative Scenario A scenario that is illustrative for each of the six scenario groups reflected in the Summary for Policymakers of Nakićenović and Swart (2000). They include four revised *scenario markers* for the scenario groups A1B, A2, B1, B2, and two additional scenarios for the A1FI and A1T groups. All scenario groups are equally sound.

Marker Scenario A scenario that was originally posted in draft form on the SRES website to represent a given scenario family. The choice of markers was based on which of the initial quantifications best reflected the storyline, and the features of specific models. Markers are no more likely than other scenarios, but are considered by the SRES writing team as illustrative of a particular storyline. They are included in revised form in Nakićenović and Swart (2000). These scenarios received the closest scrutiny of the entire writing team and via the SRES open process. Scenarios were also selected to illustrate the other two scenario groups.

Storyline A narrative description of a scenario (or family of scenarios), highlighting the main scenario characteristics, relationships between key driving forces and the dynamics of their evolution.

Steric See *Sea level change*.

Stock See *Reservoir*.

Storm surge The temporary increase, at a particular locality, in the height of the sea due to extreme meteorological conditions (low atmospheric pressure and/or strong winds). The storm surge is defined as being the excess above the level expected from the tidal variation alone at that time and place.

Storm tracks Originally, a term referring to the tracks of individual cyclonic weather systems, but now often generalised to refer to the *regions* where the main tracks of extratropical disturbances occur as sequences of low (cyclonic) and high (anticyclonic) pressure systems.

Stratosphere The highly stratified region of the *atmosphere* above the *troposphere* extending from about 10 km (ranging from 9 km at high latitudes to 16 km in the tropics on average) to about 50 km altitude.

Subduction Ocean process in which surface waters enter the ocean interior from the surface mixed layer through *Ekman pumping* and lateral *advection*. The latter occurs when surface waters are advected to a region where the local surface layer is less dense and therefore must slide below the surface layer, usually with no change in density.

Sunspots Small dark areas on the Sun. The number of sunspots is higher during periods of high *solar activity*, and varies in particular with the *solar cycle*.

Surface layer See *Atmospheric boundary layer*.

Surface temperature See *Global surface temperature*; *Ground temperature*; *Land surface air temperature*; *Sea surface temperature*.

Teleconnection A connection between *climate variations* over widely separated parts of the world. In physical terms, teleconnections are often a consequence of large-scale wave motions, whereby energy is transferred from source regions along preferred paths in the *atmosphere*.

Thermal expansion In connection with sea level, this refers to the increase in volume (and decrease in density) that results from warming water. A warming of the ocean leads to an expansion of the ocean volume and hence an increase in sea level. See *Sea level change*.

Thermal infrared radiation Radiation emitted by the Earth's surface, the *atmosphere* and the clouds. It is also known as *terrestrial* or *longwave radiation*, and is to be distinguished from the near-infrared radiation that is part of the solar spectrum. Infrared radiation, in general, has a distinctive range of wavelengths (*spectrum*) longer than the wavelength of the red colour in the visible part of the spectrum. The spectrum of thermal infrared radiation is practically distinct from that of shortwave or *solar radiation* because of the difference in temperature between the Sun and the Earth-atmosphere system.

Thermocline The layer of maximum vertical temperature gradient in the ocean, lying between the surface ocean and the abyssal ocean. In subtropical regions, its source waters are typically surface waters at higher latitudes that have *subducted* and moved equatorward. At high latitudes, it is sometimes absent, replaced by a *halocline*, which is a layer of maximum vertical salinity gradient.

Thermohaline circulation (THC) Large-scale circulation in the ocean that transforms low-density upper ocean waters to higher-density intermediate and deep waters and returns those waters back to the upper ocean. The circulation is asymmetric, with conversion to dense waters in restricted regions at high latitudes and the return to the surface involving slow upwelling and diffusive processes over much larger geographic regions. The THC is driven by high densities at or near the surface, caused by cold temperatures and/or high salinities, but despite its suggestive though common name, is also driven by mechanical forces such as wind and tides. Frequently,

the name THC has been used synonymously with *Meridional Overturning Circulation*.

Thermokarst The process by which characteristic landforms result from the thawing of ice-rich *permafrost* or the melting of massive *ground ice* (Van Everdingen, 1998).

Thermosteric See *Sea level change*.

Tide gauge A device at a coastal location (and some deep-sea locations) that continuously measures the level of the sea with respect to the adjacent land. Time averaging of the sea level so recorded gives the observed secular changes of the *relative sea level*.

Total solar irradiance (TSI) The amount of *solar radiation* received outside the Earth's *atmosphere* on a surface normal to the incident radiation, and at the Earth's mean distance from the Sun.

Reliable measurements of solar radiation can only be made from space and the precise record extends back only to 1978. The generally accepted value is 1,368 W m⁻² with an accuracy of about 0.2%. Variations of a few tenths of a percent are common, usually associated with the passage of *sunspots* across the solar disk. The *solar cycle* variation of TSI is of the order of 0.1% (AMS, 2000). See also *Insolation*.

Transient climate response See *Climate sensitivity*.

Tree rings Concentric rings of secondary wood evident in a cross-section of the stem of a woody plant. The difference between the dense, small-celled late wood of one season and the wide-celled early wood of the following spring enables the age of a tree to be estimated, and the ring widths or density can be related to *climate* parameters such as temperature and precipitation. See *Proxy*.

Trend In this report, the word *trend* designates a change, generally monotonic in time, in the value of a variable.

Tropopause The boundary between the *troposphere* and the *stratosphere*.

Troposphere The lowest part of the *atmosphere*, from the surface to about 10 km in altitude at mid-latitudes (ranging from 9 km at high latitudes to 16 km in the tropics on average), where clouds and weather phenomena occur. In the troposphere, temperatures generally decrease with height.

Turnover time See *Lifetime*.

Uncertainty An expression of the degree to which a value (e.g., the future state of the *climate system*) is unknown. Uncertainty can result from lack of information or from disagreement about what is known or even knowable. It may have many types of sources, from quantifiable errors in the data to ambiguously defined concepts or terminology, or uncertain *projections* of human behaviour. Uncertainty can therefore be represented by quantitative measures, for example, a range of values calculated by various models, or by qualitative statements, for example, reflecting the judgement of a team of experts (see Moss and Schneider, 2000; Manning et al., 2004). See also *Likelihood*; *Confidence*.

United Nations Framework Convention on Climate Change (UNFCCC)

The Convention was adopted on 9 May 1992 in New York and signed at the 1992 Earth Summit in Rio de Janeiro by more than 150 countries and the European Community. Its ultimate objective is the 'stabilisation of greenhouse gas concentrations in the atmosphere at a level that would prevent dangerous anthropogenic interference with the climate system'. It contains commitments for all Parties. Under the Convention, Parties included in Annex I (all OECD

countries and countries with economies in transition) aim to return *greenhouse gas* emissions not controlled by the *Montreal Protocol* to 1990 levels by the year 2000. The convention entered in force in March 1994. See *Kyoto Protocol*.

Uptake The addition of a substance of concern to a *reservoir*. The uptake of carbon containing substances, in particular *carbon dioxide*, is often called (carbon) *sequestration*.

Urban heat island (UHI) The relative warmth of a city compared with surrounding rural areas, associated with changes in runoff, the *concrete jungle* effects on heat retention, changes in surface *albedo*, changes in pollution and *aerosols*, and so on.

Ventilation The exchange of ocean properties with the *atmospheric surface layer* such that property concentrations are brought closer to equilibrium values with the *atmosphere* (AMS, 2000).

Volume mixing ratio See *Mole fraction*.

Walker Circulation Direct thermally driven zonal overturning circulation in the *atmosphere* over the tropical Pacific Ocean, with rising air in the western and sinking air in the eastern Pacific.

Water mass A volume of ocean water with identifiable properties (temperature, salinity, density, chemical tracers) resulting from its unique formation process. Water masses are often identified through a vertical or horizontal extremum of a property such as salinity.

Younger Dryas A period 12.9 to 11.6 kya, during the deglaciation, characterised by a temporary return to colder conditions in many locations, especially around the North Atlantic.

REFERENCES

- AMS, 2000: *AMS Glossary of Meteorology*, 2nd Ed. American Meteorological Society, Boston, MA, <http://amsglossary.allenpress.com/glossary/browse>.
- Charlson, R.J., and J. Heintzenberg (eds.), 1995: *Aerosol Forcing of Climate*. John Wiley and Sons Limited, pp. 91–108. Copyright 1995 ©John Wiley and Sons Limited. Reproduced with permission.
- Heim, R.R., 2002: *A Review of Twentieth-Century Drought Indices Used in the United States*. *Bull. Am. Meteorol. Soc.*, **83**, 1149–1165
- IPCC, 1992: *Climate Change 1992: The Supplementary Report to the IPCC Scientific Assessment* [Houghton, J.T., B.A. Callander, and S.K. Varney (eds.)]. Cambridge University Press, Cambridge, United Kingdom and New York, NY, USA, 116 pp.
- IPCC, 1996: *Climate Change 1995: The Science of Climate Change. Contribution of Working Group I to the Second Assessment Report of the Intergovernmental Panel on Climate Change* [Houghton, J.T., et al. (eds.)]. Cambridge University Press, Cambridge, United Kingdom and New York, NY, USA, 572 pp.
- IPCC, 2000: *Land Use, Land-Use Change, and Forestry. Special Report of the Intergovernmental Panel on Climate Change* [Watson, R.T., et al. (eds.)]. Cambridge University Press, Cambridge, United Kingdom and New York, NY, USA, 377 pp.
- IPCC, 2001: *Climate Change 2001: The Scientific Basis. Contribution of Working Group I to the Third Assessment Report of the Intergovernmental Panel on Climate Change* [Houghton, J.T., et al. (eds.)]. Cambridge University Press, Cambridge, United Kingdom and New York, NY, USA, 881 pp.
- IPCC, 2003: *Definitions and Methodological Options to Inventory Emissions from Direct Human-Induced Degradation of Forests and Devegetation of Other Vegetation Types* [Penman, J., et al. (eds.)]. The Institute for Global Environmental Strategies (IGES), Japan, 32 pp.
- Manning, M., et al., 2004: *IPCC Workshop on Describing Scientific Uncertainties in Climate Change to Support Analysis of Risk of Options*. Workshop Report. Intergovernmental Panel on Climate Change, Geneva.
- Moss, R., and S. Schneider, 2000: *Uncertainties in the IPCC TAR: Recommendations to Lead Authors for More Consistent Assessment and Reporting*. In: IPCC Supporting Material: Guidance Papers on Cross Cutting Issues in the Third Assessment Report of the IPCC. [Pachauri, R., T. Taniguchi, and K. Tanaka (eds.)]. Intergovernmental Panel on Climate Change, Geneva, pp. 33–51.
- Nakićenović, N., and R. Swart (eds.), 2000: *Special Report on Emissions Scenarios. A Special Report of Working Group III of the Intergovernmental Panel on Climate Change*. Cambridge University Press, Cambridge, United Kingdom and New York, NY, USA, 599 pp.
- Schwartz, S.E., and P. Warneck, 1995: Units for use in atmospheric chemistry. *Pure Appl. Chem.*, **67**, 1377–1406.
- Van Everdingen, R. (ed.): 1998. *Multi-Language Glossary of Permafrost and Related Ground-Ice Terms*, revised May 2005. National Snow and Ice Data Center/World Data Center for Glaciology, Boulder, CO, <http://nsidc.org/fgdc/glossary/>.

Annex II

Contributors to the IPCC WGI Fourth Assessment Report

ACHUTARAO, Krishna

Lawrence Livermore National Laboratory
USA

ADLER, Robert

National Aeronautics and
Space Administration
USA

ALEXANDER, Lisa

Hadley Centre for Climate Prediction
and Research, Met Office
UK, Australia, Ireland

ALEXANDERSSON, Hans

Swedish Meteorological and
Hydrological Institute
Sweden

ALLAN, Richard

Environmental Systems Science
Centre, University of Reading
UK

ALLEN, Myles

Climate Dynamics Group, Atmospheric,
Oceanic and Planetary Physics, Department
of Physics, University of Oxford
UK

ALLEY, Richard B.

Department of Geosciences,
Pennsylvania State University
USA

ALLISON, Ian

Australian Antarctic Division and
Antarctic Climate and Ecosystems
Cooperative Research Centre
Australia

AMBENJE, Peter

Kenya Meteorological Department
Kenya

AMMANN, Caspar

Climate and Global Dynamics Division,
National Center for Atmospheric Research
USA

ANDRONOVA, Natalia

University of Michigan
USA

ANNAN, James

Frontier Research Center for Global
Change, Japan Agency for Marine-
Earth Science and Technology
Japan, UK

ANTONOV, John

National Oceanic and
Atmospheric Administration
USA, Russian Federation

ARBLASTER, Julie

National Center for Atmospheric Research
and Bureau of Meteorology Research Center
USA, Australia

ARCHER, David

University of Chicago
USA

ARORA, Vivek

Canadian Centre for Climate Modelling
and Analysis, Environment Canada
Canada

ARRITT, Raymond

Iowa State University
USA

ARTALE, Vincenzo

Italian National Agency for
New Technologies, Energy and
the Environment (ENEA)
Italy

ARTAXO, Paulo

Instituto de Fisica, Universidade
de Sao Paulo
Brazil

AUER, Ingeborg

Central Institute for Meteorology
and Geodynamics
Austria

AUSTIN, John

National Oceanic and Atmospheric
Administration, Geophysical
Fluid Dynamics Laboratory
USA

BAEDE, Alphonsus

Royal Netherlands Meteorological
Institute (KNMI) and Ministry of Housing,
Spatial Planning and the Environment
Netherlands

BAKER, David

National Center for Atmospheric Research
USA

BALDWIN, Mark P.

Northwest Research Associates
USA

BARNOLA, Jean-Marc

Laboratoire de Glaciologie et
Géophysique de l'Environnement
France

BARRY, Roger

National Snow and Ice Data
Center, University of Colorado
USA

BATES, Nicholas Robert

Bermuda Institute of Ocean Sciences
Bermuda

BAUER, Eva

Potsdam Institute for Climate
Impact Research
Germany

BENESTAD, Rasmus

Norwegian Meteorological Institute
Norway

BENISTON, Martin

University of Geneva
Switzerland

BERGER, André

Université catholique de Louvain,
Institut d'Astronomie et de
Géophysique G. Lemaître
Belgium

BERNTSEN, Terje

Centre for International Climate and
Environmental Research (CICERO)
Norway

BERRY, Joseph A.

Carnegie Institute of Washington,
Department of Global Ecology
USA

BETTS, Richard A.

Hadley Centre for Climate Prediction
and Research, Met Office
UK

BIERCAMP, Joachim

Deutsches Klimarechenzentrum GmbH
Germany

BINDOFF, Nathaniel L.

Antarctic Climate and Ecosystems
Cooperative Research Centre and CSIRO
Marine and Atmospheric Research
Australia

BITZ, Cecilia

University of Washington
USA

BLATTER, Heinz

Institute for Atmospheric and
Climate Science, ETH Zurich
Switzerland

BODEKER, Greg

National Institute of Water and
Atmospheric Research
New Zealand

BOJARIU, Roxana

National Institute of Meteorology
and Hydrology (NIMH)
Romania

BONAN, Gordon

National Center for Atmospheric Research
USA

Coordinating lead authors, lead authors, and contributing authors are listed alphabetically by surname.

BONFILS, C line

School of Natural Sciences,
University of California, Merced
USA, France

BONY, Sandrine

Laboratoire de M t eorologie Dynamique,
Institut Pierre Simon Laplace
France

BOONE, Aaron

CNRS CNRM at M teo France
France, USA

BOONPRAGOB, Kansri

Department of Biology, Faculty of
Science, Ramkhamhaeng University
Thailand

BOUCHER, Olivier

Hadley Centre for Climate Prediction
and Research, Met Office
UK, France

BOUSQUET, Philippe

Institut Pierre Simon Laplace,
Laboratoire des Sciences du
Climat et de l'Environnement
France

BOX, Jason

Ohio State University
USA

BOYER, Tim

National Oceanic and
Atmospheric Administration
USA

BRACONNOT, Pascale

Pascale Braconnot Institut Pierre Simon
Laplace, Laboratoire des Sciences
du Climat et de l'Environnement
France

BRADY, Esther

National Center for Atmospheric Research
USA

BRASSEUR, Guy

Earth and Sun Systems Laboratory,
National Center for Atmospheric Research
USA, Germany

BREHERTON, Christopher

Department of Atmospheric Sciences,
University of Washington
USA

BRIFFA, Keith R.

Climatic Research Unit, School
of Environmental Sciences,
University of East Anglia
UK

BROCCOLI, Anthony J.

Rutgers University
USA

BROCKMANN, Patrick

Laboratoire des Sciences du
Climat et de l'Environnement
France

BROMWICH, David

Byrd Polar Research Center,
The Ohio State University
USA

BROVKIN, Victor

Potsdam Institute for Climate
Impact Research
Germany, Russian Federation

BROWN, Ross

Environment Canada
Canada

BUJA, Lawrence

National Center for Atmospheric Research
USA

BUSUIOC, Aristita

National Meteorological Administration
Romania

CADULE, Patricia

Institut Pierre Simon Laplace
France

CAI, Wenju

CSIRO Marine and Atmospheric Research
Australia

CAMILLONI, In s

Universidad de Buenos Aires, Centro de
Investigaciones del Mar y la Atm sfera
Argentina

CANAPELL, Josep

Global Carbon Project, CSIRO
Australia

CARRASCO, Jorge

Direccion Meteorologica de Chile
and Centro de Estudios Cientificos
Chile

CASSOU, Christophe

Centre National de Recherche Scientifique,
Centre Europeen de Recherche et de
Formation Avancee en Calcul Scientifique
France

CAYA, Daniel

Consortium Ouranos
Canada

CAYAN, Daniel R.

Scripps Institution of Oceanography,
University of California, San Diego
USA

CAZENAVE, Anny

Laboratoire d'Etudes en G ophysique et
Oc anographie Spatiale (LEGOS), CNES
France

CHAMBERS, Don

Center for Space Research, The
University of Texas at Austin
USA

CHANDLER, Mark

Columbia University and NASA
Goddard Institute for Space Studies
USA

CHANG, Edmund K.M.

Stony Brook University, State
University of New York
USA

CHAO, Ben

NASA Goddard Institute for Space Studies
USA

CHEN, Anthony

Department of Physics, University
of the West Indies
Jamaica

CHEN, Zhenlin

Dept of International Cooperation,
China Meteorological Administration
China

CHIDTHAISONG, Amnat

The Joint Graduate School of Energy
and Environment, King Mongkut's
University of Technology Thonburi
Thailand

CHRISTENSEN, Jens Hesselbjerg

Danish Meteorological Institute
Denmark

CHRISTIAN, James

Fisheries and Oceans, Canada, Canadian
Centre for Climate Modelling and Analysis
Canada

CHRISTY, John

University of Alabama in Huntsville
USA

CHURCH, John

CSIRO Marine and Atmospheric
Research and Ecosystems
Cooperative Research Centre
Australia

CIAIS, Philippe

Laboratoire des Sciences du
Climat et de l'Environnement
France

CLARK, Deborah A.

University of Missouri, St. Louis
USA

CLARKE, Garry

Earth and Ocean Sciences,
University of British Columbia
Canada

CLAUSSEN, Martin

Potsdam Institute for Climate
Impact Research
Germany

CLEMENT, Amy

University of Miami, Rosenstiel School
of Marine and Atmospheric Science
USA

COGLEY, J. Graham

Department of Geography, Trent University
Canada

COLE, Julia

University of Arizona
USA

- COLLIER, Mark**
CSIRO Marine and Atmospheric Research
Australia
- COLLINS, Matthew**
Hadley Centre for Climate Prediction
and Research, Met Office
UK
- COLLINS, William D.**
Climate and Global Dynamics Division,
National Center for Atmospheric Research
USA
- COLMAN, Robert**
Bureau of Meteorology Research Centre
Australia
- COMISO, Josefino**
National Aeronautics and Space
Administration, Goddard
Space Flight Center
USA
- CONWAY, Thomas J.**
National Oceanic and Atmospheric
Administration, Earth System
Research Laboratory
USA
- COOK, Edward**
Lamont-Doherty Earth Observatory
USA
- CORTIJO, Elsa**
Laboratoire des Sciences du Climat et de
l'Environnement, CNRS-CEA-UVSQ
France
- COVEY, Curt**
Lawrence Livermore National Laboratory
USA
- COX, Peter M.**
School of Engineering, Computer Science
and Mathematics, University of Exeter
UK
- CROOKS, Simon**
University of Oxford
UK
- CUBASCH, Ulrich**
Institut für Meteorologie,
Freie Universität Berlin
Germany
- CURRY, Ruth**
Woods Hole Oceanographic Institution
USA
- DAI, Aiguo**
National Center for Atmospheric Research
USA
- DAMERIS, Martin**
German Aerospace Center
Germany
- DE ELÍA, Ramón**
Ouranos Consortium
Canada, Argentina
- DELWORTH, Thomas L.**
Geophysical Fluid Dynamics
Laboratory, National Oceanic and
Atmospheric Administration
USA
- DENMAN, Kenneth L.**
Canadian Centre for Climate Modelling
and Analysis, Environment Canada and
Department of Fisheries and Oceans
Canada
- DENTENER, Frank**
European Commission Joint Research
Centre; Institute of Environment and
Sustainability Climate Change Unit
EU
- DESER, Clara**
National Center for Atmospheric Research
USA
- DETHLOFF, Klaus**
Alfred Wegener Institute for Polar and
Marine Research, Research Unit Potsdam
Germany
- DIANSKY, Nikolay A.**
Institute of Numerical Mathematics,
Russian Academy of Sciences
Russian Federation
- DICKINSON, Robert E.**
School of Earth and Atmospheric Sciences,
Georgia Institute of Technology
USA
- DING, Yihui**
National Climate Centre, China
Meteorological Administration
China
- DIRMEYER, Paul**
Center for Ocean-Land-Atmosphere Studies
USA
- DIX, Martin**
CSIRO
Australia
- DIXON, Keith**
National Oceanic and
Atmospheric Administration
USA
- DLUGOKENCKY, Ed**
National Oceanic and Atmospheric
Administration, Earth System
Research Laboratory
USA
- DOKKEN, Trond**
Bjerknes Centre for Climate Research
Norway
- DOTZEK, Nikolai**
Deutsches Zentrum für Luft und Raumfahrt,
Institut für Physik der Atmosphäre
Germany
- DOUTRIAUX, Charles**
Program for Climate Model
Diagnosis and Intercomparison
USA, France
- DRANGE, Helge**
Nansen Environmental and
Remote Sensing Center, Bjerknes
Centre for Climate Research
Norway
- DRIESSCHAERT, Emmanuelle**
Université catholique de Louvain,
Institut d'Astronomie et de
Géophysique G. Lemaitre
Belgium
- DUFRESNE, Jean-Louis**
Laboratoire de Météorologie Dynamique,
Institut Pierre Simon Laplace
France
- DUPLESSY, Jean-Claude**
Centre National de la Recherche
Scientifique, Laboratoire des Sciences
du Climat et de l'Environnement
France
- DYURGEROV, Mark**
Institute of Arctic and Alpine Research,
University of Colorado at Boulder
& Department of Geography and
Quaternary Geology at Stockholm
Sweden, USA
- EASTERLING, David**
National Oceanic and Atmospheric
Administration, Earth System
Research Laboratory
USA
- EBY, Michael**
University of Victoria
Canada
- EDWARDS, Neil R.**
The Open University
UK
- ELKINS, James W.**
National Oceanic and Atmospheric
Administration, Earth System
Research Laboratory
USA
- EMERSON, Steven**
School of Oceanography,
University of Washington
USA
- EMORI, Seita**
National Institute for Environmental
Studies and Frontier Research Center
for Global Change, Japan Agency for
Marine-Earth Science and Technology
Japan
- ETHERIDGE, David**
CSIRO Marine and Atmospheric Research
Australia
- EYRING, Veronika**
Deutsches Zentrum für Luft und Raumfahrt,
Institut für Physik der Atmosphäre
Germany
- FAHEY, David W.**
National Oceanic and Atmospheric
Administration, Earth System
Research Laboratory
USA

- FASULLO, John**
National Center for Atmospheric Research
USA
- FEDDEMA, Johannes**
University of Kansas
USA
- FEELY, Richard**
National Oceanic and Atmospheric
Administration, Pacific Marine
Environmental Laboratory
USA
- FEICHTER, Johann**
Max Planck Institute for Meteorology
Germany
- FICHEFET, Thierry**
Université catholique de Louvain,
Institut d'Astronomie et de
Géophysique G. Lemaître
Belgium
- FITZHARRIS, Blair**
Department of Geography,
University of Otago
New Zealand
- FLATO, Gregory**
Canadian Centre for Climate Modelling
and Analysis, Environment Canada
Canada
- FLEITMANN, Dominik**
Institute of Geological Sciences,
University of Bern
Switzerland, Germany
- FLEMING, James Rodger**
Colby College
USA
- FOGT, Ryan**
Polar Meteorology Group, Byrd Polar
Research Center and Atmospheric
Sciences Program, Department of
geography, The Ohio State University
USA
- FOLLAND, Christopher**
Hadley Centre for Climate Prediction
and Research, Met Office
UK
- FOREST, Chris**
Massachusetts Institute of Technology
USA
- FORSTER, Piers**
School of Earth and Environment,
University of Leeds
UK
- FOUKAL, Peter**
Heliophysics, Inc.
USA
- FRASER, Paul**
CSIRO Marine and Atmospheric Research
Australia
- FRAUENFELD, Oliver**
National Snow and Ice Data Center,
University of Colorado at Boulder
USA, Austria
- FREE, Melissa**
Air Resources Laboratory, National
Oceanic and Atmospheric Administration
USA
- FREI, Allan**
Hunter College, City
University of New York
USA
- FREI, Christoph**
Federal Office of Meteorology
and Climatology MeteoSwiss
Switzerland
- FRICKER, Helen**
Scripps Institution of Oceanography,
University of California, San Diego
USA
- FRIEDLINGSTEIN, Pierre**
Institut Pierre Simon Laplace,
Laboratoire des Sciences du
Climat et de l'Environnement
France, Belgium
- FU, Congbin**
Start Regional Center for Temperate
East Asia, Institute of Atmospheric
Physics, Chinese Academy of Science
China
- FUJII, Yoshiyuki**
Arctic Environment Research Center,
National Institute of Polar Research
Japan
- FUNG, Inez**
University of California, Berkeley
USA
- FURRER, Reinhard**
Colorado School of Mines
USA, Switzerland
- FUZZI, Sandro**
National Research Council, Institute of
Atmospheric Sciences and Climate
Italy
- FYFE, John**
Canadian Centre for Climate Modelling
and Analysis, Environment Canada
Canada
- GANOPOLSKI, Andrey**
Potsdam Institute for Climate
Impact Research
Germany
- GAO, Xuejie**
Laboratory for Climate Change,
National Climate Centre, China
Meteorological Administration
China
- GARCIA, Hernan**
National Oceanic and Atmospheric
Administration, National
Oceanographic Data Center
USA
- GARCÍA-HERRERA, Ricardo**
Universidad Complutense de Madrid
Spain
- GAYE, Amadou Thierno**
Laboratory of Atmospheric Physics,
ESP/CAD, Dakar University
Senegal
- GELLER, Marvin**
Stony Brook University
USA
- GENT, Peter**
National Center for Atmospheric Research
USA
- GERDES, Rüdiger**
Alfred-Wegener-Institute für
Polar und Meeresforschung
Germany
- GILLETT, Nathan P.**
Climatic Research Unit, School
of Environmental Sciences,
University of East Anglia
UK
- GIORGI, Filippo**
Abdus Salam International Centre
for Theoretical Physics
Italy
- GLEASON, Byron**
National Climatic Data Center, National
Oceanic and Atmospheric Administration
USA
- GLECKLER, Peter**
Lawrence Livermore National Laboratory
USA
- GONG, Sunling**
Air Quality Research Division, Science &
Technology Branch, Environment Canada
Canada
- GONZÁLEZ-DAVILA, Melchor**
University of Las Palmas de Gran Canaria
Spain
- GONZÁLEZ-ROUCO, Jesus Fidel**
Universidad Complutense de Madrid
Spain
- GOOSSE, Hugues**
Université catholique de Louvain
Belgium
- GRAHAM, Richard**
Hadley Centre, Met Office
UK
- GREGORY, Jonathan M.**
Department of Meteorology, University of
Reading and Hadley Centre for Climate
Prediction and Research, Met Office
UK
- GRIESER, Jürgen**
Deutscher Wetterdienst, Global
Precipitation Climatology Centre
Germany
- GRIGGS, David**
Hadley Centre for Climate Prediction
and Research, Met Office
UK

GROISMAN, Pavel

University Corporation for Atmospheric Research at the National Climatic Data Center, National Oceanic and Atmospheric Administration
USA, Russian Federation

GRUBER, Nicolas

Institute of Geophysics and Planetary Physics, University of California, Los Angeles and Department of Environmental Sciences, ETH Zurich
USA, Switzerland

GUJGEL, Richard

National Oceanic and Atmospheric Administration
USA

GUDMUNDSSON, G. Hilmar

British Antarctic Survey
UK, Iceland

GUENTHER, Alex

National Center for Atmospheric Research
USA

GULEV, Sergey

P. P. Shirshov Institute of Oceanography
Russian Federation

GURNEY, Kevin

Department of Earth and Atmospheric Science, Purdue University
USA

GUTOWSKI, William

Iowa State University
USA

HAAS, Christian

Alfred Wegener Institute
Germany

HABIBI NOKHANDAN, Majid

National Center for Climatology
Iran

HAGEN, Jon Ove

University of Oslo
Norway

HAIGH, Joanna

Imperial College London
UK

HALL, Alex

Department of Atmospheric and Oceanic Sciences, University of California, Los Angeles
USA

HALLEGATTE, Stéphane

Centre International de Recherche sur l'Environnement et le Développement, Ecole Nationale des Ponts-et-Chaussées and Centre National de Recherches Meteorologique, Meteo-France
USA, France

HANAWA, Kimio

Physical Oceanography Laboratory, Department of Geophysics, Graduate School of Science, Tohoku University
Japan

HANSEN, James

Goddard Institute for Space Studies
USA

HANSSEN-BAUER, Inger

Norwegian Meteorological Institute
Norway

HARRIS, Charles

School of Earth, Ocean and Planetary Science, Cardiff University
UK

HARRIS, Glen

Hadley Centre for Climate Prediction and Research, Met Office
UK, New Zealand

HARVEY, Danny

University of Toronto
Canada

HASUMI, Hiroyasu

Center for Climate System Research, University of Tokyo
Japan

HAUGLUSTAINE, Didier

Institut Pierre Simon Laplace, Laboratoire des Sciences du Climat et de l'Environnement, CEA-CNRS-UVSQ
France

HAYWOOD, James

Hadley Centre for Climate Prediction and Research, Met Office
UK

HEGERL, Gabriele C.

Division of Earth and Ocean Sciences, Nicholas School for the Environment and Earth Sciences, Duke University
USA, Germany

HEIMANN, Martin

Max-Planck-Institut für Biogeochemie
Germany, Switzerland

HEINZE, Christoph

University of Bergen, Geophysical Institute and Bjerknes Centre for Climate Research
Norway, Germany

HELD, Isaac

National Oceanic and Atmospheric Administration, Geophysical Fluid Dynamics Laboratory
USA

HENDERSON-SELLERS, Ann

World Meteorological Organization
Switzerland

HENDON, Henry

Bureau of Meteorology Research Centre
Australia

HEWITSON, Bruce

Department of Environmental and Geographical Sciences, University of Cape Town
South Africa

HINZMAN, Larry

University of Alaska, Fairbanks
USA

HOCK, Regine

Stockholm University
Sweden

HODGES, Kevin

Environmental Systems Science Centre
UK

HOELZLE, Martin

University of Zürich, Department of Geography
Switzerland

HOLLAND, Elisabeth

Atmospheric Chemistry Division, National Center for Atmospheric Research (NCAR)
USA

HOLLAND, Marika

National Center for Atmospheric Research
USA

HOLTSLAG, Albert A. M.

Wageningen University
Netherlands

HOSKINS, Brian J.

Department of Meteorology, University of Reading
UK

HOUSE, Joanna

Quantifying and Understanding the Earth System Programme, University of Bristol
UK

HU, Aixue

National Center for Atmospheric Research
USA, China

HUNKE, Elizabeth

Los Alamos National Laboratory
USA

HURRELL, James

National Center for Atmospheric Research
USA

HUYBRECHTS, Philippe

Departement Geografie, Vrije Universiteit Brussel
Belgium

INGRAM, William

Hadley Centre for Climate Prediction and Research, Met Office
UK

ISAKSEN, Ketil

Norwegian Meteorological Institute
Norway

ISHII, Masayoshi

Frontier Research Center for Global Change, Japan Agency for Marine-Earth Science and Technology
Japan

JACOB, Daniel

Department of Earth and Planetary Sciences, Harvard University
USA, France

JALLOW, Babu

Department of Water Resources
The Gambia

JANSEN, Eystein

University of Bergen, Department of Earth Sciences and Bjerknes Centre for Climate Research Norway

JANSSON, Peter

Department of Physical Geography and Quaternary Geology, Stockholm University Sweden

JENKINS, Adrian

British Antarctic Survey, Natural Environment Research Council UK

JONES, Andy

Hadley Centre for Climate Prediction and Research, Met Office UK

JONES, Christopher

Hadley Centre for Climate Prediction and Research, Met Office UK

JONES, Colin

Universite du Quebec a Montreal, Canadian Regional Climate Modelling Network Canada

JONES, Gareth S.

Hadley Centre for Climate Prediction and Research, Met Office UK

JONES, Julie

GKSS Research Centre Germany, UK

JONES, Philip D.

Climatic Research Unit, School of Environmental Sciences, University of East Anglia UK

JONES, Richard

Hadley Centre for Climate Prediction and Research, Met Office UK

JOOS, Fortunat

Climate and Environmental Physics, Physics Institute, University of Bern Switzerland

JOSEY, Simon

National Oceanography Centre, University of Southampton UK

JOUGHIN, Ian

Applied Physics Laboratory, University of Washington USA

JOUZEL, Jean

Institut Pierre Simon Laplace, Laboratoire des Sciences du Climat et de l'Environnement, CEA-CNRS-UVSQ France

JOYCE, Terrence

Woods Hole Oceanographic Institution USA

JUNGCLAUS, Johann H.

Max Planck Institute for Meteorology Germany

KAGEYAMA, Masa

Laboratoire des Sciences du Climat et de l'Environnement France

KÅLLBERG, Per

European Centre for Medium-Range Weather Forecasts ECMWF

KÄRCHER, Bernd

Deutsches Zentrum für Luft und Raumfahrt, Institut für Physik der Atmosphäre Germany

KARL, Thomas R.

National Oceanic and Atmospheric Administration, National Climatic Data Center USA

KAROLY, David J.

University of Oklahoma USA, Australia

KASER, Georg

Institut für Geographie, University of Innsbruck Austria, Italy

KATTSOV, Vladimir

Voeikov Main Geophysical Observatory Russian Federation

KATZ, Robert

National Center for Atmospheric Research USA

KAWAMIYA, Michio

Frontier Research Center for Global Change, Japan Agency for Marine-Earth Science and Technology Japan

KEELING, C. David

Scripps Institution of Oceanography USA

KEELING, Ralph

Scripps Institution of Oceanography USA

KENNEDY, John

Hadley Centre, Met Office UK

KENYON, Jesse

Duke University USA

KETTLEBOROUGH, Jamie

British Atmospheric Data Centre, Space Science and Technology Department, Council for the Central Laboratory of the Research Councils UK

KHARIN, Viatcheslar

Canadian Centre for Climate Modelling and Analysis, Environment Canada Canada

KHODRI, Myriam

Institut de Recherche Pour le Developpement France

KILADIS, George

National Oceanic and Atmospheric Administration USA

KIM, Kuh

Seoul National University Republic of Korea

KIMOTO, Masahide

Center for Climate System Research, University of Tokyo Japan

KING, Brian

National Oceanography Centre, Southampton UK

KINNE, Stefan

Max-Planck Institute for Meteorology Germany

KIRTMAN, Ben

Center for Ocean-Land-Atmosphere Studies, George Mason University USA

KITOH, Akio

First Research Laboratory, Climate Research Department, Meteorological Research Institute, Japan Meteorological Agency Japan

KLEIN, Stephen A.

Lawrence Livermore National Laboratory USA

KLEIN TANK, Albert

Royal Netherlands Meteorological Institute (KNMI) Netherlands

KNUTSON, Thomas

Geophysical Fluid Dynamics Laboratory, National Oceanic and Atmospheric Administration USA

KNUTTI, Reto

Climate and Global Dynamics Division, National Center for Atmospheric Research Switzerland

KOERTZINGER, Arne

Leibniz Institut für Meereswissenschaften an der Universität Kiel and Institut für Ostseeforschung Warnemünde Germany

KOIKE, Toshio

Department of Civil Engineering, University of Tokyo Japan

KOLLI, Rupa Kumar

Climatology and Hydrometeorology Division, Indian Institute of Tropical Meteorology India

- KOSTER, Randal**
National Aeronautics and
Space Administration
USA
- KOTTMEIER, Christoph**
Institut für Meteorologie, und
Klimaforschung, Universität Karlsruhe/
Forschungszentrum Karlsruhe
Germany
- KRIPALANI, Ramesh**
Indian Institute of Tropical Meteorology
India
- KRYNYTZKY, Marta**
University of Washington
USA
- KUNKEL, Kenneth**
Illinois State Water Survey
USA
- KUSHNER, Paul J.**
Department of Physics,
University of Toronto
Canada
- KWOK, Ron**
Jet Propulsion Laboratory, California
Institute of Technology
USA
- KWON, Won-Tae**
Climate Research Laboratory,
Meteorological Research Institute (METRI),
Korean Meteorological Administration
Republic of Korea
- LABEYRIE, Laurent**
Laboratoire des Sciences du
Climat et de l'Environnement
France
- LAINE, Alexandre**
Laboratoire des Sciences du
Climat et de l'Environnement
France
- LAM, Chiu-Ying**
Hong Kong Observatory
China
- LAMBECK, Kurt**
Australia National University
Australia
- LAMBERT, F. Hugo**
Atmospheric, Oceanic and Planetary
Physics, University of Oxford
UK
- LANZANTE, John**
National Oceanic and
Atmospheric Administration
USA
- LAPRISE, René**
Département des Sciences de la Terre
et de l'Atmosphère, University
of Quebec at Montreal
Canada
- LASSEY, Keith**
National Institute of Water and
Atmospheric Research
New Zealand
- LATIF, Mojib**
Leibniz Institut für Meereswissenschaften,
IFM-GEOMAR
Germany
- LAU, Ngar-Cheung**
Geophysical Fluid Dynamics
Laboratory, National Oceanic and
Atmospheric Administration
USA
- LAVAL, Katia**
Laboratoire de Météorologie
Dynamique du CNRS
France
- LAVINE, Michael**
Duke University
USA
- LAWRENCE, David**
National Center for Atmospheric Research
USA
- LAWRIMORE, Jay**
National Oceanic and Atmospheric
Administration, National
Climatic Data Center
USA
- LAXON, Seymour**
Centre for Polar Observation and
Modelling, University College London
UK
- LE BROCCQ, Anne**
Centre for Polar Observation and
Modelling, University of Bristol
UK
- LE QUÉRÉ, Corinne**
University of East Anglia and
British Antarctic Survey
UK, France, Canada
- LE TREUT, Hervé**
Laboratoire de Météorologie
Dynamique du CNRS
France
- LEAN, Judith**
Naval Research Laboratory
USA
- LECK, Caroline**
Department of Meteorology,
Stockholm University
Sweden
- LEE, Terry C.K.**
University of Victoria
Canada
- LEE-TAYLOR, Julia**
National Center for Atmospheric Research
USA, UK
- LEFEVRE, Nathalie**
Institut de Recherche Pour le
Développement, Laboratoire
d'Océanographie et de Climatologie
France
- LEMKE, Peter**
Alfred Wegener Institute for
Polar and Marine Research
Germany
- LEULIETTE, Eric**
University of Colorado, Boulder
USA
- LEUNG, Ruby**
Pacific Northwest National
Laboratory, National Oceanic and
Atmospheric Administration
USA
- LEVERMANN, Anders**
Potsdam Institute for Climate
Impact Research
Germany
- LEVINSON, David**
National Oceanic and Atmospheric
Administration, National
Climatic Data Center
USA
- LEVITUS, Sydney**
National Oceanic and
Atmospheric Administration
USA
- LIE, Øyvind**
Bjerknes Centre for Climate Research
Norway
- LIEPERT, Beate**
Lamont-Doherty Earth Observatory,
Columbia University
USA
- LIU, Shiyin**
Cold and Arid Regions Environmental
and Engineering Research Institute,
Chinese Academy of Sciences
China
- LOHMANN, Ulrike**
ETH Zürich, Institute for Atmospheric
and Climate Science
Switzerland
- LOUTRE, Marie-France**
Université catholique de Louvain,
Institut d'Astronomie et de
Géophysique G. Lemaître
Belgium
- LOWE, David C.**
National Institute of Water and
Atmospheric Research
New Zealand
- LOWE, Jason**
Hadley Centre for Climate Prediction
and Research, Met Office
UK
- LUO, Yong**
Laboratory for Climate Change,
National Climate Centre, China
Meteorological Administration
China
- LUTERBACHER, Jürg**
Institute of Geography, Climatology
and Meteorology, and National
Centre of Competence in Research
on Climate, University of Bern
Switzerland

LYNCH, Amanda H.

School of Geography and Environmental Science, Monash University
Australia

MACAYEAL, Douglas

University of Chicago
USA

MACCRACKEN, Michael

Climate Institute
USA

MAGAÑA RUEDA, Victor

Centro de Ciencias de la Atmósfera, Ciudad Universitaria, Universidad Nacional Autónoma de México
Mexico

MALHI, Yadvinder

University of Oxford
UK

MALANOTTE-RIZZOLI, Paola

Massachusetts Institute of Technology
USA, Italy

MANNING, Andrew C.

University of East Anglia
UK, New Zealand

MANNING, Martin

IPCC WGI TSU, National Oceanic and Atmospheric Administration, Earth System Research Laboratory
USA, New Zealand

MANZINI, Elisa

National Institute for Geophysics and Volcanology
Italy

MARENGO ORSINI, Jose Antonio

CPTEC/INPE
Brazil, Peru

MARSH, Robert

National Oceanography Centre, University of Southampton
UK

MARSHALL, Gareth

British Antarctic Survey
UK

MARTELO, Maria

Ministerio del Ambiente y los Recursos Naturales, Dir. de Hidrología y Meteorología
Venezuela

MASARIE, Ken

National Oceanic and Atmospheric Administration, Earth System Research Laboratory, Global Monitoring Division
USA

MASSON-DELMOTTE, Valérie

Laboratoire des Sciences du Climat et de l'Environnement
France

MATSUMOTO, Katsumi

University of Minnesota, Twin Cities
USA

MATSUNO, Taroh

Frontier Research Center for Global Change, Japan Agency for Marine-Earth Science and Technology
Japan

MATTHEWS, H. Damon

University of Calgary and Concordia University
Canada

MATULLA, Christoph

Environment Canada
Canada, Austria

MAURITZEN, Cecilie

Norwegian Meteorological Institute
Norway

MCAVANEY, Bryant

Bureau of Meteorology Research Centre
Australia

MCFIGGANS, Gordon

University of Manchester
UK

MCINNES, Kathleen

CSIRO, Marine and Atmospheric Chemistry Research
Australia

MCPHADEN, Michael

National Oceanic and Atmospheric Administration
USA

MEARNS, Linda

National Center for Atmospheric Research
USA

MEARS, Carl

Remote Sensing Systems
USA

MEEHL, Gerald A.

Climate and Global Dynamics Division, National Center for Atmospheric Research
USA

MEINSHAUSEN, Malte

Potsdam Institute for Climate Impact Research
Germany

MELLING, Humphrey

Fisheries and Oceans Canada
Canada

MENÉNDEZ, Claudio Guillermo

Centro de Investigaciones del Mar y de la Atmósfera, (CONICET-UBA)
Argentina

MENON, Surabi

Lawrence Berkeley National Laboratory
USA

MESCHERSKAYA, Anna V.

Russian Federation

MILLER, John B.

National Oceanic and Atmospheric Administration
USA

MILLOT, Claude

Centre National de la Recherche Scientifique
France

MILLY, Chris

United States Geological Survey
USA

MITCHELL, John

Hadley Centre for Climate Prediction and Research, Met Office
UK

MOKSSIT, Abdalah

Direction de la météorologie Nationale
Morocco

MOLINA, Mario

Scripps Institution of Oceanography, Dept. of Chemistry and Biochemistry, University of California, San Diego
USA, Mexico

MOLINARI, Robert

National Oceanic and Atmospheric Administration, Atlantic Oceanographic and Meteorological Laboratory
USA

MONAHAN, Adam H.

School of Earth and Ocean Sciences, University of Victoria
Canada

MONNIN, Eric

Climate and Environmental Physics, Physics Institute, University of Bern
Switzerland

MONTZKA, Steve

National Oceanic and Atmospheric Administration
USA

MOSLEY-THOMPSON, Ellen

Ohio State University
USA

MOTE, Philip

Climate Impacts Group, Joint Institute for the Study of the Atmosphere and Oceans (JIASO), University of Washington
USA

MUHS, Daniel

United States Geological Survey
USA

MULLAN, A. Brett

National Institute of Water and Atmospheric Research
New Zealand

MÜLLER, Simon A.

Climate and Environmental Physics, Physics Institute, University of Bern
Switzerland

MURPHY, James M.

Hadley Centre for Climate Prediction and Research, Met Office
UK

MUSCHELER, Raimund

Goddard Earth Sciences and Technology Center, University of Maryland & NASA/Goddard Space Flight Center, Climate & Radiation Branch
USA

MYHRE, Gunnar

Department of Geosciences, University of Oslo
Norway

NAKAJIMA, Teruyuki

Center for Climate System Research, University of Tokyo
Japan

NAKAMURA, Hisashi

Department of Earth, Planetary Science, University of Tokyo
Japan

NAWRATH, Susanne

Potsdam Institute for Climate Impact Research
Germany

NEREM, R. Steven

University of Colorado at Boulder
USA

NEW, Mark

Centre for the Environment, University of Oxford
UK

NGANGA, John

University of Nairobi
Kenya

NICHOLLS, Neville

Monash University
Australia

NODA, Akira

Meteorological Research Institute, Japan Meteorological Agency
Japan

NOJIRI, Yukihiko

Secretariat of Council for Science and Technology Policy, Cabinet Office
Japan

NOKHANDAN, Majid Habibi

Iranian Meteorological Organization
Iran

NORRIS, Joel

Scripps Institution of Oceanography
USA

NOZAWA, Toru

National Institute for Environmental Studies
Japan

OERLEMANS, Johannes

Institute for Marine and Atmospheric Research, Utrecht University
Netherlands

OGALLO, Laban

IGAD Climate Prediction and Application Centre
Kenya

OHMURA, Atsumu

Swiss Federal Institute of Technology
Switzerland

OKI, Taikan

Institute of Industrial Science, The University of Tokyo
Japan

OLAGO, Daniel

Department of Geology, University of Nairobi
Kenya

ONO, Tsuneo

Hokkaido National Fisheries Research Institute, Fisheries Research Agency
Japan

OPPENHEIMER, Michael

Princeton University
USA

ORAM, David

University of East Anglia
UK

ORR, James C.

Marine Environment Laboratories, International Atomic Energy Agency
Monaco, USA

OSBORN, Tim

University of East Anglia
UK

O'SHAUGHNESSY, Kath

National Institute of Water and Atmospheric Research
New Zealand

OTTO-BLIESNER, Bette

Climate and Global Dynamics Division, National Center for Atmospheric Research
USA

OVERPECK, Jonathan

Institute for the Study of Planet Earth, University of Arizona
USA

PAASCHE, Øyvind

Bjerknes Centre for Climate Research
Norway

PAHLOW, Markus

Dalhousie University, Bedford Institute of Oceanography
Canada

PAL, Jeremy S.

Loyola Marymount University, The Abdus Salam International Centre for Theoretical Physics
USA, Italy

PALMER, Timothy

European Centre for Medium-Range Weather Forecasting
ECMWF, UK

PANT, Govind Ballabh

Indian Institute of Tropical Meteorology
India

PARKER, David

Hadley Centre for Climate Prediction and Research, Met Office
UK

PARRENIN, Frédéric

Laboratoire de Glaciologie et Géophysique de l'Environnement
France

PAVLOVA, Tatyana

Voikov Main Geophysical Observatory
Russian Federation

PAYNE, Antony

University of Bristol
UK

PELTIER, W. Richard

Department of Physics, University of Toronto
Canada

PENG, Tsung-Hung

Atlantic Oceanographic and Meteorological Laboratory, National Oceanic and Atmospheric Administration
USA

PENNER, Joyce E.

Department of Atmospheric, Oceanic, and Space Sciences, University of Michigan
USA

PETERSON, Thomas

National Oceanic and Atmospheric Administration, National Climatic Data Center
USA

PETOUKHOV, Vladimir

Potsdam Institute for Climate Impact Research
Germany

PEYLIN, Philippe

Laboratoire des Modélisation du Climat et de l'Environnement
France

PFISTER, Christian

University of Bern
Switzerland

PHILLIPS, Thomas

Program for Climate Model Diagnosis and Intercomparison, Lawrence Livermore National Laboratory
USA

PIERCE, David

Scripps Institution of Oceanography
USA

PIPER, Stephen

Scripps Institution of Oceanography
USA

PITMAN, Andrew

Department of Physical Geography, Macquarie University
Australia

PLANTON, Serge

Météo-France
France

PLATTNER, Gian-Kasper

Climate and Environmental Physics,
Physics Institute, University of Bern
Switzerland

PLUMMER, David

Environment Canada
Canada

POLLACK, Henry

University of Michigan
USA

PONATER, Michael

Deutsches Zentrum für Luft und Raumfahrt,
Institut für Physik der Atmosphäre
Germany

POWER, Scott

Bureau of Meteorology Research Centre
Australia

PRATHER, Michael

Earth System Science Department,
University of California at Irvine
USA

PRINN, Ronald

Department of Earth, Atmospheric
and Planetary Sciences, Massachusetts
Institute of Technology
USA, New Zealand

PROSHUTINSKY, Andrey

Woods Hole Oceanographic Institution
USA

PROWSE, Terry

Environment Canada, University of Victoria
Canada

QIN, Dahe

Co-Chair, IPCC WGI, China
Meteorological Administration
China

QIU, Bo

University of Hawaii
USA

QUAAS, Johannes

Max Planck Institute for Meteorology
Germany

QUADFASSEL, Detlef

Institut für Meereskunde, Centre for Marine
and Atmospheric Sciences Hamburg
Germany

RAGA, Graciela

Centro de Ciencias de la Atmósfera,
Universidad Nacional Autónoma de México
México, Argentina

RAHIMZADEH, Fatemeh

Atmospheric Science & Meteorological
Research Center (ASMER), I.R. of Iran
Meteorological Organization (IRIMO)
Iran

RAHMSTORF, Stefan

Potsdam Institute for Climate
Impact Research
Germany

RÄISÄNEN, Jouni

Department of Physical Sciences,
University of Helsinki
Finland

RAMACHANDRAN, Srikanthan

Space & Atmospheric Sciences Division,
Physical Research Laboratory
India

RAMANATHAN, Veerabhadran

Scripps Institution of Oceanography
USA

RAMANKUTTY, Navin

University of Wisconsin, Madison
USA, India

RAMASWAMY, Venkatachalam

National Oceanic and Atmospheric
Administration, Geophysical
Fluid Dynamics Laboratory
USA

RAMESH, Rengaswamy

Physical Research Laboratory
India

RANDALL, David A.

Department of Atmospheric Science,
Colorado State University
USA

RAPER, Sarah C.B.

Manchester Metropolitan University
UK

RAUP, Bruce H.

National Snow and Ice Data
Center, University of Colorado
USA

RAUPACH, Michael

CSIRO
Australia

RAYMOND, Charles

University of Washington, Department
of Earth and Space Sciences
USA

RAYNAUD, Dominique

Laboratoire de Glaciologie et
Géophysique de l'Environnement
France

RAYNER, Peter

Institut Pierre Simon Laplace,
Laboratoire des Sciences du
Climat et de l'Environnement
France

REHDER, Gregor

Leibniz Institut für Meereswissenschaften
an der Universität Kiel and Institut
für Ostseeforschung Warnemünde
Germany

REID, George

National Oceanic and
Atmospheric Administration
USA

REN, Jiawen

Cold and Arid Regions Environmental
and Engineering Research Institute,
Chinese Academy of Sciences
China

RENSEN, Hans

Faculty of Earth and Life Sciences,
Vrije Universiteit Amsterdam
Netherlands

RENWICK, James A.

National Institute of Water and
Atmospheric Research
New Zealand

RIEBESELL, Ulf

Leibniz Institute for Marine
Sciences, IFM-GEOMAR
Germany

RIGNOT, Eric

Jet Propulsion Laboratory
USA

RIGOR, Ignatius

Polar Science Center, Applied Physics
Laboratory, University of Washington
USA

RIND, David

National Aeronautics and Space
Administration, Goddard
Institute for Space Studies
USA

RINKE, Annette

Alfred Wegener Institute for
Polar and Marine Research
Germany

RINTOUL, Stephen

CSIRO, Marine and Atmospheric
Research and Antarctic Climate and
Ecosystems Cooperative Research Centre
Australia

RIXEN, Michel

University of Liege and NATO
Undersea Research Center
NATO, Belgium

RIZZOLI, Paola

Massachusetts Institute of Technology
USA, Italy

ROBERTS, Malcolm

Hadley Centre for Climate Prediction
and Research, Met Office
UK

ROBERTSON, Franklin R.

National Aeronautics and
Space Administration
USA

ROBINSON, David

Rutgers University
USA

RÖDENBECK, Christian

Max Planck Institute for
Biogeochemistry Jena
Germany

- ROECKNER, Erich**
Max Planck Institute for Meteorology
Germany
- ROSATI, Anthony**
National Oceanic and
Atmospheric Administration
USA
- ROSENLOF, Karen**
National Oceanic and
Atmospheric Administration
USA
- ROTHROCK, David**
University of Washington
USA
- ROTSTAYN, Leon**
CSIRO Marine and Atmospheric Research
Australia
- ROULET, Nigel**
McGill University
Canada
- RUMMUKAINEN, Markku**
Rossby Centre, Swedish Meteorological
and Hydrological Institute
Sweden, Finland
- RUSSELL, Gary L.**
National Aeronautics and Space
Administration, Goddard
Institute for Space Studies
USA
- RUSTICUCCI, Matilde**
Departamento de Ciencias de la
Atmósfera y los Océanos, FCEN,
Universidad de Buenos Aires
Argentina
- SABINE, Christopher**
National Oceanic and Atmospheric
Administration, Pacific Marine
Environmental Laboratory
USA
- SAHAGIAN, Dork**
Lehigh University
USA
- SALAS Y MÉLIA, David**
Météo-France, Centre National de
Recherches Météorologiques
France
- SANTER, Ben D.**
Program for Climate Model Diagnosis
and Intercomparison, Lawrence
Livermore National Laboratory
USA
- SARR, Abdoulaye**
Service Météorologique, DMN Sénégal
Senegal
- SAUSEN, Robert**
Deutsches Zentrum für Luft und Raumfahrt,
Institut für Physik der Atmosphäre
Germany
- SCHÄR, Christoph**
ETH Zürich, Institute for Atmospheric
and Climate Science
Switzerland
- SCHERRER, Simon Christian**
Federal Office of Meteorology
and Climatology MeteoSwiss
Switzerland
- SCHMIDT, Gavin**
National Aeronautics and Space
Administration, Goddard
Institute for Space Studies
USA, UK
- SCHMITTNER, Andreas**
College of Oceanic and Atmospheric
Sciences, Oregon State University
USA, Germany
- SCHNEIDER, Birgit**
Leibniz Institut für Meereswissenschaften
Germany
- SCHOTT, Friedrich**
Leibniz Institut für Meereswissenschaften,
IFM-GEOMAR
Germany
- SCHULTZ, Martin G.**
Max Planck Institute for Meteorology
Germany
- SCHULZ, Michael**
Institut Pierre Simon Laplace,
Laboratoire des Sciences du Climat et de
l'Environnement, CEA-CNRS-UVSQ
France, Germany
- SCHWARTZ, Stephen E.**
Brookhaven National Laboratory
USA
- SCHWARZKOPF, Dan**
National Oceanic and
Atmospheric Administration
USA
- SCINOCICA, John**
Canadian Centre for Climate Modelling
and Analysis, Environment Canada
Canada
- SEIDOV, Dan**
Pennsylvania State University
USA
- SEMAZZI, Fred H.**
North Carolina State University
USA
- SENIOR, Catherine**
Hadley Centre for Climate Prediction
and Research, Met Office
UK
- SEXTON, David**
Hadley Centre for Climate Prediction
and Research, Met Office
UK
- SHEA, Dennis**
National Center for Atmospheric Research
USA
- SHEPHERD, Andrew**
School of Geosciences, The
University of Edinburgh
UK
- SHEPHERD, J. Marshall**
University of Georgia,
Department of Geography
USA
- SHEPHERD, Theodore G.**
University of Toronto
Canada
- SHERWOOD, Steven**
Yale University
USA
- SHUKLA, Jagadish**
Center for Ocean-Land-Atmosphere
Studies, George Mason University
USA
- SHUM, C.K.**
Geodetic Science, School of Earth
Sciences, The Ohio State University
USA
- SIEGMUND, Peter**
Royal Netherlands Meteorological
Institute (KNMI)
Netherlands
- SILVA DIAS, Pedro Leite da**
Universidade de Sao Paulo
Brazil
- SIMMONDS, Ian**
University of Melbourne
Australia
- SIMMONS, Adrian**
European Centre for Medium-
Range Weather Forecasts
ECMWF, UK
- SIROCKO, Frank**
University of Mainz
Germany
- SLATER, Andrew G.**
Cooperative Institute for Research
in Environmental Sciences,
University of Colorado, Boulder
USA, Australia
- SLINGO, Julia**
National Centre for Atmospheric
Science, University of Reading
UK
- SMITH, Doug**
Hadley Centre for Climate Prediction
and Research, Met Office
UK
- SMITH, Sharon**
Geological Survey of Canada,
Natural Resources Canada
Canada
- SODEN, Brian**
University of Miami, Rosentiel School
for Marine and Atmospheric Science
USA
- SOKOLOV, Andrei**
Massachusetts Institute of Technology
USA, Russian Federation

SOLANKI, Sami K.

Max Planck Institute for
Solar System Research
Germany, Switzerland

SOLOMINA, Olga

Institute of Geography RAS
Russian Federation

SOLOMON, Susan

Co-Chair, IPCC WGI, National Oceanic
and Atmospheric Administration,
Earth System Research Laboratory
USA

SOMERVILLE, Richard

Scripps Institution of Oceanography,
University of California, San Diego
USA

SOMOT, Samuel

Météo-France, Centre National de
Recherches Météorologiques
France

SONG, Yuhe

Jet Propulsion Laboratory
USA

SPAHLI, Renato

Climate and Environmental Physics,
Physics Institute, University of Bern
Switzerland

SRINIVASAN, Jayaraman

Centre for Atmospheric and Oceanic
Sciences, Indian Institute of Science
India

STAINFORTH, David

Atmospheric, Oceanic and
Planetary Physics, Department of
Physics, University of Oxford
UK

STAMMER, Detlef

Institut fuer Meereskunde Zentrum
fuer Meeres und Klimaforschung
Universitaet Hamburg
Germany

STANFORTH, Andrew

Hadley Centre for Climate Prediction
and Research, Met Office
UK

STARK, Sheila

Hadley Centre for Climate Prediction
and Research, Met Office
UK

STEFFEN, Will

Australian National University
Australia

STENCHIKOV, Georgiy

Rutgers, The State University of New Jersey
USA

STERN, William

National Oceanic and
Atmospheric Administration
USA

STEVENSON, David

University of Edinburgh
UK

STOCKER, Thomas F.

Climate and Environmental Physics,
Physics Institute, University of Bern
Switzerland

STONE, Daithí A.

University of Oxford
UK, Canada

STOTT, Lowell D.

Department of Earth Sciences,
University of Southern California
USA

STOTT, Peter A.

Hadley Centre for Climate Prediction
and Research, Met Office
UK

STOUFFER, Ronald J.

National Oceanic and Atmospheric
Administration, Geophysical
Fluid Dynamics Laboratory
USA

STUBER, Nicola

Department of Meteorology,
University of Reading
UK, Germany

SUDO, Kengo

Nagoya University
Japan

SUGA, Toshio

Tohoku University
Japan

SUMI, Akimasa

Center for Climate System
Research, University of Tokyo
Japan

SUPPIAH, Ramasamy

CSIRO
Australia

SWEENEY, Colm

Princeton University
USA

TADROSS, Mark

Climate Systems Analysis Group,
University of Cape Town
South Africa

TAKEMURA, Toshihiko

Research Institute for Applied
Mechanics, Kyushu University
Japan

TALLEY, Lynne D.

Scripps Institution of Oceanography,
University of California, San Diego
USA

TAMISIEA, Mark

Harvard-Smithsonian Center
for Astrophysics
USA

TAYLOR, Karl E.

Program for Climate Model Diagnosis
and Intercomparison, Lawrence
Livermore National Laboratory
USA

TEBALDI, Claudia

National Center for Atmospheric Research
USA

TENG, Haiyan

National Center for Atmospheric Research
USA, China

TENNANT, Warren

South African Weather Service
South Africa

TERRAY, Laurent

European Centre for Research and Advanced
Training in Scientific Computation
France

TETT, Simon

Hadley Centre for Climate Prediction
and Research, Met Office
UK

TEXTOR, Christiane

Laboratoire des Sciences du
Climat et de l'Environnement
France, Germany

THOMAS, Robert H.

EG&G Technical Services, Inc. and
Centro de Estudios Científicos (CECS)
USA, Chile

THOMPSON, Lonnie

Ohio State University
USA

THORNCROFT, Chris

Department of Earth and Atmospheric
Science, University at Albany, SUNY
USA, UK

THORNE, Peter

Hadley Centre for Climate Prediction
and Research, Met Office
UK

TIAN, Yuhong

Georgia Institute of Technology
USA, China

TRENBERTH, Kevin E.

Climate Analysis Section, National
Center for Atmospheric Research
USA

TSELIODIS, George

National Aeronautics and Space
Administration, Goddard Institute for
Space Studies, Columbia University
USA, Greece

TSIMPLIS, Michael

National Oceanography Centre,
University of Southampton
UK, Greece

UNNIKRISHNAN, Alakkat S.

National Institute of Oceanography
India

UPPALA, Sakari

European Centre for Medium-
Range Weather Forecasts
ECMWF

VAN DE WAL, Roderik Sylvester Willo
Institute for Marine and Atmospheric
Research, Utrecht University
Netherlands

VAN DORLAND, Robert
Royal Netherlands Meteorological
Institute (KNMI)
Netherlands

VAN NOIJE, Twan
Royal Netherlands Meteorological
Institute (KNMI)
Netherlands

VAUGHAN, David
British Antarctic Survey
UK

VILLALBA, Ricardo
Departamento de Dendrocronología e
Historia Ambiental, Instituto Argentino
de Novología, Glaciología y Ciencias
Ambientales (IANIGLA - CRICYT)
Argentina

VOLODIN, Evgeny M.
Institute of Numerical Mathematics
of Russian Academy of Sciences
Russian Federation

VOSE, Russell
National Oceanic and Atmospheric
Administration, National
Climatic Data Center
USA

WAELBROECK, Claire
Institut Pierre Simon Laplace,
Laboratoire des Sciences du Climat
et de l'Environnement, CNRS
France

WALSH, John
University of Alaska
USA

WANG, Bin
National Key Laboratory of Numerical
Modeling for Atmospheric Sciences
and Geophysical Fluid Dynamics,
Institute of Atmospheric Physics,
Chinese Academy of Sciences
China

WANG, Bin
University of Hawaii
USA

WANG, Minghuai
Department of Atmospheric, Oceanic, and
Space Sciences, University of Michigan
USA

WANG, Ray
Georgia Institute of Technology
USA

WANNINKHOF, Rik
Atlantic Oceanographic and Meteorological
Laboratory, National Oceanic and
Atmospheric Administration
USA

WARREN, Stephen
University of Washington
USA

WASHINGTON, Richard
UK, South Africa

WATTERSON, Ian G.
CSIRO Marine and Atmospheric Research
Australia

WEAVER, Andrew J.
School of Earth and Ocean
Sciences, University of Victoria
Canada

WEBB, Mark
Hadley Centre for Climate Prediction
and Research, Met Office
UK

WEISHEIMER, Antje
European Centre for Medium-
Range Weather Forecasting and
Free University, Berlin
ECMWF, Germany

WEISS, Ray
Scripps Institution of Oceanography,
University of California, San Diego
USA

WHEELER, Matthew
Bureau of Meteorology Research Centre
Australia

WHETTON, Penny
CSIRO Marine and Atmospheric Research
Australia

WHORF, Tim
Scripps Institution of Oceanography,
University of California, San Diego
USA

WIDMANN, Martin
GKSS Research Centre, Geesthacht
and School of Geography, Earth
and Environmental Sciences,
University of Birmingham
Germany, UK

WIELICKI, Bruce
National Aeronautics and Space
Administration, Langley Research Center
USA

WIGLEY, Tom M.L.
National Center for Atmospheric Research
USA

WILBY, Rob
Environment Agency of England and Wales
UK

WILD, Martin
ETH Zürich, Institute for Atmospheric
and Climate Science
Switzerland

WILD, Oliver
Frontier Research Center for Global
Change, Japan Agency for Marine-
Earth Science and Technology
Japan, UK

WILES, Gregory
The College of Wooster
USA

WILLEBRAND, Jürgen
Leibniz Institut für Meereswissenschaften
an der Universität Kiel
Germany

WILLIS, Josh
Jet Propulsion Laboratory
USA

WOFSY, Steven C.
Division of Engineering and Applied
Science, Harvard University
USA

WONG, A.P.S.
School of Oceanography,
University of Washington
USA, Australia

WONG, Takmeng
National Aeronautics and Space
Administration, Langley Research Center
USA

WOOD, Richard A.
Hadley Centre for Climate Prediction
and Research, Met Office
UK

WOODWORTH, Philip
Proudman Oceanographic Laboratory
UK

WORBY, Anthony
Australian Antarctic Division and
Antarctic Climate and Ecosystems
Cooperative Research Centre
Australia

WRATT, David
National Climate Centre, National Institute
of Water and Atmospheric Research
New Zealand

WUERTZ, David
National Oceanic and Atmospheric
Administration, National
Climatic Data Center
USA

WYMAN, Bruce L.
Geophysical Fluid Dynamics
Laboratory, National Oceanic and
Atmospheric Administration
USA

XU, Li
Department of Atmospheric, Oceanic, and
Space Sciences, University of Michigan
USA, China

YAMADA, Tomomi
Japanese Society of Snow and Ice
Japan

YASHAYAEV, Igor
Maritimes Region of the Department
of Fisheries and Oceans
Canada

YASUDA, Ichiro
University of Tokyo
Japan

YOSHIMURA, Jun

Meteorological Research Institute
Japan

YU, Rucong

China Meteorological Administration
China

YUKIMOTO, Seiji

Meteorological Research Institute
Japan

ZACHOS, James

University of California, Santa Cruz
USA

ZHAI, Panmao

National Climate Center, China
Meteorological Administration
China

ZHANG, De'er

National Climate Center, China
Meteorological Administration
China

ZHANG, Tingjun

National Snow and Ice Data Center, CIRES,
University of Colorado at Boulder
USA, China

ZHANG, Xiaoye

Chinese Academy of Meteorological
Sciences, Centre for Atmosphere
Watch & Services
China

ZHANG, Xuebin

Climate Research Division,
Environment Canada
Canada

ZHAO, Lin

Cold and Arid Regions Environmental
and Engineering Research Institute,
Chinese Academy of Science
China

ZHAO, Zong-Ci

National Climate Center, China
Meteorological Administration
China

ZHENGTEG, Guo

Institute of Geology and Geophysics,
Chinese Academy of Science
China

ZHOU, Liming

Georgia Institute of Technology
USA, China

ZORITA, Eduardo

Helmholtz Zentrum Geesthacht
Germany, Spain

ZWIERS, Francis

Canadian Centre for Climate Modelling
and Analysis, Environment Canada
Canada

Annex III

Reviewers of the IPCC WGI Fourth Assessment Report

Algeria

AMAR, Matari
IHFR, Oran

MATARI, Amar
IHFR, Oran

Australia

CAI, Wenju
CSIRO Marine and Atmospheric Research

CHURCH, John
CSIRO Marine and Atmospheric
Research and Ecosystems
Cooperative Research Centre

COLMAN, Robert
Bureau of Meteorology Research Centre

ENTING, Ian
University of Melbourne

GIFFORD, Roger
CSIRO Plant Industry

HIRST, Anthony
CSIRO Marine and Atmospheric Research

HOBBINS, Michael
Australian National University

HOWARD, William
Antarctic Climate and Ecosystems
Cooperative Research Centre

HUNTER, John
Antarctic Climate and Ecosystems
Cooperative Research Centre

JONES, Roger
CSIRO Marine and Atmospheric Research

KININMONTH, William

LYNCH, Amanda H.
School of Geography and Environmental
Science, Monash University

MANTON, Michael
Bureau of Meteorology Research Centre

MCAVANEY, Bryant
Bureau of Meteorology Research Centre

MCDUGALL, Trevor
CSIRO Marine and Atmospheric Research

MCGREGOR, John
CSIRO Marine and Atmospheric Research

MCNEIL, Ben
University of New South Wales

MOISE, Aurel
Bureau of Meteorology Research Centre

NICHOLLS, Neville
Monash University

PITMAN, Andrew
Department of Physical Geography,
Macquarie University

RAUPACH, Michael
CSIRO

RINTOUL, Stephen
CSIRO, Marine and Atmospheric
Research and Antarctic Climate and
Ecosystems Cooperative Research Centre

RODERICK, Michael
Australian National University

ROTSTAYN, Leon
CSIRO Marine and Atmospheric Research

SIEMS, Steven
Monash University

SIMMONDS, Ian
University of Melbourne

TREWIN, Blair
National Climate Centre,
Bureau of Meteorology

VAN OMMEN, Tas
Australian Antarctic Division

WALSH, Kevin
School of Earth Sciences,
University of Melbourne

WATKINS, Andrew
National Climate Centre,
Bureau of Meteorology

WHEELER, Matthew
Bureau of Meteorology Research Centre

WHITE, Neil
CSIRO Marine and Atmospheric Research

Austria

BÖHM, Reinhard
Central Institute for Meteorology
and Geodynamics

KIRCHENGAST, Gottfried
University of Graz

O'NEILL, Brian
IIASA and Brown University

RADUNSKY, Klaus
Umweltbundesamt

Belgium

BERGER, André
Université catholique de Louvain,
Institut d'Astronomie et de
Géophysique G. Lemaître

DE BACKER, Hugo
Royal Meteorological Institute

GOOSSE, Hugues
Université catholique de Louvain

JANSSENS, Ivan A.
University of Antwerp

LOUTRE, Marie-France
Université catholique de Louvain,
Institut d'Astronomie et de
Géophysique G. Lemaître

VAN LIPZIG, Nicole
Katholieke Universiteit Leuven

Benin

BOKO, Michel
Université de Bourgogne

GUENDEHOU, G. H. Sabin
Benin Centre for Scientific
and Technical Review

VISSIN, Expédit Wilfrid
LECREDE/DGAT/FLASH/
Université d'Abomey-Calavi

YABI, Ibouaïma
Laboratoire de Climatologie/DGAT/UAC

Brazil

CARDIA SIMÕES, Jefferson
Departamento de Geografia, Instituto
de Geociências, Universidade
Federal do Rio Grande do Sul

GOMES, Marcos S.P.
Department of Mechanical
Research, Pontifical Catholic
University of Rio de Janeiro

MARENGO ORSINI, Jose Antonio
CPTEC/INPE

Canada

BELTRAMI, Hugo
St. Francis Xavier University

BROWN, Ross
Environment Canada

Expert reviewers are listed by country. Experts from international organizations are listed at the end.

CAYA, Daniel

Consortium Ouranos

CHYLEK, Petr

Dalhousie University, Departments of Physics and Oceanography

CLARKE, Garry

Earth and Ocean Sciences, University of British Columbia

CLARKE, R. Allyn

Bedford Institute of Oceanography

CULLEN, John

Dalhousie University

DERKSEN, Chris

Climate Research Branch, Meteorological Service of Canada

FERNANDES, Richard

Canada Centre for Remote Sensing, Natural Resources Canada

FORBES, Donald L.

Natural Resources Canada, Geological Survey of Canada

FREELAND, Howard

Department of Fisheries and Oceans

GARRETT, Chris

University of Victoria

HARVEY, Danny

University of Toronto

ISAAC, George

Environment Canada

JAMES, Thomas

Geological Survey of Canada, Natural Resources Canada

LEWIS, C.F. Michael

Geological Survey of Canada, Natural Resources Canada

MACDONALD, Robie

Department of Fisheries and Oceans

MATTHEWS, H. Damon

University of Calgary and Concordia University

MCINTYRE, Stephen

University of Toronto

MCKITRICK, Ross

University of Guelph

PELTIER, Wm. Richard

Department of Physics, University of Toronto

SAVARD, Martine M.

Geological Survey of Canada, Natural Resources Canada

SMITH, Sharon

Geological Survey of Canada, Natural Resources Canada

TRISHCHENKO, Alexander P.

Canada Centre for Remote Sensing, Natural Resources Canada

WANG, Shusen

Canada Centre for Remote Sensing, Natural Resources Canada

WANG, Xiaolan L.

Climate Research Branch, Meteorological Service of Canada

ZWIERS, Francis

Canadian Centre for Climate Modelling and Analysis, Environment Canada

Chile**ACEITUNO, Patricio**

Department Geophysics, Universidad de Chile

China**CAI, Zucong**

Institute of Soil Science, Chinese Academy of Sciences

CHAN, Johnny

City University of Hong Kong

DONG, Zhaoqian

Polar Research Institute of China

GONG, Dao-Yi

College of Resources Science and Technology, Beijing Normal University

GUO, Xueliang

Institute of Atmospheric Physics, Chinese Academy of Sciences

LAM, Chiu-Ying

Hong Kong Observatory

REN, Guoyu

National Climate Center, China Meteorological Administration

SHI, Guang-yu

Institute of Atmospheric Physics, Chinese Academy of Sciences

SU, Jilan

Lab of Ocean Dynamic Processes and Satellite Oceanography, Second Institute of Oceanography, State Oceanic Administration

SUN, Junying

Centre for Atmosphere Watch and Services, Chinese Academy of Meteorological Sciences, CMA

WANG, Dongxiao

South China Sea Institute of Oceanology, Chinese Academy of Sciences

WANG, Mingxing

Institute of Atmospheric Physics, Chinese Academy of Sciences

XIE, Zhenghui

Institute of Atmospheric Physics, Chinese Academy of Sciences

XU, Xiaobin

Chinese Academy of Meteorological Sciences

YU, Rucong

China Meteorological Administration

ZHAO, Zong-Ci

National Climate Center, China Meteorological Administration

ZHOU, Tianjun

Institute of Atmospheric Physics, Chinese Academy of Sciences

Denmark**GLEISNER, Hans**

Atmosphere Space Research Division, Danish Met. Institute

STENDEL, Martin

Danish Meteorological Institute

Egypt**EL-SHAHAWY, Mohamed**

Cairo University, Egyptian Environmental Affairs Agency

Estonia**JAAGUS, Jaak**

University of Tartu

Fiji**LAL, Murari**

University of the South Pacific

Finland**CARTER, Timothy**

Finnish Environment Institute

KORTELAJAINEN, Pirkko

Finnish Environment Institute

KULMALA, Markku

University of Helsinki

LAAKSONEN, Ari

University of Kuopio

MÄKIPÄÄ, Raisa

Finnish Forest Research Institute

RÄISÄNEN, Jouni

Department of Physical Sciences, University of Helsinki

SAVOLAINEN, Iikka

Technical Research Centre of Finland

France**BONY, Sandrine**

Laboratoire de Météorologie Dynamique, Institut Pierre Simon Laplace

BOUSQUET, Philippe

Institut Pierre Simon Laplace, Laboratoire des Sciences du Climat et de l'Environnement

BRACONNOT, Pascale

Pascale Braconnot Institut Pierre Simon Laplace, Laboratoire des Sciences du Climat et de l'Environnement

CAZENAVE, Anny

Laboratoire d'Etudes en Géophysique et Océanographie Spatiale (LEGOS), CNES

CLERBAUX, Cathy

Centre National de Recherche Scientifique

CORTIJO, Elsa

Laboratoire des Sciences du Climat et de l'Environnement, CNRS-CEA-UVSQ

DELECLUSE, Pascale

CEA, CNRS

DÉQUÉ, Michel

Météo-France

DUFRESNE, Jean-Louis

Laboratoire de Météorologie Dynamique, Institut Pierre Simon Laplace

FRIEDLINGSTEIN, Pierre

Institut Pierre Simon Laplace, Laboratoire des Sciences du Climat et de l'Environnement

GENTHON, Christophe

Centre National de Recherche Scientifique, Laboratoire de Glaciologie et Géophysique de l'Environnement

GUILYARDI, Eric

Laboratoire des Sciences du Climat et de l'Environnement

GUIOT, Joel

CEREGE, Centre National de Recherche Scientifique

HAUGLUSTAINE, Didier

Institut Pierre Simon Laplace, Laboratoire des Sciences du Climat et de l'Environnement, CEA-CNRS-UVSQ

JOUSSAUME, Sylvie

Centre National de Recherche Scientifique

KANDEL, Robert

Laboratoire de Météorologie Dynamique, Ecole Polytechnique

KHODRI, Myriam

Institut de Recherche Pour le Développement

LABEYRIE, Laurent

Laboratoire des Sciences du Climat et de l'Environnement

MARTIN, Eric

Météo-France

MOISSELIN, Jean-Marc

Météo-France

PAILLARD, Didier

Laboratoire des Sciences du Climat et de l'Environnement

PETIT, Michel

CGTI

PLANTON, Serge

Météo-France

RAMSTEIN, Gilles

Laboratoire des Sciences du Climat et de l'Environnement

SCHULZ, Michael

Institut Pierre Simon Laplace, Laboratoire des Sciences du Climat et de l'Environnement, CEA-CNRS-UVSQ

SEGUIN, Bernard

INRA

TEXTOR, Christiane

Laboratoire des Sciences du Climat et de l'Environnement

WALBROECK, Claire

Institut Pierre Simon Laplace, Laboratoire des Sciences du Climat et de l'Environnement, CNRS

Germany**BANGE, Hermann W.**

Leibniz Institut für Meereswissenschaften, IFM-GEOMAR

BAUER, Eva

Potsdam Institute for Climate Impact Research

BECK, Christoph

Global Precipitation Climatology Centre

BROVKIN, Victor

Potsdam Institute for Climate Impact Research

CHURKINA, Galina

Max Planck Institute for Biogeochemistry

COTRIM DA CUNHA, Leticia

Max-Planck-Institut für Biogeochemie

DOTZEK, Nikolai

Deutsches Zentrum für Luft und Raumfahrt, Institut für Physik der Atmosphäre

FEICHTER, Johann

Max Planck Institute for Meteorology

GANOPOLSKI, Andrey

Potsdam Institute for Climate Impact Research

GIORGETTA, Marco A.

Max Planck Institute for Meteorology

GRASSL, Hartmut

Max Planck Institute for Meteorology

GREWE, Volker

Deutsches Zentrum für Luft und Raumfahrt, Institut für Physik der Atmosphäre

GRIESER, Jürgen

Deutscher Wetterdienst, Global Precipitation Climatology Centre

HARE, William

Potsdam Institute for Climate Impact Research

HELD, Hermann

Potsdam Institute for Climate Impact Research

HOFZUMAHAUS, Andreas

Forschungszentrum Jülich, Institut für Chemie und Dynamik der Geosphäre II: Troposphäre

KOPPMANN, Ralf

Institut für Chemie und Dynamik der Geosphäre, Institut II: Troposphäre, Forschungszentrum Jülich, Jülich, Germany

LATIF, Mojib

Leibniz Institut für Meereswissenschaften, IFM-GEOMAR

LAWRENCE, Mark

Max Planck Institute for Chemistry

LELIEVELD, Jos

Max Planck Institute for Chemistry

LEVERMANN, Anders

Potsdam Institute for Climate Impact Research

LINGNER, Stephan

Europäische Akademie Bad Neuenahr-Ahrweiler GmbH

LUCHT, Wolfgang

Potsdam Institute for Climate Impact Research

MAROTZKE, Jochem

Max Planck Institute for Meteorology

MATA, Louis Jose

Center for Development Research, University of Bonn

MEINSHAUSEN, Malte

Potsdam Institute for Climate Impact Research

MICHAELOWA, Axel

Hamburg Institute of International Economics

MÜLLER, Rolf

Research Centre Jülich

RAHMSTORF, Stefan

Potsdam Institute for Climate Impact Research

RHEIN, Monika

Institute for Environmental Physics, University Bremen

SAUSEN, Robert

Deutsches Zentrum für Luft und Raumfahrt, Institut für Physik der Atmosphäre

SCHOENWIESE, Christian-D.

University Frankfurt a.M., Institute for Atmosphere and Environment

SCHOTT, Friedrich

Leibniz Institut für Meereswissenschaften, IFM-GEOMAR

SCHULZ, Michael
University of Bremen

SCHÜTZENMEISTER, Falk
Technische Universität Dresden,
Institut für Soziologie

STAMMER, Detlef
Institut fuer Meereskunde Zentrum
fuer Meeres und Klimaforschung
Universitaet Hamburg

TEGEN, Ina
Institute for Tropospheric Research

VÖLKER, Christoph
Alfred Wegener Institute for
Polar and Marine Research

WEFER, Gerold
University of Bremen, Research
Center Ocean Margins

WURZLER, Sabine
North Rhine-Westphalia State
Environment Agency

ZENK, Walter
Leibniz Institut für Meereswissenschaften,
IFM-GEOMAR

ZOLINA, Olga
Meteorologisches Institut
der Universität Bonn

ZORITA, Eduardo
Helmholtz Zentrum Geesthacht

Hungary

ZAGONI, Miklos
Budapest University

India

SRIKANTHAN, Ramachandran
Physical Research Laboratory

TULKENS, Philippe
The Energy and Research Institute (TERI)

Iran

RAHIMZADEH, Fatemeh
Atmospheric Science & Meteorological
Research Center (ASMER), I.R. of Iran
Meteorological Organization (IRIMO)

Ireland

FEALY, Rowan
National University of Ireland, Maynooth

SWEENEY, John
National University of Ireland, Maynooth

Italy

ARTALE, Vincenzo
Italian National Agency for
New Technologies, Energy and
the Environment (ENEA)

BALDI, Marina
Consiglio Nazionale delle Ricerche
(CNR), Inst of Biometeorology

BERGAMASCHI, Peter
European Commission, Joint
Research Centre, Institute for
Environment and Sustainability

BRUNETTI, Michele
Istituto di Scienze dell'atmosfera
e del Clima (ISAC) Consiglio
Nazionale delle Ricerche (CNR)

CAMPOSTRINI, Pierpaolo
CORILA

COLOMBO, Tiziano
Italian Met Service

CORTI, Susanna
Istituto di Scienze dell'atmosfera
e del Clima (ISAC) Consiglio
Nazionale delle Ricerche (CNR)

DESIATO, Franco
Agenzia per la protezione dell'ambiente
e per i servizi tecnici (APAT)

DI SARRA, Alcide
Italian National Agency for
New Technologies, Energy and
the Environment (ENEA)

DRAGONI, Walter
Perugia University

ETIOPE, Giuseppe
Istituto Nazionale di Geofisica e
Vulcanologia

FACCHINI, Maria Cristina
Consiglio Nazionale delle Ricerche (CNR)

GIORGI, Filippo
Abdus Salam International Centre
for Theoretical Physics

LIONELLO, Piero
Univ. of Lecce, Dept. "Scienza dei materiali"

MARIOTTI, Annarita
Italian National Agency for New
Technologies, Energy and the Environment
(ENEA) and Earth System Science
Interdisciplinary Center (ESSIC-USA)

MOSETTI, Renzo
OGS

NANNI, Teresa
Istituto di Scienze dell'atmosfera e
del Clima (ISAC) Consiglio
Nazionale delle Ricerche (CNR)

RUTI, Paolo Michele
Italian National Agency for New
Technologies, Energy and the Environment

SANTINELLI, Chiara
Consiglio Nazionale delle Ricerche (CNR)

VAN DINGENEN, Rita
European Commission, Joint
Research Centre, Institute for
Environment and Sustainability

VIGNUDELLI, Stefano
Consiglio Nazionale delle Ricerche
(CNR), Istituto di Biofisica

Japan

ALEXANDROV, Georgii
National Institute for Environmental Studies

ANNAN, James
Frontier Research Center for Global
Change, Japan Agency for Marine-
Earth Science and Technology

AOKI, Teruo
Meteorological Research Institute,
Japan Meteorological Agency

AWAJI, Toshiyuki
Kyoto University

EMORI, Seita
National Institute for Environmental
Studies and Frontier Research Center
for Global Change, Japan Agency for
Marine-Earth Science and Technology

HARGREAVES, Julia
Frontier Research Center for Global
Change, Japan Agency for Marine-
Earth Science and Technology

HAYASAKA, Tadahiro
Research Institute for Humanity and Nature

IKEDA, Motoyoshi
Hokkaido University

ITOH, Kiminori
Yokohama National University

KAWAMIYA, Michio
Frontier Research Center for Global
Change, Japan Agency for Marine-
Earth Science and Technology

KIMOTO, Masahide
Center for Climate System
Research, University of Tokyo

KITOH, Akio
First Research Laboratory, Climate Research
Department, Meteorological Research
Institute, Japan Meteorological Agency

KOBAYASHI, Shigeki
TRDL

KONDO, Hiroki
Frontier Research Center for Global
Change, Japan Agency for Marine-
Earth Science and Technology

MAKI, Takashi
Meteorological Research Institute,
Japan Meteorological Agency

MAKSYUTOV, Shamil

National Institute for Environmental Studies

MARUYAMA, Koki

CRIEPI

MATSUNO, Taroh

Frontier Research Center for Global Change, Japan Agency for Marine-Earth Science and Technology

MIKAMI, Masao

Meteorological Research Institute, Japan Meteorological Agency

MIKAMI, Takehiko

Tokyo Metropolitan University

NAKAJIMA, Teruyuki

Center for Climate System Research, University of Tokyo

NAKAWO, Masayoshi

Research Institute for Humanity and Nature

NODA, Akira

Meteorological Research Institute, Japan Meteorological Agency

OHATO, Tetsuo

JAMSTEC

ONO, Tsuneo

Hokkaido National Fisheries Research Institute, Fisheries Research Agency

SASAKI, Hidetaka

Meteorological Research Institute, Japan Meteorological Agency

SATO, Yasuo

Meteorological Research Institute, Japan Meteorological Agency

SEKIYA, Akira

National Institute of Advanced Industrial Science and Technology (AIST)

SHINODA, Masato

Tottori University, Arid Land Research Center

SUGA, Toshio

Tohoku University

SUGI, Masato

Meteorological Research Institute, Japan Meteorological Agency

TOKIOKA, Tatsushi

Frontier Research Center for Global Change, Japan Agency for Marine-Earth Science and Technology

TOKUHASHI, Kazuaki

National Institute of Advanced Industrial Science and Technology (AIST)

TSUSHIMA, Yoko

Japan Agency for Marine-Earth Science and Technology

UCHIYAMA, Akihiro

Meteorological Research Institute, Japan Meteorological Agency

YAMAMOTO, Susumu

Graduate School of Environmental Science, Okayama University

YAMANOUCI, Takashi

National Institute of Polar Research

YAMASAKI, Masanori

Japan Agency for Marine-Earth Science and Technology

YAMAZAKI, Koji

Graduate School of Environmental Science, Hokkaido University

YOKOYAMA, Yusuke

Department of Earth and Planetary Sciences, University of Tokyo

TSUTSUMI, Yukitomo

Meteorological Research Institute, Japan Meteorological Agency

Republic of Korea**KIM, Kyung-Ryul**

Seoul National University, School of Earth and Environmental Services

Mexico**LLUCH-BELDA, Daniel**

Centro Interdisciplinario de Ciencias Marinas del IPN

Mozambique**QUEFACE, Antonio Joaquim**

Physics Department, Eduardo Mondlane University

Netherlands, Antilles and Aruba**MARTIS, Albert**

Climate Research Center, Meteorological Service Netherlands, Antilles & Aruba

Netherlands**BAEDE, Alphonsus**

Royal Netherlands Meteorological Institute (KNMI) and Ministry of Housing, Spatial Planning and the Environment

BURGERS, Gerrit

Royal Netherlands Meteorological Institute (KNMI)

DE BRUIN, Henk

Meteorology and Air Quality Group, Wageningen University

DE WIT, Florens**DILLINGH, Douwe**

National Institute for Coastal and Marine Management / RIKZ

HAARSMA, Reindert

Royal Netherlands Meteorological Institute (KNMI)

HAZELEGER, Wilco

Royal Netherlands Meteorological Institute (KNMI)

HOLTSLAG, Albert A. M.

Wageningen University

KROON, Dick

Vrije Universiteit, Amsterdam

SIEGMUND, Peter

Royal Netherlands Meteorological Institute (KNMI)

STERL, Andreas

Royal Netherlands Meteorological Institute (KNMI)

VAN AKEN, Hendrik M.

Royal Netherlands Institute for Sea Research (NIOZ)

VAN DE WAL, Roderik Sylvester Willo

Institute for Marine and Atmospheric Research, Utrecht University

VAN DEN HURK, Bart

Royal Netherlands Meteorological Institute (KNMI)

VAN NOIJE, Twan

Royal Netherlands Meteorological Institute (KNMI)

VAN VELTHOVEN, Peter

Royal Netherlands Meteorological Institute (KNMI)

VANDEBERGHE, Jef

Vrije Universiteit, Inst. of Earth Sciences

VEEFKIND, Pepijn

Royal Netherlands Meteorological Institute (KNMI)

VELDERS, Guus J.M.

Netherlands Environmental Assessment Agency (MNP)

New Zealand**ALLOWAY, Brent**

Institute of Geological and Nuclear Sciences

BARRETT, Peter

Antarctic Research Centre, Victoria University of Wellington

BODEKER, Greg

National Institute of Water and Atmospheric Research

BOWEN, Melissa

National Institute of Water and Atmospheric Research

CRAMPTON, James

Institute of Geological and Nuclear Sciences

GRAY, Vincent

Climate Consultant

LASSEY, Keith

National Institute of Water and Atmospheric Research

LAW, Cliff

National Institute of Water and Atmospheric Research

MACLAREN, Piers

NZ Forest Research Institute

MULLAN, A. Brett

National Institute of Water and Atmospheric Research

NODDER, Scott

National Institute of Water and Atmospheric Research

RENWICK, James A.

National Institute of Water and Atmospheric Research

SALINGER, M. James

National Institute of Water and Atmospheric Research

SHULMEISTER, James

University of Canterbury

WILLIAMS, Paul W.

Auckland University

WRATT, David

National Climate Centre, National Institute of Water and Atmospheric Research

Norway**BENESTAD, Rasmus**

Norwegian Meteorological Institute

FUGLESTVEDT, Jan

Centre for International Climate and Environmental Research (CICERO)

GODAL, Odd

Department of Economics, University of Bergen

HANSSSEN-BAUER, Inger

Norwegian Meteorological Institute

ISAKSEN, Ketil

Norwegian Meteorological Institute

JOHANNESSEN, Ola M.

Nansen Environmental and Remote Sensing Center

KRISTJÁNSSON, Jón Egill

University of Oslo

NESJE, Atle

Department of Earth Science, University of Bergen

PAASCHE, Øyvind

Bjerknes Centre for Climate Research

Peru**GAMBOA, Nadia**

Pontificia Universidad Católica del Perú

Romania**BOJARIU, Roxana**

National Institute of Meteorology and Hydrology (NIMH)

BORONEANT, Constanta-Emilia

National Meteorological Administration

BUSUIOC, Aristita

National Meteorological Administration

MARES, Constantin

Romanian Academy, Geodynamics Institute

MARES, Ileana

Romanian Academy of Technical Studies

Russian Federation**MELESHKO, Valentin**

Voeykov Main Geophysical Observatory

Slovakia**LAPIN, Milan**

Slovak National Climate Program

Spain**AGUILAR, Enric**

Climate Change Research Group, Universitat Rovira i Virgili de Tarragona

BLADÉ, Ileana

Department of Astronomy and Meteorology, University of Barcelona

BRUNET, Manola

University Rovira i Virgili

CALVO COSTA, Eva

Institut de Ciències del Mar

GARCÍA-HERRERA, Ricardo

Universidad Complutense de Madrid

GONZÁLEZ-ROUCO, Jesus Fidel

Universidad Complutense de Madrid

LAVIN, Alicia M.

Instituto Español de Oceanografía

MARTIN-VIDE, Javier

Physical Geography of the University of Barcelona

MONTOYA, Marisa

Dpto. Astrofísica y Física de la Atmosfera, Facultad de Ciencias Físicas, Universidad Complutense de Madrid

PELEJERO, Carles

Institut de Ciències del Mar, CMIMA-CSIC

RIBERA, Pedro

Universidad Pablo de Olavide

Sweden**HOLMLUND, Per**

Stockholm University

KJELLSTRÖM, Erik

Swedish Meteorological and Hydrological Institute

LECK, Caroline

Department of Meteorology, Stockholm University

RUMM AINEN, Markku

Rosby Centre, Swedish Meteorological and Hydrological Institute

Switzerland**APPENZELLER, Christof**

Federal Office of Meteorology and Climatology MeteoSwiss

BLUNIER, Thomas

Climate and Environmental Physics, University of Bern

BRÖNNIMANN, Stefan

ETH Zürich

CASTY, Carlo

Climate and Environmental Physics

CHERUBINI, Paolo

Swiss Federal Research Institute WSL

ESPER, Jan

Swiss Federal Research Institute WSL

FREI, Christoph

Federal Office of Meteorology and Climatology MeteoSwiss

GHOSH, Sucharita

Swiss Federal Research Institute WSL

HAEBERLI, Wilfried

Geography Department, University of Zürich

JOOS, Fortunat

Climate and Environmental Physics, Physics Institute, University of Bern

KNUTTI, Reto

Climate and Global Dynamics Division, National Center for Atmospheric Research

LUTERBACHER, Jürg

Institute of Geography, Climatology and Meteorology, and National Centre of Competence in Research on Climate, University of Bern

MARCOLLI, Claudia

ETH Zürich, Institute for Atmosphere and Climate

PETER, Thomas

ETH Zürich

PHILIPONA, Rolf

Observatory Davos

PLATTNER, Gian-Kasper

Climate and Environmental Physics, Physics Institute, University of Bern

RAIBLE, C. Christoph

Climate and Environmental Physics, University of Bern

REBETEZ, Martine

Swiss Federal Research Institute WSL

ROSSI, Michel J.

Ecole Polytechnique Fédérale de Lausanne, Laboratoire de Pollution Atmosphérique et Sol

ROZANOV, Eugene

IAC ETHZ and PMOD/WRC

SCHÄR, Christoph

ETH Zürich, Institute for Atmospheric and Climate Science

SIDDALL, Mark

Climate and Environmental Physics, University of Bern

SPAHNI, Renato

Climate and Environmental Physics, Physics Institute, University of Bern

STAEHELIN, Johannes

ETH Zürich

STOCKER, Thomas F.

Climate and Environmental Physics, Physics Institute, University of Bern

WANNER, Heinz

National Centre of Competence in Research on Climate, University of Bern

WILD, Martin

ETH Zürich, Institute for Atmospheric and Climate Science

Thailand**GARIVAIT, Savitri**

The Joint Graduate School of Energy and Environment, King Mongkut's University of Technology Thonburi

LIMMEECHOKCHAI, Bundit

Sirindhorn International Institute of Technology, Thammasat Univ.

Togo**AJAVON, Ayite-Lo N.**

Atmospheric Chemistry Laboratory

UK**ALEXANDER, Lisa**

Hadley Centre for Climate Prediction and Research, Met Office

ALLAN, Richard

Environmental Systems Science Centre, University of Reading

BANKS, Helene

Hadley Centre for Climate Prediction and Research, Met Office

BETTS, Richard A.

Hadley Centre for Climate Prediction and Research, Met Office

BODAS-SALCEDO, Alejandro

Hadley Centre for Climate Prediction and Research, Met Office

BOUCHER, Olivier

Hadley Centre for Climate Prediction and Research, Met Office

BROWN, Simon

Hadley Centre for Climate Prediction and Research, Met Office

BRYDEN, Harry

University of Southampton

CAESAR, John

Hadley Centre for Climate Prediction and Research, Met Office

CARSLAW, Kenneth

University of Leeds

COLLINS, Matthew

Hadley Centre for Climate Prediction and Research, Met Office

COLLINS, William

Hadley Centre for Climate Prediction and Research, Met Office

CONNOLLEY, William

British Antarctic Survey

COURTNEY, Richard S.

European Science and Environment Forum

CRUCIFIX, Michel

Hadley Centre for Climate Prediction and Research, Met Office

FALLOON, Pete

Hadley Centre for Climate Prediction and Research, Met Office

FOLLAND, Christopher

Hadley Centre for Climate Prediction and Research, Met Office

FORSTER, Piers

School of Earth and Environment, University of Leeds

FOWLER, Hayley

Newcastle University

GEDNEY, Nicola

Hadley Centre for Climate Prediction and Research, Met Office

GILLETT, Nathan P.

Climatic Research Unit, School of Environmental Sciences, University of East Anglia

GRAY, Lesley

Reading University

GREGORY, Jonathan M.

Department of Meteorology, University of Reading and Hadley Centre for Climate Prediction and Research, Met Office

GRIGGS, David

Hadley Centre for Climate Prediction and Research, Met Office

HAIGH, Joanna

Imperial College London

HARANGOZO, Steve

British Antarctic Survey

HAWKINS, Stephen J.

The Marine Biological Association of the UK

HIGHWOOD, Eleanor

University of Reading

HINDMARSH, Richard

British Antarctic Survey

HOSKINS, Brian J.

Department of Meteorology, University of Reading

HOUSE, Joanna

Quantifying and Understanding the Earth System Programme, University of Bristol

INGRAM, William

Hadley Centre for Climate Prediction and Research, Met Office

JOHNS, Timothy

Hadley Centre for Climate Prediction and Research, Met Office

JONES, Christopher

Hadley Centre for Climate Prediction and Research, Met Office

JONES, Gareth S.

Hadley Centre for Climate Prediction and Research, Met Office

JONES, Philip D.

Climatic Research Unit, School of Environmental Sciences, University of East Anglia

JOSEY, Simon

National Oceanography Centre, University of Southampton

KING, John

British Antarctic Survey

LE QUÉRÉ, Corrine

University of East Anglia and British Antarctic Survey

LEE, David

Manchester Metropolitan University

LOWE, Jason

Hadley Centre for Climate Prediction and Research, Met Office

MARSH, Robert

National Oceanography Centre, University of Southampton

MARTIN, Gill

Hadley Centre for Climate Prediction and Research, Met Office

MCCARTHY, Mark

Hadley Centre for Climate Prediction and Research, Met Office

MCDONALD, Ruth

Hadley Centre for Climate Prediction and Research, Met Office

MITCHELL, John

Hadley Centre for Climate Prediction and Research, Met Office

MURPHY, James

Hadley Centre for Climate Prediction and Research, Met Office

NICHOLLS, Robert

School of Civil Engineering and the Environment, University of Southampton

PARKER, David

Hadley Centre for Climate Prediction and Research, Met Office

PRENTICE, Iain Colin

Quantifying and Understanding the Earth System Programme, Department of Earth Sciences, University of Bristol

RAPER, Sarah

Manchester Metropolitan University

RAYNER, Nick

Hadley Centre for Climate Prediction and Research, Met Office

REISINGER, Andy

IPCC Synthesis Report TSU

RIDLEY, Jeff

Hadley Centre for Climate Prediction and Research, Met Office

ROBERTS, C. Neil

University of Plymouth, School of Geography

RODGER, Alan

British Antarctic Survey

ROSCOE, Howard

British Antarctic Survey

ROUGIER, Jonathan

Durham University

ROWELL, Dave

Hadley Centre for Climate Prediction and Research, Met Office

SENIOR, Catherine

Hadley Centre for Climate Prediction and Research, Met Office

SEXTON, David

Hadley Centre for Climate Prediction and Research, Met Office

SHINE, Keith

University of Reading

SLINGO, Julia

National Centre for Atmospheric Science, University of Reading

SMITH, Leonard A.

London School of Economics

SROKOSZ, Meric

National Oceanography Centre

STARK, Sheila

Hadley Centre for Climate Prediction and Research, Met Office

STEPHENSON, David

Department of Meteorology, University of Reading

STONE, Daithí A.

University of Oxford

STOTT, Peter A.

Hadley Centre for Climate Prediction and Research, Met Office

THORNE, Peter

Hadley Centre for Climate Prediction and Research, Met Office

TSIMPLIS, Michael

National Oceanography Centre, University of Southampton

TURNER, John

British Antarctic Survey

VAUGHAN, David

British Antarctic Survey

VELLINGA, Michael

Hadley Centre for Climate Prediction and Research, Met Office

WASDELL, David

Meridian Programme

WILLIAMS, Keith

Hadley Centre for Climate Prediction and Research, Met Office

WOLFF, Eric

British Antarctic Survey

WOOD, Richard A.

Hadley Centre for Climate Prediction and Research, Met Office

WOODWORTH, Philip

Proudman Oceanographic Laboratory

WU, Peili

Hadley Centre for Climate Prediction and Research, Met Office

Uruguay**BIDEGAIN, Mario**

Universidad de la Republica

USA**ALEXANDER, Becky**

University of Washington

ALEXANDER, Michael

National Oceanic and Atmospheric Administration, Climate Diagnostics Branch, Physical Science Division, Earth System Research Lab

ALLEY, Richard B.

Department of Geosciences, Pennsylvania State University

ANDERSON, David M.

National Center for Atmospheric Research, Paleoclimatology

ANDERSON, Theodore

University of Washington

ANDERSON, Wilmer

University of Wisconsin, Madison, Physics Department

ANTHES, Richard

University Corporation for Atmospheric Research

ARRITT, Raymond

Iowa State University

AVERYT, Kristen

IPCC WGI TSU, National Oceanic and Atmospheric Administration, Earth System Research Laboratory

BAER, Paul

Stanford University, Center for Environmental Science and Policy

BAKER, Marcia

University of Washington

BARRY, Roger

National Snow and Ice Data Center, University of Colorado

BATES, Timothy

National Oceanic and Atmospheric Administration

BAUGHCUUM, Steven

Boeing Company

BENTLEY, Charles R.

University of Wisconsin, Madison

BERNSTEIN, Lenny

International Petroleum Industry Environmental Conservation Association & L.S. Bernstein & Associates, LLC

BOND, Tami

University of Illinois at Urbana-Champaign

BROCCOLI, Anthony J.

Rutgers University

BROMWICH, David

Byrd Polar Research Center, The Ohio State University

BROOKS, Harold

National Oceanic and Atmospheric Administration, National Severe Storms Laboratory

BRYAN, Frank

National Center for Atmospheric Research

CAMERON-SMITH, Philip

Lawrence Livermore National Laboratory

CHIN, Mian

National Aeronautics and Space Administration, Goddard Space Flight Center

- CHRISTY, John**
University of Alabama in Huntsville
- CLEMENS, Steven**
Brown University
- COFFEY, Michael**
National Center for Atmospheric Research
- COLLINS, William D.**
Climate and Global Dynamics Division,
National Center for Atmospheric Research
- CROWLEY, Thomas**
Duke University
- CUNNOLD, Derek**
School of Earth and Atmospheric Sciences,
Georgia Institute of Technology
- DAI, Aiguo**
National Center for Atmospheric Research
- DANIEL, John S.**
National Oceanic and Atmospheric
Administration, Earth System
Research Laboratory
- DANILIN, Mikhail**
The Boeing Company
- D'ARRIGO, Rosanne**
Lamont Doherty Earth Observatory
- DAVIES, Roger**
Jet Propulsion Laboratory, California
Institute of Technology
- DEL GENIO, Anthony**
National Aeronautics and Space
Administration, Goddard
Institute for Space Studies
- DIAZ, Henry**
National Oceanic and Atmospheric
Administration, Climate Diagnostics
Branch, Physical Science Division,
Earth System Research Lab
- DICKINSON, Robert E.**
School of Earth and Atmospheric Sciences,
Georgia Institute of Technology
- DIXON, Keith**
National Oceanic and
Atmospheric Administration
- DONNER, Leo**
Geophysical Fluid Dynamics
Laboratory, National Oceanic and
Atmospheric Administration
- DOUGLAS, Bruce**
International Hurricane Research Center
- DOUGLASS, Anne**
National Aeronautics and Space
Administration, Goddard
Space Flight Center
- DUTTON, Ellsworth**
National Oceanic and Atmospheric
Administration, Earth System Research
Laboratory, Global Monitoring Division
- EASTERLING, David**
National Oceanic and Atmospheric
Administration, Earth System
Research Laboratory
- EMANUEL, Kerry A.**
Massachusetts Institute of Technology
- EVANS, Wayne F.J.**
North West Research Associates
- FAHEY, David W.**
National Oceanic and Atmospheric
Administration, Earth System
Research Laboratory
- FEELY, Richard**
National Oceanic and Atmospheric
Administration, Pacific Marine
Environmental Laboratory
- FEINGOLD, Graham**
National Oceanic and
Atmospheric Administration
- FELDMAN, Howard**
American Petroleum Institute
- FEYNMAN, Joan**
Jet Propulsion Laboratory, California
Institute of Technology
- FITZPATRICK, Melanie**
University of Washington
- FOGT, Ryan**
Polar Meteorology Group, Byrd Polar
Research Center and Atmospheric
Sciences Program, Department of
geography, The Ohio State University
- FREE, Melissa**
Air Resources Laboratory, National
Oceanic and Atmospheric Administration
- FU, Qiang**
Department of Atmospheric Sciences,
University of Washington
- GALLO, Kevin**
National Oceanic and Atmospheric
Administration, NESDIS
- GARCIA, Hernan**
National Oceanic and Atmospheric
Administration, National
Oceanographic Data Center
- GASSÓ, Santiago**
University of Maryland, Baltimore
County and NASA
- GENT, Peter**
National Center for Atmospheric Research
- GERHARD, Lee C.**
Thomasson Partner Associates
- GHAN, Steven**
Pacific Northwest National Laboratory
- GNANADESIKAN, Anand**
National Oceanic and Atmospheric
Administration, Geophysical
Fluid Dynamics Laboratory
- GORNITZ, Vivien**
National Aeronautics and Space
Administration, Goddard Institute for
Space Studies, Columbia University
- GROISMAN, Pavel**
University Corporation for Atmospheric
Research at the National Climatic
Data Center, National Oceanic and
Atmospheric Administration
- GRUBER, Nicolas**
Institute of Geophysics and Planetary
Physics, University of California,
Los Angeles and Department of
Environmental Sciences, ETH Zurich
- GURWICK, Noel**
Carnegie Institution of Washington,
Department of Global Ecology
- HAKKARINEN, Chuck**
Electric Power Research Institute, retired
- HALLEGATTE, Stéphane**
Centre International de Recherche sur
l'Environnement et le Développement,
Ecole Nationale des Ponts-et-Chaussées
and Centre National de Recherches
Météorologique, Météo-France
- HALLETT, John**
Desert Research Institute
- HAMILL, Patrick**
San Jose State University
- HARTMANN, Dennis**
University of Washington
- HAYHOE, Katharine**
Texas Tech University
- HEGERL, Gabriele**
Division of Earth and Ocean Sciences,
Nicholas School for the Environment
and Earth Sciences, Duke University
- HELD, Isaac**
National Oceanic and Atmospheric
Administration, Geophysical
Fluid Dynamics Laboratory
- HEMMING, Sidney**
Lamont Doherty Earth Observatory,
Columbia University
- HOULTON, Benjamin**
Stanford University, Dept. of Biological
Sciences; Carnegie Institution of
Washington, Dept. of Global Ecology
- HU, Aixue**
National Center for Atmospheric Research
- HUGHES, Dan**
Hughes and Associates
- ICHOKU, Charles**
Science Systems & Applications,
Inc. (SSAI), NASA-GSFC
- JACOB, Daniel**
Department of Earth and Planetary
Sciences, Harvard University

- JACOBSON, Mark**
Stanford University
- JIN, Menglin**
Department of Atmospheric and Oceanic Sciences, University of Maryland, College Park
- JOYCE, Terrence**
Woods Hole Oceanographic Institution
- KARL, Thomas R.**
National Oceanic and Atmospheric Administration, National Climatic Data Center
- KAROLY, David J.**
University of Oklahoma
- KAUFMAN, Yoram**
National Aeronautics and Space Administration, Goddard Space Flight Center
- KELLER, Klaus**
Pennsylvania State University
- KHESHGI, Haroon**
ExxonMobil Research and Engineering Company
- KNUTSON, Thomas**
Geophysical Fluid Dynamics Laboratory, National Oceanic and Atmospheric Administration
- KO, Malcolm**
National Aeronautics and Space Administration, Langley Research Center
- KOUTNIK, Michelle**
University of Washington
- KUETER, Jeffrey**
Marshall Institute
- LACIS, Andrew**
National Aeronautics and Space Administration, Goddard Institute for Space Studies
- LASZLO, Istvan**
National Oceanic and Atmospheric Administration
- LEULIETTE, Eric**
University of Colorado, Boulder
- LEVY, Robert**
Science Systems & Applications, Inc. (SSAI), NASA-GSFC
- LEWITT, Martin**
- LI, Zhanqing**
University of Maryland, Department of Atmospheric and Oceanic Science and ESSIC
- LIU, Yangang**
Brookhaven National Laboratory
- LOVEJOY, Edward R.**
National Oceanic and Atmospheric Administration
- LUNCH, Claire**
Stanford University, Carnegie Institution of Washington
- LUPO, Anthony**
University of Missouri, Columbia
- MACCRACKEN, Michael**
Climate Institute
- MAGI, Brian**
University of Washington
- MAHLMAN, Jerry**
National Center for Atmospheric Research
- MAHOWALD, Natalie**
National Center for Atmospheric Research
- MANN, Michael**
Pennsylvania State University
- MANNING, Martin**
IPCC WGI TSU, National Oceanic and Atmospheric Administration, Earth System Research Laboratory
- MARQUIS, Melinda**
IPCC WGI TSU, National Oceanic and Atmospheric Administration, Earth System Research Laboratory
- MARTIN, Scot**
Harvard University
- MASSIE, Steven**
National Center for Atmospheric Research
- MASTRANDREA, Michael**
Stanford University
- MATSUMOTO, Katsumi**
University of Minnesota, Twin Cities
- MATSUOKA, Kenichi**
University of Washington
- MAURICE, Lourdes**
Federal Aviation Administration
- MICHAELS, Patrick**
University of Virginia
- MILLER, Charles**
Jet Propulsion Laboratory, California Institute of Technology
- MILLER, Laury**
National Oceanic and Atmospheric Administration, Lab for Satellite Altimetry
- MILLER, Ron**
National Aeronautics and Space Administration, Goddard Institute for Space Studies
- MILLET, Dylan**
Harvard University
- MILLY, Chris**
United States Geological Survey
- MINNIS, Patrick**
National Aeronautics and Space Administration, Langley Research Center
- MOLINARI, Robert**
National Oceanic and Atmospheric Administration, Atlantic Oceanographic and Meteorological Laboratory
- MOTE, Philip**
Climate Impacts Group, Joint Institute for the Study of the Atmosphere and Oceans (JIASO), University of Washington
- MURPHY, Daniel**
National Oceanic and Atmospheric Administration, Earth System Research Laboratory
- MUSCHELER, Raimund**
Goddard Earth Sciences and Technology Center, University of Maryland & NASA/Goddard Space Flight Center, Climate & Radiation Branch
- NEELIN, J. David**
University of California, Los Angeles
- NELSON, Frederick**
Department of Geography, University of Delaware
- NEREM, R. Steven**
University of Colorado at Boulder
- NOLIN, Anne**
Oregon State University
- NORRIS, Joel**
Scripps Institution of Oceanography
- OPPENHEIMER, Michael**
Princeton University
- OTTO-BLIESNER, Bette**
Climate and Global Dynamics Division, National Center for Atmospheric Research
- OVERPECK, Jonathan**
Institute for the Study of Planet Earth, University of Arizona
- OWENS, John**
3M
- PATT, Anthony**
Boston University
- PENNER, Joyce E.**
Department of Atmospheric, Oceanic, and Space Sciences, University of Michigan
- PETERS, Halton**
Carnegie Institution of Washington, Department of Global Ecology
- PRINN, Ronald**
Department of Earth, Atmospheric and Planetary Sciences, Massachusetts Institute of Technology
- PROFETA, Timothy H.**
Nicholas Institute of Environmental Policy Solutions, De University
- RAMANATHAN, Veerabhadran**
Scripps Institution of Oceanography

RAMASWAMY, Venkatachalam

National Oceanic and Atmospheric Administration, Geophysical Fluid Dynamics Laboratory

RANDERSON, James

University of California, Irvine

RAVISHANKARA, A. R.

National Oceanic and Atmospheric Administration

RIGNOT, Eric

Jet Propulsion Laboratory

RIND, David

National Aeronautics and Space Administration, Goddard Institute for Space Studies

RITSON, David

Stanford University

ROBOCK, Alan

Rutgers University

RUSSO, Felicita

UMBC/JCET

SABINE, Christopher

National Oceanic and Atmospheric Administration, Pacific Marine Environmental Laboratory

SCHIMEL, David

National Center for Atmospheric Research

SCHMIDT, Gavin

National Aeronautics and Space Administration, Goddard Institute for Space Studies

SCHWARTZ, Stephen E.

Brookhaven National Laboratory

SCHWING, Franklin

National Oceanic and Atmospheric Administration Fisheries Service, SWFSC/ERD

SEIDEL, Dian

National Oceanic and Atmospheric Administration, Air Resources Laboratory

SEINFELD, John

California Institute of Technology

SETH, Anji

University of Connecticut, Department of Geography

SEVERINGHAUS, Jeffrey

Scripps Institution of Oceanography, University of California, San Diego

SHERWOOD, Steven

Yale University

SHINDELL, Drew

National Aeronautics and Space Administration, Goddard Institute for Space Studies

SHUKLA, Jagadish

Center for Ocean-Land-Atmosphere Studies, George Mason University

SIEVERING, Herman

University of Colorado - Boulder and Denver

SODEN, Brian

University of Miami, Rosentiel School for Marine and Atmospheric Science

SOLOMON, Susan

Co-Chair, IPCC WGI, National Oceanic and Atmospheric Administration, Earth System Research Laboratory

SOULEN, Richard**STEFFAN, Konrad**

University of Colorado

STEIG, Eric

University of Washington

STEVENS, Bjorn

UCLA Department of Atmospheric & Oceanic Sciences

STONE, Peter

Massachusetts Institute of Technology

STOUFFER, Ronald J.

National Oceanic and Atmospheric Administration, Geophysical Fluid Dynamics Laboratory

TAKLE, Eugene

Iowa State University

TAMISIEA, Mark

Harvard-Smithsonian Center for Astrophysics

TERRY, Joyce

Woods Hole Oceanographic Institution

THOMPSON, Anne

Pennsylvania State University, Department of Meteorology

THOMPSON, David

Department of Atmospheric Science, Colorado State University

THOMPSON, LuAnne

University of Washington

THOMPSON, Robert

United States Geological Survey

TRENBERTH, Kevin E.

Climate Analysis Section, National Center for Atmospheric Research

VINNIKOV, Konstantin

University of Maryland

VONDER HAAR, Thomas

Colorado State University

WAITZ, Ian

Massachusetts Institute of Technology

WANG, James S.

Environmental Defense

WEBB, Robert

National Oceanic and Atmospheric Administration, Earth System Research Laboratory

WEISS, Ray

Scripps Institution of Oceanography, University of California, San Diego

WELTON, Ellsworth

National Aeronautics and Space Administration, Goddard Space Flight Center

WIELICKI, Bruce

National Aeronautics and Space Administration, Langley Research Center

WILES, Gregory

The College of Wooster

WINTON, Michael

Geophysical Fluid Dynamics Laboratory, National Oceanic and Atmospheric Administration

WOODHOUSE, Connie

National Climatic Data Center

YU, Hongbin

National Aeronautics and Space Administration, Goddard Space Flight Center

YU, Jin-Yi

University of California, Irvine

ZENDER, Charles

University of California, Irvine

ZHAO, Xuepeng

ESSIC/UMCP & National Oceanic and Atmospheric Administration

International Organizations**PALMER, Timothy**

European Centre for Medium-Range Weather Forecasting

RIXEN, Michel

University of Liege and NATO Undersea Research Center

SIMMONS, Adrian

European Centre for Medium-Range Weather Forecasts

Annex IV

Acronyms & Regional Abbreviations

Acronyms

μmol	micromole	ASOS	Automated Surface Observation Systems
20C3M	20th Century Climate in Coupled Models	ASTEX	Atlantic Stratocumulus Transition Experiment
AABW	Antarctic Bottom Water	ATCM	Atmospheric Transport and Chemical Model
AAIW	Antarctic Intermediate Water	ATSR	Along Track Scanning Radiometer
AAO	Antarctic Oscillation	AVHRR	Advanced Very High Resolution Radiometer
AATSR	Advanced Along Track Scanning Radiometer	BATS	Bermuda Atlantic Time-series Study
ACC	Antarctic Circumpolar Current	BC	black carbon
ACCENT	Atmospheric Composition Change: a European Network	BCC	Beijing Climate Center
ACE	Accumulated Cyclone Energy or Aerosol Characterization Experiment	BCCR	Bjerknes Centre for Climate Research
ACRIM	Active Cavity Radiometer Irradiance Monitor	BIOME 6000	Global Palaeovegetation Mapping project
ACRIMSAT	Active Cavity Radiometer Irradiance Monitor Satellite	BMRC	Bureau of Meteorology Research Centre
ACW	Antarctic circumpolar wave	C⁴MIP	Coupled Carbon Cycle Climate Model Intercomparison Project
ADEC	Aeolian Dust Experiment on Climate	CaCO₃	calcium carbonate
ADNET	Asian Dust Network	CAMS	Climate Anomaly Monitoring System (NOAA)
AeroCom	Aerosol Model Intercomparison	CAPE	Convective Available Potential Energy
AERONET	Aerosol RObotic NETwork	CCl₄	carbon tetrachloride
AGAGE	Advanced Global Atmospheric Gases Experiment	CCM	Chemistry-Climate Model
AGCM	Atmospheric General Circulation Model	CCCma	Canadian Centre for Climate Modelling and Analysis
AGWP	Absolute Global Warming Potential	CCN	cloud condensation nuclei
AIACC	Assessments of Impacts and Adaptations to Climate Change in Multiple Regions and Sectors	CCSR	Centre for Climate System Research
AIC	aviation-induced cloudiness	CDIAC	Carbon Dioxide Information Analysis Center
ALAS	Autonomous Lagrangian Current Explorer	CDW	Circumpolar Deep Water
ALE	Atmospheric Lifetime Experiment	CERES	Clouds and the Earth's Radiant Energy System
AMIP	Atmospheric Model Intercomparison Project	CERFACS	Centre Europeen de Recherche et de Formation Avancee en Calcul Scientific
AMO	Atlantic Multi-decadal Oscillation	CF₄	perfluoromethane
AMSU	Advanced Microwave Sounding Unit	CFC	chlorofluorocarbon
AO	Arctic Oscillation	CFCI₃	CFC-11
AOGCM	Atmosphere-Ocean General Circulation Model	CH₂I₂	di-iodomethane (methylene iodide)
APEX	Atmospheric Particulate Environment Change Studies	CH₂O	formaldehyde
AR4	Fourth Assessment Report	CH₃CCl₃	methyl chloroform
ARM	Atmospheric Radiation Measurement	CH₃COOH	acetic acid
		CH₄	methane

CLAMS	Chesapeake Lighthouse and Aircraft Measurements for Satellites	DTR	diurnal temperature range
CLARIS	Europe-South America Network for Climate Change Assessment and Impact Studies	DU	Dobson unit
CLIMAP	Climate: Long-range Investigation, Mapping, and Prediction	EARLINET	European Aerosol Research Lidar Network
CLIVAR	Climate Variability and Predictability Programme	EBM	Energy Balance Model
CMAP	CPC Merged Analysis of Precipitation	ECMWF	European Centre for Medium Range Weather Forecasts
CMDL	Climate Monitoring and Diagnostics Laboratory (NOAA)	ECS	equilibrium climate sensitivity
CMIP	Coupled Model Intercomparison Project	EDGAR	Emission Database for Global Atmospheric Research
CNRM	Centre National de Recherches Météorologiques	EMIC	Earth System Model of Intermediate Complexity
CO	carbon monoxide	ENSO	El Niño-Southern Oscillation
CO₂	carbon dioxide	EOF	Empirical Orthogonal Function
CO₃²⁻	carbonate	EOS	Earth Observing System
COADS	Comprehensive Ocean-Atmosphere Data Set	EPICA	European Programme for Ice Coring in Antarctica
COARE	Coupled Ocean-Atmosphere Response Experiment	ERA-15	ECMWF 15-year reanalysis
COBE-SST	Centennial in-situ Observation-Based Estimates of SSTs	ERA-40	ECMWF 40-year reanalysis
COWL	Cold Ocean-Warm Land	ERBE	Earth Radiation Budget Experiment
CPC	Climate Prediction Center (NOAA)	ERBS	Earth Radiation Budget Satellite
CREAS	Regional Climate Change Scenarios for South America	ERS	European Remote Sensing satellite
CRIEPI	Central Research Institute of Electric Power Industry	ESRL	Earth System Research Library (NOAA)
CRUTEM2v	CRU/Hadley Centre gridded land-surface air temperature version 2v	ESTOC	European Station for Time-series in the Ocean
CRUTEM3	CRU/Hadley Centre gridded land-surface air temperature version 3	EUROCS	EUROpean Cloud Systems
CSIRO	Commonwealth Scientific and Industrial Research Organization	FACE	Free Air CO ₂ Enrichment
CTM	Chemical Transport Model	FAO	Food and Agriculture Organization (UN)
DEMETER	Development of a European Multimodel Ensemble System for Seasonal to Interannual Prediction	FAR	First Assessment Report
DIC	dissolved inorganic carbon	FRGCG	Frontier Research Center for Global Change
DJF	December, January, February	FRSGC	Frontier Research System for Global Change
DLR	Deutsches Zentrum für Luft- und Raumfahrt	GAGE	Global Atmospheric Gases Experiment
DMS	dimethyl sulphide	GARP	Global Atmospheric Research Program
D-O	Dansgaard-Oeschger	GATE	GARP Atlantic Tropical Experiment
DOC	dissolved organic carbon	GAW	Global Atmosphere Watch
DORIS	Determination d'Orbite et Radiopositionnement Intégrés par Satellite	GCM	General Circulation Model
DSOW	Denmark Strait Overflow Water	GCOS	Global Climate Observing System
DSP	Dynamical Seasonal Prediction	GCSS	GEWEX Cloud System Study
		GEIA	Global Emissions Inventory Activity
		GEOS	Goddard Earth Observing System
		GEWEX	Global Energy and Water Cycle Experiment
		GFDL	Geophysical Fluid Dynamics Laboratory

GHCN	Global Historical Climatology Network	HCO₃⁻	bicarbonate
GHG	greenhouse gas	HFC	hydrofluorocarbon
GIA	glacial isostatic adjustment	HIRS	High Resolution Infrared Radiation Sounder
GIN Sea	Greenland-Iceland-Norwegian Sea	HLM	High Latitude Mode
GISP2	Greenland Ice Sheet Project 2	HNO₃	nitric acid
GISS	Goddard Institute for Space Studies	HO₂	hydroperoxyl radical
GLACE	Global Land Atmosphere Coupling Experiment	HONO	nitrous acid
GLAMAP	Glacial Ocean Mapping	HOT	Hawaii Ocean Time-Series
GLAS	Geoscience Laser Altimeter System	hPa	hectopascal
GLODAP	Global Ocean Data Analysis Project	HYDE	HistorY Database of the Environment
GLOSS	Global Sea Level Observing System	IABP	International Arctic Buoy Programme
GMD	Global Monitoring Division (NOAA)	ICESat	Ice, Cloud and land Elevation Satellite
GOME	Global Ozone Monitoring Experiment	ICOADS	International Comprehensive Ocean-Atmosphere Data Set
GPCC	Global Precipitation Climatology Centre	ICSTM	Imperial College of Science, Technology and Medicine
GPCP	Global Precipitation Climatology Project	IGBP	International Geosphere-Biosphere Programme
GPS	Global Positioning System	IGBP-DIS	IGBP Data and Information System
GRACE	Gravity Recovery and Climate Experiment	IGRA	Integrated Global Radiosonde Archive
GRIP	Greenland Ice Core Project	IMO	International Meteorological Organization
GSA	Great Salinity Anomaly	INDOEX	Indian Ocean Experiment
Gt	gigatonne (10 ⁹ tonnes)	InSAR	Interferometric Synthetic Aperture Radar
GWE	Global Weather Experiment	IO	iodine monoxide
GWP	Global Warming Potential	IOCI	Indian Ocean Climate Initiative
H₂	molecular hydrogen	IOD	Indian Ocean Dipole
HadAT	Hadley Centre Atmospheric Temperature data set	IOZM	Indian Ocean Zonal Mode
HadAT2	Hadley Centre Atmospheric Temperature data set Version 2	IPAB	International Programme for Antarctic Buoys
HadCRUT2v	Hadley Centre/CRU gridded surface temperature data set version 2v	IPO	Inter-decadal Pacific Oscillation
HadCRUT3	Hadley Centre/CRU gridded surface temperature data set version 3	IPSL	Institut Pierre Simon Laplace
HadISST	Hadley Centre Sea Ice and Sea Surface Temperature data set	IS92	IPCC Scenarios 1992
HadMAT	Hadley Centre Marine Air Temperature data set	ISCCP	International Satellite Cloud Climatology Project
HadRT	Hadley Centre Radiosonde Temperature data set	ITCZ	Inter-Tropical Convergence Zone
HadRT2	Hadley Centre Radiosonde Temperature data set	JAMSTEC	Japan Marine Science and Technology Center
HadSLP2	Hadley Centre MSLP data set version 2	JJA	June, July, August
HadSST2	Hadley Centre SST data set version 2	JMA	Japan Meteorological Agency
HALOE	Halogen Occultation Experiment	ka	thousand years ago
HCFC	hydrochlorofluorocarbon	KMA	Korea Meteorological Administration
		KNMI	Royal Netherlands Meteorological Institute
		kyr	thousand years

LASG	National Key Laboratory of Numerical Modeling for Atmospheric Sciences and Geophysical Fluid Dynamics	MODIS	Moderate Resolution Imaging Spectrometer
LBA	Large-Scale Biosphere-Atmosphere Experiment in Amazonia	mol	mole
LBC	lateral boundary condition	MONEX	Monsoon Experiment
LBL	line-by-line	MOPITT	Measurements of Pollution in the Troposphere
LGM	Last Glacial Maximum	MOZAIC	Measurement of Ozone by Airbus In-service Aircraft
LIG	Last Interglacial	MPI	Max Planck Institute
LKS	Lanzante-Klein-Seidel	MPIC	Max Planck Institute for Chemistry
LLGHG	long-lived greenhouse gas	MPLNET	Micro-Pulse Lidar Network
LLJ	Low-Level Jet	MRI	Meteorological Research Institute of JMA
LLNL	Lawrence Livermore National Laboratory	MSLP	mean sea level pressure
LMD	Laboratoire de Météorologie Dynamique	MSU	Microwave Sounding Unit
LOA	Laboratoire d'Optique Atmosphérique	Myr	million years
LOSU	level of scientific understanding	N₂	molecular nitrogen
LSCE	Laboratoire des Sciences du Climat et de l'Environnement	N₂O	nitrous oxide
LSM	land surface model	N₂O₅	dinitrogen pentoxide
LSW	Labrador Sea Water	NADW	North Atlantic Deep Water
LW	longwave	NAH	North Atlantic subtropical high
LWP	liquid water path	NAM	Northern Annular Mode
Ma	million years ago	NAMS	North American Monsoon System
MAM	March, April, May	NAO	North Atlantic Oscillation
MARGO	Multiproxy Approach for the Reconstruction of the Glacial Ocean surface	NARCCAP	North American Regional Climate Change Assessment Program
mb	millibar	NASA	National Aeronautics and Space Administration
MDI	Michelson Doppler Imager	NCAR	National Center for Atmospheric Research
Meteosat	European geostationary meteorological satellite	NCDC	National Climatic Data Center
MFR	Maximum Feasible Reduction	NCEP	National Centers for Environmental Prediction
MHT	meridional heat transport	NEAQS	New England Air Quality Study
MINOS	Mediterranean Intensive Oxidants Study	NEP	net ecosystem production
MIP	Model Intercomparison Project	NESDIS	National Environmental Satellite, Data and Information Service
MIRAGE	Megacity Impacts on Regional and Global Environments	NGRIP	North Greenland Ice Core Project
MISO	Monsoon Intra-Seasonal Oscillation	NH	Northern Hemisphere
MISR	Multi-angle Imaging Spectro-Radiometer	NH₃	ammonia
MJO	Madden-Julian Oscillation	NH₄⁺	ammonium ion
MLS	Microwave Limb Sounder	NIES	National Institute for Environmental Studies
MMD	Multi-Model Data set (at PCMDI)	NIWA	National Institute of Water and Atmospheric Research
MOC	Meridional Overturning Circulation	NMAT	Nighttime Marine Air Temperature

NMHC	non-methane hydrocarbon	PMOD	Physikalisch-Meteorologisches Observatorium Davos
NMVOC	non-methane volatile organic compound	PNA	Pacific-North American pattern
NO	nitric oxide	PNNL	Pacific Northwest National Laboratory
NO₂	nitrogen dioxide	PNV	potential natural vegetation
NO₃	nitrate radical	POA	primary organic aerosol
NOAA	National Oceanic and Atmospheric Administration	POC	particulate organic carbon
NO_x	reactive nitrogen oxides (the sum of NO and NO ₂)	POLDER	Polarization and Directionality of the Earth's Reflectance
NPI	North Pacific Index	POM	particulate organic matter
NPIW	North Pacific Intermediate Water	ppb	parts per billion
NPP	net primary productivity	ppm	parts per million
NRA	NCEP/NCAR reanalysis	PR	Precipitation Radar
NVAP	NASA Water Vapor Project	PREC/L	Precipitation Reconstruction over Land (PREC/L)
O('D)	oxygen radical in the 1D excited state	PROVOST	Prediction of Climate Variations on Seasonal to Interannual Time Scales
O₂	molecular oxygen	PRP	Partial Radiative Perturbation
O₃	ozone	PSA	Pacific-South American pattern
OASIS	Ocean Atmosphere Sea Ice Soil	PSC	polar stratospheric cloud
OCTS	Ocean Colour and Temperature Scanner	PSMSL	Permanent Service for Mean Sea Level
ODS	ozone-depleting substances	PSU	Pennsylvania State University
OECD	Organisation for Economic Co-operation and Development	psu	Practical Salinity Unit
OGCM	Ocean General Circulation Model	QBO	Quasi-Biennial Oscillation
OH	hydroxyl radical	RATPAC	Radiosonde Atmospheric Temperature Products for Assessing Climate
OIO	iodine dioxide	RCM	Regional Climate Model
OLR	outgoing longwave radiation	REA	Reliability Ensemble Average
OMI	Ozone Monitoring Instrument	REML	restricted maximum likelihood
OPAC	Optical Parameters of Aerosols and Clouds	RF	radiative forcing
PCMDI	Program for Climate Model Diagnosis and Intercomparison	RFI	Radiative Forcing Index
pCO₂	partial pressure of CO ₂	RH	relative humidity
PDF	probability density function	RMS	root-mean square
PDI	Power Dissipation Index	RSL	relative sea level
PDO	Pacific Decadal Oscillation	RSS	Remote Sensing Systems
PDSI	Palmer Drought Severity Index	RTMIP	Radiative-Transfer Model Intercomparison Project
PET	potential evapotranspiration	SACZ	South Atlantic Convergence Zone
PETM	Palaeocene-Eocene Thermal Maximum	SAFARI	Southern African Regional Science Initiative
PFC	perfluorocarbon	SAGE	Stratospheric Aerosol and Gas Experiment or Centre for Sustainability and the Global Environment
Pg	petagram (10 ¹⁵ grams)	SAM	Southern Annular Mode or Stratospheric Aerosol Measurement
PMIP	Paleoclimate Modelling Intercomparison Project		

SAMS	South American Monsoon System	STARDEX	STAtistical and Regional dynamical Downscaling of EXtremes for European regions
SAMW	Subantarctic Mode Water	STE	stratosphere-troposphere exchange
SAR	Second Assessment Report or Synthetic Aperture Radar	STMW	Subtropical Mode Water
SARB	Surface and Atmosphere Radiation Budget	SUNY	State University of New York
SARR	Space Absolute Radiometric Reference	Sv	Sverdrup ($10^6 \text{ m}^3 \text{ s}^{-1}$)
SAT	surface air temperature	SW	shortwave
SCA	snow-covered area	SWE	snow water equivalent
SCIAMACHY	SCanning Imaging Absorption SpectroMeter for Atmospheric CHartographY	SWH	significant wave height
SCM	Simple Climate Model	T/P	TOPEX/Poseidon
SeaWiFs	Sea-Viewing Wide Field-of-View Sensor	T12	HIRS channel 12
SF₆	sulphur hexafluoride	T2	MSU channel 2
SH	Southern Hemisphere	T2_L	MSU lower-troposphere channel
SIO	Scripps Institution of Oceanography	T3	MSU channel 3
SIS	Small Island States	T4	MSU channel 4
SLE	sea level equivalent	TAR	Third Assessment Report
SLP	sea level pressure	TARFOX	Tropospheric Aerosol Radiative Forcing Experiment
SMB	surface mass balance	TBO	Tropospheric Biennial Oscillation
SMM	Solar Maximum Mission	TCR	transient climate response
SMMR	Scanning Multichannel Microwave Radiometer	TEAP	Technology and Economic Assessment Panel
SO	Southern Oscillation	TGBM	Tide Gauge Bench Mark
SO₂	sulphur dioxide	TGICA	Task Group on Data and Scenario Support for Impact and Climate Analysis (IPCC)
SO₄	sulphate	THC	Thermohaline Circulation
SOA	secondary organic aerosol	THIR	Temperature Humidity Infrared Radiometer
SOHO	Solar Heliospheric Observatory	TIM	Total Solar Irradiance Monitor
SOI	Southern Oscillation Index	TIROS	Television InfraRed Observation Satellite
SOM	soil organic matter	TMI	TRMM microwave imager
SON	September, October, November	TOA	top of the atmosphere
SORCE	Solar Radiation and Climate Experiment	TOGA	Tropical Ocean Global Atmosphere
SPARC	Stratospheric Processes and their Role in Climate	TOM	top of the model
SPCZ	South Pacific Convergence Zone	TOMS	Total Ozone Mapping Spectrometer
SPM	Summary for Policymakers	TOPEX	TOPOgraphy EXperiment
SRALT	Satellite radar altimetry	TOVS	TIROS Operational Vertical Sounder
SRES	Special Report on Emission Scenarios	TransCom 3	Atmospheric Tracer Transport Model Intercomparison Project
SSM/I	Special Sensor Microwave/Imager	TRMM	Tropical Rainfall Measuring Mission
SST	sea surface temperature	TSI	total solar irradiance
		UAH	University of Alabama in Huntsville

UARS	Upper Atmosphere Research Satellite
UCDW	Upper Circumpolar Deep Water
UCI	University of California at Irvine
UEA	University of East Anglia
UHI	Urban Heat Island
UIO	University of Oslo
UKMO	United Kingdom Meteorological Office
ULAQ	University of L'Aquila
UMD	University of Maryland
UMI	University of Michigan
UNEP	United Nations Environment Programme
UNFCCC	United Nations Framework Convention on Climate Change
USHCN	US Historical Climatology Network
UTC	Coordinated Universal Time
UTRH	upper-tropospheric relative humidity
UV	ultraviolet
UVic	University of Victoria
VIRGO	Variability of Irradiance and Gravity Oscillations
VIRS	Visible Infrared Scanner
VOC	volatile organic compound
VOS	Voluntary Observing Ships
VRGCM	Variable-Resolution General Circulation Model
W	watt
WAIS	West Antarctic Ice Sheet
WCRP	World Climate Research Programme
WDCGG	World Data Centre for Greenhouse Gases
WGI	IPCC Working Group I
WGII	IPCC Working Group II
WGIII	IPCC Working Group III
WGMS	World Glacier Monitoring Service
WMDW	Western Mediterranean Deep Water
WMO	World Meteorological Organization
WOCE	World Ocean Circulation Experiment
WRE	Wigley, Richels and Edmonds (1996)
WWR	World Weather Records
ZIA	0°C isotherm altitude
τ_{aer}	aerosol optical depth

Regional Abbreviations used in Chapter 11

ALA	Alaska
AMZ	Amazonia
ANT	Antarctic
ARC	Arctic
CAM	Central America
CAR	Caribbean
CAS	Central Asia
CGI	East Canada, Greenland and Iceland
CNA	Central North America
EAF	East Africa
EAS	East Asia
ENA	Eastern North America
IND	Indian Ocean
MED	Mediterranean Basin
NAS	Northern Asia
NAU	North Australia
NEU	Northern Europe
NPA	North Pacific Ocean
SAF	South Africa
SAH	Sahara
SAS	South Asia
SAU	South Australia
SEA	Southeast Asia
SEM	Southern Europe and Mediterranean
SPA	South Pacific Ocean
SSA	Southern South America
TIB	Tibetan Plateau
TNE	Tropical Northeast Atlantic
WAF	West Africa
WNA	Western North America

